The role of claudin-1 in the initiation and progression of hepatocellular carcinoma

Dayus, James

Award date:
2019

Awarding institution:
Coventry University

The Role of Claudin-1 in the Initiation and Progression of Hepatocellular Carcinoma

By

James Dayus

September 2017

A thesis submitted in partial fulfilment of the University's requirements for the Degree of Doctor of Philosophy

Content removed due to data protection considerations

Certificate of Ethical Approval

Applicant:

James Dayus

Project Title:

Differential expression of Claudin-1 influences cellular migration and protein trafficking in HepG2 cells.

This is to certify that the above named applicant has completed the Coventry University Ethical Approval process and their project has been confirmed and approved as High Risk

Date of approval:

23 May 2018

Project Reference Number:

P60814

Abstract

During cancer progression, tight junctions behave as mechanical restraints by anchoring malignant cells to their neighbours thereby inhibiting the metastatic development of primary tumours. Tight junctions not only behave as cell-cell junctional barriers but active participants in cell signalling pathways regulating cell proliferation, polarity, and differentiation.

The increased and decreased expression of the tight junctional protein claudin-1 has been associated with higher tumour grades and lower survival rates in hepatocellular carcinoma. Despite these observations, little is known about how claudin-1 influences the molecular mechanisms involved in the initiation and progression of the disease. By overexpressing and silencing claudin-1 in the HepG2 hepatocellular carcinoma cell line, we have demonstrated that the aberrant expression of claudin-1 induces an invasive phenotype with increased migratory capacity that is consistent with the observational evidence published in the literature.

Overexpression of claudin-1 in the HepG2 cell line resulted in an increase in the mRNA levels of mesenchymal and tumour metastasis genes such as vimentin, MMP -2, -9 and -13, SNAIL, SLUG, TWIST, and ZEB1/2. Furthermore, a significant decrease in the mRNA levels of epithelial markers E-cadherin, cytokeratin-7, -14, -19 and miR-200a, b, c was also observed in these cells. Silencing of claudin-1 in HepG2 cells resulted in increased mRNA expression of vimentin, N-cadherin, MMP -2, -9, and -13, FOXC2, TWIST, and ZEB2. These cells also displayed increased mRNA levels of stem cell markers CD44, CK19, NOTCH, and JAGGED. The classical downregulation of epithelial markers combined with the upregulation of mesenchymal markers provide evidence that aberrant expression of claudin-1 induces EMT in these cells.

Acknowledgments

I want to express my gratitude and deepest thanks to an amazing supervisor and mentor, Dr Christopher Mee. Your guidance and support have kept me focused and determined throughout this work, which has ultimately shaped my development into the scientist I am today. I wouldn't be where I am without you!

Other members of staff I would like to thank are Dr Elaine Green and Dr Aftab Hussain for their continued help and support. I am also incredibly grateful for all the advice and guidance given from all the technical staff, in particular Susan Tompsett who regularly went above and beyond to help me.

Throughout my PhD journey, I have met some amazing people who I now consider close friends. I would like to thank everyone who has worked alongside me, in particular Sarah Siverns, Gurpreet Sandu, Dorota Dobrzanska, Pavneet Singh, Henry Nden, Danielle Meyer, Chloe Jagpal, Natasha Browne-Marke, Refik Kuburas and Charlie Gamage

A particular friend who has been with me through thick and thin is Eliot Barson. His friendship, support, guidance and importantly bad jokes have kept me strong though any challenges I may have faced. Our friendship has developed from the start of my university life and I hope it continues for life! Thank you for everything!

Most importantly I would like to express my upmost thanks and appreciation to my amazing girlfriend Lauren Chandler and my two beautiful daughters Lily and Chloe Dayus. You have been through it all with me, supporting me every step of the way. I certainly could not have done it without you!

Abbreviations

Akt	-	Protein Kinase B
APC	-	Adenomatous polyposis coli
Apg-2	-	Sec-independent protein translocase
ARP2/3	-	Actin-Related Proteins ARP2 and ARP3
BMP-7	-	Bone morphogenetic protein 7
BRG1	-	ATP-dependent helicase SMARCA4
BSA	-	Bovine serum albumin (Fraction V)
C/EBP	-	CCAAT-enhancer-binding protein
CAMK2N1	-	Ca2+/calmodulin-dependent protein kinase II
CAV-1	-	Caveolin 1
CD133	-	Prominin-1
CDC42	-	Cell division control protein 42 homolog
CDK4	-	Cyclin-dependent kinase 4
cDNA	-	Complementary DNA
CK1	-	Casein kinase 1
CLDN1	-	Claudin-1
CMV	-	Cytomegalovirus promotor
CPE	-	Clostridium perfringens enterotoxin
Crumbs3	-	Crumbs protein homolog 3

CSC	-	Cancer Stem Cell
CT	-	Cycle Threshold
CtBP	-	C-terminal-binding protein 1
CXCL12	-	C-X-C Motif Chemokine Ligand 12
CXCR4	-	C-X-C chemokine receptor type 4
DAPI	-	4',6-diamidino-2-phenylindole
DMEM	-	Dulbecco's Modified Eagle's Medium
DMSO	-	Dimethylsulphoxide
DNA	-	Deoxyribonucleic acid
TRAIL-RI	-	TNF-related apoptosis-inducing ligand receptor 1
TRAIL-RII	-	TNF-related apoptosis-inducing ligand receptor 2
DVL	-	Dishevelled
E2-2	-	Alternative name of transcription factor 4 (TCF4 or TCF7L2)
E2A	-	Alternative name of transcription factor 4 (TCF3 or TCF7L1)
E47	-	Alternative name of transcription factor 4 (TCF3)
E-box	-	Enhancer box (Protein binding region in DNA)
ECM	-	Extracellular matrix
EDTA	-	Ethylenediaminetetraacetic acid
EGF	-	Epithelial Growth Factor
EGFR	-	Epithelial Growth Factor Receptor

EIF5A2	-	Eukaryotic translation initiation factor 5A-2
EMMPRIN)	-	Extracellular MMP Inducer
EMT	-	Epithelial to mesenchymal transition
EMT-TFs	-	EMT inducing transcription factors
EphB2	-	Ephrin Type-B receptor 2
ERBB3	-	Receptor tyrosine-protein kinase erbB-3
ERK1/2	-	Extracellular signal–regulated kinases 1 and 2
EZH2	-	Enhancer of zeste homolog 2
FBS	-	Foetal Bovine Serum
FGF-2	-	Basic fibroblast growth factor
FOXC2	-	Forkhead box protein C2
FOXO1	-	Forkhead box protein O2
FOXQ1	-	Forkhead box protein Q1
GAPDH	-	Glyceraldehyde 3-phosphate dehydrogenase
GDP	-	Guanosine diphosphate
GNAI1	-	Guanine nucleotide-binding protein alpha-1 subunit
GSC	-	Homeobox Goosecoid
GSK-3β	-	Glycogen synthase kinase-3β
GTP	-	Guanosine triphosphate
GTPase	-	Guanosine triphosphatase

GuK	-	Guanylate kinase
HCC	-	Hepatocellular Carcinoma
HCV	-	Hepatitis C virus
HER2	-	Receptor tyrosine-protein kinase erbB-2
HGF	-	Hepatocyte growth factor
HIF-1α	-	Hypoxia-inducible factor-1alpha
HIF-2α	-	Endothelial PAS domain protein 1
HNF-1α	-	Hepatic Nuclear Factor 1 Alpha
HRE	-	Hypoxia-response element HRE
HRP	-	Horseradish Peroxidase
IGF2BP1	-	Insulin-like growth factor 2
IKKs	-	IκB kinases
ILK	-	Integrin linked kinase
IMS	-	Industrial Methylated Spirits (Denatured Alcohol)
JAG1	-	JAGGED1
JAM	-	Junctional Adhesion Molecule
JNK	-	c-Jun N-terminal kinase
KISS1	-	Kisspeptin
KISS1R	-	KiSS1-derived peptide receptor
LEF1	-	Lymphoid enhancer-binding factor 1

LRP6	-	Lipoprotein receptor related protein 6
LSD1	-	Lys-specific demethylase 1
MAGUK	-	Membrane-Associated Guanylate Kinase-like homologs
MAP1b	-	Microtubule Associated Protein 1B
MAPK	-	Mitogen-activated protein kinases
MBCD	-	Methyl-β-cyclodextrin
MDCK II	-	Madin-Darby canine kidney cells
MET	-	Mesenchymal to Epithelial Transition
MMP	-	Matrix Metalloprotease
MTSS1	-	Metastasis suppressor protein 1
MUPP1	-	Multi-PDZ domain protein
NF-κB	-	Nuclear factor kappa-light-chain-enhancer of activated B cells
NUDT13	-	Nudix Hydrolase 13
P38	-	P38 mitogen-activated protein kinase
PAR	-	Protease activated receptor
PATJ	-	PALS-1 associated TJ protein
PBS	-	Phosphate Buffered Saline
PBST	-	Phosphate Buffered Saline/Tween 20
PCAF	-	P300/CBP-associated factor
PCR	-	Polymerase Chain Reaction

PDGF	-	Platelet Derived Growth Factor
PDGFRB	-	Beta-type platelet-derived growth factor receptor
PDZ	-	PSD -95/D iscs-large/ZO -l
PFA	-	Paraformaldehyde
PI3K	-	Phosphoinositide 3-kinase
PKC	-	Protein Kinase C
PRC2	-	Polycomb Repressive Complex 2
PTEN	-	Phosphatase and tensin homolog
PTPRJ	-	Protein Tyrosine Phosphatase, Receptor Type J
PVDF	-	Polyvinylidene fluoride
Rac1	-	Ras-related C3 botulinum toxin substrate 1
RNA	-	Ribonucleic acid
RO/DI water	-	Reverse Osmosis (RO) Deionized (DI) water
ROCK	-	Rho-associated, coiled-coil-containing protein kinase 1
RT	-	Room Temperature
RT-PCR	-	Real-Time PCR
SAPK	-	Stress-activated protein kinases
SDS	-	Sodium dodecyl sulphate
SDS-PAGE	-	Sodium dodecyl sulphate polyacrylamide gel electrophoresis
SETD8	-	Histone-lysine N-methyltransferase SETD8

SH3	-	SRC Homology 3
SIN3A	-	SIN3 Transcription Regulator Family Member A
siRNA	-	Small interfering RNA
SLUG	-	Zinc finger protein SNAI2
SNAIL	-	Zinc finger protein SNAI1
snRNA	-	Small nuclear RNA
SOX	-	SRY box
SP1	-	Specificity Protein 1
SPARC	-	Osteonectin or Secreted Protein Acidic and Rich in Cysteine
STAT3	-	Signal transducer and activator of transcription 3
T.A.E	-	Tris-base/Acetic acid/EDTA Buffer
T.B.E	-	Tris base/Borate/EDTA
TAB2/3	-	TGF-Beta Activated Kinase 1/MAP3K7 Binding Protein 2 & 3
TAMP	-	Tight Junction-associated MARVEL Proteins
TBST	-	Tri-base, Sodium Chloride, Tween)
TCF1	-	T-Cell-Specific Transcription Factor 1 or TCF7
TGF-β	-	Transforming growth factor beta
TIMP	-	Tissue Inhibitor of Metalloproteinases
TRAIL	-	TNF-related apoptosis-inducing ligand
TSS Buffer	-	Transformation Storage Solution Buffer

TWIST	-	Twist-related protein 1
USP9X	-	Ubiquitin Specific Peptidase 9, X-Linked
VEGF	-	Vascular endothelial growth factor
WASP	-	Wiskott–Aldrich Syndrome protein (also known as WAVE)
WNK4	-	WNK lysine deficient protein kinase
ZEB	-	Zinc Finger E-Box Binding Homeobox 1
ZO	-	Zonula Occludens
ZONAB	-	ZO-1-associated Y-box factor
β-Trcp	-	F-box/WD repeat-containing protein 1A

Table of Contents

List of Figures

List of Tables

Chapter 1: Introduction

1.1 Hepatocellular carcinoma

1.1.1 Global epidemiology

Hepatocellular carcinoma (HCC) is the most common primary liver cancer representing approximately 90% of hepatic malignancies (McGlynn et al 2015). It predominantly presents in patients with a history of chronic inflammation and/or cirrhosis but can also develop as a result of viral Hepatitis infections, chronic alcohol abuse, or fatty liver disease (Kanwal et al 2011). The underlying aetiology varies based on age, geography, gender, and other risk factors. HCC is the fifth most common cancer for men and the seventh most common for women with 523,000 and 226,000 new cases worldwide each year, respectively (El-Serag 2012). This accounts for around 7% of all cancers for both men and women across the globe. Despite this, HCC is the second largest contributor to cancer mortality (El-Serag 2012).

The distribution of HCC varies most based on geographical location, with the highest incidence in Africa and Asia. Sub-Saharan Africa and Eastern Asia account for more than 80% of HCC cases with a typical incidence rate of 20 per 100,000 individuals. Its prevalence correlates with the epidemic prevalence of Hepatitis B and C viral infections in these regions (Raza et al 2007). Southern european and mediterranean countries such as Greece, Spain, and Italy have lower incidence levels ranging from 10-20 cases per 100,000 individuals. North America and Northern Europe have the lowest incidence of HCC globally, with less than 5 cases per 100,000 individuals. Reports suggest that cases of HCC are decreasing in certain regions in China such as Hong Kong, Shanghai and Singapore as well as Japan. However, cases of the disease have been increasing in countries with otherwise low incidences levels such as America and Canada (Mittal et al 2013).

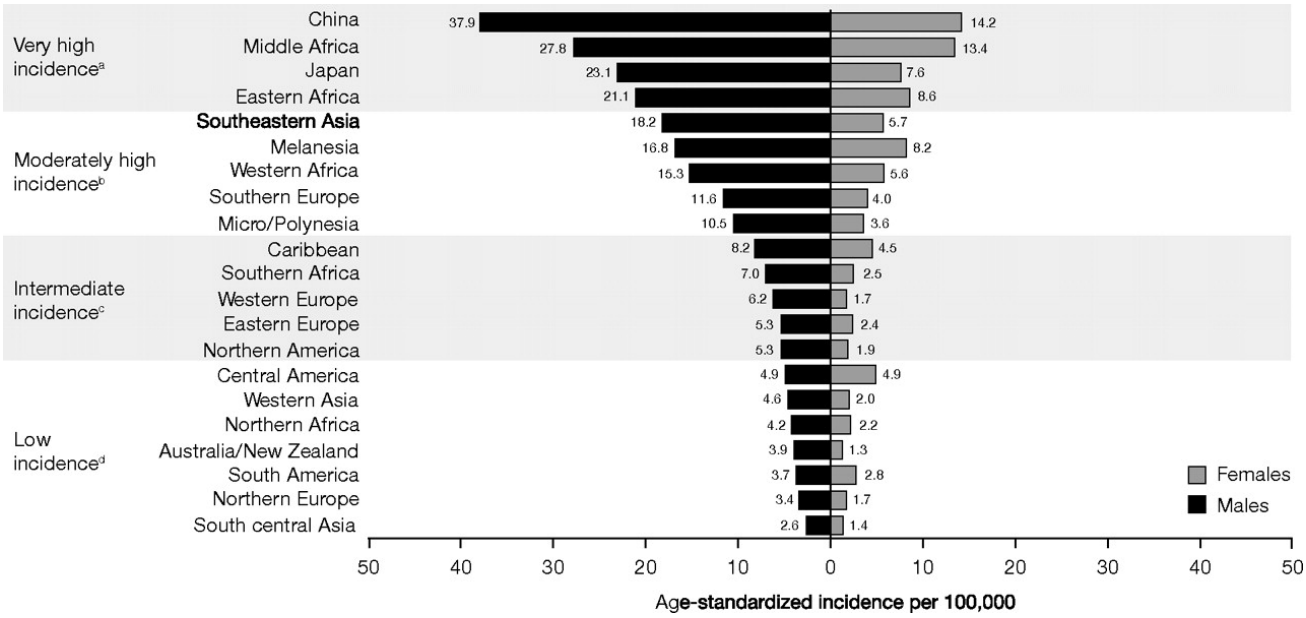

Figure 1.1 Global variation in hepatocellular carcinoma incidence rates. Age-adjusted incidences per 100,000 of hepatocellular carcinoma among men and women by region, 2003-2010. Data taken from Venook et al 2010.

The incidence of HCC, like the majority of cancers, increases with age. It is rarely seen in individuals under the age of 40, with the exception of areas where Hepatitis B and C infection is hyperendemic (Kanwal et al 2011). As the predominant causation factor is viral Hepatitis, the age of diagnosis correlates with the incidence of infection. In high incidence areas, such as China, the most common causation factor for HCC is viral Hepatitis transmitted at birth (El-Serag 2012). As a result, HCC is diagnosed on average 10 years earlier compared to lower incidence areas such as northern Europe and America, where viral Hepatitis is contracted at a later age. In China, the mean age of HCC diagnosis is 55-59 years, and in Europe and America around 63-65 years. Areas with low incidences of viral Hepatitis have average HCC diagnosis ages of 75 or older (Venook et al 2010)

1.1.2 Risk factors of hepatocellular carcinoma

The most important clinical risk factor in the causation of HCC is macronodular cirrhosis. It has been linked to 70-90% of HCC cases and is therefore the largest single risk factor (Nordenstedt et al. 2010). Cirrhosis is characterised by alterations to the normal structure of the liver resulting in areas of abnormal nodules, inflammation, and fibrosis. After macronodular cirrhosis, the most common aetiologies include chronic viral Hepatitis, alcoholic liver disease, steatohepatitis (fatty liver disease), and Wilson's disease (Okuda 2007). Other less common causative factors include Obesity, Diabetes Mellitus, Autoimmune Hepatitis, Alpha-1-antitrypsin deficiency, cigarette smoking, and Aflatoxin exposure (Herbst & Reddy 2012)

1.1.3 Treatment of HCC

Treatment of HCC is significantly based on the staging of the tumour. Unfortunately, the diagnosis of the disease is often missed until patients present with signs and symptoms of advanced hepatic impairment. As a result, the tumours are often of an advanced stage, making resection and transplantation unsuitable for many people (Malek et al 2014). The treatment with the highest curative rate for patients with early stage HCC, prior to lymph node or portal vein invasion, is a partial hepatectomy. The resectability of the tumour depends on a number of factors such as the stage, location, liver function, and the volume of liver requiring resection (Wong & Frenette 2011). Successful resection can result in a 41-74%, 5-year survival rate. However, the operative mortality rate can be as high as 10%, dependent on the degree of cirrhosis. Liver transplantation can be offered if the tumour is too large for resection, providing an organ is available, no extrahepatic invasion has occurred, and the patient presents with a good operative risk. Patients that are not suitable for resection or transplantation can be offered loco-regional therapies such as transarterial

chemoembolization, radioembolization, percutaneous alcohol injection, and radiofrequency treatment, providing no extrahepatic invasion has occurred (Balogh et al 2016). Patients diagnosed with advanced HCC presenting with extrahepatic invasion, nodal spread, and general metastasis that are unacceptable for resection, translation, and locoregional therapies are often treated with systemic Sorafenib. The therapeutic action of Sorafenib is inhibition of Raf kinases, VEGF and platelet-derived growth factor receptors. Inhibiting these signalling pathways has been shown to limit cell proliferation and angiogenesis in cancer, although the effectiveness of the drug is dependent on the molecular profile of the disease (Clark et al 2016).

Molecular profiling describes the process of understanding the genetic and epigenetic processes underlying the development of diseases such as cancer. This process makes it possibly to understand how specific molecular signatures correspond to clinical outcomes which can ultimately allow the development of targeted treatment options based on these signatures (Piris 2011). Ras activation resulting from several molecular mechanisms such as point mutations, and epigenetic silencing of associated tumour suppressors are common progressive factors in hepatocellular carcinoma. Sorafenib has been shown to be effective treatment against HCC tumours derived from aberrant Ras activation, by blocking the kinase activity of Ras (Newell et al 2009). However, cases of HCC with mutations that lead to inactivation of the wild-type p53 tumor suppressor gene have been shown to be significantly more likely to be resistant to sorafenib. This is mainly due to these cells being less dependent on their vascular supply which sorafenib targets though blocking VEGF (He and Goldenberg 2013). Furthermore, hepatocellular carcinomas with elevated stem cell marks such as CD133/CD44 have been shown to respond poorly to the treatment (Rimassa et al 2009).

1.2 Hepatocellular carcinoma metastasis

Metastatic cancer is defined by the ability of cancer cells to invade the tumour microenvironment and subsequently spread and recolonise in distant parts of the body. This process defines the major difference between benign and malignant tumours and has significant clinical implications as over 90% of cancer related deaths are caused by metastasis (Hanahan & Weinberg 2000). Metastasising cells cause fatalities by creating local obstructions, disturbing organ function and competing with normal bodily cells for nutrients and oxygen. Unfortunately, many cancers are likely to metastasise before they are clinically detectable, leading to a poor prognosis and limiting treatment options for many people (Hutchinson 2015).

The majority of cancers invade and utilise the immediate vasculature and lymphatic systems as means of transport from primary to metastatic sites (Gobardhan et al 2011). As a result, the predominant location of secondary tumours is in close proximity, usually following the routes of these systems. However, it has been observed that specific cancers favour certain metastatic niches that cannot be explained by the routes of anatomical channels (Williams et al 2013). In 1889, Stephen Paget, found patients with breast cancer often presented with liver metastasis with none recorded in the spleen, despite both organs receiving similar blood volumes. He later proposed the terms “seed and soil”, stating that metastasising cancer cells, ‘the seeds’, may require a metastatic niche, ‘the soil’, with conditions favourable to those cells to allow recolonisation (Paget 1889). Sugarbaker, and later Kinsey, experimentally proved Paget’s theory correct when they transplanted melanoma-containing organs into DBA/2 syngeneic mice. They found that the melanoma cells only metastasised to the lungs and no other organs, despite no obvious anatomical explanation (Sugarbaker 1952; Kinsey 1960).

The occurrence of extrahepatic metastases of HCC are not rare. The aggressive

nature of the cancer means patients on average develop metastases only 10 months after initial diagnosis. The average life expectance for these patients is 7 months, which is often significantly reduced in patients with multiple organ metastases (Natsuizaka et al 2005).

The most frequent site for extrahepatic metastases is the lung, representing by an average 55% of secondary malignancies (Katyal et al 2000). The bone, abdominal lymph nodes, and adrenal glands are also common metastatic sites occurring in up to 38%, 33%, and 17% of patients respectively (Katyal et al 2000). The brain, and less commonly skeletal muscle, are also metastasised to in 8% and 1.5% of patients respectively (Katyal et al 2000). Up to 45% of patients present with multiple organ metastases, with the majority of patients with brain metastases also having lung metastases (Natsuizaka et al 2005).

The frequency of extrahepatic metastases, short survival rate, and limited treatment options for patients with HCC poses a significant problem in management of the disease. Further understanding of the molecular mechanisms which initiate metastasis are needed to provide adequate therapeutic options.

1.2.1 The molecular process of metastasis initiation

The process of metastasis follows a progressive acquisition of traits causing cells to gain an invasive phenotype and recolonise a secondary site. The major steps in the process are invasion, intravasation, transport, extravasation, metastatic colonisation and angiogenesis. Although these processes are often described as distinct biological events, the acquisition of the traits required to implement any of these stages may be obtained simultaneously or in a different order as described above. This is due to many of these mechanisms sharing conserved molecular pathways (Gupta & Massagué 2006).

The process of metastasis often begins with the acquisition of an invasive phenotype. Epigenetic and genomic instability coupled with oncogenic mutations drive

molecular mechanisms which cause cells to disseminate from the primary tumours. Before cells can begin to invade they first must acquire cancerous prerequisites such as self-renewal, and detachment survival both from neighbouring cells and the extracellular matrix (Hutchinson 2015).

Cellular adhesion between neighbouring cells and the extracellular matrix is predominantly achieved by coordinating tight junctions, cell adhesion molecules (CAMs), and integrins (Farahani et al 2014). A loss or mislocalisation of tight junction and cell adhesion molecules, predominantly claudins, occludin, and cadherins, has been shown to promote motility and metastasis in a number of cancers (Cavallaro & Christofori 2004). Cells must regulate these molecular restraints, so they can gain motility and break away from the primary tumour and surrounding ECM.

Integrins have also been shown to modulate the malignant phenotype. The upregulation of integrin $\alpha_6\beta_4$ has been shown to form signalling complexes with oncogenic tyrosine kinases c-Met, EGFR, and Her2, upregulating cell proliferation and the invasive phenotype (Guo & Giancotti 2004).

During cancer progression, malignant cells are required to break integrin-ECM ligand binding to migrate and colonise secondary sites. Ordinarily, in normal cells this causes a specific type of apoptosis called anoikis. Anoikis is mediated by activation of death receptors (via the extrinsic pathway) and mitochondria (via the intrinsic pathway). Death receptors such as Fas and TNFR1 active caspase 8 causing cleavage and activation of executor caspases such as caspase 3 leading to cell death. Bax-Bak oligomers can also be formed via the intrinsic pathway leading to cytochrome c release from the mitochondria into the cytoplasm. Once released it can induce the development the apoptosome and ultimately the activation of the executor caspases leading to cell death. Cancer cells that are able to invade and disrupt this interaction are required to gain apoptosis resistance to

overcome this response (Paoli et al 2013). Cancer cells which can initiate the EMT program are able to downregulate pro-apoptotic proteins such as p21, Bim and Bax allowing detachment from the ECM and subsequent migration without initiating anoikis (Wu and Zhou 2010)

Once malignant cells have modulated their cell-cell adhesion properties, they must manipulate the ECM and surrounding tumour stroma to access the neighbouring vasculature or lymphatic tissue. Serine proteases and matrix metalloproteases secreted directly from tumour cells or induced from surrounding tumour stromal cells, are able to degrade elements of the tumour microenvironment facilitating the invasion of malignant cells. A number of tumours have been shown to secrete extracellular MMP inducer (EMMPRIN) which binds to non-malignant stromal cells such as fibroblasts and infiltrating inflammatory cells, causing them to secrete proteases (Reunanen & Kähäri 2000).

The MMP family not only remodel and degrade ECM components but also cleave extracellular and cell surface proteins such as growth factors (EGF and TGF-β) and extracellular ligands, promoting cell proliferation, angiogenesis, and resistance to apoptosis (Nissinen and Kähäri 2014). Due to their potent effect during metastasis, the gene expression of MMPs are stringently regulated. They are secreted in an inactive form and inhibited by a family of appropriately named Tissue Inhibitor of Metalloproteinases (TIMPS). A downregulated expression of TIMP family members in cancer is commonly observed, which consequently causes a decrease in their anti-metastatic activity and an increase in MMP activity promoting tumour progression (Hadler-Olsen et al 2013).

The remodelling of cell-cell contacts and surrounding extracellular matrix allows individual cells to behave more independently. However, metastasising cells must gain motility to leave the primary tumour site. The acquisition of a mobile phenotype is a complex and highly orchestrated process guided by internal and external signals. Integrins,

chemokines, and growth factor receptors can interpret the surrounding environment and modulate signal transduction pathways influencing cell migration (Polacheck et al 2013). These factors also activate Rho, Rac1, and CDC42, members of the small GTPase family. The expression of Rho, Rac1 and CDC42 are commonly upregulated in the hepatocellular carcinoma and have been linked to increased cell migration and invasion (Grise et al 2009). Rho GTPases act as sensitive molecular switches which are activated by internal and external signals. Figure (1.2) illustrates the mechanism of activation/inactivation of Rho GTPases.

Figure 1.2: The Rho GTPase cycle. Rho GTPases cycle between an active (GTP-bound) and an inactive (GDP-bound) conformation. This is facilitated by guanine nucleotide exchange factors (GEFs) which catalyse nucleotide exchange and maintain activation. GTPase-activating proteins (GAPs) facilitate GTP hydrolysis, leading to inactivation. Guanine nucleotide exchange inhibitors (GDIs) prevent exchange of GDP to GTP (maintaining the small GTPase in an inactive state) but also remove the inactive GTPase from the membrane which is the site of action (Etienne-Manneville and Hall 2002)

Rho GTPases are responsible for initiating cell migration which ultimately creates protrusions of lamellipodia and filopodia at the leading ledge, whilst contracting the cell, and detaching the trailing edge. Both lamellipodia and filopodia are created by actin polymerisation and filament elongation mediated by the Arp2/3 complex. CDC42 and Rac

activate the Arp2/3 complex via WASP/N-WASP and WAVE respectively, stimulating actin polymerization and driving forward the leading edge (Ridley 2015). Rho in conjunction with ROCK, mediate cell contraction and detachment of the trailing edge by modifying integrin based focal adhesion (Parri & Chiarugi 2010). Taken together, these mechanisms promote cell migration and contribute to the invasive phenotype seen in HCC.

Figure 1.3: Regulation of cell migration via signal transduction. Signalling pathways for cell migration mediated by Ras. Extracellular stimuli, such as serum, EGF and TGF-β activate Rac though Ras. Rac is then able to activate Cdc42 and IRSp53 resulting in actin polymerisation and ultimately filopodia and lamellipodia formation. Rac can also regulate focal adhesion to favour cell mitigation by activating vinculin (VCL) and inhibiting gelsolin (GSN) though PI(4)P 5-Kinase (PIP5KI) (Thomas et al 2013).

The traits acquired by metastasising cells to invade and intravasate can theoretically be obtained independently of one another. Although, the molecular mechanisms that control these changes link a number of these invasive attributes together. The most common

process linking these characteristics and driving the metastatic phenotype is epithelial to mesenchymal transition (Thiery 2002).

1.3 Epithelial to Mesenchymal Transition (EMT)

EMT is the physiological process by which closely connected, polarised epithelial cells are converted into highly mobile and invasive mesenchymal cells (He et al 2017). The process involves a multitude of changes that alters cellular shape, production of intra and extracellular components and the way cells interact with their immediate environment (Ogden et al 2013). The process is essential in a number of normal biological settings such as during wound healing and early embryogenesis. However, EMT is also implemented in a number of diseases, organ fibrosis, and often the initiation of metastasis, tumour invasion, and cell migration (Kalluri & Weinberg 2009).

Normal epithelial tissue is organised into polarised sheets, functioning as a barrier between distinct environments, and enabling the body to be compartmentalised (Giepmans et al 2009). Ordinarily, these cells have extensive interactions between the neighbouring cells and the underlying extracellular matrix utilising tight junctions, adherence junctions, and cellular adhesion molecules (Anderson & Van Itallie 2009). During EMT cells undergo gene expression changes and biochemical alterations which allow detachment and degradation or remodelling of these cell-cell tight junctions/gap junctions, and cell-ECM integrin attachments (Moreno-Bueno et al 2008). These changes also alter the cellular phenotype allowing increased proliferation (via upregulation of cyclin D1), increased migratory capacity (via upregulation of Rock, Rac1 and CDC42) and increased resistance to apoptosis and chemotherapy (via upregulating the expression of the pro-survival protein Bcl-XL) (Shibue and Weinberg 2017). The resulting mesenchymal cells are depolarised

with a fibroblastic morphology, often only interacting with other cells via focal points (Thiery 2002).

The process of EMT can be observed in three district biological settings, producing three classifications of the process. Whilst these classifications share many overlapping features, the outcomes of the transition differ significantly. Type 1 EMT is almost exclusively involved in foetal implantation and embryogenesis. Every aspect of this type of EMT is rigorously controlled by highly conserved mechanisms that have not been corrupted by mutations associated with cancer (Chaffer et al 2016). As a result of this, and the absence of inflammation, the process does not allow for fibrosis formation or uncontrolled growth. Instead the mesenchyme created, termed primary mesenchyme, facilitates invasion of the endometrium and encourages placental formation, as well as expanding and specifying the different tissues required during embryogenesis. Embryonic mesenchyme cells then differentiate into secondary epithelia by the reverse process, mesenchymal to epithelial transition, a process crucial to the successful development of the foetus (Kalluri & Weinberg 2009).

Type 2 EMT is associated with wound healing and tissue regeneration, initiated by inflammatory mediators, immune cells, and fibroblasts. Cellular damage in response to injury or pathogens attracts immune cells such macrophages that activate resident fibroblasts present at the site of injury (Kalluri & Weinberg 2009). Growth factors including TGF-β, PDGF, EGF, and FGF-2 are released by fibroblasts, macrophages and other inflammation inducing immune cells, as well as from the interstitial fluid surrounding the damaged cells. The binding of these factors, particularly TGF-β, increases proliferation and initiates the EMT program via the SMAD2/3 and MAPK pathway. (Nawshad et al 2005). As a result, epithelial, progenitor, and stellate cells resident in the surrounding stromal tissue are subject to direct myofibroblastic differentiation as part of the EMT program, adopting a

mesenchymal phenotype. These cells further release growth factors (such as TGF-β, PDGF, EGF, and FGF-2), chemokines (such as CXCL12), and MMPs, remodelling the ECM and creating a chemoattractive gradient for epithelial cells and fibroblasts to attend and repair the affected area. Myofibroblastic cells can contract using a smooth muscle type actin-myosin complex, pulling the wound edges together whilst proliferating to replace damaged cells (Kalluri & Neilson 2003).

Remodelling of the ECM during wound healing and inflammation causes myofibroblasts to produce excessive amounts of ECM components, especially collagen. Under normal circumstances when the reconstruction of the tissue is complete the inflammation subsides, and the modification of the ECM stops (Darby et al 2014). However, prolonged inflammatory exposure, such as during chronic viral Hepatitis infection, induces continuous ECM remodelling and continuous depositing of ECM components thereby causing bands of hepatic scarring and eventual cirrhosis (Bishayee 2014). The continuous increase in inflammation seen during Hepatitis infection is thought to be a great risk factor for HCC initiation (Gomaa et al 2008). The abundance of growth factors, coupled with a number of epithelial and progenitor stem cells undergoing the EMT program creates an environment of invasive, proliferative cells that are more likely to gain mutations and initiate HCC. (Levrero & Zucman-Rossi 2016).

Type 3 EMT is the third biologically distinct classification of the process and the one most associated with tumour initiation and progression (Banyard & Bielenberg 2015). It is thought to occur predominantly in epithelial cells that have gained genetic mutations and epigenetic modifications (Tam & Weinberg 2013). During neoplasm formation and cancer progression, permanent alterations in the DNA sequence of oncogenes and tumour suppressor genes can signal and initiate the EMT program thereby producing the frequently observed hallmarks of cancer (Zeisberg & Neilson 2009). Epigenetic modifications such as

DNA methylation and histone modifications can also alter the expression of oncogenes and tumour suppressor genes by orchestrating repressor proteins that attach to silencer regions of the DNA. Disruption of epigenetic processes can lead to altered gene function, malignant cellular transformation and initiation of the EMT program (Biswas and Rao 2017). The initiation of EMT has been linked to the acquisition of an invasive phenotype and associated metastasis in a number of cancers, including HCC (Thiery 2002).

Type 3 EMT has a number of characteristics typically associated with type 1 EMT, as type 3 does not typically result in fibrosis and is able to be reversed by MET. It is poorly understood how type 3 EMT cells reverse their phenotype to perform MET, however, it is thought that this process is responsible for the colonisation step at secondary sites (Huang et al 2008). It has been suggested that the local microenvironment of the secondary tumour can influence the reversal of EMT and promote colonisation. Proteins such as Bone morphogenic protein-7 (BMP-7), which is usually involved in osteoblast differentiation, has been described as a major inducer of MET and could in part explain the frequent colonisation of bone by metastasising cells (Langley & Fidler 2011). It is also thought that the absence of EMT inducing signals experienced in the primary tumour environment could trigger MET and the colonisation process (Kalluri & Weinberg 2009).

The mechanisms by which type 1 and 2 EMT are initiated are well documented, although the exact mechanisms that promote type 3 are still yet to be completely understood (Kalluri & Weinberg 2009). In many cases the inflammatory environment associated with cancer, contains an abundance of growth factors and chemokines. The presence of HGF, EGF, PDGF, and especially TGF-β, are suspected to be heavily involved in initiating EMT during cancer progression. Binding of these modules to their respective cell surface receptors causes a cascade of intercellular signal transduction, activating targets such as ERK1/2, PI3K, AKT, SMADs, Rho GTPases, and β-catenin (Shi &

Massagué 2003). Figure (1.4) illustrates the epidermal growth factor (EGF) Signaling pathway which can initiate EMT via MAPK signalling.

Figure 1.4: Epidermal growth factor (EGF) signalling pathway. The diagram on the left shows the signalling pathway prior to stimulation, with the components in their inactive form. These include the soluble ligand, EGF, its receptor (EGFR, a tyrosine kinase), Ras (a G protein), several kinases (RAF, MEK, MAPK), and transcription factors (TF). The diagram on the right shows the activation of the signalling pathway. Binding of EGF to EGFR causes autophosphorylation of the receptor. Though a series of proteins not shown here, Ras is activated to its active GTP bound form. Ras can now continue the signalling process by phosphorylating a series of kinases and ultimately the transcriptions factors which promote the expression of genes associated with cell proliferation and EMT activation (Kim et al 2016).

Mutations can also occur in one or more of these EMT regulatory proteins. These mutations can result in activation and/or loss of inhibitory factors thereby initiating EMT independently of external signals. Ras mutations are commonly implicated in the causation and progression cancers. Mutations at specific loci in Ras exons have been shown to inhibit

GTPase activity, modulate the guanine nucleotide exchange rate, or desensitize their activation by GTPase-activating proteins. Ultimately, this results in constitutive active Ras and inappropriate activation of downstream MAPK signalling, irrespective of any inhibition of cell surface receptor kinases (Hecht et al 2015).

Figure 1.5: Changes associated with mutant Ras. The diagram on the left demonstrates the normal mode of action of wild-type Ras. The controlled activation of Ras mediates normal cellular growth, proliferation and differentiation. This process can be activated/inactivated in response to the needs of the cell. The diagram on the right demonstrates mutant Ras. This form of Ras contains one or more of the mutations previously discussed, resulting in resistance to inactivation with associated abnormal growth and proliferation.

GAP (guanosine triphosphatase-activating proteins) ; GDP (guanosine diphosphate); GEF (guanine exchange factors); GTP (guanosine triphosphate) (Hecht et al 2015).

1.3.1 Hallmarks of EMT

The biomarkers of EMT consist of transcription factors and signal transduction kinases that choreograph the transitional process. As a result, EMT modifies cell surface markers, cytoskeleton/intermediate filaments, and ECM proteins creating the hallmarks associated with cancer progression.

As cells progress from an epithelial phenotype to a mesenchymal one, they change

their cell surface markers in an attempt to regulate intercellular and ECM adherence. E-cadherin is a transmembrane cellular adhesion molecule, found to be almost exclusive to epithelial cells. Its downregulation or complete loss is an important indicator for EMT, and often the first step in the progression towards a more mesenchymal phenotype (Huber et al 2005). Despite this, not all cadherin members are downregulated during EMT. In fact, a process called cadherin switching upregulates other cadherin members such as -N, -T, -P, -11 and -OB. This process is important for type 1 EMT during primitive streak formation and neural plate invagination in embryonic development, as the switching of cadherin members causes segregation of cells, allowing the formation of different tissues. This mechanism is also often observed in type 3 EMT, when E-cadherin is commonly replaced with N-cadherin, promoting cellular motility and invasion of the basal membrane. In this way, the upregulation of the N-cadherin is recognised as a mesenchymal marker (Wheelock et al 2008).

β-catenin is a cytoplasmic plaque protein that associates with E-cadherin at the cell membrane, and with α-catenin and the actin cytoskeleton intracellularly. The loss of E-cadherin associated with cancer progression and EMT causes the dissociation of β-catenin into the cytoplasm of the cell. Under normal conditions, β-catenin is then targeted for proteosomal degradation by the destruction complex, consisting of the scaffolding protein axin along with APC, CK1 and GSK-3β. Together they phosphorylate the amino terminal region of β-catenin. An E3 ubiquitin ligase, β-Trcp recognises this phosphorylated region and targets the protein for destruction by ubiquitination. Binding of extracellular WNT ligands to frizzled receptors located on the cell surface recruits an intracellular, membrane bound complex of low-density lipoprotein receptor related protein 6 (LRP6) and dishevelled (Dvl). This membrane bound complex recruits axin and GSK-3β, thereby preventing the phosphorylation of β-catenin and its associated proteosomal degradation (MacDonald et al

2009). The stabilised β-catenin is now able to translocate to the nucleus and bind to TCF/LEF1 transcription factors. These transcription factors have been found to up regulate HIF-2α, EGFR, c-MYC, and cyclinD1 expression as well as EMT transcription factors SNAIL, SLUG, and TWIST, thereby driving the EMT program (Liu et al 2016).

Most commonly, β-catenin mediated EMT in cancer is triggered by mutations in one or more members of the destruction complex, rendering it ineffective in the ubiquitination of β-catenin. Mutations in β-catenin itself can also be present, making its destruction more difficult, or entirely ineffective (Morin et al 2016). However, β-catenin can be stabilised by other signalling pathways, irrespective WNT signalling or mutations. The EMT transcription factor SNAIL has also been shown to directly bind to β-catenin during EMT, thereby stabilising it and preventing its degradation by GSK-3β. The β-catenin/TCF/LEF complex can then upregulate SNAIL in a positive feedback loop, further promoting EMT (Stemmer et al 2008). IκB kinases (IKKs), the primary regulators of NF-κB, and extracellular signal-regulated kinase (ERK1/2), a downstream kinase in growth factor signalling, have also both been reported to inhibit GSK-3β, promoting the stabilisation of β-catenin (Yamaguchi et al 2012). Other intracellular signalling molecules such as integrin linked kinase (ILK) and PI3K activate AKT in response to TGF-β and other stimuli, thereby inactivating GSK-3β and promoting the stabilisation of β-catenin independently of external WNT signalling (Medici et al 2008). These findings outline how central β-catenin is in the EMT program and how integral it is to a number of other initiating signalling pathways.

In addition to cadherins, the expression and localisation of tight junctions, adherence junctions, and desmosomes at lateral surfaces are also modulated under the EMT program. Upon the initiation of the process, zonula occluden-1 (ZO-1), an important scaffold protein in cell junction formation, is frequently relocalised and/or degraded (Foroni et al 2012). In type 1 and 2 EMT, the downregulation and/or delocalisation of ZO-1 destabilises the

junctional proteins, particularly occludin and claudin, resulting in downregulated cell-cell adherence and subsequent cell migration. However, in type 3 EMT associated with cancer, the role of tight junctions and other junctional proteins is far more complex. While it is true that in the vast majority of human cancers tight junctions are dysregulated, they are not always downregulated, nor are they always localised in the correct places. In fact, some cancers have presented with increased levels of tight junction proteins, with a poor prognosis documented as a result (Latorre et al 2006).

Integrin composition, in terms of the expression of α/β subunits, is also altered during EMT to adapt to the changes in ECM composition and to mediate cell migration (Li et al 2003). An example of this is the upregulation of the integrin subunit α5. A common biomarker of EMT, its expression is regulated by TWIST1 and is documented to be upregulated in all three EMT biological groups promoting cell migration (Nam et al 2015). In type 1 EMT during development, the expression of fibronectin binding integrin α5β1 is upregulated (Davidson et al 2006). The α5 integrin has also been documented to be increased in type 2 EMT seen in kidney fibrosis experiments (White et al 2007) and associated with increased migration and invasion in HCC (Nejjari et al 2002).

The binding to fibronectin via integrins has also been shown to initiate EMT. Furthermore, the initiation of EMT causes the secretion of fibronectin as part of the remodelling of the ECM. This positive feedback mechanism can be found in all three types of EMT (Park & Schwarzbauer 2014). In tumour initiation and progression, the increased expression of fibronectin is described as a cause and result of the process, with elevated levels correlating with the severity the disease. As a result, fibronectin is recognised as a biomarker for EMT and associated cancer progression (Ioachim et al 2002).

During EMT, cells change the composition of their intermediate filaments to mediate changes in cell shape and morphology. Epithelial cells classically produce type I and II

cytokeratin filaments which are well suited to maintaining their epithelial phenotype by promoting the formation of adherence junctions and directing E-cadherin to the cell membrane (Toivola et al 2005). During the transition to a mesenchymal phenotype, cells downregulate the epithelial associated cytokeratin and upregulate vimentin, a type III intermediate filament (Huang et al 2012). Vimentin has been reported to be involved in signal transduction. Upregulation of the intermediate filament has been shown to induce ERK1/2 activation, as well as upregulate SLUG expression thereby progressing the EMT phenotype (Mendez et al 2010). Vimentin is thought to facilitate a more dynamic cell structure that allows cancer cells to survive the mechanical stresses of the tumour microenvironment. This dynamic cell structure also facilitates migration, intravasation, and extravasation though a changing and challenging environment (Liu et al 2015). As vimentin is almost exclusively associated with mesenchymal cells it has become a common hallmark of the transition.

1.3.2 Transcriptional regulation of EMT

The initiation of EMT is orchestrated at the molecular level by an array of transcription factors (EMT-TFs). These regulators interact with epigenetic components which repress epithelial gene expression and promote a mesenchymal phenotype (Puisieux et al 2014). Almost all of the phenotypic changes associated with the transition are mediated by SNAIL, TWIST, and ZEB1/2, although the importance of other transcription factors such as FOXC2 and homeobox goosecoid are only just being realised. The changes in gene expression induced by these transcription factors relies considerably on the extracellular ligands and signal transduction pathways involved. Although, during cancer they can be significantly influenced by the mutations and epigenetic changes driving the malignancy (Peinado et al 2007)

The SNAIL family of transcription factors consists of three members SNAIL -1, -2, and -3. Although only SNAIL1 and SNAIL2 (SLUG) have been implicated in the initiation of EMT. Both SNAIL and SLUG are able to promote and repress the transcription of a number of EMT related genes via binding though their carboxy-terminal zinc-finger domains to E-box DNA sequences present in the proximal promotor region of these genes (Peinado et al 2007). Binding in this way recruits the polycomb repressive complex 2 (PRC2) consisting of methyltransferases (EZH2, SUV39H1), co-repressors (SIN3A), the lys-specific demethylase 1 (LSD1), and histone deacetylases. This complex is able to initiate histone modifications and produce bivalent chromatin (Herranz et al 2008). Bivalent chromatin are segments of DNA, bound to histone proteins, that have both repressing and activating epigenetic regulators in the same region. This acts as an epigenetic switch that is able to both repress and activate expression of EMT genes. Bivalent chromatin is crucial in developing and differentiating pluripotent embryonic stem cells and is thought to contribute to the revisable nature of the EMT program (Bernstein et al 2006).

SNAIL and SLUG are often defined by their ability to initiate the EMT program by epigenetically repressing E-cadherin (Lin et al 2014). However, they have also been shown to regulate a number of other aspects of the EMT phenotype. In a further attempt to regulate cellular adhesion, SNAIL family members are able to bind and repress the promotors of claudin-1, occludin, cytokeratin and ZO-1 (Lin et al 2014). Cell polarity is also decreased due to the suppression of crumbs3, PALS1 and PATJ by SNAIL and SLUG (Lamouille et al 2014). Cell proliferation is increased by these transcription factors as they supress cyclin D proteins, cyclin-dependent kinase 4 (CDK4) and promote WNT5a and LEF1 (Peiro et al 2006). Suppression of caspases, DNA fragmentation factor, and Bcl-interacting death agonist by SNAIL and SLUG significantly increase the resistance to apoptosis during EMT (Nieto 2009). While the up-regulation of fibronectin, N-cadherin, and

vimentin, as well as MMP-2 and -9 by SNAIL and SLUG drive the mesenchymal phenotype and induce cell migration and invasion (Zeisberg et al 2009). Both SNAIL and SLUG have also been documented to induce the transcription of other EMT transcription factors ZEB1/2 and TWIST, further promoting the initiation of transition (Lamouille et al 2014).

SNAIL is regulated post-translationally by glycogen synthase kinase-3β (GSK-3β). Phosphorylation of SNAIL by GSK-3β on Serine 97 and Serine 101 amino acids cause a change in the subcellular localisation of the transcription factor, promoting its nuclear export to the cytoplasm, thereby diminishing its transcriptional activity. Further phosphorylation of SNAIL on other serine rich residues causes the ubiquitination and subsequent proteolytic destruction of the transcription factor (Zhou et al 2004). In response to TGF-β, growth factors, or oncogenic activity, the signal transduction pathways WNT, PI3K–AKT, NOTCH, and NF-κB through receptor tyrosine kinases have all been shown to prevent phosphorylation of SNAIL by GSK-3β thereby preserving its nuclear location and associated transcriptional activity (Yook et al 2006, Sahlgren et al 2008, Wu et al 2009).

TWIST is a member of the a basic helix-loop-helix transcription factor family and a master regulator of EMT. The EMT-TF is most frequently upregulated during embryonic morphogenesis influencing cell differentiation and lineage determination (Yu et al 2008). Postnatally its expression is mainly associated with wound healing, fibrosis, and with cancer metastasis (Kida et al 2007, Yang et al 2004). The N-terminal region of TWIST shares a conserved basic amino region which binds to E-box DNA sequences present in the proximal promotor region of EMT genes, in a similar way to SNAIL (Jones 2004). Binding to these regions by TWIST initiates the recruitment of histone modifying SETD8 methyltransferase, which is linked to repression or promotion of EMT related genes (Yang et al 2012). It is thought that TWIST is involved in regulating up to 500 genes in EMT and development (Margetts et al 2012). TWIST has been shown to downregulate E-cadherin,

claudins, occludin, and other adherence proteins such as desmoplaskin and plakoglobin, whilst upregulating N-cadherin, vimentin, fibronectin, SPARC, and the α5 integrin subunit (Lamouille et al 2014). Stabilisation and subsequent nuclear import of TWIST is required to enable its transcription activity. MAPK signalling as a result of TGF-β or oncogenic activity causes p38, JNK and ERK1/2 to phosphorylate the Serine 68 amino acid in TWIST, thereby stabilizing the transcription factor and protecting it from ubiquitin-mediated degradation (Hong et al 2011). TWIST has also been shown to be upregulated by mechanical stress and the hypoxic conditions associated with cancer (Farge 2003). Inducing mechanical stress in *Drosophila melanogaster* epithelia increases TWIST expression, a process that is thought be modulated by β-catenin. It has been proposed that the mechanical restrains associated with cancer could also induce TWIST expression by a similar mechanism (Farge 2003). Hypoxia-inducible factor-1alpha (HIF-1α) is upregulated during the anaerobic conditions of some cancers and has been shown to directly bind to the TWIST hypoxia-response element (HRE) in the TWIST proximal promoter, thereby upregulating its expression (Yang et al 2008).

ZEB1 and 2 are important regulatory EMT transcription factors able to activate and repress associated genes via E-box binding (Gregory et al 2008). Their DNA binding capacity is mediated by the presence of two zinc finger domains that enable attachment to the promotor region of a number of genes, such as E-cadherin, crumbs3 and PATJ (Aigner et al 2007). Once bound ZEB1/2 are able to recruit transcriptional co-repressors and co-activators, thereby regulating EMT gene transcription (Liu et al 2008). During cancer progression, the overexpression of ZEB1/2 is most commonly associated with the decrease of E-cadherin (Sanchez-Tillo et al 2010). Binding of ZEB1/2 to the E-box promotor region of E-cadherin, recruits CtBP transcriptional co-repressors and chromatin-remodelling protein BRG1, thus preventing the transcription of the gene (Shi et al 2003). ZEB1/2 are also able

to repress a number of cell polarity genes such as crumbs3, HUGL2 and PATJ and tight junction associated scaffold ZO-1 further promoting the mesenchymal phenotype (Aigner et al 2007).

Recruiting and binding PCAF and SMAD proteins enable ZEB1/2 to become transcriptional activators, enabling transcription activity of TGF-β-responsive genes N-cadherin and MMPs (Postigo 2003). They have also been shown to recruit lys-specific demethylase 1 (LSD1) which is involved in the epigenetic histone demethylation in EMT and developmental processes (Wang et al 2007). The extent of which ZEB1/2 regulated EMT and cancer progression is still under investigation, but its documented involvement seems to be increasing. Experimental evidence has suggested that in certain breast cancer cell lines, ZEB1/2 are involved in repressing over 200 genes, whilst activating more than 30, most of which are key regulators of EMT, cellular adhesion, and cell-cell contact (Zhang et al 2015).

There has been an emergence in the literature of the importance of the role of less conventional EMT inducing transcription factors such as the forkhead box (FOX), goosecoid homeobox (GSC) and SRY box (SOX) (Lamouille et al 2014). In a similar way to the well-established EMT-TFs they are able to bind and repress or activate EMT related genes, both independently and in conjunction with SNAIL, TWIST, and ZEB1/2. Although their exact role in the transition is still being realised, their presence has been considered a hallmark of the program (Lamouille et al 2014).

1.3.3 MicroRNA meditation in the initiation and progression of EMT

Micro-RNAs are short, non-coding RNA strands capable of post-transcriptionally regulating gene expression by complimentary binding to target mRNA transcripts, preventing their translation or promoting their degradation (Iorio & Croce 2017). Present in virtually all cell

types, these regulatory nucleotides are thought to be master regulators in both normal cellular physiology and in diseases such as Alzheimer's, osteoporosis, diabetes, and cancer (Abba et al 2016).

Figure 1.6: miRNA bio-genesis. A diagram outlining the biogenesis and function of miRNAs. The process begins in the nucleus where the polyadenylated primary miRNA transcript (pri-miRNA) is transcribed by RNA-polymerase II-dependent (RNAPII). This transcript is processed by Drosha, a RNase III endonuclease, and its co-factor Dgcr8. This creates a smaller stem-looped structure known as precursor miRNA (pre-miRNA). Exportin-5 transports pre-miRNAs out of the nucleus and into the cytosol where Dicer, a RNase III enzyme further modifies them to create the mature miRNA. The mature miRNA associates with the RISC complex (miRNA-induced silencing complex) and binds to the target mRNA sequence via complementary base pair binding. The binding of the miRNA-RISC complex induces translational repression and/or mRNA degradation (Lin and Gregory 2015).

During EMT, the molecular reprogramming and phenotypic changes associated with the transition are thought to be significantly regulated by miRNAs (Sassen et al 2008). It has

been estimated that 30% of all genes and almost every genetic pathway involved in EMT is under some form of miRNA control, the regulation of miRNAs that target EMT transcription factors is thought to be key in the initiation and progression of the process (Yan et al 2013). The complex interplay between microRNAs and transcription factors means that they are able to regulate each other, forming both positive and negative feedback loops that can either promote or inhibit the progression of EMT. For example, ZEB1 is inhibited by miR-200, but the increased expression of ZEB1 during EMT initiation causes the decrease of these miRNAs in a double negative feedback loop (Lamouille et al 2014).

Figure 1.7: ZEB1/miR-200 Double-Negative Feedback Loop. A diagram which represents the double negative feedback loop between ZEB1 and the miRNA 200 family. In epithelial cells, the epithelial phenotype is maintained by high expression of miR-200 which inhibits ZEB1, a key regulator of EMT progression. Upon EMT initiation, in this example via TGF-β induction, ZEB1 expression is increased causing cells to transition toward a mesenchymal phenotype. ZEB1 represses the expression of the miR-200 family by binding to ZEB-type E-Boxes within the miR-200b∼200a∼429 promoter. Together this system forms a double negative feedback loop, whereby the either the epithelial or mesenchymal state is maintained depending on the relative levels of ZEB1 and miR-200 (Ocana and Nieto 2008)

A large number of regulatory miRNAs are downregulated during cancer progression, resulting in a decrease in their inhibitory effect on the EMT program. As a result, cancer cells are able to obtain the EMT related hallmarks that enable increased proliferation, invasion and metastasis (Sassen et al 2008).

Figure 1.8: Regulation of EMT by miRNAs. Regulation of epithelial mesenchymal transition (EMT) by miRNAs. Green arrows represent the upregulation/activation and the red lines indicate the inhibition or transcriptional repression. Many miRNAs, such as miR-29a, b, c, miR-200c, miR-34a, regulate EMT by suppressing EMT-related transcription factors and signalling pathways. These miRNAs are commonly downregulated during cancer progression, resulting in the initiation of EMT (Chi and Zhou 2016).

1.3.4 Hybrid EMT

Existing evidence for EMT suggests that cells either adopt an epithelial or a mesenchymal phenotype, possessing exclusive markers unique to either state (Zeisberg et al 2009). Recent research has suggested that this transition is not a binary process, and in fact it is possible for cells to express and display co-expression of epithelial and mesenchymal markers, in a process termed partial or hybrid EMT (Grigore et al 2016). In an apparent contradictory notion, it appears that cells expressing a hybrid EMT phenotype have a 50 times higher tumour-initiating and metastatic potential than those in a complete mesenchymal phenotype (Jolly et al 2015).

Interestingly, cells that possess this hybrid EMT phenotype display increased stem cell properties and markers, such as CD44. Interestingly, the increase in these markers appears to be greater in hybrid EMT cells than cells that display a complete mesenchymal transition. Ruscetti et al provided evidence of this by separating hybrid EMT cells from complete EMT cells in a prostate cancer mouse model. The hybrid EMT cells displayed higher stem cell properties and tumour initiating potential compared to complete EMT cells (Ruscetti et al 2015). Jolly et al, in combination with Ombrato and Malanchi, furthered this work and created the figure below, outlining the stem-ness window model during hybrid EMT (Jolly et al 2015; Ombrato and Malanchi 2014)

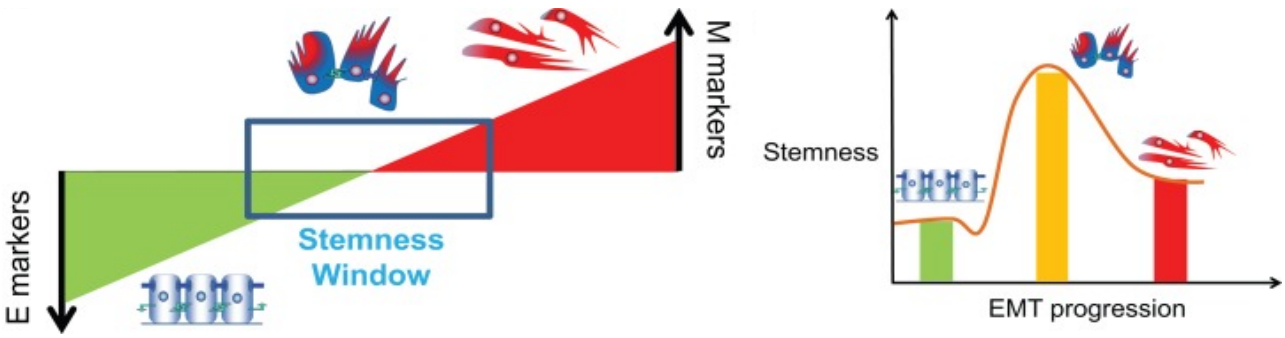

Figure 1.9: Stemness window of hybrid EMT. A diagram representing the 'EMT gradient' where partial/hybrid EMT is associated with stemness. Ombrato and Malanchi propose a model whereby stemness is maintained in a window between epithelial and mesenchymal states. This window represents cells which have increased stem cell markers and significantly higher tumor-initiating potential.

The increase in stemness associated with hybrid EMT is thought to promote chemoresistance and immune tolerance, creating a selective advantage during chemotherapy treatments (Chouaib et al 2014). As a result, it is thought that hybrid EMT cells may be selected for during chemotherapy.

A major marker of stemness associated with hybrid EMT is the upregulation of NOTCH/JAGGED1 signalling. Although not unique to stem cells/cancer stem cells,

NOTCH/JAGGED1 signalling features heavily in embryonic stem cell development as it contributes to stem cell maintenance, cell differentiation, and cellular homeostasis (Koch et al 2013). NOTCH/JAGGED1 signalling has also been shown to upregulate stem cell markers during HCC (Govaere et al 2014). Cell to cell communication between hybrid EMT cells by NOTCH/JAGGED1 signalling is thought to stabilise the hybrid phenotype and can induce the phenotype in adjacent cells via lateral induction. Hybrid EMT cells connecting this way can form clusters and exhibit collective cell migration (Jolly et al 2015). Hybrid EMT-induced collective migration in the form of multicellular aggregates were found to be more efficient at extravasation and display sufficient plasticity to enable metastatic colonisation at secondary sites (Bednarz-Knoll et al 2012). Ultimately, this would contribute to the significantly higher tumour-initiating and metastatic potential observed by these cells.

The idea of partial EMT conserves the notion that tight junctional proteins, often downregulated during the process, are not always silenced during EMT and cancer. In fact, a growing body of evidence continues to implicate tight junction proteins in the progression of the disease and in the initiation of EMT (Martin et al 2011). This highlights the importance of research into understanding the mechanisms surrounding their role in initiating EMT and ultimately metastasis.

1.4 Tight junctions

Tight junctions are a group of protein constituents that form junctional complexes responsible for the production of comprehensive sheets of polarised epithelial and endothelial cells. They act as paracellular barriers that regulate the diffusion of intercellular solutes and maintain the apical/basolateral plasma membrane domains (Itoh & Bissell 2003). Tight junctions are comprised of transmembrane and peripheral membrane proteins that interact with one another and connect the complex to a scaffold of intracellular proteins.

The scaffold proteins provide the link between transmembrane proteins and the cytoskeleton, whilst connecting and influencing many signal transduction pathways. The transmembrane and peripheral membrane proteins are able to form intercellular junctional complexes that act as adhesive contacts between adjacent cells (Giepmans & van IJzendoorn 2009). Tight junctions are vital in the formation of many tissues, particularly epithelial. Epithelial cells make up tissues, and line the majority of organs, ducts and lobules. Tight junctions present between epithelial cells create an effective seal producing selectively permeable barriers between body compartments and regulate the passage of solutes (Gunzel & Yu 2013). The presence of tight junctions dictates the boundaries of the apical and basolateral membrane domains of the cell, thereby creating a fence function regulating intramembrane diffusion and passage of proteins and macromolecules (Trimble & Grinstein 2015).

Tight junctions were conventionally viewed as static, mechanical structures used to maintain paracellular permeability and cell-to-cell contact. However, tight junctions are known to be highly dynamic structures involved in regulating intracellular polarity complexes, and directly targeting and modulating gene transcription relating to cellular proliferation and differentiation (González-Mariscal et al 2008)

Disruption of tight junctions is thought to directly initiate a variety of pathological disorders and cancers. Viruses, bacteria, and other pathogens often target junctional complexes, for example Hepatitis C virus and Adenovirus exploit tight junction proteins to gain entry to cells. The inflammatory conditions induced by these viruses have been observed to disrupt cellular polarity, increasing the infection and transmission of the virus as a result (Mee et al 2009).

More than 40 proteins have been identified within the tight junction complex. These can be divided into three major categories (Latorre et al. 2006):

Transmembrane proteins

Tight junctional transmembrane proteins include the tight junction–associated MARVEL protein (TAMP) family (occludin, tricellulin and marvelD3), the claudin family 1-24, and Junctional Adhesion Molecules (JAMs). All transmembrane proteins span the cell membrane and are anchored to the cytoskeleton via cytoplasmic plaques/scaffold proteins (Latorre et al. 2006).

Cytoplasmic plaques/scaffold proteins

Cytoplasmic plaques/scaffold proteins include Zonula Occluden proteins (ZO-1, ZO-2, and ZO-3), PATJ, MUPP1, cingulin and the angiomotin family. These proteins are responsible for linking tight junctional proteins to the cytoskeleton and are involved in regulating numerous signal transduction pathways (Guillemot et al. 2008)

Associated/regulatory proteins

Associated/regulatory proteins include such families as the RAB and Rho subfamily along with important polarity complexes such as crumbs and PAR. They are often targets involved in scaffold protein signal transduction (Anderson & Van itallie 2009)

1.4.1 Claudins: Distribution and Function

Claudins are tight junctional membrane proteins that form paracellular barriers and pores which regulate the selective permeability to small ions and solutes. They were first identified in 1998 by Mikio Furuse and Shoichiro Tsukita in purified junctional fractions of chicken liver (Furuse et al 1998). Furuse (1999) later demonstrated claudins to be the major structural component of the tight junction by overexpressing them in fibroblasts that ordinarily do not produce tight junctions. As a result, strands of fibroblasts formed with junctional complexes that resembled tight junctions. Since then a multitude of studies focusing on overexpression or silencing of claudins has provided evidence of their role in forming both paracellular

barriers and pores within the tight junction and determining the permeability properties of epithelial and endothelial cells (Oliveira and Morgado-Diaz 2007)

The human claudin family to date is comprised of 27 members, which exhibit complex tissue-specific patterns of expression. They range from 20 to 34 kDa in size, with most around 22 to 24 kDa. Claudins are expressed in all known epithelial tissues in a variable tissue-specific manner of expression. Expression of different combinations of claudins can give rise to differences in the sealing properties of tight junctions and ultimately the permeability properties of tissues. The differing requirements of selective permeability in tissues means multiple different claudins are often co-expressed to achieve this (Capaldo and Nusrat 2015).

Tissue	**Claudin**	**Reference**
Stomach	3, 4, 5, 12, 18, 23	(Rahner et al. 2001) (Hewitt et al. 2006) (Katoh 2003)
Intestine	1, 2, 3, 4, 5, 7, 8, 10, 12, 15, 18, 20, 21, 23	(Fujita et al. 2006) (Holmes et al. 2006)
Liver	1 (Tight junctions of hepatocytes, lateral membrane of bile duct cholangiocytes) 2 (Tight junctions of hepatocytes. Levels increase from periportal to pericentral hepatocytes) 3 (Expressed in hepatocyte and cholangiocyte tight junctions) 5 (Expressed in endothelial cells of the portal veins and hepatic arteries) 6	(Hadj-Rabia et al. 2004) (Rahner et al. 2001) (Zheng et al. 2007) (Jakab et al. 2010)

Tissue	Claudin	Reference
	7 (Expressed in the basolateral membrane of cholangiocytes but not in hepatocytes) 8, 9, 14	
Gall bladder	(Strongly expressed) 1, 2, 3 ,4, 10 (Weakly expressed) 7, 8	(Laurila et al. 2007)
Respiratory tract	(Proximal) 1, 3, 4, 5, 7, 10 (Confined to Clara cells), 18 (distal) 3, 4, 5, 7, 8, 15, 18	(Coyne et al. 2003) (Moldvay et al. 2007) (Wang et al. 2003)
Epidermis	1, 4, 7 > 3, 5, 8, 11, 12, 17	(Brandner et al. 2002)
Eye	(Cornea and conjunctiva)1, 4, 7 (Conjunctiva) 10	(Yoshida et al. 2009)
Salivary gland	10 > 1, 2, 3, 4, 7, 8, 12	(Maria et al. 2008)
Mammary gland	1, 2, 3, 4, 5, 7, 8, 15, 16	(Markov et al. 2012) (Jakab et al. 2008)
Taste bud	4, 6, 7, 8	(Michlig et al. 2007)
Exocrine pancreas	1, 2, 3, 4, 5, 7	(D'Souza et al. 2009)
Retinal pigment epithelium	19 > 3, 10	(Xu et al 2005)
Choroid plexus	1, 2, 5, 11	(Lippoldt et al. 2007) (Morita et al. 1999)
Cochlea	(Organ of Corti & striae vascularis marginal cells); 1, 2, 3, 8, 9, 10, 12, 14, 18 (Striae vascularis basal cells) 11	(Kitajiri et al. 2004)
Ovary	1, 5	(Zhu et al. 2007)
Prostate	1, 3, 4, 5, 7, 8, 10	(Sakai et al. 2007)
Epididymis	4, 7 > 2, 5, 10	(Dube et al. 2007)

Tissue	Claudin	Reference
Seminiferous tubule	3, 5, 11	(Morita et al. 1999) (Morrow et al. 2010)
Urinary bladder	4, 8, 12	(Acharya et al. 2004)

Table 1.1: Normal tissue specific claudin expression. The table outlines the expression patterns in of claudin family members in normal tissue development.

1.4.1.2 Claudin structure

The structure of claudins within the protein family is highly conserved throughout the animal kingdom, showing little change between species (Simske 2013). Claudins along with the tight junction–associated MARVEL protein (TAMP) family (occludin, tricellulin and MARV3D) are all tetraspanin proteins that share the same topology of four transmembrane domains, two extracellular domains, and cytoplasmic N- and C-termini. Although similar in structure, no members of the claudin family show any sequence homology to occludin (Koval 2013). The two extracellular domains (EL1, EL2) are formed as the protein chain crosses the cell membrane four times, thereby simultaneously creating the four transmembrane domains (TM1-4). The first extracellular domain forms a loop of approximately 60 amino acids that mediates paracellular ion selectivity. Motifs in this first extracellular loop create a region important for Hepatitis C virus (HCV) entry. The first extracellular domain also contains two highly conserved cysteine residues that from an intramolecular disulphide bond thought to improve the stability of the protein chain. The second extracellular domain also forms a shorter loop of approximately 24 amino acids and is thought to aid in claudin oligomerization and Clostridium perfringens enterotoxin (CPE) binding. The cytoplasmic carboxy-terminal typically ranges from 21 to 63 amino acids in

length but in the case of claudin-23 can be as large as 106 amino acids (Lal-Nag & Morin 2009). The cytoplasmic N-terminal region however is much shorter, usually around 7 amino acids in length, and to date appears not to interfere with claudin assembly or function (Koval 2013). Figure 1.10 shows the generalised structure of the claudin monomer.

Figure 1.10: Schematic representation of the claudin monomer. The diagram illustrates the conserved structural features present in all claudin monomers with some known interactions labelled. EL1 and EL2 represent the two extracellular loops 1 and 2, respectively. EL1 is known to be important in regulating paracellular ion selectivity and EL2 is involved in claudin-claudin oligomerization. The four transmembrane domains are labelled TM1 to TM4. Regions which are important for Hepatitis C virus (HCV) entry and Clostridium perfringens enterotoxin (CPE) binding are shown (Lal-Nag and Morin 2009).

The carboxy-terminal of claudins contains a PDZ binding domain that enables signal transduction to PDZ containing cytoplasmic scaffolding proteins such as ZO-1, ZO-2, ZO-3, multi-PDZ domain protein (MUPP)-1 and PALS-1 associated TJ protein (PATJ). This region shows the greatest amount of sequence and size heterogeneity despite being the most highly conserved region within the claudin family.

1.4.1.3 Claudin-Claudin interactions

Claudins are known to display complex tissue-specific patterns of expression. The claudin composition of any given tissue dictates the paracellular permeability that will be variable to compounds of different molecular weights and charges. Intermolecular Claudin-Claudin interactions are responsible for regulating the function of the tight junction. Claudin isoforms have the potential to intermix, producing variable tight junction strands. The interactions between different claudin isoforms may provide a mechanism of selective barrier permeability (Findley & Koval 2009).

Claudins have been observed to interact in two orthogonal orientations similar to that of the adherence junctional proteins cadherins. As a result, claudins have adopted the same nomenclature of that of cadherin interactions. Claudin molecules which interact with other claudins laterally in same plane of the plasma membrane are termed cis-interactions, whereas claudins that interact with other claudins on opposing plasma membranes are termed trans-interactions. Claudins can also form homo and heterophilic interactions with other claudin isoforms as shown in figure 1.11 (Krause et al 2008).

Figure 1.11: Example homophilic and heterophilic cis- and trans-interaction possibilities of claudin-1 and -3. The diagrams represent possible interactions between claudin family members, the example given here involved claudin-1 and claudin-3. The upper table represents tight junctional strands consisting of (A) homophilic *cis*- and *trans*-interactions, (B) heterophilic *trans*-interaction and homophilic *cis*-interaction (C) homophilic *trans*-interaction and heterophilic *cis*-interaction as well as (D) heterophilic *cis*- and *trans*-interactions. The lower part of the diagram illustrates how individual claudin monomers can interact via homo/heterophilic and cis/trans interactions (Krause et al 2008).

1.4.2 Occludin

Occludin is a 522 amino acid, ~65 kDa integral membrane tight junction protein, first discovered in avian tissue by Furuse et al in 1993. It was confirmed as the first tetraspan tight junction protein to be identified and is present in the tight junctions of epithelial and endothelial cells, but not fibroblasts (Cummins 2012). Two isoforms of occludin exist that are formed via alternative mRNA splicing, however no difference has been observed in their

function or tissue distribution (Muresan et al 2000).

As a tetraspan tight junctional protein, occludin shares a similar structure to claudin. They both consist of two extracellular domains, four transmembrane domains, N- and C-termini and a short cytoplasmic loop. Unlike claudin, the two extracellular domains are almost identical in size; EL1 and EL2 are approximately 46 and 48 amino acids long. Occludin also contains substantially larger cytoplasmic C-termini, which is represented by a significantly larger molecular mass compared to claudin (Morrow et al 2010). The extended C-terminus is essential in signal transduction involved in facilitating occludin dimerization and interactions with cytoplasmic proteins such as ZO-1, which mediates occludins intracellular trafficking to the tight junction (Cummins 2012). Localisation of occludins within the tight junction of both epithelial and endothelial cells are also depended upon is phosphorylation. Phosphorylated occludin is intergraded into the tight junction complex whereas non-phosphorylated occludin is located toward the basolateral membrane and cytoplasmic vesicles (Wong 1997).

The C-terminal domain of occludin has been identified as regulator of signal transduction. Osanai et al (2006) has demonstrated that this domain is able to receive and transmit cell survival signals. Loss of occludin during carcinogenesis is common in many cell types and often correlates to increased invasion and metastasis. Overexpression of occludin in several cancer cell lines has resulted in an upregulation of apoptotic factors via an increased gene expression of apoptotic pathways. As a result, overexpression of occludin in these cell lines presents a reduction in tumor progression and invasion. This suggests that occludin functions not only as a structural constituent of the tight junction, but a regulator of signal transduction of a number of pathways.

The role of occludin in the tight junction is complex; it is thought to function as a paracellular barrier and participate in tight junction stability (Cummins 2012). However,

Saitou et al (2000) demonstrated that genetically altered occludin −/− mice produced tight junctions that did not appear to be affected morphologically. The barrier function of the intestinal epithelium was also examined electrophysiologically and also appeared to be normal, however, the mice displayed may other defects such as chronic inflammation, hyperplasia of the gastric epithelium, calcification in the brain, and thinning of several bone structures. The data therefore indicated that occludin is likely to regulate the tight junction rather than uphold the structure and assembly itself (Saitou et al 2000).

1.4.3 Tricellulin

Tricellulin, otherwise known as marvelD2, is a tetraspan tight junction protein uniquely concentrated at tricellular contacts in epithelial cellular sheets. They consist of two extracellular domains, four transmembrane domains, N- and C-termini, and a short cytoplasmic loop. Four isoforms of tricellulin can be found in humans ranging from 51-64 kDa via alternative splicing of the human tricellulin gene, TRIC. The structure of tricellulin resembles that of occludin with approximately 133 amino acids conserved between them, predominantly at the C-terminus, which accounts for 32% homology (Mariano et al 2011).

Tricellulin knockouts in mouse Eph4 epithelial clones drastically compromised tight junction organization. An increase in paracellular permeability, and a decrease in transepithelial electrical resistance, were observed, suggesting that tricellulin is directly involved in barrier formation within the tight junction (Ikenouchi et al 2005).

Tricellulin was reported to relocate from the tricellular to the bicellular tight junction in occludin knockdown MDCK II cells, in part restoring the phenotype of normal occludin expression. This suggests that tricellulin may compensate, to some degree for some of occludins function (Ikenouchi et al 2008).

Mutations in a tricellulin isoform tricellulin-a (TRIC-a) have been observed to cause

nonsyndromic deafness in humans. This is particularly interesting as only the hearing is affected given the widespread tissue distribution of tricellulin in human epithelial cells (Riazuddin et al 2006)

1.4.4 Junctional Adhesion Molecules (JAM)

Junctional adhesion molecules JAM-A, -B and -C are members of the immunoglobulin (Ig)-like glycoproteins involved in cellular adhesion and tight junction formation. All three JAM molecules consist of a single peptide approximately 30-40ka, with two Ig-like domains, a transmembrane domain and a cytoplasmic tail (Bazzoni 2003). The intracellular cytoplasmic tail contains a PDZ domain-binding sequence, similar to other tight junction proteins. This domain mediates binding to ZO-1, AF-6, MUPP1 and the cell polarity proteins PAR-3 and -6. In this way they are thought to be involved in tight junction and cell polarity formation. JAM-A, JAM-B, and JAM-C can all dimerise via homophilic binding forming junctions between adjacent cells. They have also displayed the capacity to bind to leukocytes and platelets via interactions with integrins, and other JAM molecules. Therefore, JAMs are recognised to have two main purposes; to mediate cell to cell adhesion and tight junction formation, and to mediate leukocyte-endothelial cell interactions in immune responses (Ebnet et al 2004).

1.4.5 Zonula Occludens

Zonula Occludens, or ZO proteins, as they are often referred to, are scaffold proteins associated with intercellular junctions. The first TJ-associated protein to be identified was ZO-1 (220kDa), using a specific monoclonal antibody raised against a preparation of liver membranes. ZO-2 (160 kDa) and ZO-3 (130 kDa) were later identified as proteins that co-immunoprecipitated with ZO-1 (Guillemot et al. 2008). ZO proteins are comprised of three

variants ZO-1, ZO-2, and ZO-3 which belong to the MAGUK (membrane-associated guanylate kinase-like homologs) family. They contain PDZ domains followed by SH3 and GuK regions with a carboxyl end that features an acidic domain and proline-rich region. These characteristics are common to all MAGUK proteins (Bauer et al. 2010). Figure 1.12 shows a number of proteins that able to bind to ZO-1, -2, and -3. Although they share the same basic structure, sequence variation changes the binding properties of these proteins which ultimately gives them differing characteristics.

Figure 1.12: Interaction of proteins with Zonula Occludens, ZO-1, -2, and -3. The diagram illustrates interactions between zonula occludens (ZO)-1, -2, and -3 and tight junctional/cytoskeleton proteins. ZO proteins contain 3 PDZ (post-synaptic density 95/Drosophila disc large/zona-occludens) domains, a SH3 (Src homology-3) domain and a GUK (region of homology to guanylate kinase). Several junctional and cytoskeleton proteins interact with ZO proteins via these domains. In this way ZO proteins form a scaffold linking these junctional proteins to the actin cytoskeleton (Lee 2015).

The multiple protein binding domains featured in ZO-1, -2 and -3, create and maintain multi-molecular complexes at subcellular sites that are usually clustered at the tight junction. They comprise of cell adhesion molecules, receptors, cytoskeletal proteins, ion channels, transcription factors, and signalling compounds. All ZO proteins directly bind to actin filaments, creating a scaffold and producing the structural basis of multi protein complexes that link junctional proteins to the cytoskeleton. ZO-1 and -2 bind to the actin skeleton via

the terminal –COOH regions, whereas ZO-3 binds through a domain located in the N-terminal region. ZO proteins also possess the ability to indirectly bind to the actin skeleton via a number of actin binding proteins such as α-catenin, cortactin, and cingulin (González-Mariscal et al 2008).

Evidence has proposed ZO proteins are not only involved in structural barrier mechanisms but participate in signal transduction and transcriptional modulation. For example, ZONAB has a high affinity for the Src-homology-3 (SH3) domain of ZO-1. However, if ZO-1 is downregulated or missocialised, ZONAB translocated to the nucleus and promotes cell proliferation via the upregulation of cyclin D1 (Pozzi & Zent 2010).

ZO proteins are known to interact directly with a number of tight junctional transmembrane proteins such as occludin, claudins, JAM, and tricellulin (González-Mariscal et al 2008). Their role as a scaffolding protein allows them to interact with a number of molecules and receptors, thereby acting as an intermediate between extracellular proteins and intracellular signalling molecules. The ability of ZO proteins to cross talk to intracellular signalling pathways enables them to regulate gene transcription and cell proliferation in response to changes in cellular adhesion, intercellular permeability, and other changes to extracellular conditions. ZO proteins are known to influence transcriptions factors such as Fos, Jun, ZONAB, C/EBP and KyoT2, heat shock protein Apg-2, and cell cycle regulators such as cyclin D1 (González-Mariscal et al 2008).

1.5 Tight junctions in cancer

Tight junctions are conventionally known for their barrier forming and paracellular solute regulating roles (Trimble & Grinstein 2015). However, tight junctional complexes have been found to maintain cellular adhesion between epithelial cells and are important in maintaining the strict organisation of tissues. One of the initiating steps during cancer invasion and

metastasis is the disassociation of malignant cells from the primary tumour, and the penetration of the neighbouring vasculature. Therefore, tight junctions and associated adhesion must be moderated to enable cancer cells to overcome this barrier and subsequently metastasise (Martin & Jiang 2009).

During cancer progression, tight junctions can be modulated in a number of ways. The upregulation of growth factors and cytokines secreted by the tumour cells themselves or by inflammatory cells in the tumour stroma can cause a dysregulation of tight junctional constituents. Regulatory mechanisms such as EMT, which are frequently involved during cancer metastasis, can upregulate associated transcription factors causing epigenetic changes to tight junction constituent promoter regions (Ikenouchi et al 2003). Mutations present in the functional regions of tight junctional proteins can cause non-functional proteins, creating leaky barriers and reduced cellular adhesion (Runkle & Mu 2013). Other regulatory elements such as RhoGTPases are able to disrupt cellular polarity and prevent effective TJ formation (Gopalakrishnan et al 1998). All of these mechanisms can be exploited by cancer cells during metastasis in response to physiological and environment-specific requirements.

The extent in which tight junctions are involved in tumour progression is still unknown. While it is true that their barrier function must be controlled to mediate migration, it appears that tight junctions, in conjunction with their associated multiprotein structures, can regulate core cellular processes such as polarity, proliferation, and differentiation. Furthermore, it is becoming clear that tight junctions not only further the progression of cancer, but their dysregulation may orchestrate the processes required for oncogenesis (Shin et al 2006).

The dysregulation of tight junctions in human cancer and cancer cell lines is well documented. Both the upregulation and downregulation of tight junction constituents along

with their localisation and epigenetic regulation have all be implicated in the progression of the disease. The disruption of cell-cell adhesion does not always mean the downregulation of tight junctional proteins. The localisation, orientation, and possible modifications that take place in cancer can disrupt tight junctional proteins even if they are overexpressed. However, it appears the dysregulation of tight junctions and the effects on tumour progression as a result, appear to be cancer specific (Martin & Jiang 2009).

1.5.1 Bladder cancer

In bladder cancer, claudin-4 has been reported to be upregulated in well-differentiated carcinomas but subsequently downregulated in invasive/high-grade tumours. This is thought to be due to hypermethylation of the claudin-4 promotor region in these cancers. Boireau et al (2007) reported alterations in claudin-4 in 26/39 tumours examined, with abnormal cellular localisation of claudins -1, -4 and -7. Boireau et al (2007) also linked the downregulated expression of claudin-4 with an approximate 1-year survival rate in these patients.

1.5.2 Breast cancer

In breast cancer, claudin-1 has been described as a prognostic marker as it is frequently downregulated, associated with increased lymph node metastasis and short-term patient survival (Morohashi et al 2007). The expression of claudin-1 has also been documented to be undetectable in breast cancer cell lines MDA-MB-435 and MDA-MB-361, along with occludin and ZO-1 (Hoevel et al 2002). Interestingly, no genetic alterations in the promoter or coding sequences of claudin-1 have been identified in sporadic tumours and hereditary breast cancer patients, suggesting that the dysregulated expression of claudin-1 during breast cancer progression occurs as a result of epigenetic silencing or other regulatory

factors (Krämer et al 2000).

A comparative study investigated the expression of claudin-1, -3 and -4, by immunohistochemistry and real-time PCR, in 56 cases of malignant breast tumours and benign lesions. The study revealed significant dysregulation of these claudin family members in all 56 sections of breast cancer sections examined. Claudin-1 stained positively and was shown to be present, in normal membrane location in non-malignant duct cells, and in a small percentage of malignant ductal carcinoma in situ sections. However, claudin-1 was either undetectable or displayed abnormal/scattered localisation in over 90% of secondary breast cancer metastasises, suggesting its downregulation or mislocalisation promotes cancer progression away from the primary site (Tőkés et al 2005).

Claudin-3 stained positively in 49 of the 56 sections and did not appear to affect the invasive nature of the cancer. Claudin-4 stained positively in all sections but was significantly higher in benign lesions and almost undetectable in grade 1 ductal carcinomas. Taken together, it appears that both claudin-1 and -4 may play a role in the invasion and metastasis of breast cancer (Tőkés et al 2005).

Both occludin and ZO-1 expression are frequently downregulated in breast cancer compared to normal breast tissue. The downregulation of occludin in breast cancer has been associated with tumour progression. Experimental forced expression of occludin promoted oxidative stress, and anoikis based apoptosis (Osanai et al 2007). ZO-1 is documented to be significantly reduced or absent in 42% of well differentiated breast cancers, 83% of moderately differentiated and of 93% of poorly differentiated tumours. The decreased expression of ZO-1 correlates with the increase in tumour grade and inversely with tumour differentiation in breast cancer (Hoover et al 1998).

1.5.3 Colon cancer

A study investigating the expression of claudin-1, -4, occludin, and ZO-1 in 129 patients with stage II colon cancer found the expression of all of these tight junction constituents to be dysregulated. Claudin-1 was normal or elevated in 75% of tumours, claudin-4 in 58%, occludin in 54% and ZO-1 in 44%. However, they found that low expression of claudin-1 and ZO-1 correlated with increasing tumour grade and associated poor prognosis. Further analysis indicated that low claudin-1 levels in colon cancer was linked to increased lymphovascular invasion and was a strong independent predictor of recurrence (Resnick et al 2005). Interestingly, other studies have reported increased claudin-1 and decreased levels of claudins -8 and -12 in colon cancer with both membranous and intracellular vesicular staining. Both the overexpression and the absence of claudin-1 in colon cancer has be associated with a poor prognosis and increased tumour staging (de Oliveira et al 2005). The increased expression of claudin-1 in colon cancer is thought to correlate with the increase of β-catenin/TCF4 and ZEB1 and has been shown to induce EMT in those cells (Huang et al 2014). The differential expression of claudin-1 in colon cancer is thought to be associated with the initiation and progression of the disease, where both the increased and decreased levels of the protein are of prognostic value.

1.5.4 Lung cancer

The composition of tight junction constituents seems to be cell type specific in lung carcinomas. Squamous cell carcinomas and basal cells of bronchial epithelium have been shown to have increased expression of claudin-1 and decreased expression of claudin-5. Whereas, adenocarcinomas, normal cylindrical cells, and pneumocytes presented with increased claudin-5 and decreased claudin-1 expression (Paschoud et al 2007). The authors of this study made an interesting observation, noting that squamous cell

carcinomas and colon cancers often present with high claudin-1 levels, whilst glandular-based lung cancers and breast cancers present with low claudin-1 levels. This divide suggests that cancers originating from epithelial/squamous cells are likely to develop a high claudin-1 associated carcinoma, whereas cancers originating from glandular components are more likely to present with a claudin-1 low phenotype.

Both squamous cell carcinomas and adenocarcinomas presented with positive claudin-4 and ZO-1 staining. Although, at the mRNA level both lung carcinomas presented with decreased expressions of claudin-3, claudin-4, claudin-7, ZO-2 and ZO-3, with squamous cell carcinomas also showing decreased levels of JAM-1, occludin, and Cingulin (Paschoud et al 2007).

Occludin staining did not show any positivity in any cases of squamous cell carcinoma, large cell carcinoma, small cell carcinoma, or large cell neuroendocrine carcinoma despite showing strong staining in all other surrounding normal lung tissues. These results suggest occludin could be an accurate Immunohistochemical indicator distinguishing between normal and malignant lung tissues (Tobioka et al 2004).

1.5.5 Pancreas cancer

In a similar pattern to lung carcinomas, carcinomas originating in different tissues of the pancreas express differing tight junction profiles. Carcinomas originating from normal pancreatic acini and ductal cells show strong immunological staining and increased mRNA expression of claudins-1, -3, -4, and -7 but were negative for claudin-13. Pancreatic endocrine tumours displayed no staining for claudin-1 and -4. However, both Langerhans islets and pancreatic endocrine tumours displayed claudin-3 and -7 positive immunohistochemistry. Claudin-2 expression was detected in around 50% of ductal adenocarcinomas, although the staining pattern was irregular and scattered. Claudin-2

expression was undetectable in the majority of Pancreatic endocrine tumours (Borka et al 2007).

A study investigating the expression and localisation of ZO-1 found that pancreatic ductal adenocarcinoma samples contained significantly higher (6-fold) levels compared with normal pancreatic samples. In normal pancreatic tissue with or without chronic pancreatitis, ZO-1 is located the apical/apicolateral domains. However, during metastasis pancreatic carcinoma cells display a range of ZO-1 localised staining from apical and apicolateral, to diffuse membranous staining. The increased expression of ZO-1 and its abnormal localisation during the lymphatic invasion of these cells, may imply that the scaffold protein confers a metastatic advantage to pancreatic cancer cells (Kleeff et al 2001).

A decreased expression of JAM-A has been associated with a poor prognosis in pancreatic cancer (Fong et al 2012). Over 40% of samples specimens examined presented with low or delocalised JAM-A staining. The low expression of the junction protein was shown to correlate with increased lymph node invasion, distant metastasis, and increased tumour grade. As a result, JAM-A has been described as an independent predictor of poor outcome and a potential biomarker of the disease (Fong et al 2012).

1.6 Tight Junctions in hepatocellular carcinoma

As with the majority of cancers, HCC presents with a defining profile of junctional proteins during the initiation and progression of the disease. The profile produced has been suggested to confer an advantage during malignant transformation, with the expression of a number of tight junctional proteins correlating with patient prognosis.

1.6.1 Junctional proteins downregulated in hepatocellular carcinoma

Claudin-2 is frequently downregulated in HCC, with decreased expression recorded at both the protein and mRNA level compared to normal and surrounding liver tissues. The dysregulation of claudin-2 coincides with the decreased expression of hepatocyte nuclear factor–1α (HNF-1α) in the disease. HNF-1α is thought to be a positive regulator of claudin-2 in HCC. Claudin-2 has been documented to be required for cell polarity in hepatic cells. Taken together, it appears claudin-2 acts as a tumour suppressor by maintaining cellular polarity in HCC (Holczbauer et al 2013).

Claudin-3 is either undetectable or found at very low levels in the majority of HCC cases. Over 75% of HCC tissue samples and 65% of HCC cell lines contain downregulated or undetectable levels of the tight junction protein. In both cases, the downregulation is commonly associated with claudin-3 promoter hypermethalation (Holczbauer et al 2013). The low levels of claudin-3 in HCC have also been associated with increased cell motility, cell invasiveness, and tumor formation in experiments involving nude mice. Claudin-3 was shown to supress the invasive phenotype of HCC by inactivating Wnt/β-catenin and subsequently inhibiting epithelial mesenchymal transition. Claudin-3 has therefore been described as a metastasises suppressor in HCC (Jiang et al 2014).

Claudin-4 is typically undetectable or found at very low levels in HCC but is significantly increased in biliary tract cancers (Lódi et al 2006). The decreased expression of claudin-4 is associated with increased tumour grade (grade III and IV), increased recurrence rate and low disease-free survival rate in the disease. The increased levels of the protein are an independent prognostic factor for survival prognosis in the disease (Bouchagier et al 2014).

The expression of claudin-5 has been documented to decrease with increasing tumour grade in HCC. It is normally expressed in hepatocytes and in sinusoidal endothelial

cells but is frequently downregulated during hepatitis or fibrosis. The downregulation of claudin-5 has been associated with poor overall survival, with an increase in the protein representing an independent prognostic factor for the disease (Bouchagier et al 2014).

The expression of ZO-1, occludin and tricellulin have been documented to be decreased in both primary HCCs and secondary metastases compared with normal liver tissue (Holczbauer et al 2013). In normal liver tissue, both occludin and ZO-1 are strongly expressed at the bile canaliculi with weaker, sometimes absent expression on apical, apicolateral, and basal membranes. In HCC, occludin and ZO-1 are commonly localised in the cytoplasm, if at all. The intracellular localisation is thought to indicate the loss of function of the tight junctional proteins (Bouchagier et al 2014). The expression of occludin and tricellulin is thought to not have any prognostic value in HCC, but the decreased expression of ZO-1 has been described as a predictive marker associated with poor prognosis in patients with HCC after hepatectomy (Nagai et al 2016).

1.6.2 Junctional proteins upregulated in hepatocellular carcinoma

Reports have suggested differing expression levels of claudin-7 in HCC. Holczbauer et al reported no significant change of claudin-7 expression immunochemistry during HCC compared to non-tumorous liver (Holczbauer et al 2013). Whereas, Bouchagier et al reported an increase of claudin-7 expression during the disease, and that a downregulation of the protein is an independent prognostic factor for increased overall survival (Bouchagier et al 2014).

Claudin-10 has emerged as an interesting inducer of invasive qualities during HCC development. Experimental overexpression of the tight junction protein in Hep3B cells, which ordinarily show undetectable levels of claudin-10, promoted cancer cell survival, motility, and invasiveness. Further analysis revealed that the overexpression of claudin-10

in these cells increased MMP2 and MT1-MMP as well as claudin-1, -2, and -4 (Martin & Jiang 2009). The same authors used siRNA knockdown to silence claudin-10 in an invasive HCC cell line, HLE, which is associated with overexpression of the tight junction protein. As a result, the siRNA knockdown of claudin-10 reduced the expression of MMPS and claudin-1, whilst decreasing the invasive nature of the cells. Despite this, as yet no data exists about the typical expression levels of claudin-10 in HCC patient samples (Ip et al 2007)

1.7 Claudin-1 in hepatocellular carcinoma

The documented expression of claudin-1 and its effects in HCC have been controversial in the literature. As with a number of other cancers, claudin-1 has been linked to the progression of the disease, but the mechanisms in which it elicits its effects are under dispute. Previous studies believed that many cancers followed the breast cancer expression prolife of claudin-1, where low expression promoted invasion and metastasis, and increased expression caused suppression of this phenotype (Myal et al 2010). While this is still true for some cancers, such as breast and lung, other cancers such as colon, show a greater complexity of claudin-1 involvement in the disease (Chao et al 2009). In colon cancer, both claudin-1 overexpression and silencing has been reported to promote tumour progression and metastasis. Overexpression of the tight junction constituent has been linked to the upregulation of invasive markers and even the induction of EMT in a recent study (Bhat et al 2016). While the decreased expression of claudin-1 has been associated with increased tumour grade and lymph node metastasis (Ersoz et al 2011). This duel role of claudin-1 in colon cancer is not unique, with similar occurrences observed in HCCs, where both increased and decreased expression of claudin-1 is associated with a poor patient prognosis. HCC cell lines with increased claudin-1 levels are reported to be more invasive with upregulated expression of MMPs (Yoon et al 2010). Furthermore, data

obtained from HCC tissue sections has demonstrated that increased claudin-1 levels correlated with higher grades of tumour. Interestingly, the decreased expression of claudin-1 has also been shown to be associated with tumour dedifferentiation, poor prognosis, and lower survival rates after hepatectomy (Higashi et al 2007). Despite these observations, very little is known about how claudin-1 influences the initiation and progression of HCC, particularly the underlying mechanisms that drive hepatocarcinogenesis, and the invasive and metastatic phenotype that is strongly associated with the disease.

1.8 Aims and Objectives

Evidence suggests that both the increased and decreased expression of claudin-1 contributes to in the initiation and progression of HCC. However, this data originates from the observational findings of previous HCC cases, the exact underlying mechanisms by which claudin-1 modulates this invasive phenotype remains unclear. In this study, we aim to investigate the role of claudin-1 in the initiation and progression of HCC. The HepG2 hepatocellular carcinoma cell line was used to examining the molecular mechanisms in which claudin-1 orchestrates the biochemical and functional changes that are observed during the disease. Therefore, the aims of this thesis are to:

1. Investigate the *in vitro* migratory capacity of claudin-1 overexpressing and claudin-1 silenced HepG2 cells.
2. Determine the expression of the tight junction profile in the claudin-1 overexpressing and claudin-1 silenced HepG2 cells.
3. Determine the expression of genes associated with epithelial-mesenchymal transition in the claudin-1 overexpressed and claudin-1 silenced HepG2 cells.
4. Determine the expression of tumour metastasis and associated genes in the claudin-1 overexpressing and claudin-1 silenced HepG2 cells.

5. Determine the expression profile of MicroRNAs in claudin-1 overexpressing and claudin-1 silenced HepG2 cells.

Determining the migratory capacity, the gene expression profile of miRNAs and the gene expression profile of tight junctional, EMT and tumour metastasis genes will allow a greater understanding of how claudin-1 can influence the malignant hallmarks often seen in hepatocellular carcinoma. The intention is that this data can aid in stratifying HCC patient groups using the molecular markers outlined during this work. Ultimately this could aid in determining patient treatment and possibly give an indication of patient prognosis.

Chapter 2: Materials and methods

2.1 Materials

2.1.1 Standard solutions

2.1.1.1 Solutions for cell culture

X10 Phosphate Buffered Saline (PBS) (Ca^{2+} and Mg^{2+} free)

80g of NaCl (sigma S7653-5KG), 2g of KCL (sigma P9541-500G), 14.4g of $Na_2HPO_4.12H_2O$ (sigma S5136-500G), and 2g of KH_2PO_4 (sigma P5655-500G) were dissolved in 1 litre of RO/DI water. The solution was adjusted to PH 7.4 and autoclaved. PBS can be stored at room temperature until needed.

X1 PBS

X10 PBS was diluted to x1PBS (100ml with 900ml RO/DI water) prior to use.

Trypsin/EDTA x10

100ml of x10 Trypsin/EDTA (LabTech XC-T1717/100) was diluted in 400ml sterile PBS. The diluted trypsin/EDTA was divided into 10ml aliquots stored at -20^{o}C until needed. Trypsin/EDTA is used for enzymatic cellular detachment in routine cell culture.

70% IMS

700ml of 99% Ethanol denatured with methanol (industrial methylated spirit) (VWR 23684.444) was mixed with 300ml RO/DI water. IMS was transferred to spray bottle for use in sterilisation. IMS can be stored at room temperature until needed.

2.1.1.2 Microbiological solutions

Luria Bertani (LB) broth with glucose

10g of tryptone (sigma T7293-1KG), 5g of yeast extract (sigma Y1625-1KG), 5g of NaCl and 1g of glucose (sigma 49159-1KG) was dissolved in 1 litre final volume of RO/DI water. The solution was adjusted to PH7.5, autoclaved, allowed to cool and stored at room temperature. The addition of selective antibiotics (if required) must only be added once cooled.

Luria Bertani (LB) agar

10g of tryptone, 5g of yeast extract, 5g of NaCl, 1g of glucose and 15g of Bacteriological agar (sigma A5306-250GF) was dissolved in 1 litre final volume of RO/DI water. The solution was adjusted to PH7.5, autoclaved, allowed to cool and stored at room temperature. The solution was steamed for 45 minutes until liquefied. Once liquid, the solution was placed in a 55^{o}C water bath to reduce the temperature but allow the solution to remain in a liquid state. At this stage selective antibiotics were added. The solution was then poured into 10cm^{2} petri dishes (ThermoFisher 263991) in a category II laminar flow cupboard (NuAire) allowed to cool until solid, inverted and stored at 4^{o}C.

TSS buffer

5g Poly (ethylene glycol) 8000 (Sigma P5413-500G), 0.30g $MgCl_2.6H_20$ (Sigma M2670-100G) and 2.5ml 100% Dimethylsulphoxide (DMSO) (Sigma D8418-100ML) were mixed and made up to 50ml using LB broth. TSS buffer was filtered through 0.2um minisart filters (Sartorius 17764ACK), divided into 500µl aliquots and stored at -20^{o}C.

Ampicillin, sodium salt (50mg/ml)

500mg of ampicillin, sodium salt (Sigma A0166-5G) was dissolved in 10ml of autoclaved Milli Q water, filtered through 0.2µm minisart filter (Sartorius 17764ACK), divided into 1ml aliquots and stored at -20^{o}C. 100 microliters of ampicillin, sodium salt was diluted in 100ml of LB broth/agar for use as a selective antibiotic.

Chloramphenicol (Water Soluble) (25mg/ml)

250mg Chloramphenicol (Sigma C3175-100MG) was dissolved in 10ml of autoclaved Milli Q water, filtered through 0.2µm minisart filter (Sartorius 17764ACK), divided into 1ml aliquots and stored at -20^{o}C. 25 microliters of Chloramphenicol solution were diluted in 100ml of LB broth/agar for use as a selective antibiotic.

2.1.1.3 Molecular solutions

75% Ethanol

75ml molecular biology grade absolute ethanol (Fisher Scientific 10041814) was mixed with 25ml Milli Q water and stored at RT in an RNase/DNase free container.

0.3M guanidine hydrochloride in 95% ethanol

2.86g guanidine hydrochloride (Sigma G3272-100G) was dissolved in 95ml molecular biology grade absolute ethanol and made up to 100ml total volume with 5ml Milli Q water. Solution was stored at RT in an RNase/DNase free container.

Tris/Acetate/EDTA Buffer (T.A.E)

48.4g of Tris-base (sigma T1503-500G), 7.44g of EDTA.$Na_2$2H_2O (sigma EDS-500G) and 11.42ml of glacial acetic acid (sigma A6283-500ML-D) was dissolved in autoclaved Milli Q water and made up to 900ml. The solution was then PH adjusted to 8.5 and made up to 1 litre final volume using autoclaved Milli Q water, autoclaved and stored at room temperature. The solution will need to be diluted to x1 concentration prior to use in agarose gels or running buffer.

T.A.E Agarose Gels

Table 2.1 shows the amount of agarose (sigma A9539-100G) and T.A.E buffer need to create agarose gels used in the separation of RNA during electrophoresis. Once mixed, the solution was autoclaved, allowed to cool and solidify, stored at room temperature.

Gel concentration	Agarose	x1 T.A.E
1.0%	0.35g	35ml
2.0%	0.70g	35ml
2.5%	0.85g	35ml

Table 2.1: Amounts of Agarose and T.A.E buffer needed for a range of agarose electrophoresis gels. The table outlines reagents required to produce different percentage agarose gels. Percentage gel varied based on the length of DNA/RNA separated. Volumes provided are per gel.

Tris base/Borate/EDTA buffer (T.B.E) x10

108g of Tris-base, 55g of boric acid (sigma B7901-500G) and 9.5g of EDTA.$Na_2$2H_2O was dissolved in autoclaved Milli Q water and made up to 900ml. The solution was then pH adjusted to 8 using HCL and made up to 1 litre final volume using autoclaved Milli Q water, autoclaved and stored at room temperature. The solution was diluted to x1 concentration prior to use in agarose gels or running buffer.

T.B.E Agarose Gels

Table 2.2 shows the amount of agarose and T.B.E buffer need to create agarose gels used in the separation of DNA during electrophoresis. Once mixed, the solution was autoclaved, allowed to cool and solidify, and stored at room temperature.

Gel concentration	Agarose	x1 T.B.E
1.0%	0.35g	35ml
2.0%	0.70g	35ml
2.5%	0.85g	35ml

Table 2.2: Amounts of Agarose and T.B.E buffer needed for a range of agarose electrophoresis gels. The table outlines reagents required to produce different percentage agarose gels. Percentage gel varied based on the length of DNA/RNA separated. Volumes provided are per gel.

2.1.1.4 Immunocytochemistry solutions

Blocking buffer

(1% BSA, 22.52 mg/mL glycine in PBST (PBS+ 0.1% Tween 20)

200mg Bovine Serum Albumin (sigma A9418-50G), 450mg glycine (sigma G8898-500G) and 20µl Tween 20 (sigma P1379-100ML) were added to 20ml PBS pH7.4 and mixed gently on a tube roller. Blocking buffer was stored at 4^{o}C for a maximum of 48hours.

Antibody dilution buffer

(1% BSA in PBST (PBS+ 0.1% Tween 20)

200mg Bovine Serum Albumin and 20µl Tween 20 were added to 20ml PBS pH7.4 and mixed gently on a tube roller. Antibody dilution buffer was stored at 4^{o}C for a maximum of 48 hours.

Permeabilization buffer (0.2% Triton x-100/PBS)

40µl of Triton x-100 (sigma 93443-100ML) was added to 20ml PBS and agitated gently until dissolved. Permeabilization buffer was stored at 4^{o}C for a maximum of 2 weeks.

2.1.1.5 Western blotting solutions

10% (w/v) SDS

10g Sodium dodecyl sulphate (Sigma L4509-250G) was dissolved in 90ml RO/DI water and adjusted to 100ml final volume. SDS was stored at room temperature.

0.5M Tris-HCL (pH6.8)

6g of Tris-Base was dissolved in 60ml RO/DI water, adjusted to pH6.8 with HCL and the total volume adjusted to 100mil with RO/DI water. Tris-HCL was stored at room temperature.

0.5% (w/v) Bromophenol blue

100µg of Bromophenol blue (sigma B0126-25G) was dissolved in 10ml RO/DI water and stored at room temperature.

Sample buffer (SDS reducing buffer)

2ml of 10% (w/v) SDS, 1.25ml 0.5M Tris-HCL (pH6.8), 2.5ml glycerol (Sigma G5516-100ML), 0.2ml 0.5% (w/v) bromophenol blue and 3.55ml RO/DI water (total volume 9.5ml) were gently mixed and stored at room temperature. Before use add 1/20 volume β-Mercaptoethanol (sigma M6250-100ML) i.e. 50ul per 950ul sample buffer.

10x Electrode running buffer (pH8.3)

10g SDS, 30.3g Tris base (sigma T1503-500G) and 144g Glycine (sigma G8898-500G) were dissolved in 900ml RO/DI water and adjusted to final volume 1000ml. 10x Electrode running buffer was diluted (100ml with 900ml RO/DI water) prior to use. Electrode running buffer was stored at 4^{o}C, warmed to room temperature when needed.

Transfer buffer

500µl of 10% (w/v) SDS, 200ml Methanol (Fisher Scientific 10002070), 14.4g Glycine, 3.03g Tris-Base were mixed and made up to 1000ml with RO/DI water. Transfer buffer was stored at 4^{o}C, warmed to room temperature when needed.

TBST, Washing/Ab/blocking buffer pH7.5

500µl Tween 20 (sigma P1379-100ML), 5.84g Sodium Chloride (sigma S7653-5KG), 1.21g Tris-Base were dissolved in 900ml RO/DI water, adjusted to pH 7.5 using HCL and made up to 1000ml final volume. TBST was stored at 4^{o}C, warmed to room temperature when needed.

Blocking buffer

5% (w/v) milk blocking buffer

5g of non-fat dried milk powder was dissolved in 100ml TBST buffer and filtered through general purpose filter paper to remove any undissolved milk. The blocking buffer was immediately or stored at 4^{o}C for a maximum 24hours.

0.5% (w/v) milk blocking buffer

Dilute 5% (w/v) blocking buffer 1/10 with TBST

2.2 Mammalian cell culture

All cell culture work was performed inside a NuAire category II laminar flow cupboard using aseptic technique. 70% IMS spray was used to sterilise laminar flow cupboards upon initiation and completion of cell culture. This method of sterilisation was also used when switching between cell lines to avoid cross contamination. Laminar flow cupboards were also subjected to a minimum of 60 minutes of ultraviolet radiation after finishing cell culture, to insure all work surfaces are free from microbiological contaminants. All consumables used in cell culture were either purchased sterile or sterilised by autoclaving, prior to cell culture taking place. All other instruments were sterilised using 70% IMS spray where

necessary. A plastic discard container filled with diluted Distel (VWR 141-0933) was used to disinfect and hold any waste liquids, discarded pipette tips and small plastic containers used during cell culture. Cell culture flasks, automatic pipette tips and larger plastic containers were discarded in external biohazard bins. Lab coats and latex gloves were used throughout the cell culture procedure. Gloves were changed periodically, upon entering and exiting the laminar flow cupboard, and between cell lines to minimise the risk of contamination.

2.2.1 Mammalian cell culture media

HepG2 and HEK293T cell lines were maintained using Dulbecco's Modified Eagle's Medium supplemented with 1% L-Glutamate (LabTech LM-D1109/500), 1% penicillin and streptomycin (x100) (LabTech XC-A4122/100) and 10% foetal bovine serum (ThermoFisher 10500064).

Transfection procedures for claudin-1 siRNA silencing and lentiviral overexpression require antibiotic free media supplemented with L-Glutamate and FBS at 10%.

Only enough antibiotic free media was produced for the procedure at any one time to avoid any possible contamination.

2.2.2 Mammalian cell lines

Liver cancer cell line (HepG2) as well as human embryonic kidney cells (HEK293T) were used throughout this study.

Cell Line	Species	Morphology	Gender	Age	Disease	Feature
HepG2	Homo sapiens	Epithelial	Male	15 years' adolescent	Hepatocellular Carcinoma	Adherent, polarising cells which form apical and basolateral cell surface domains along with structures that resemble the bile canaliculi and sinusoidal domains, derived from liver tissue
HEK293T	Homo sapiens	Epithelial	Unknown	Foetus	N/A	Semi adherent, foetus derived cell line. They are easily cultured, and transfectable with episomal DNA so are primarily used for the production of various retroviral vectors.

Table 2.3: Cell lines used in this study. The table outlines the cell lines used during this thesis with information regarding the key features of each one.

2.2.3 Mammalian cell line maintenance

All cells were grown in 25cm^2 (T-25) (ThermoScientific 163371) and 75cm^2 (T-75) (ThermoScientific 153732) Nunc cell culture treated flasks with vent/close caps until 80-90% confluent. Cells were always allowed to reach confluency before being removed for experimental procedures. All cells lines were incubated at 37^{o}C, 5% carbon dioxide and 95% humidification (containing copper sulfate) (NuAir AutoFlow NU-5500).

2.2.4 Trypsinisation of cells

As all cell lines used in this study were adherent therefore trypsinisation must occur to detach cells from the surface of the flask for either sub-culture or experimentation. The confluency was assessed by observing at the proportion of the flask surface that was occupied by cells using an invert light microscope (Nikon Eclipse TS100). Culture media was then removed aseptically and discarded. Cells were then washed in sterile, pre-warmed (37^{o}C) PBS to remove any dead cells and remaining media. Around 2-3ml of PBS was added to T-25 flask and 9-10ml for T-75 flasks. Flasks were tilted side-to-side several times in a gentle rocking motion to rinse cells. The PBS was then removed and discarded. An appropriate volume of x2 trypsin was then added to each flask. Around 1ml for T-25 and 1.5-2ml for T-75 flasks. The flasks were incubated at 37^{o}C for around 3-5 minutes to activate the trypsin. After 3-5 minutes, the cells should detach from the flask surface once agitated, this was checked using an invert light microscope. Growth media was then added to the flask to inhibit the trypsin: around 2-4ml for T-25 and 4-8ml for T75 flasks. The cell suspension was then pipetted up and down against the surface of the monolayer to disrupt any remaining cells and break up clumps. Flasks were tilted up-right and the cell suspension was pipetted from the bottom corner or edge and transferred to a 30ml sterile centrifuge tube. Cells were centrifuged at 1500rpm for 5 minutes to pellet the cells. The

supernatant was discarded, leaving a pellet of cells ready for counting for experimentation, subculture or freezing.

2.2.5 Subculture of cells

The pelleted cells were re-suspended in around 10ml of pre-warmed (37^{o}C) growth media by pipetting up and down thoroughly to ensure cells are singular. Antibiotic free media was used here for silencing or overexpression experiments. Cells were divided into new culture flasks; the split ratio depended on cell type and growth behavior. HepG2 cells at 80-90% confluency were split 1:5 every 96 hours. HEK293T cells at 80-90% confluency were split 1:8 every 96hours. Growth media was replaced every 48hours. Cells were incubated at 37^{o}C and 5% CO_2.

2.2.6 Cell counting

The pelleted cells, post trypsinisation, were re-suspended in 8-10ml of pre-warmed (37^{o}C) growth media by pipetting up and down thoroughly to ensure cells were singular. 20µl of the cell suspension was transferred into a sterile eppendorf tube. 20µl trypan blue dye was added to the cell suspension and mixed by pipetting. 20µl of the cell suspension/dye mix as loaded onto a hemocytometer counting chamber, viewed at 10x magnification under an invert light microscope and counted.

The haemocytometer contains four 16 square areas in which cell were counted. The dimension of each 16 square is 1mm x 1mm x 0.2mm which allows the number of cells per millilitre to be determined by the following equation.

$$\text{Cell number/ml} = \left(\frac{\text{Number of live cells in the four corner,16 square areas}}{4} \times 2\right) \text{x}10^4$$

2.2.7 Cell freezing and storage

Cells from an 80-90% confluent, 75cm^3 flask were trypsinised and pelleted as previously described. Pelleted cells were re-suspended in a mixture of 750µl of FBS and 750µl growth media and transferred to a 1.8ml cryopreservation tube (Sarstedt 72.379) placed on ice. 10% Dimethylsulphoxide (DMSO) (Sigma D8418-100ML) was added drop-wise to the FBS/Media/cell suspension to limit any cytotoxic effects. The cryopreservation tubes were transferred to the -80^{o}C freezer overnight in a CoolCell LX Cell Freezing Container (Corning 432001), before long term storage in a liquid nitrogen tank.

2.2.8 Recovery of frozen cells

Frozen cells stored in liquid nitrogen were carefully removed and incubated at room temperature for 30 seconds, this allowed any remaining liquid nitrogen to dissipate. Cells were transferred to a preheated 37^{o}C water bath for three minutes to facilitate rapid thawing. Once thawed, cells were transferred to a 20ml centrifuge tube containing 10ml complete growth media, preheated to 37^{o}C. Cells were centrifuged at 1500 rpm for five minutes to form a pellet. The supernatant was discarded and the cells were re-suspended in 15ml of fresh complete growth media and placed in a T75 cell culture flask. Cells were then incubated at 37^{o}C, 5% carbon dioxide and 95% humidification overnight. The following day, growth media was replaced and cells rinsed in PBS to remove any dead cells and cell debris.

2.2.9 Cellular migration assay protocol

Migration assays were performed using ibidi 2 well culture inserts (ibidi 80209) in accordance with the ibidi protocol, that has been modified as a result of optimization. Inserts were sterilised in 100% ethanol for one minute before being washed in PBS and

placed on the 6 well plate. The plate was incubated at 37°C until dry, usually 15-20 minutes. Inverting the plate identified any poorly stuck inserts. Inserts were attached in triplicate to allow for some failing to stick. HepG2 cells were counted at seeded into the inserts at $5x10^4$ cells per side. Growth media was added so the total volume per side of the insert was 100µl. The plate containing the inserts was incubated overnight in a humidified 37°C + 5% CO_2 incubator. The following morning inserts were checked for leaking compartments. The wells containing intact and sealed inserts were filled with 2ml/well cell culture media. The inserts were then carefully removed with sterile tweezers and retained. The 6 well plate was then imaged under an invert microscope to examine for the pattern made by the inserts. Two clear compartments of HepG2 cells divided by a 500µm gap should be present. Subsequent images and measurements were taken every 4 hours throughout the day. The experiment was terminated if the gap closed completely or if 96 hours was reached.

2.3 Lentiviral plasmid production

2.3.1 Preparation of competent Stbl3 *E. coli*

Stbl3 *E. coli* cells stored at -80°C were thawed in a 37°C water bath until completely defrosted. The *E. coli* were then plated on LB-agar plates and then incubated overnight in a 37°C incubator. A single colony was selected from the streak plate and used to inoculate 5ml of LB-broth, creating a liquid culture. The liquid culture was incubated overnight at 37°C until a thick bacterial culture is formed. 2.5 milliliters of the *E. coli* culture was transferred into a conical flask containing 50ml of LB-broth, and incubated for an estimated 3 hours, until a spectrophotometer reading at OD_{600} of 0.3 was achieved. The culture was then chilled on ice for 20 minutes before centrifuging at 4000rpm for 15 minutes at 4°C. The

supernatant was discarded leaving a pellet of Stbl3 *E. coli* cells. This pellet was re-suspended in 500µl of sterile, ice-cold TSS buffer. At this point cells could be mixed with 20% glycogen and stored at -80ºC.

2.3.2 DNA transformation protocol

Competent *E. coli* Stbl3 cells were taken from the freezer and allowed to thaw on wet ice. Competent *E. coli* cells were divided into 100µl aliquots, allowing for both positive and negative controls for each DNA transformation. 100ng of plasmid DNA (CLDN-1 pLenti-C-Myc-DDK-IRES-Puro and pLenti-C-Myc-DDK-IRES-Puro) was added to separate aliquots of competent *E. coli*. The same volume of sterile water was also added to the negative control. Both positive and negative controls were left on ice for 30 minutes. Competent *E. coli* were placed in a 42ºC water bath for 45 seconds, then immediately back on ice for 2 minutes to induce heat-shock. 500µl of LB-Broth containing no antibiotics was added to both positive and negative controls and allowed to incubate at 37ºC for 60 minutes. 100 microliters of the transformed *E. coli* and the negative control *E. coli* were spread on LB-agar plates containing selective antibiotics, dependent on resistance gene, using aseptic technique. Plates were incubated overnight at 37ºC. Positive control plates with bacterial colonies contained transformed *E. coli* producing the plasmid of interest. A single colony was selected and amplified in a liquid bacterial culture. Negative control plates should contain no colonies, as the *E. coli* do not possess the resistance gene to survive on the LB-agar plates containing selective antibiotics.

2.3.3 Amplifying transformed *E. coli* in liquid bacterial culture

Colonies selected from positive control plates were grown in liquid bacterial culture to amplify the amount of plasmid before extraction. A single colony from a positive control plate was selected and transferred into a sterile centrifuge tube or equivalent containing 5ml of LB-Broth with corresponding selective antibiotics, using aseptic technique. A second sterile centrifuge tube or equivalent containing 5ml of LB-Broth with the same selective antibiotics was used to represent a negative control. A flamed loop was placed into the negative control tube without touching any colonies. Once both tubes were treated, the lids were sealed and incubated in an orbital shaking incubator at 37^{o}C overnight. The next day the tubes were inspected, positive cultures were cloudy, whereas negative tubes were clear.

2.3.4 Extracting plasmid DNA from transformed *E. coli*

Plasmid DNA was extracted from transformed *E. coli* using Qiagen QIAprep spin miniprep kit (Qiagen 27104) in accordance to the provided protocol. Positive *E. coli* cultures in LB broth, containing transformed plasmid DNA, were centrifuged at 4400 rpm for 10 minutes to pellet the cells. The supernatant was then discarded and the pelleted cells re-suspended in 250µl lysis buffer containing RNase A. The re-suspended cells were transferred to a sterile 1.5ml Eppendorf tube where 250µl of LyseBlue reagent was added. This aided in the alkaline lysis of *E. coli*, shown by the solution turning blue once mixed by inversion 4-6 times with the lysed *E. coli*. Once blue, 350µl of neutralization buffer was added and mixed immediately and thoroughly by inversion 4-6 times. The cell lysate turned colourless indicating a neutralization of Ph. Microcentrifuge tubes containing the neutralized cell lysate were centrifuged at 13,000 rpm for 10 minutes, separating the cell debris from the plasmid DNA in solution. The supernatant was pipetted into the QIAprep spin column, insuring no

cell debris was transferred. The prepared column was centrifuged for 60 seconds at 13,000 rpm. The flow-through was discarded and 750µl wash buffer was added to the QIAprep spin column. The column was then centrifuged for 60 seconds at 13,000 rpm. The flow-through was discarded and the spin column was further centrifuged for 60 seconds at 13,000 rpm. The spin column was transferred to a labelled, sterile, 1.5ml Eppendorf tube. The DNA was eluted by adding 50µl elution buffer directly to the center of the QIAprep spin column, leaving to stand for 1 minute then centrifuging for a 1 minute at 13,000 rpm. Eluted DNA was tested on a Nanodrop One spectrophotometer (ThermoFisher) and ran on a 1% T.B.E agarose gel to test plasmid concentration, purity and size. Plasmid DNA was either used immediately or stored at -20^{o}C until needed.

2.4 Claudin-1 overexpression protocol

A custom expression vector was ordered from Origene technologies which incorporated a CLDN-1 cDNA clone taken from the TrueORF vector (CAT#: RC204466) and inserted into a pLenti-C-Myc-DDK-IRES-Puro plasmid backbone (CAT#: PS100069) creating the custom CLDN-1 pLenti-C-Myc-DDK-IRES-Puro plasmid (CAT#: CW301818). The CLDN-1 pLenti-C-Myc-DDK-IRES-Puro plasmid was used to produce lentiviral particles which were transduced into HepG2 cells. Though selection and clonal expansion a HepG2 cell line with stable overexpression of the CLDN-1 gene was created. This process was repeated in a separate group of HepG2 cells using the original pLenti-C-Myc-DDK-IRES-Puro plasmid backbone which contains no ORF insert to create a HepG2 control cell line, HepG2$^{pCMV\text{-}ve}$.

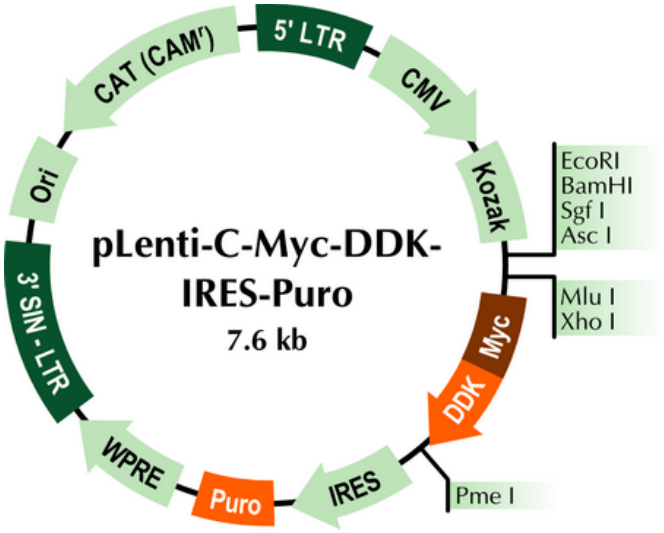

Figure 2.1: Plasmid map for pLenti-C-Myc-DDK-IRES-Puro. Plasmid map for pLenti-C-Myc-DDK-IRES-Puro. Purchased from Origene technologies, this lentiviral plasmid vector contains a multiple cloning site which is expressed under the CMV promoter. Other features include a chloramphenicol bacterial resistance gene (CAM^r), a mammalian puromycin resistance gene under a IRES promoter (Puro), a bacterial origin of replication (Ori) and 3'/5' LTR regions necessary for lentiviral integration.

GCGATCGCCATGGCCAACGCGGGGCTGCAGCTGTTGGGCTTCATTCTCGCCTTCCTGGGATGGATCGGCG

CCATCGTCAGCACTGCCCTGCCCCAGTGGAGGATTTACTCCTATGCCGGCGACAACATCGTGACCGCCCA

GGCCATGTACGAGGGGCTGTGGATGTCCTGCGTGTCGCAGAGCACCGGGCAGATCCAGTGCAAAGTCTTT

GACTCCTTGCTGAATCTGAGCAGCACATTGCAAGCAACCCGTGCCTTGATGGTGGTTGGCATCCTCCTGG

GAGTGATAGCAATCTTTGTGGCCACCGTTGGCATGAAGTGTATGAAGTGCTTGGAAGACGATGAGGTGCA

GAAGATGAGGATGGCTGTCATTGGGGGCGCGATATTTCTTCTTGCAGGTCTGGCTATTTTAGTTGCCACA

GCATGGTATGGCAATAGAATCGTTCAAGAATTCTATGACCCTATGACCCCAGTCAATGCCAGGTACGAAT

TTGGTCAGGCTCTCTTCACTGGCTGGGCTGCTGCTTCTCTCTGCCTTCTGGGAGGTGCCCTACTTTGCTG

TTCCTGTCCCCGAAAAACAACCTCTTACCCAACACCAAGGCCCTATCCAAAACCTGCACCTTCCAGCGGG

AAAGACTACGTGACGCGT

Figure 2.2: CLDN-1 mRNA sequence including restriction sites. Red sequence is the cloning site for SgfI restriction enzyme, Blue sequence is the CLDN-1 mRNA (NCBI GenBank: EF564137.1) and the Green sequence is the cloning site for the MluI restriction enzyme. This sequence was inserted into the pLenti-C-Myc-DDK-IRES-Puro vector by Origene technologies to create the CLDN-1 pLenti-C-Myc-DDK-IRES-Puro plasmid.

2.4.1 Lentiviral production

The expression vector was transduced using the lentivirus method due to the resistant nature of HepG2 cells to conventional transfection.

Prior to seeding cells, a 6 well plate (ThermoFisher 140675) was coated with 0.5ml 0.01% Poly-L-lysine solution (sigma P4707-50ML) per well and incubated at room temperature for 5 minutes. The plate was rocked gently to insure an even coating of the culture surface. After 5 minutes the solution was removed by aspiration and washed twice with 2ml PBS per well. The plate was allowed to dry for 2 hours at room temperature before seeding cells.

Once dry, HEK293T cells were seeded at $5x10^5$ cells per well in 2ml growth media and incubated overnight at 37^oC + 5% CO_2. The following day a transfection mastermix was produced in two separate 1.5ml Eppendorf tubes.

Tube 1 contained 1µg of either pLenti-CLDN-1 expression construct (CLDN-1 pLenti-C-Myc-DDK-IRES-Puro) or the pLenti-C-Myc-DDK-IRES-Puro vector, 1.2µg Lenti-vpak packaging mix (Origene TR30022) and 100µl Opti-MEM (ThermoFisher Scientific 31985070)

Tube 2 contained 100µl Opti-MEM and 10µl FuGENE HD Transfection Reagent (Promega E2311)

(The above amounts were for one well of a 6 well plate, these needed to be scaled up accordingly depended on application)

The contents of tubes 1 and 2 were allowed to incubate at room temperature for 5 minutes. The DNA solution from tube 1 was then transferred to tube 2, briefly vortexed and incubated for a further 15 minutes at room temperature. The culture media was changed on the HEK293T cells while transfection mixture was incubating. After 15 minutes, the

transfection mixture was added directly onto the cells containing fresh growth media. Cells were then incubated overnight at 37^{o}C + 5% CO_2.

After 12-18 hours, the transfection mixture was removed and replaced with 2ml per well fresh growth media.

The first batch of viral supernatant was harvested and stored at 4^{o}C, 24 hours after the transfection mixture was removed.

The second batch of viral supernatant was harvested 48 hours after the transfection mixture was removed and combined with the first batch of viral supernatant.

The viral supernatant was centrifuged at 3000rpm for 5 minutes at 4^{o}C and filtered through a 0.45-micron filter to remove cellular debris. The viral supernatant was used immediately if possible, stored at 4^{o}C for maximum 48hours or stored at -80^{o}C long term. However, freezing reduced titre by 30-50%.

2.4.1.2 Lentiviral transduction

HepG2 cells were seeded in a 6 well plate at 2.5x10^{5} cells per well in 2 ml growth media 24 hours prior to transduction. The following day the growth media was removed. In a separate tube viral supernatant and fresh growth media was mixed in a 2:1 ratio. The viral media was then supplemented with 8µg/ml Polybrene (santa cruz sc-134220). Around 2-4ml of viral media should be added to each well. Cells were incubated for 24 hours at 37^{o}C + 5% CO_2. The viral media was then replaced with 2ml per well fresh growth media.

2.4.2 Stable cell line production

After 72 hours post transduction, HepG2 cells containing the control pLenti vector (HepG2$^{pCMV\text{-}ve}$) and HepG2 cells containing the claudin-1 pLenti overexpression vector

(HepG2$^{CLDN-1+}$) were selected for using puromycin dihydrochloride (santa cruz sc-108071B). The transduced HepG2 cells (both HepG2$^{CLDN-1+}$ and HepG2$^{pCMV-ve}$) were trypsinised and transferred to two separate T25 flasks. Growth media containing puromycin 4µg/ml was added to each flask to select for transduced HepG2 cells. Only cells containing either the control pLenti vector (HepG2$^{pCMV-ve}$) or the claudin-1 pLenti overexpression vector (HepG2$^{CLDN-1+}$) were resistant. Puromycin (4µg/ml) containing media was changed every 24 hours and cells were sub-cultured once 60-80% confluency was reached. Five single isolated colonies of resistant cells were obtained and transferred into individual wells of a 24 well plate for clonal expansion, this was performed for both control pLenti vector containing cells (HepG2$^{pCMV-ve}$) and CLDN-1 pLenti overexpression vector containing cells (HepG2$^{CLDN-1+)}$. All 5 colonies for both control (HepG2$^{pCMV-ve}$) and claudin-1 overexpressing cells (HepG2$^{CLDN-1+}$) were tested by RT-qPCR to determine increased expression of claudin-1. HepG2 cells containing the CLDN-1 pLenti overexpression vector (HepG2$^{CLDN-1+}$) were compared against cells containing the control pLenti vector (HepG2$^{pCMV-ve}$). A colony was chosen that displayed a statistically significant increase of expression of claudin-1 and was puromycin resistant. Only 1 of the 5 clones contained both properties.

2.5 Claudin-1 siRNA transfection protocol

2.5.1 HepG2 cell plating

HepG2 cells were initially plated 24 hours in advance at the optimum cell densities listed in table 1. Cell plating densities are depended upon growth characteristics that are unique to each cell line. Cells were trypsinised and counted in complete antibiotic free DMEM, 10%

FBS. Once plated at optimum cell densities, cells were diluted with complete antibiotic free media and incubated overnight at 37ºC with 5% CO_2.

2.5.2 siRNA transfection

Transfection was performed using SMARTpool CLDN-1 siRNA (Dharmacon L-017369-00-0005). SMARTpool siRNA consists of four siRNA duplexes all designed to target distinct sites within the specific gene of interest, in this case claudin-1. The siRNA sequences are selected using the Dharmacon SMARTselection design algorithm and then analysed for significant sequence identity with other non-targeted genes using a unique, modified BLAST analysis against a curated database for the appropriate species.

Claudin-1 SMARTpool siRNA (Dharmacon L-017369-00-0005) was briefly centrifuged to ensure a pellet collected at the bottom of a 1.5ml Eppendorf tube. The pelleted siRNA was then resuspended in 250µl of 1x siRNA Buffer (Dharmacon B-002000-UB-100) to create a concentrated 20uM stock. A preparation of the recommended 5uM siRNA solution was created by diluting the 20uM stock in 1x siRNA buffer in a 1:4 ratio.

A transfection mastermix was produced in two separate 1.5ml Eppendorf tubes, 24 hours after cell plating. The required reagents and volumes per well are outlined in table 2.4. If more than one well of transfected cell was needed the amounts were scaled up accordingly.

		Tube 1: Diluted siRNA		Tube 2: Diluted DharmaFECT			
Plating Format (wells per plate)	Surface Area (cm2 per well)	Volume of 5uM siRNA (µl)	Volume of Opti-Mem (µl)	Volume of DharmaFECT (µl)	Volume of Opti-Mem (µl)	Antibiotic-free Media (µl/well)	Total Transfection Volume (µl/well)
96	0.3	0.5	9.5	0.25	9.75	80	100
24	2.0	2.5	47.5	2.00	48.00	400	500
12	4.0	5.0	95.0	3.50	96.50	800	1000
6	10.0	10.0	190.0	5.00	195.00	1600	2000

Table 2.4: Required reagents needed for siRNA transfection per well. The table outlines the volumes of required reagents to perform siRNA mediated silencing of claudin-1. Volumes outlined are per well of the indicated multi-well plate.

Once prepared, the contents of tube 1 and 2 were incubated at room temperature for 5 minutes. The siRNA solution from tube 1 was then transferred to tube 2, briefly vortexed and incubated for a further 15 minutes at room temperature. After 15 minutes, the culture media was removed on the HepG2 cells and replaced with a volume of fresh complete antibiotic-free media minus the volume of the transfection mixture as shown in Table (2.4). The transfection mixture was added dropwise, directly onto the cells. Cells were then incubated overnight at 37^{o}C + 5% CO_2. Cell culture media was removed and replaced with 2ml fresh antibiotic-free media, 24 hours post transfection. The level of claudin-1 expression was quantified via qPCR at 24hrs, 48hrs, 72hrs and 96hours to determine the optimum silencing incubation time. The maximum decrease in claudin-1 expression was achieved after 72hours incubation and this time point was therefore chosen for subsequent experiments.

2.6 RNA extraction

RNA extraction from cells was performed in accordance with the TRIsure protocol (Bioline BIO-38033), which has been modified as a result of optimization, using sterile RNase-free plastic ware and tips. Cells intended for RNA extraction were plated as a monolayer in 6 well plates at $5x10^5$ cells per well. 1ml of TRIsure was used to lyse cells directly on the plate; it was divided equally between the occupied wells and incubated at room temperature for five minutes. The lysate was pipetted against the plate surface to insure complete cell detachment and lysis. The TRIsure/cell lysate mixture was pooled, transferred to a sterile 1.5ml Eppendorf tube and 200µl chloroform (Fisher Scientific 10053213) was added. The caps of the centrifuge tubes were tightly closed and shaken vigorously for 15 seconds until a pale green emulsion was formed. Samples were incubated at room temperature for 2-3 minutes and centrifuged at 12,000xg for 15 minutes in a refrigerated centrifuge at 2-4^{o}C. The resulting sample contained three separate phases; a colorless upper aqueous phase containing RNA, an intermediate cell debris phase, and a lower pale green organic phase. The upper aqueous phase was then carefully transferred to a new sterile 1.5ml Eppendorf tube by pipetting, insuring no intermediate or organic phase is disturbed or transferred. The sample was mixed with 0.5ml ice-cold isopropyl alcohol, incubated for 10 minutes at room temperature and centrifuged at 12,000xg for 10 minutes at 2-4^{o}C to precipitate the RNA. The supernatant was removed, and the pelleted RNA was by resuspended and washed in 1ml of 75% ethanol. The sample was then vortexed and centrifuged at 7500xg for five minutes at 2-4^{o}C. The ethanol was discarded and the pellet left to air-dry at room temperature for approximately 10 minutes. The pelleted RNA was resuspended in 50µl Milli Q water, quantified on a Nanodrop spectrophotometer and ran on a 1% T.A.E agarose gel to test RNA concentration, purity and size. RNA was either used immediately or stored at -80^{o}C.

2.7 Protein extraction

After the upper aqueous phase was been removed and the RNA extracted, the remaining interphase and lower organic phase were processed to extract DNA and protein. DNA was first precipitated out of the sample by adding 0.3ml 100% ethanol. The sample was then mixed by inversion, incubated at RT for three minutes and then centrifuged at 2000 x g for five minutes at 4°C. The supernatant was retained and transferred to a new 2ml Eppendorf tube, leaving the pelleted precipitated DNA. DNA at this stage can be further purified or discarded if not needed. The retained supernatant was mixed with 1.5ml isopropyl alcohol and incubated for 10 minutes at room temperature on an orbital shaker (med/high speed). The sample was centrifuged at 12000 x g, for 10 minutes at 4°C to precipitate the protein. The supernatant was removed, and 2ml 0.3M guanidine hydrochloride in 95% ethanol was added to wash the protein pellet. The sample was incubated at room temperature for 20 minutes on an orbital shaker (med/high speed) followed by centrifuging at 7500 x g for five minutes at 4°C. The guanidine hydrochloride/ethanol was discarded and the pellet wash was repeated at least once more to remove organic contaminants. Following the wash steps, 2ml of 100% ethanol was added to the pellet. The sample was vortexed and incubated at room temperature for 20 minutes on an orbital shaker (med/high speed) followed by centrifuging at 7500 x g for five minutes, at 4°C. The supernatant was removed and the pellet dried using either a vacuum or silica filled desiccator. Once completely dry, 250µl 1% SDS was added and sample heated to 50°C to aid resuspension. Pipetting and freeze thaw cycling was used to aid resuspension if the protein pellet was large. Once re-suspended, protein samples were stored at -20°C.

2.8 T.A.E/T.B.E Gel electrophoresis

Gel electrophoresis was used to separate and analyse RNA and DNA molecules. RNA and DNA were separated on T.A.E and T.B.E gels respectively, to assess the purity and size of the nucleic molecules. Premade T.A.E/T.B.E gels were melted as required by steaming for 45 minutes or microwaving for 1 minute 30 seconds in a 750-watt microwave. Once cooled but still molten, 2µl of Gel-Red (Biotium 41003-1) was added to the gel and gently agitated until fully dissolved. The gel was then poured into a Fisherbrand Midi Horizontal Gel System (FisherScientific 11853303) with two end plates to contain the gel, and a comb to create wells for loading the RNA/DNA. Once set, the end plates and comb were removed and either T.A.E/T.B.E buffer, to match gel type, was added until the max fill mark. Samples were then mixed with 5µl loading dye and carefully pipetted into the loading wells. Once loaded, the gel system was connected to an omniPAC MIDI Power Supply (Cleaverscientific CS-300v) and ran at 50v. When the sample had fully entered the gel the voltage was increase to 100v. The gel was run until the solvent front reached ¾ of the length of the gel, then imaged using a ChemiDoc MP System (Bio-Rad 1708280)

2.9 cDNA synthesis Protocol

Extracted RNA was converted to a cDNA template for use in real-time PCR amplification. cDNA synthesis was performed in accordance with the Tetro cDNA synthesis kit (Bio-line BIO-65043) using sterile RNase-free plastic ware and tips.

Reagent	Volume
Random Hexamer Primer	1µl
10mM dNTP mix	1µl
5x RT Buffer	4µl
RiboSafe RNase Inhibitor	1µl
Tetro Reverse Transcriptase (200u/µl)	1µl
1500ng RNA	*n*µl
Milli Q water	to 20µl

Table 2.5: cDNA synthesis mastermix reagents. The table outlines the volumes of required reagents to perform cDNA synthesis reaction from mRNA template. Volumes outlined are enough for a single reaction.

The cDNA master mix was prepared on ice, in an RNase free environment. Samples were gently mixed by pipetting, briefly centrifuged and incubated in a Mastercycler nexus gradient PCR machine (Eppendorf 6331000017) for:

- 10 minutes at 25^{o}C
- 30 minutes at 45^{o}C
- 5 minutes at 85^{o}C
- Hold 4^{o}C

The samples were immediately placed on ice following the 85^{o}C termination step. cDNA was diluted 1/5 before use by adding 80µl MilliQ water per sample. The cDNA template was then either used immediately or stored at -20^{o}C.

2.10 Real-Time PCR

Real-Time PCR was performed in accordance with the iTaq Universal SYBR Green supermix (Bio-Rad 1725124) protocol which has been modified as a result of optimization. Table 2.6 outlines the reagents required to make a master mix for each sample. Primer sequences used to amplify specific DNA targets are outlined in table 2.9.

Reagent	Volume
iTaq Universal SYBR Green supermix	5µl
Forward Primer	1µl*
Reverse Primer	1µl*
Milli Q Water	2µl
cDNA (Diluted cDNA)	1µl

*working concentration of primers = 300nM in a 10µl reaction

Table 2.6: Real-Time PCR mastermix reagents per well. The table outlines the volumes of required reagents to perform a RT-PCR reaction using cDNA template. Volumes outlined are enough for a single reaction.

Real-Time PCR mastermix was prepared on ice, in an RNase free environment using sterile, RNase-free plastic ware and tips. Triple replicates of each reaction were produced for each target gene and the housekeeping genes. An 10% extra mastermix was produced to allow for minor pipetting errors. The 10µl mastermix produced for each sample and housekeeping genes were pipetted into a Hard-Shell 96-Well PCR Plate (Bio-Rad 1845098) and covered using an adhesive Microseal (Bio-Rad MSB1001). A negative control containing Milli Q water in place of cDNA was used to monitor contamination. The PCR plate was then centrifuged at 1000rpm for 1 minute in an Eppendorf 5430R centrifuge with a swing bucket rotor A-2-MTP (Eppendorf 5428000414) before being placed into the CFX

Connect Real-Time PCR Detection System (Bio-Rad 1855196)

All samples were ran using the following protocol:

Stage	Temp	Time
Initial denaturation	95°C	2 minutes
40 Cycles	95°C	15 secs
	60°C	1 min
Melt Curve	60°C-95°C	Varies
Hold 4°C		

Table 2.7: Real-Time PCR cycling conditions. The table outlines the RT-PCR cycling conditions required to amplify genes of interest.

A melt curve, ranging from 60ºC to 95ºC in 0.5ºC increments, was produced to identify if the amplified targets produced were single, specific products. This was also verified by running the product out on a 2% T.B.E gel

The expression of each gene was assessed against β-actin and GAPDH as the endogenous controls. Each sample was amplified on a separate plate which contained a minimum of two repeats, no template and no reverse transcription controls. Each sample was ran twice on two separate occasions creating four amplification profiles for each gene. Any amplification in controls rendered results void. CFX manager software determined baseline threshold, PCR efficiency and CT valves for each gene. Relative expression was calculated by the software by normalising the target gene against the endogenous controls.

2.10.1 PCR primers

All PCR Primers were designed, tested and supplied by PrimerDesign Ltd. They are for Human targets only to be used with SYBR technology. Primers are delivered lyophilized in 600 reaction aliquots. Primers were resuspended in 660µl RNase/DNase free water.

Gene of Interest	Primer Sequence (5' to 3')		Amplicon Size (Base Pairs)
B-Actin	Forward Primer	GCCAACACAGTGCTGTCTGG	202
	Reverse Primer	TACTCCTGCTTGCTGATCCA	
GAPDH	Forward Primer	GTGAAGGTCGGAGTCAACG	192
	Reverse Primer	GGTGAAGACGCCAGTGGACTC	
Claudin-1	Forward Primer	CTGTCATTGGGGGTGCGATA	118
	Reverse Primer	CTGGCATTGACTGGGGTCAT	
E-cadherin	Forward Primer	GGTGCTCTTCCAGGAACCTC	195
	Reverse Primer	GAAACTCTCTCGGTCCAGCC	
Vimentin	Forward Primer	CGGGAGAAATTGCAGGAGGA	105
	Reverse Primer	AAGGTCAAGACGTGCCAGAG	

Table 2.8: List of primer sequences used in Real-Time PCR.The table outlines the RT-PCR primers used during this study to determine mRNA levels of beta-actin, GAPDH, claudin-1, E-cadherin and vimentin. Primers were synthesised by Thermofisher Scientific.

2.11 PrimePCR array protocol

PrimePCR array plates consist of either a 96 or 384 well PCR plate that contain expertly designed and fully wet-lab validated primers which are used to determine gene expression. The plates are available as pathway panels, which contain primers to determine the gene expression profile assorted with certain diseases, pathways or conditions. Three different types of PrimePCR plates were used during the following experiment which are:

- Cell adhesion - Tight junctions (Bio-Rad 10025728)
- Epithelial to mesenchymal transition (EMT) (Bio-Rad 10034143)

- Tumor metastasis (Bio-Rad 10034254)

PrimePCR plates were chosen for the following experiments as they are fully validated, meet all MIQE guidelines and enable quantification of multiple genes in a time efficient and cost-effective way.

A Real-Time PCR mastermix was prepared on ice, in an RNase free environment. Table 2.9 outlines the reagents required to produce a mastermix required for each 96well PrimePCR array plate (Bio-Rad).

Reagent	Volume*
iTaq Universal SYBR Green supermix	550µl
Milli Q Water	440µl
cDNA (Diluted cDNA)	110µl

Table 2.9: Real-Time PCR mastermix reagents per array. The table outlines the volumes of required reagents to run a PrimePCR array plate using cDNA template. Volumes outlined are enough for a single array. *Volumes have been adjusted by 10% to allow for minor pipetting errors. These volumes were x4 if a 384well plate was used.

PrimePCR array plates are produced with lyophilized primers preloaded into each well. To each well, 10µl PCR mastermix was added using an Eppendorf multipette E3 electronic dispenser (Eppendorf 4987000010). Each plate contained wells free for experimental controls and negative controls. Experimental controls were supplied with the PrimePCR plates and added in accordance with the Bio-Rad PrimePCR protocol. Negative control wells contained 10µl PCR mastermix with no lyophilized primers present. Once complete, PrimePCR array plates were sealed using adhesive microseal. The arrays were centrifuged in an Eppendorf 5430R at 1000rpm for one minute.

PrimePCR arrays were available in either 96 or 384 well formats. The Bio-Rad CFX96 Real-Time PCR detection system in conjunction with the CFX manger software was used to amplify and analyse 96 well array formats, whereas the Applied Biosystems 7900HT Fast Real-Time PCR system with 384-well block module (ThermoFisher 4351405), in conjunction with SDS2.4 and RQ manager was used to amplify and analyse 384 well array formats. Each PrimePCR array has a runfile, available from the Bio-Rad website, which allows target, reference and control information to be imported directly into the CFX or SDS PCR software.

Once centrifuged the PrimePCR arrays are loaded into their respective PCR machine dependent on well format. The Runfile is imported and protocol ran, the analysis is then carried out using either CFX or RQ manager software.

2.12 miRNA extraction

miRNA extraction was performed using the mirVana™ miRNA Isolation Kit (ThermoFisher AM1560). Mammalian cells were cultured on a 6 well plate prior to miRNA extraction, cell density and incubation time was dependent on experiment. Three wells containing minimum $2.5x10^5$ cells per well, usually provided sufficient yield of miRNA to progress to PCR. Preceding cell lysis, cell culture medium was aspirated and cells washed in 2ml PBS. The remaining PBS was removed, the plate placed on ice and 250µl lysis/binding solution was added to each well. No more than three wells were processed per column. Cells were incubated in the lysis/binding solution for 5 minutes on an orbital shaker (low/medium speed). Cell lysate was finally broken up using a p1000 pipette, pooled and transferred to a 2ml Eppendorf tube. Cell lysate was then cooled on ice and 1/10 volume of miRNA homogenate additive was added to each sample. Samples were vortexed for 30-60 seconds and returned to the ice for 10 minutes. A volume of Acid-Phenol: Chloroform

(ThermoFisher AM9720) equal to the volume of cell lysate prior to the addition of miRNA homogenate additive was added to each sample (E.g three wells produce 750µl cell lysate, therefore 750µl Acid-Phenol: Chloroform should be added at this stage.) Samples were vortexed for 30-60seconds and centrifuged 10,000xg for 5 minutes at room temperature. Samples at this stage should have distinct aqueous and organic phases separated by a compact interphase, if not repeat the centrifuge step. The aqueous (upper) phase was then removed without disturbing the lower phase and transferred to a fresh tube. It is important to note the volume of aqueous phase transferred. Per sample, 1.25 volumes of 100% ethanol were added to the aqueous phase (E.g 500µl aqueous phase, 625µl 100% ethanol should be added at this stage.) A filter cartridge was then placed into a collection tube and 700µl ethanol/lysate mixture was added. The cartridge was briefly centrifuged at 10,000xg for ~15 sec to pass the mixture though the column and the flowthrough discarded. This process was repeated until all the ethanol/lysate mixture passed through the column. Once all the ethanol/lysate mixture has passed through, 700 µl miRNA Wash Solution 1 was added to the column and briefly centrifuged at 10,000xg for ~5-10 seconds. The flowthrough was discarded and 500µl Wash Solution 2/3 was added and briefly centrifuged at 10,000xg for ~5-10 seconds. The flowthrough was discarded and the process repeated. After two washes in Wash Solution 2/3 the column was centrifuged at 10,000xg for one minute to remove residual fluid from the filter. The filter cartridge was then transferred to a new collection tube insuring no fluid was present on the outside of the cartridge. The elution solution was heated to 95°C and 100µl pipetted onto the centre of the filter. The column was incubated at room temperature for two minutes followed by two minutes centrifuge at max speed. The filter cartridge was then discarded, and the sample quantified on the nanodrop spectrophotometer.

2.13 Megaplex miRNA reverse transcription protocol

The following reverse transcription components were thawed on ice, Megaplex RT Primers A2.1 and B3.0 (ThermoFisher 4399966 and 4444281) and TaqMan MicroRNA Reverse Transcription Kit (ThermoFisher 4366596). The following master mix outlined in table (2.10) should be made separately for both A and B primer sets. To minimise pipetting errors, only ten sample reaction volumes were made, and any remaining reaction mix was frozen at -20°C

Reverse Transcription Reaction Mix Components	**Volume for One Sample (µl)**	**Volume for Ten Samples (µl)‡**
Megaplex™ RT Primers (10×)	0.8	9.00
dNTPs with dTTP (100mM)	0.2	2.25
MultiScribe™ Reverse Transcriptase (50U/µl)	1.5	16.88
10× RT Buffer	0.8	9.00
MgCl2 (25mM)	0.9	10.12
RNase Inhibitor (20U/µl)	0.1	1.12
Nuclease-free water	0.2	2.25
Total:	4.5	50.62

‡ Includes 12.5% excess for volume loss from pipetting.

Table 2.10: miRNA Reverse transcription reaction mix. The table outlines the volumes of required reagents to perform a miRNA reverse transcription reaction from miRNA template. Volumes outlined are for a single reaction (middle column) or for 10 reactions (right hand column)

Each reverse transcription reaction was prepared in an 0.5ml Eppendorf tube and contained:

4.5µL reverse transcription reaction mix + 3µL (1000ng) total RNA

(This produced enough reverse transcribed miRNA for one TaqMan miRNA array plate)

The reaction mixture was then vortexed, briefly centrifuged and placed in a PCR machine using the following conditions:

Stage	Temp	Time
40 Cycles	16°C	2 minutes
	42°C	1 min
Hold	50°C	1 sec
Hold	85°C	5 minutes
Hold 4°C		

Table 2.11: TaqMan MicroRNA cDNA cycling conditions. The table outlines the PCR cycling conditions required to synthesis cDNA from the miRNA template.

The cDNA can be stored at -20°C for up to 6 months if not required immediately.

2.14 TaqMan MicroRNA array protocol

The following components were thawed on ice and combined in accordance with table 2.12

Component	**Volume for One Array** (µl)‡
TaqMan® Universal PCR Master Mix, No AmpErase® UNG, 2✕	450
Megaplex™ RT product	7.5
Nuclease-free water	442.5
Total	900

‡ Includes 12.5% excess for volume loss from pipetting.

Table 2.12: TaqMan miRNA array reaction mix components. The table outlines the volumes of required reagents to run a TaqMan miRNA array card. Volumes outlined are enough for a single array card.

The reaction mix was vortexed and briefly centrifuged. The TaqMan miRNA array card was unpackaged and 100µl reaction mixture was pipetted into reservoirs 1-8 via the fill port. The TaqMan array card was then placed vertically in a Sorvall Legend RT centrifuge with a rotor for TaqMan Array Micro Fluidic Cards (Sorvall 100715). The card was then centrifuged at 1200rpm (331xg) for one minute and checked to see if the fluid had migrated into the card evenly. If so, the card was centrifuged again for one minute, if not, the card was discarded. Once centrifuged, the array was placed foil side down on the TaqMan array card sealer insuring the correct orientation and starting position of the carriage. The carriage was

then drawn across the array card sealing it. Using scissors, the fill strip was removed from the TaqMan array card and discarded.

The TaqMan array card was then inserted into the Applied Biosystems 7900HT Fast Real-Time PCR system with TLDA block (ThermoFisher 4329012) installed. The SDS setup file supplied with the TaqMan array cards was imported into the SDS software and the protocol ran, Table 2.13 outlines the cycling conditions for each array. The run file was then analysed using RQ manager.

Stage	Temp	Time
Initial denaturation (Step1)	50°C	2 minutes
Initial denaturation (Step2)	94.5°C	10 minutes
40 Cycles	97°C	30 secs
	59.7°C	1 min
Melt Curve	60°C-95°C	Varies
Hold 4°C		

Table 2.13: TaqMan miRNA array cycling conditions. The table outlines the RT-PCR cycling conditions required to amplify miRNA genes of interest.

2.15 Western blot protocol

2.15.1 Sample preparation

Protein samples prepared using the TRIsure protocol were quantified using a Nanodrop spectrometer. Equal volumes of Protein sample and sample buffer (β-Mercaptoethanol added) were mixed in a 1.5ml Eppendorf tube. Samples were boiled at 95^{o}C for 5 minutes using a dry bath to reduce and denature proteins. Protein sample can be aliquoted at this point and stored at -20^{o}C.

2.15.2 SDS-PAGE

The outer packaging, comb and foil tape were removed from an Any kD Mini-PROTEAN TGX Stain-Free Protein Gel (Bio-Rad 4568123). The gel was then loaded into the running module of a Mini-PROTEAN Tetra electrophoresis cell for precast gels (Bio-Rad 1658004). Electrode running buffer (x1) was added to the inner and outer chambers to the reference line. If only one gel was run, a blanking plate was added to the opposing site of the cassette. 20-30ug of prepared sample was loaded per well of the gel, up to 30µl of sample could be loaded per well. Samples should be run against wells containing 3ul Precision Plus Protein Dual Colour Standards (Bio-Rad 1610374) as a band size comparison. Once loaded, the tetra electrophoresis cell was assembled and connected to a PowerPac power supply (Bio-Rad 1645052) and ran at 50v (per gel) until the sample had completely entered the gel, at which point the voltage could be increased 100v (per gel). Gels were ran for about 1 hour, or until the samples reach the bottom of the gel. Once run, the gel cassette was opened using a lever (Bio-Rad 456-0000) by levering the top side of the plastic cassette at the points marked by an arrow. The top plastic cover could then be removed and the gel either imaged or blotted.

2.15.3 Stain-free imaging of Mini-PROTEAN TGX Stain-Free protein gel

Once removed from the cassette the stain-free gel was activated and imaged using a ChemiDoc MP System (Bio-Rad 1708280) to assess the quality of the protein separation. The gel was placed directly on the transilluminator after protein separation and the auto exposure setting selected. The software automatically chose the most appropriate settings and activated trihalo compounds which bound to proteins present in the gel and caused them to fluoresce. The software then captured an image of the separated protein bands.

This was used later for normalising the protein amounts between samples to accurately compare protein levels.

2.15.4 Blotting a protein gel

After activation and imaging, the protein was transferred onto the blotting membrane of a Trans-Blot Turbo Midi PVDF Transfer Pack (Bio-Rad 1704157). Two mini gels could be blotted onto a midi transfer pack or the pack can be cut in half if only one gel was needed. A Trans-Blot Turbo Transfer System (Bio-Rad 1704155) was used to electrochemically transfer separated proteins from the gel to the membrane in a semi-dry manor. The transfer pack contains a PVDF membrane sandwiched between two ion reservoir stacks. The base reservoir stack and membrane were placed on the base of the turbo blot cassette. The gel was then placed on top of the PVDF membrane followed by the top reservoir stack. A roller (supplied with the turbo blot system) was used to gently remove any air bubbles within the stack. The top of the cassette was secured and placed into the turbo blot system. The turbo blot system has pre-set settings based on the molecular weight of the protein of interest.

2.15.5 Blocking the membrane

The blot was then transferred into a 50ml falcon tube and 15ml of blocking buffer was added. The tube was placed on a tube roller in the fridge at 4^{o}C over night to block against unspecific antibody binding.

2.15.6 Incubation with primary antibody

Primary antibody was diluted in 2ml of 0.5% (w/v) blocking buffer in accordance with Table 2.14. The blocking solution was removed from the tube containing the blot. The blot was

then washed once for 5 minutes in 15ml TBST of the tube roller at 4ºC. After the wash, the diluted primary antibody was added and incubated on the tube roller for 2 hours at 4ºC. Less specific antibodies require a longer incubation.

2.15.7 Incubation with secondary antibody

The blot was washed 3 times for 5 minutes each in 15ml TBST on the tube roller at 4ºC. Secondary HRP antibody was diluted 1:1000 in 2ml 0.5% (w/v) blocking buffer and added to the tube containing the blot. Blot was incubated on the tube roller for 1 hours at 4ºC.

2.15.8 Protein detection using West Femto Maximum Sensitivity Substrate

Blot was washed 3 times for 5 minutes each in 15ml TBST on the tube roller at 4ºC. The blot was then placed in a plastic tray containing 1ml equal parts stable peroxide solution and the luminol/enhancer solution (SuperSignal West Femto Maximum Sensitivity Substrate, ThermoFisher scientific 34095). The blot was imaged using the ChemiDoc system using auto-exposure settings. The ChemiDoc software also calculated protein normalisation in conjunction with the stain free gels.

2.16 Immunocytochemistry and immunofluorescence protocol

2.16.1 Preparation of 4% paraformaldehyde fixative

For the preparation of 500ml 4% PFA fixative, 400ml 1x PBS was heated to 60ºC in a fume cupboard. Twenty grams of paraformaldehyde powder (sigma P6148-500G) was weighted and added to the PBS, a magnetic stirrer was used to mix the solution. Whilst being mixed, 2M Sodium Hydroxide was added dropwise until the solution cleared. Once dissolved the solution was cooled. The volume was then adjusted up to 500ml using 1x PBS and pH

adjusted to 7.4 using small amounts of dilute HCL. The solution was filtered using a 0.22-micron Nalgene Disposable Filter (ThermoFisher scientific 450-0045) used immediately or stored at -20^{o}C.

2.16.2 Sample preparation

Immunofluorescence staining of cells was performed on glass coverslips (ThermoFisher 150067) in a 24 well plate (ThermoFisher 142485). Slides were coated in 0.1ml 0.01% Poly-L-lysine solution, incubated for 5 minutes, washed in PBS and allowed to dry for 2 hours. Cells were counted and seeded between 3-5x10^{4} cells per well dependent on the length of time before fixing, 72 hours is the average.

2.16.3 Fixation

After 72 hours, the growth media was removed and cells washed twice in PBS. Any remaining PBS was aspirated and 250µl 4% PFA fixative was added to each well. Cells were incubated for 10-15 minutes at room temperature. The PFA was then removed and cells washed three times for 5 minutes in PBS.

2.16.4 Immunostaining

Cells were blocked for 1 hour in 250µl blocking buffer. Primary antibody was added to antibody dilution buffer in accordance with Table 2.14. 250µl antibody/buffer was added per well. Cells were incubated in the primary antibody overnight 12-18hours at 4^{o}C.

The following day, the primary antibody was removed, and cells washed three times for 5 minutes in PBS.

The secondary antibody was added to antibody dilution buffer in accordance with Table 2.15. 250µl antibody/buffer was added per well. Typical concentration for secondary antibodies are 1:500-1:1000. Cells were incubated for 45 minutes-1hour at 37^{o}C.

After incubation, the secondary antibody was removed, and the cells washed three times for 5 minutes in PBS.

Glass coverslips were mounted on glass slides using ProLong gold antifade mountant (ThermoFisher scientific P36930) and allowed to cure for 24hours. Storage was 4^{o}C short term or -20^{o}C long term.

Primary Antibody	Use	Dilution
Claudin-1 Rabbit monoclonal antibody (Cell Signalling #13255)	Western Blotting	1:800 0.5% (w/v) milk blocking buffer
Claudin-1 Rabbit polyclonal antibody (ThermoFisher # 37-4900)	Immunofluorescence	1:100 1% BSA/PBST
β-catenin Rabbit monoclonal antibody (Cell Signalling #8480)	Western Blotting	1:800 0.5% (w/v) milk blocking buffer

Secondary Antibody	Use	Dilution
Anti-rabbit IgG, HRP-linked Antibody (Cell Signalling #7074)	Western Blotting	1:1000 0.5% (w/v) milk blocking buffer
Goat anti-Rabbit IgG, Alexa Fluor 488 (ThermoFisher # A27034)	Immunofluorescence	1:1000 1% BSA/PBST

Table 2.14: List of antibodies used in western-blotting and immunofluorescence. The tables outline primary and secondary antibodies used in western blotting and immunofluorescent procedures. All antibodies were either purchased from Thermofisher Scientific or via New England Biolabs (UK Distributor of Cell Signalling).

2.17 Statistical analysis

PCR data was analysed and normalized gene expression ($2^{-\Delta\Delta CT}$) was generated, using CFX manager analysis software (Bio-Rad). Cell migration data was generated using ImageJ software. Mean, standard deviation and statistical significance, by paired t-test was calculated for each sample and controls using GraphPad Prism (Version 7.0) software for both PCR and migration experiments. In all cases 95% confidence intervals were used. Graphs were produced using GraphPad Prism (Version 7.0) software.

P-values are indicated as below if required:

ns	$P > 0.05$
*	$P \leq 0.05$
**	$P \leq 0.01$
***	$P \leq 0.001$

Chapter 3 - Results

3.1 HepG2 cells as a model of hepatocellular carcinoma.

HepG2 cells were chosen as a model of HCC in the following experiments. Despite originating from a diseased liver, the HepG2 cell line was able to maintain a number of functions similar to normal liver. Individual cells are able to produce and maintain the majority of liver cell surface receptors. They also demonstrated the ability synthesise and secrete plasma proteins and lipoproteins (van IJzendoorn et al 1997).

To investigate how the differential expression of claudin-1 impacts the initiation and progression of HCC, groups of HepG2 cells were created, one with significantly increased levels of the protein, and the other with significantly decreased levels of the protein. A cell line with overexpressed claudin-1 was achieved by lentiviral transduction of $HepG2^{WT}$ (wild type) cells with pLenti-CLDN1 plasmid, and subsequent antibiotic selection produced a stable cell line termed $HepG2^{CLDN\text{-}1+}$. To investigate the decreased expression of claudin-1, HepG2 cells were transfected with CLDN-1 siRNA creating $HepG2^{CLDN\text{-}1-}$ (silenced) cells. $HepG2^{CLDN\text{-}1+}$ and $HepG2^{CLDN\text{-}1-}$ cells were compared their respective transfection/transduction controls $HepG2^{pCMV\text{-}ve}$ and $HepG2^{scambled\text{-}ve}$. $HepG2^{pCMV\text{-}ve}$ cells were created by lentiviral transduction of the empty vector plasmid (pLenti-C-Myc-DDK-IRES-Puro) into $HepG2^{WT}$ and acted the control for comparative $HepG2^{CLDN\text{-}1+}$ experiments. $HepG2^{scambled\text{-}ve}$ was produced by transfecting HepG2 cells with scrambled siRNA, creating a control for comparative $HepG2^{CLDN\text{-}1-}$ experiments. All cells were continuously maintained in DMEM supplemented with 10% FBS and 1% L-Glutamine.

3.2 Justification for the inclusion of results

To ensure data of the highest quality was produced, all PCR experiments followed MIQE guidelines (Bustin et al 2009). These guidelines consist of a framework of standardised requirements that are needed to ensure that data produced is repeatable, consistent and reliable. Although the previous methods section detailed experimental design it is important to outline the criteria in which data produced meets these requirements.

An important aspect outlined in the MIQE guidelines is the determination of the quality of the nucleic acids extracted. The integrity of RNA is critical to providing reliable, representative results as RNA that has been degraded will subsequently influence changes in gene expression during qPCR leading to inaccurate results. All RNA samples used in the following experiments were analysed using a RNA 6000 Nano chip on the Bioanalyzer 2100 (Agilent). The Bioanalyzer can determine RNA integrity, yield, purity and outline traces of contamination. Only RNA samples with an integrity score of 9 or higher and purity ratios (18s/28s) of 1.8 or higher were used in subsequent experiments. Figure 3.1 shows an example assay produced by the Bioanalyzer 2100 providing a visual representation of RNA assessed.

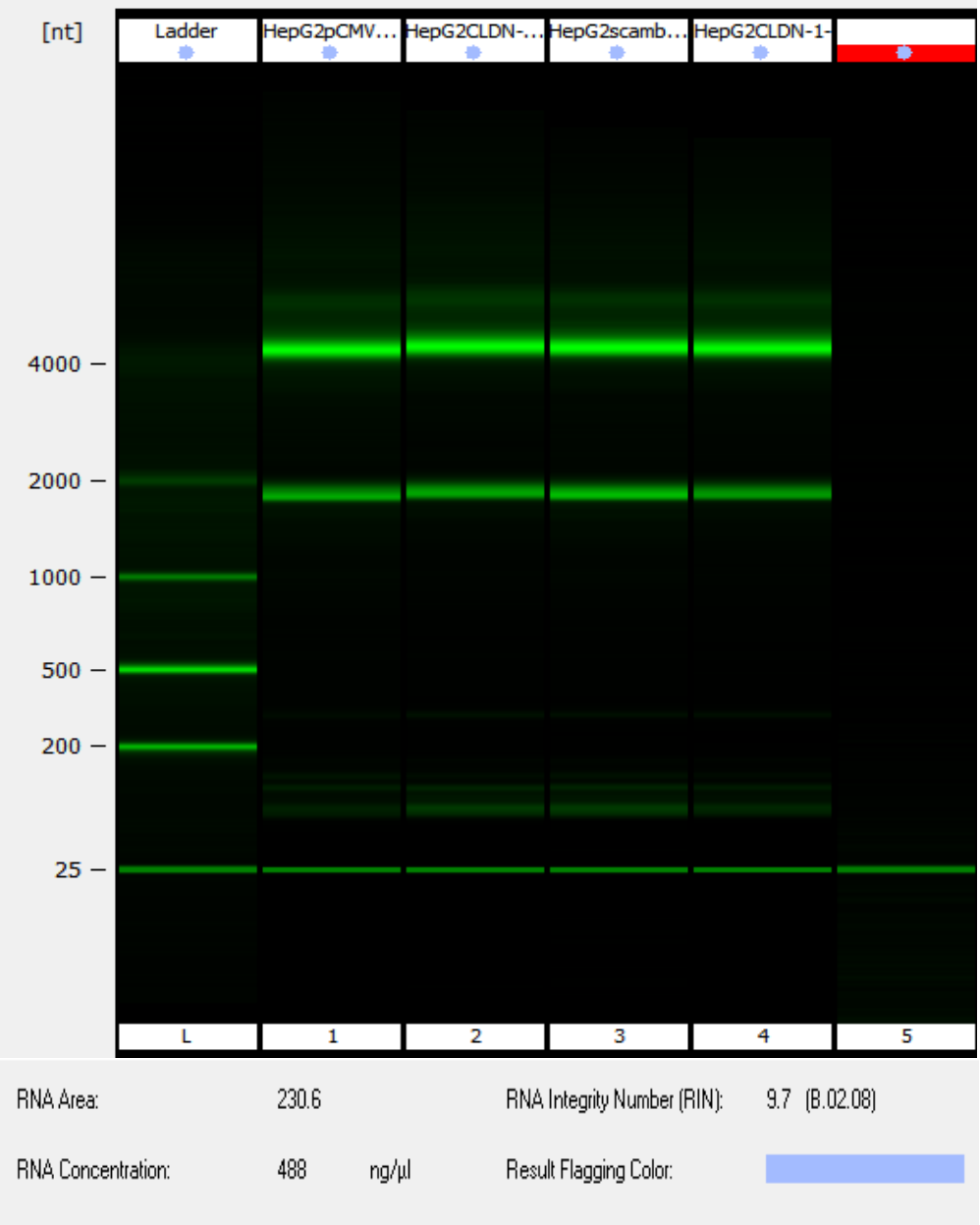

Figure 3.1 Reconstructed digitised gel image of RNA samples on an RNA 6000 Nano chip. Samples consist of Ambion® RNA 6000 Ladder (ThermoFisher) lane L, 500ng HepG2$^{pCMV\text{-}ve}$ RNA lane 1, 500ng HepG2$^{CLDN\text{-}1+}$ RNA lane 2, 500ng HepG2$^{scambled\text{-}ve}$ RNA lane 3, 500ng HepG2$^{CLDN\text{-}1-}$ lane 4. Lane 5 has been left intentionally blank. The data shown represents lane 1 (HepG2$^{pCMV\text{-}ve}$) indicating an RNA Integrity number (RIN) of 9.7.

The purity of a RNA sample was assessed using the Electropherogram produced by the

Bioanalyzer 2100. Figure 3.2 represents the electropherogram of Lane 1

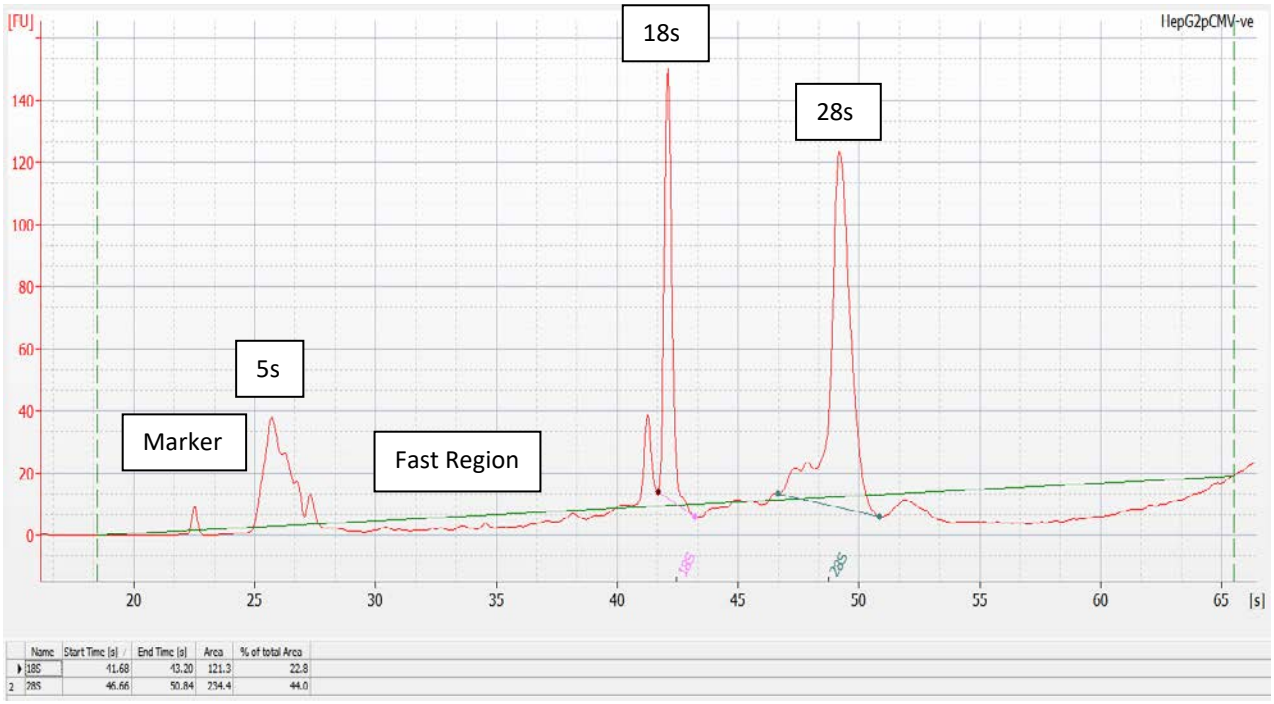

Figure 3.2: An electropherogram of HepG2$^{pCMV\text{-}ve}$ RNA. The above electropherogram shows a HepG2$^{pCMV\text{-}ve}$ RNA sample which has a purity ratio (18s/28s) of 1.9 indicating high purity. High 18s/28s peaks with a small marker peak and regular fast region also indicates non-degraded intact RNA.

Another important aspect outlined by the MIQE guidelines is the identification and exclusion of samples with poor qPCR product amplification.

Samples that displayed the following criteria were excluded from data analysis

- Negative control with a Cq less than 39
- NTC with Cq less than 39
- NRT with Cq less than 39
- Positive control with Cq greater than 35
- PCR efficiency greater than 110%
- PCR efficiency less than 90%
- Replicate group Cq Standard Deviation greater than 0.2
- Replicate group with more than 1 Cq difference
- Replicate group melt curves with more than 1°C difference
- Any melt curve with more than one product amplified (twin peak)

Figures 3.3 and 3.4 are examples of efficient qPCR, none of the above exclusion criteria apply. Whereas figures 3.5 and 3.6 represent poor qPCR and provide an example of data that would be excluded.

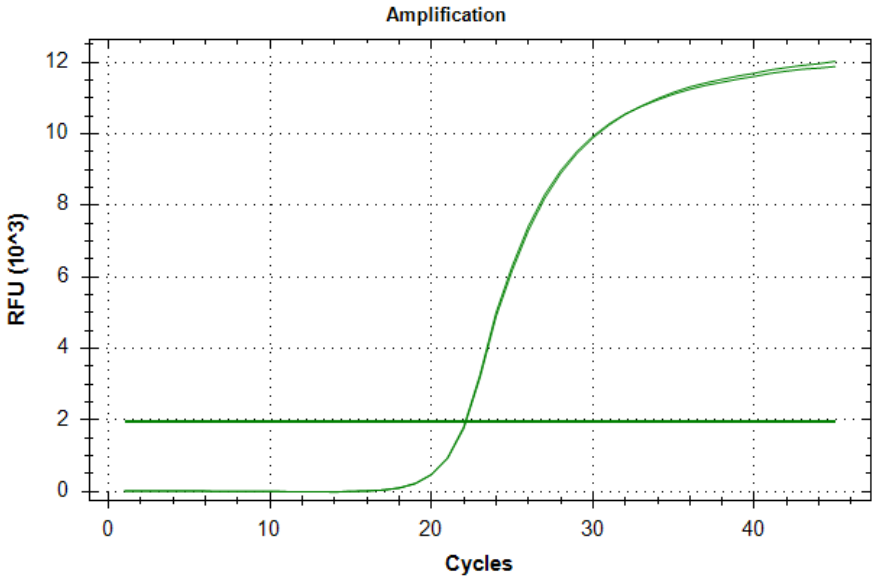

Fluor	Target	Sample	Cq
SYBR	GAPDH	HepG2pCMV-ve	22.09
SYBR	GAPDH	HepG2pCMV-ve	22.13

Figure 3.3 qPCR Amplification curve of GAPDH in HepG2$^{pCMV\text{-}ve}$ cells. The figure shows an amplification curve (relative fluorescence vs. cycle number) of an RT-PCR reaction to determine the expression of GAPDH in HepG2$^{pCMV\text{-}ve}$ cells. This is an example of an acceptable PCR, both technical replicates are only 0.04 Cq apart, are below 35 cycles and have a PCR efficiency of 100%.

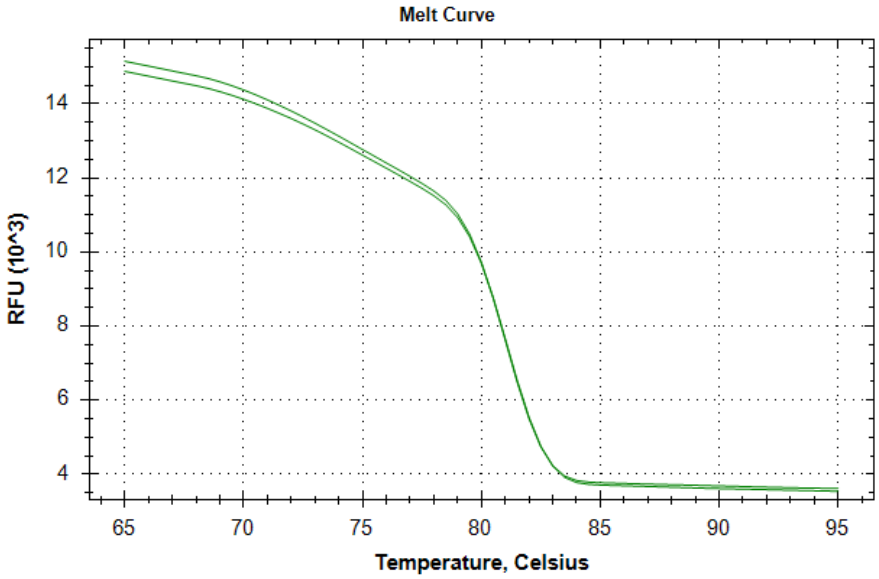

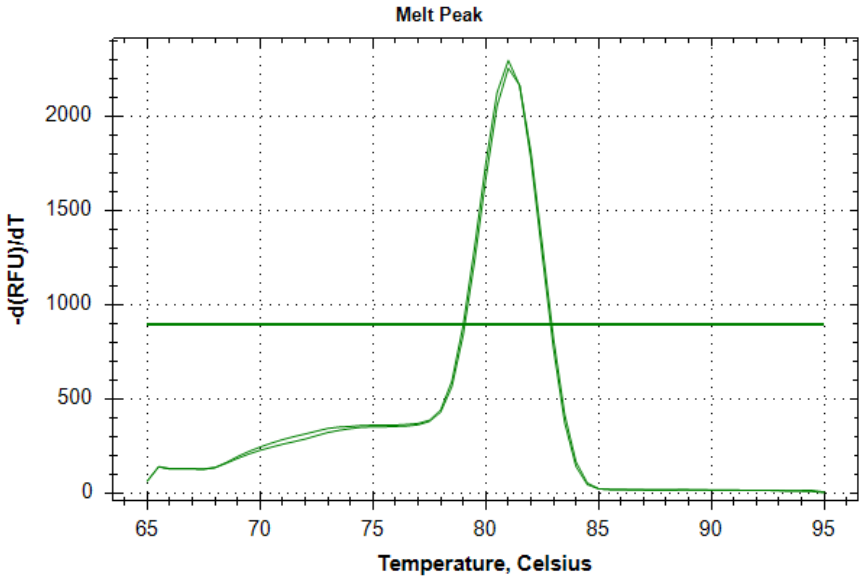

Fluor	Target	Sample	Melt Temp
SYBR	GAPDH	HepG2pCMV-ve	81.00
SYBR	GAPDH	HepG2pCMV-ve	81.00

Figure 3.4 Melt curve and melt peak of GAPDH in HepG2$^{pCMV-ve}$ cells. The figure shows a melt curve and peak (relative fluorescence vs. temperature, celsius) of an RT-PCR reaction to determine the melting temperature of the formed GAPDH PCR product generated from HepG2$^{pCMV-ve}$ cells. This is an example of an acceptable melt cure and peak, both replicates have the same melting temperature and melting peak, indicating only one product has been amplified.

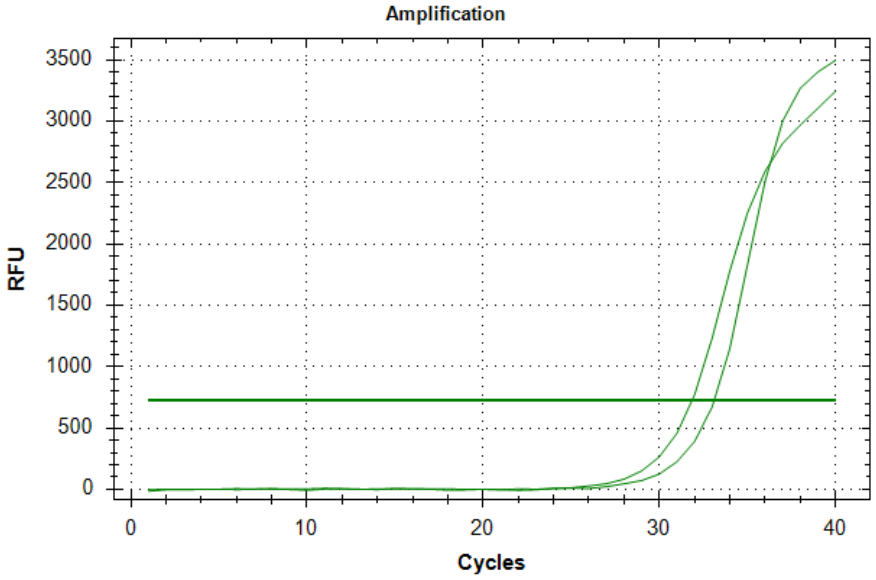

Fluor	Target	Sample	Cq
SYBR	Vimentin	HepG2pCMV-ve	33.11
SYBR	Vimentin	HepG2pCMV-ve	31.85

Figure 3.5 qPCR Amplification curve of vimentin in HepG2$^{pCMV\text{-}ve}$ cells. The figure shows an amplification curve (relative fluorescence vs. cycle number) of an RT-PCR reaction to determine the expression of vimentin in HepG2$^{pCMV\text{-}ve}$ cells. This is an example of an unacceptable PCR run, the technical replicates are over 1 cycle apart. The efficiency is within acceptable range but is less than 100%

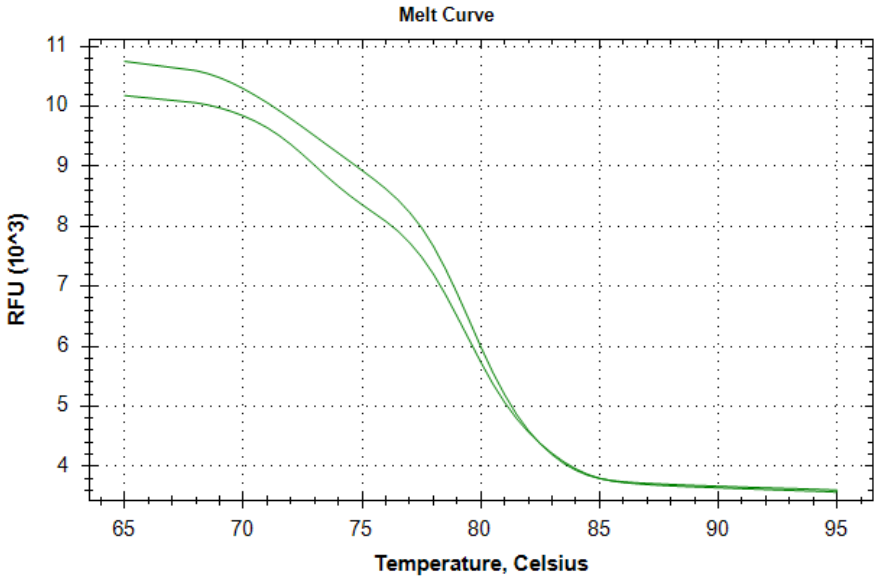

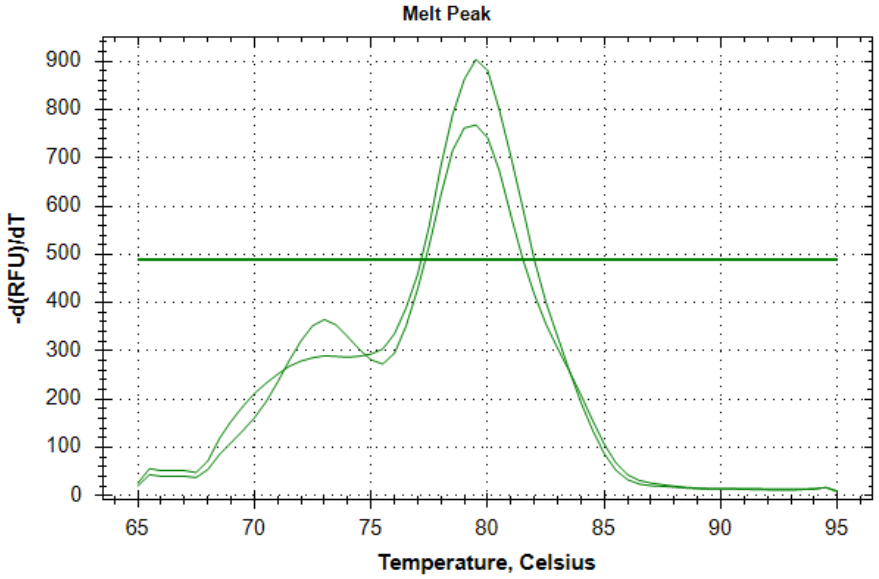

Fluor	Target	Sample	Melt Temp
SYBR	Vimentin	HepG2pCMV-ve	79.50
SYBR	Vimentin	HepG2pCMV-ve	79.50

Figure 3.6 Melt curve and melt peak of vimentin in HepG2$^{pCMV\text{-}ve}$ cells. The figure shows a melt curve and peak (relative fluorescence vs. temperature, celsius) of an RT-PCR reaction to determine the melting temperature of the formed vimentin PCR product generated from HepG2$^{pCMV\text{-}ve}$cells. This is an example of an unacceptable melt cure and peak. The melt peak shows two products formed, indicative of the formation of primer dimers. The problem here was poor primer design this was fixed in later experiments.

Only qPCR data that conforms to these exclusion criteria were analysed and included in the results section. All data was included regardless of fold change, however changes in expression were only considered to be increased/decreased if the change was statistically significant i.e the P value is less than 0.05.

3.3 Determining the localisation of claudin-1 using immunofluorescence.

The localisation of claudin-1 was determined using immunofluorescence and confocal microscopy. Cells were processed as per the immunofluorescence protocol outlined in the methods section. Cells grown on glass coverslips were mounted on glass slides using Profade mounting media, cured overnight at 4^{o}C and imaged at x20 on the confocal microscope.

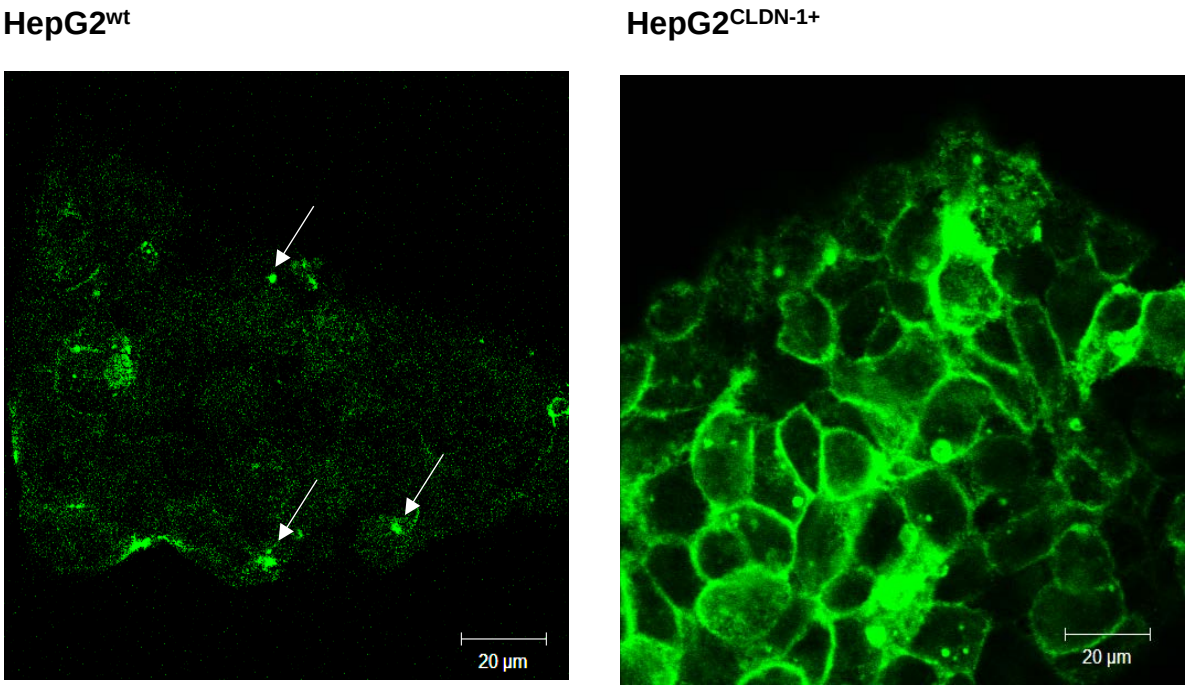

Figure 3.7: Localisation of claudin-1 in HepG2^{wt} and HepG2$^{CLDN-1+}$. Localisation of claudin-1 in cultured HepG2 cells at x20 magnification. The image on the left represents wild-type HepG2 cells and the image on the right represents HepG2 cells that overexpress claudin-1. The white arrows on the left picture indicate the localisation of bile canaliculi.

The fluorescent micrograph showed claudin-1 localisation in non-polarized HepG2^{wt} cells was evenly distributed at the cell membrane between basal/lateral surfaces, with a slight increase in concentration around the forming apical surface. When HepG2^{wt} cells began to polarise and form bile canaliculi like structures (indicated by the white arrows above), claudin-1 redistributed to the apical bile canaliculi surface from the basal/laterals edges. The overexpression of claudin-1 in HepG2$^{CLDN\text{-}1+}$ cells caused the protein to be more evenly distributed across the basal/lateral and apical surfaces with increased pools of intracellular claudin-1. Effective staining of claudin-1 in HepG2$^{CLDN\text{-}1-}$ cells could not be achieved due to the very low levels of the protein.

3.4 Determining the expression of claudin-1 by RT-PCR

The mRNA expression of claudin-1 was determined in HepG2$^{CLDN-1+}$, HepG2$^{CLDN-1-}$ and their respective controls HepG2$^{pCMV-ve}$, HepG2$^{scambled-ve}$ via RT-PCR.

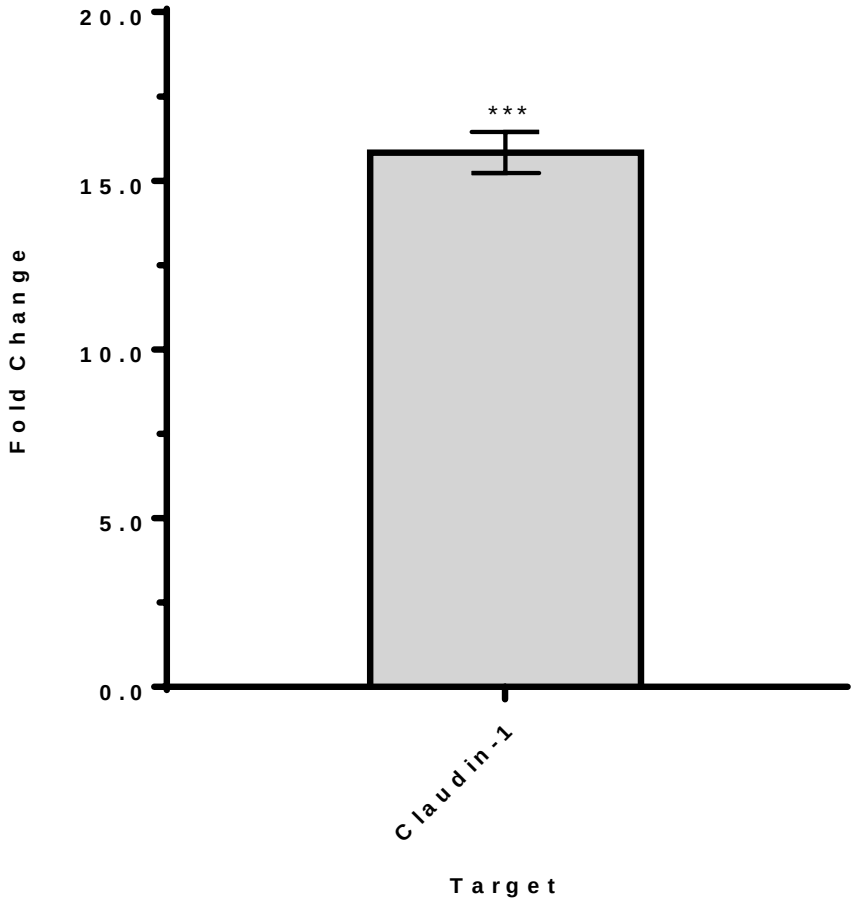

Figure 3.8: Normalized gene expression ($2^{-\Delta\Delta CT}$) of claudin-1 in HepG2$^{CLDN-1+}$ cells. HepG2$^{CLDN-1+}$ and HepG2$^{pCMV-ve}$ cells were cultured for 72 hours prior to total RNA extraction. Amplification of claudin-1 was performed alongside GAPDH as a reference gene using RT-PCR. Relative normalised gene expression was calculated using the $2^{-\Delta\Delta CT}$ method. Data presented is representative of mean fold change ±s.e.m from three biological replicates. Paired t-test was performed to determine statistical significance, *** P≤0.001.

Claudin-1 levels were shown to be significantly increased in HepG2$^{CLDN-1+}$ cells by 15.8 fold (p=0.0005) compared to HepG2$^{pCMV-ve}$.

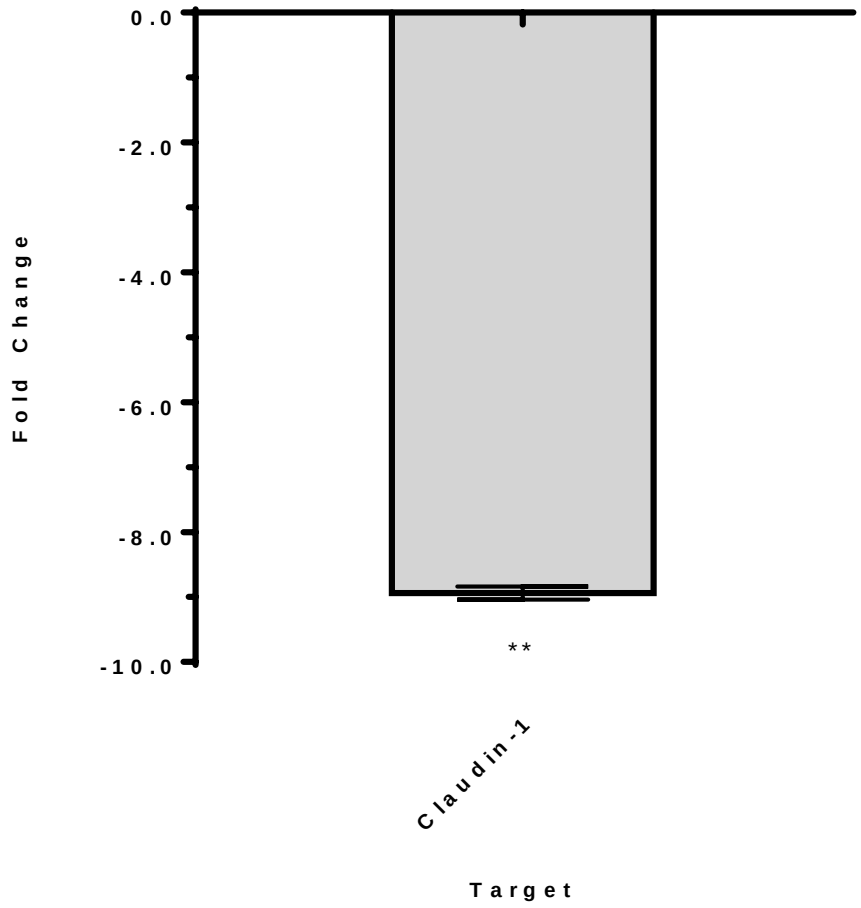

Figure 3.9: Normalized gene expression ($2^{-\Delta\Delta CT}$) of claudin-1 in HepG2$^{CLDN-1-}$ cells. HepG2$^{CLDN-1-}$ and HepG2$^{scambled-ve}$ cells were cultured for 72 hours prior to total RNA extraction. Amplification of claudin-1 was performed alongside GAPDH as a reference gene using RT-PCR. Relative normalised gene expression was calculated using the $2^{-\Delta\Delta CT}$ method. Data presented is representative of mean fold change ±s.e.m from three biological replicates. Paired t-test was performed to determine statistical significance, ** P≤0.01.

claudin-1 levels were shown to be significantly decreased in HepG2$^{CLDN-1-}$ cells by -8.9 fold (p=0.0014) compared to HepG2$^{scambled-ve}$.

3.5 Determining the expression of claudin-1 by western-blot

The protein expression of claudin-1 was determined in HepG2$^{CLDN-1+}$, HepG2$^{CLDN-1-}$ and their respective controls HepG2$^{pCMV-ve}$, HepG2$^{scambled-ve}$ via western blotting.

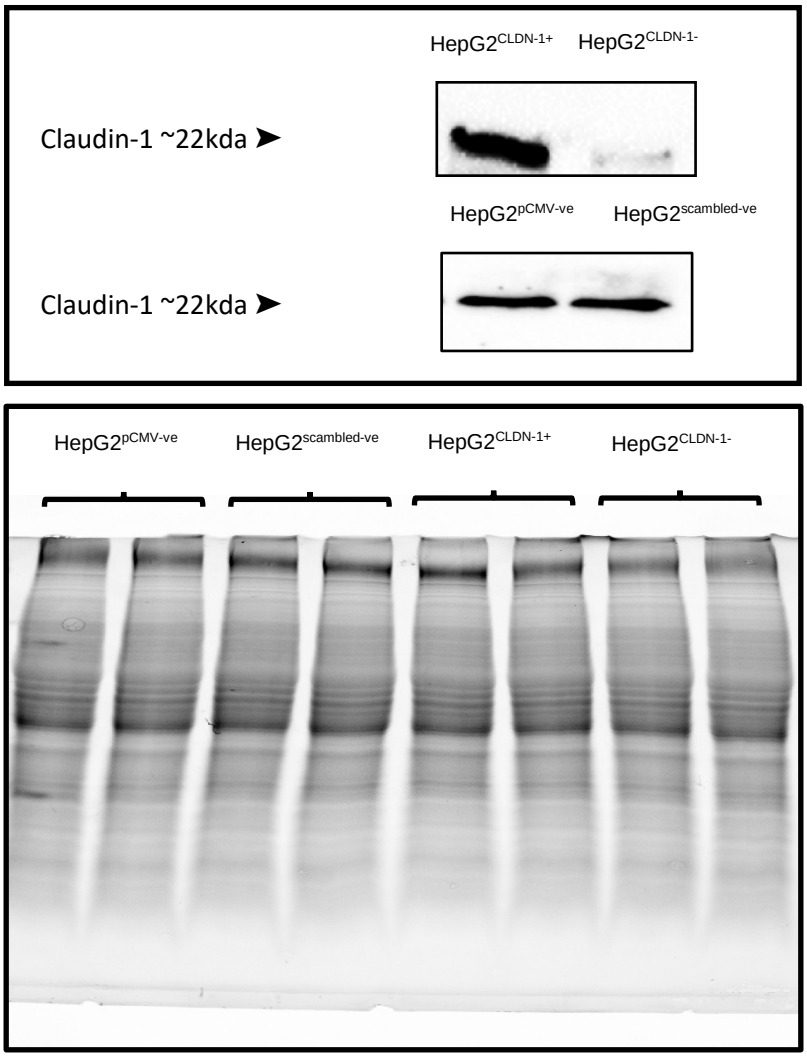

Figure 3.10: Claudin-1 protein expression in HepG2$^{CLDN-1+}$, HepG2$^{CLDN-1-}$ and the respective controls HepG2$^{pCMV-ve}$ and HepG2$^{scambled-ve}$ cells. HepG2$^{CLDN-1+}$, HepG2$^{CLDN-1-}$ and their respective controls HepG2$^{pCMV-ve}$, HepG2$^{scambled-ve}$ were cultured for 72 hours prior to cell lysis and extraction using TRIsure. Protein concentration was determined using a nanodrop spectrophotometer. Cell lysates were denatured and subjected to SDS-PAGE and immunoblot to determine the protein expression of claudin-1. The first image (above) represents an immunoblot which has been probed using a Claudin-1 Rabbit monoclonal antibody (Cell Signalling #13255) on samples HepG2$^{CLDN-1+}$, HepG2$^{CLDN-1-}$ and HepG2$^{pCMV-ve}$, HepG2$^{scambled-ve}$. The second image (below) represents a stain-free gel used as a loading control. Normalised expression was calculated using Bio-Rad Stain Free Technology and Lab Manager software. Data presented is representative of mean fold change ±s.e.m from three biological replicates. Paired t-test was performed to determine statistical significance.

Normalisation using stain-free technology determined HepG2$^{CLDN-1+}$ cells to contain a 6-fold increase in claudin-1 protein compared to HepG2$^{pCMV-ve}$ cells (P=0.009). HepG2$^{CLDN-1-}$ showed a -5 fold decrease compared to HepG2$^{scambled-ve}$ cells (P=0.03).

3.6 Determining the expression of tight junctional and associated genes in claudin-1 overexpressing and claudin-1 silenced HepG2 cells.

Claudins are arguably the main constituents of the tight junction and have been shown to regulate other tight junctional components in a number of pathophysiological events including cancers. Claudin-1, and other tight junction constituents are responsible for the maintenance of cellular contact and cell-cell adhesion. During cancer progression, tight junctional and associated genes are differentially expressed. An important initiation step in the metastasis and invasion of certain cancers involves regulation of expression of these tight junctional and associated genes to favour a less adherent phenotype. Changes in tight junction composition are thus key aspects in cancer metastasis and therefore their profile may help predict tumour behaviour.

To investigate this, the expression of tight junctional and associated genes in claudin-1 overexpressing and claudin-1 silenced HepG2 cells were analysed using a PCR panel of 21 target and housekeeping genes.

3.6.1 Expression of tight junctional and associated genes in claudin-1 overexpressing HepG2 cells

Target	Sample	Expression ($2^{-\Delta\Delta CT}$)	Expression ($2^{-\Delta\Delta CT}$) Standard Deviation	Compared to Regulation Threshold	P-Value	Exceeds P-Value Threshold (0.05)
Glyceraldehyde 3-phosphate dehydrogenase	HepG2 CLDN-1+	1.025	0.002	No change	0.856	Yes
Beta-actin	HepG2 CLDN-1+	1.033	0.366	No change	0.997	Yes
Caveolin-1	HepG2 CLDN-1+	38.952	1.976	Up regulated	0.010	No
Caveolin-2	HepG2 CLDN-1+	3.024	0.190	Up Regulated	0.010	No
Claudin-1	HepG2 CLDN-1+	15.839	0.614	Up regulated	0.001	No
Claudin-2	HepG2 CLDN-1+	2.995	0.096	Up regulated	0.003	No
Claudin-3	HepG2 CLDN-1+	1.158	0.177	No Change	0.413	Yes
Claudin-4	HepG2 CLDN-1+	-2.246	0.193	Down regulated	0.004	No
Claudin-5	HepG2 CLDN-1+	-5.694	0.040	Down regulated	0.032	No
Claudin-7	HepG2 CLDN-1+	5.468	0.236	Up regulated	0.002	No
Claudin-8	HepG2 CLDN-1+	-1.224	0.109	Down regulated	0.288	Yes
Claudin-11	HepG2 CLDN-1+	-23.084	0.004	Down regulated	0.002	No
ZONAB	HepG2 CLDN-1+	3.163	0.312	Up regulated	0.003	No
Junctional adhesion molecule A	HepG2 CLDN-1+	-10.424	0.003	Down regulated	0.002	No
Junctional adhesion molecule B	HepG2 CLDN-1+	6.208	1.576	Up regulated	0.005	No

Junctional adhesion molecule C	HepG2 CLDN-1+	1.277	2.647	No Change	0.544	Yes
Occludin	HepG2 CLDN-1+	-1.761	0.044	Down regulated	0.007	No
Zonula occludens-1 (ZO-1)	HepG2 CLDN-1+	-1.902	0.082	Down regulated	0.045	No
Zonula occludens-2 (ZO-2)	HepG2 CLDN-1+	-14.775	0.014	Down regulated	0.006	No
Zonula occludens-3 (ZO-3)	HepG2 CLDN-1+	-6.294	0.183	Down regulated	0.009	No
Serine/Threonine-Protein Kinase WNK4	HepG2 CLDN-1+	-17.176	0.013	Down regulated	0.001	No

Table 3.1: Normalised gene expression ($2^{-\Delta\Delta CT}$) of tight junctional and associated genes in claudin-1 overexpressing HepG2 cells. The table details the relative normalised gene expression of 21 tight junctional and associated genes in $HepG2^{CLDN-1+}$ cells, $HepG2^{pCMV-ve}$ cells were used as the control. $HepG2^{CLDN-1+}$ and $HepG2^{pCMV-ve}$ cells were cultured for 72 hours prior to total RNA extraction. Amplification of the genes outlined in Table 3.1 was performed alongside GAPDH and beta-actin as the reference genes using RT-PCR. Relative normalised gene expression was calculated using the $2^{-\Delta\Delta CT}$ method. Data presented is representative of mean fold change ±s.e.m from three biological replicates. Paired t-test was performed to determine statistical significance. Statistical significance is indicated if the P value is lower than the 0.05 threshold.

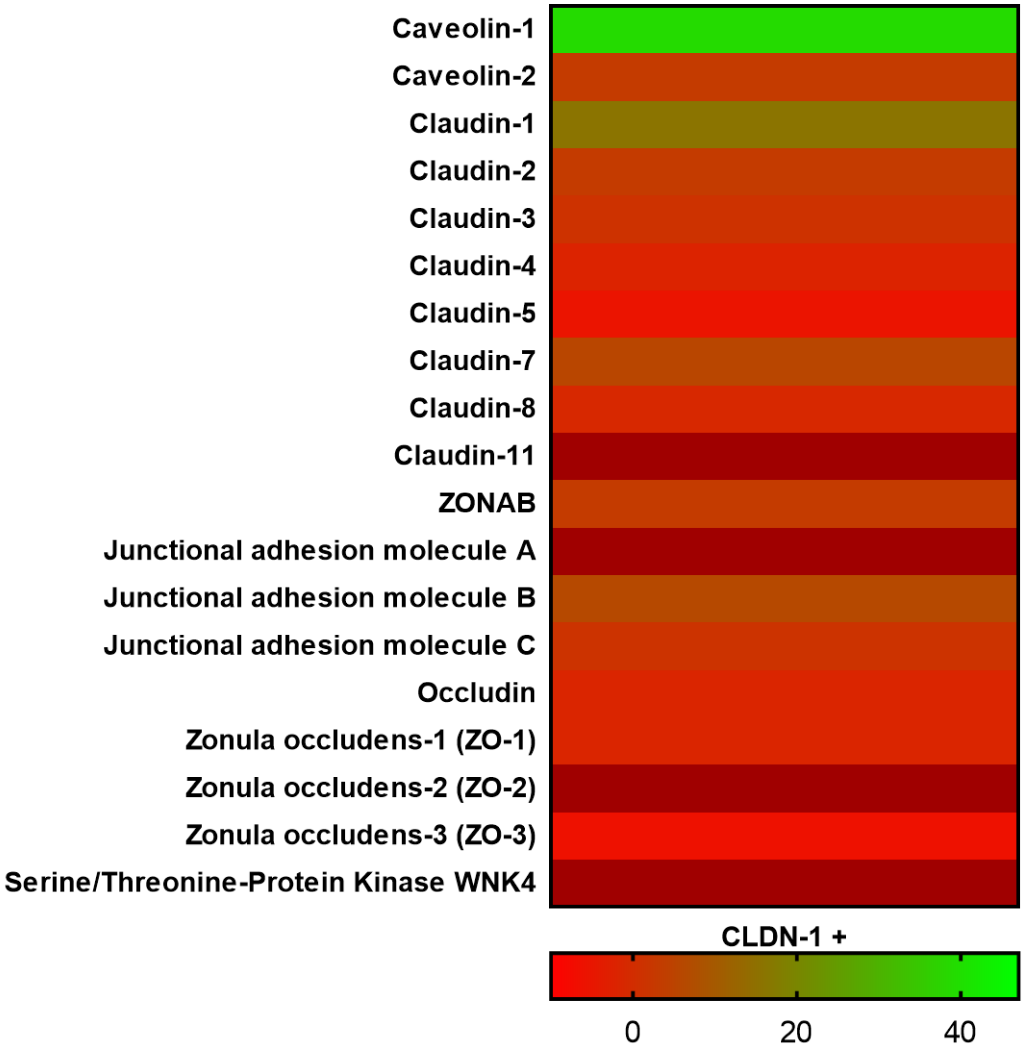

Figure 3.11 Heat map representing normalised gene expression ($2^{-\Delta\Delta CT}$) of tight junctional and associated genes in claudin-1 overexpressing HepG2 cells. Normalised gene expression values taken from Table 3.1 have been converted into a colorimetric scale outlined above to provide a visual representation of large-scale changes. Genes indicated by a green bar represent an upregulation in expression, whereas genes indicated by a red bar represent a down regulation in expression.

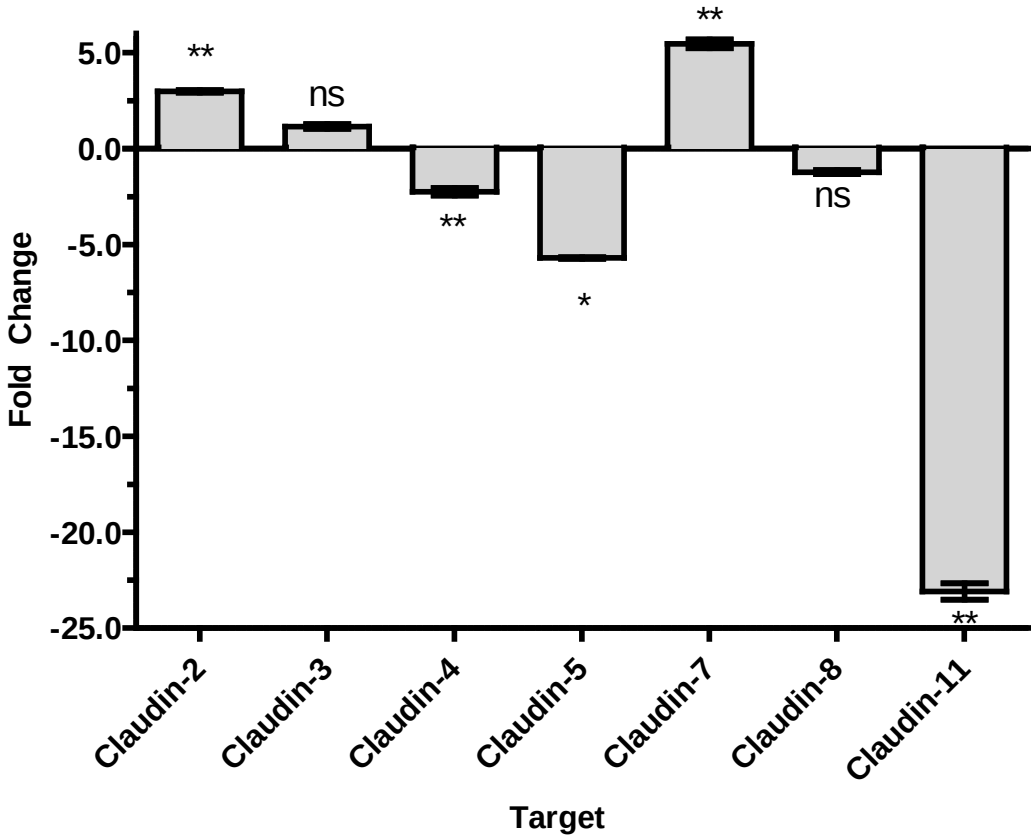

Figure 3.12: Normalized gene expression ($2^{-\Delta\Delta CT}$) of claudins-2, -3, -4, -5, -7, -8, -11 and -18 in HepG2$^{CLDN-1+}$ cells. HepG2$^{CLDN-1+}$ and HepG2$^{pCMV-ve}$ cells were cultured for 72 hours prior to total RNA extraction. Amplification of claudin-1, -2, -3, -4, -5, -7, -8, -11 was performed alongside GAPDH and beta-actin as reference genes using RT-PCR. Relative normalised gene expression was calculated using the $2^{-\Delta\Delta CT}$ method. Data presented is representative of mean fold change ±s.e.m from three biological replicates. Paired t-test was performed to determine statistical significance, ns – no significant * P≤0.05 ** P≤0.01 .

Expression of claudin family members was aberrant in response to claudin-1 overexpression. Claudin-1 levels shown in figure 3.12 were significantly increased in HepG2$^{CLDN-1+}$ cells by 15.7 fold (p=0.0005) compared to HepG2$^{pCMV-ve}$. Claudins -2, -3 and 7 were also upregulated (P=0.002, P=0.413 and P=0.0017 respectively), although claudin-3 was not significant. Claudins -4, -5 -8 and 11 were decreased in HepG2$^{CLDN-1+}$ cells (P=0.003, P=0.032, P=0.287 and P=0.002 respectively), although the decrease in claudin-8 expression was not significant. No expression of claudin-18 could be detected in either HepG2$^{CLDN-1+}$ or HepG2$^{pCMV-ve}$ cells.

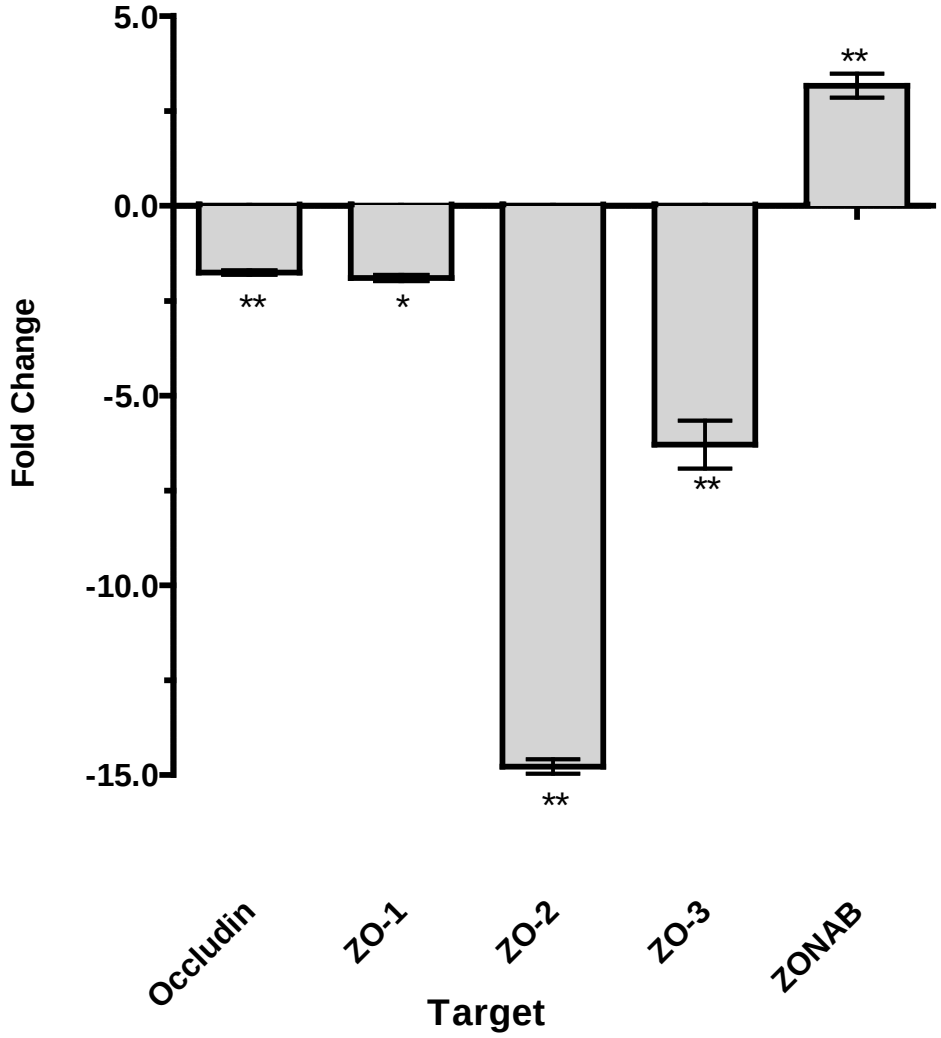

Figure 3.13: Normalized gene expression ($2^{-\Delta\Delta CT}$) of occludin, Zonula Occludens -1, -2 and -3 and ZONAB in HepG2$^{CLDN-1+}$ cells. HepG2$^{CLDN-1+}$ and HepG2$^{pCMV-ve}$ cells were cultured for 72 hours prior to total RNA extraction. Amplification of occludin, Zonula Occludens -1, -2 and -3 and ZONAB was performed alongside GAPDH and beta-actin as reference genes using RT-PCR. Relative normalised gene expression was calculated using the $2^{-\Delta\Delta CT}$ method. Data presented is representative of mean fold change ±s.e.m from three biological replicates. Paired t-test was performed to determine statistical significance, * P≤0.05 ** P≤0.01 .

The expression of occludin in HepG2$^{CLDN-1+}$ cells was decreased compared to HepG2$^{pCMV-ve}$ represented by a -1.76 fold change. Statistical analysis indicated the decrease was significant (P=0.006). The expression of ZO -1, -2 and -3 was shown to be significantly decreased in HepG2$^{CLDN-1+}$ cells compared to HepG2$^{pCMV-ve}$ (P=0.04, P=0.006 and P=0.009 respectively). Whereas the expression of transcription factor ZONAB was shown to be significantly increased compared to HepG2$^{pCMV-ve}$ (P=0.003).

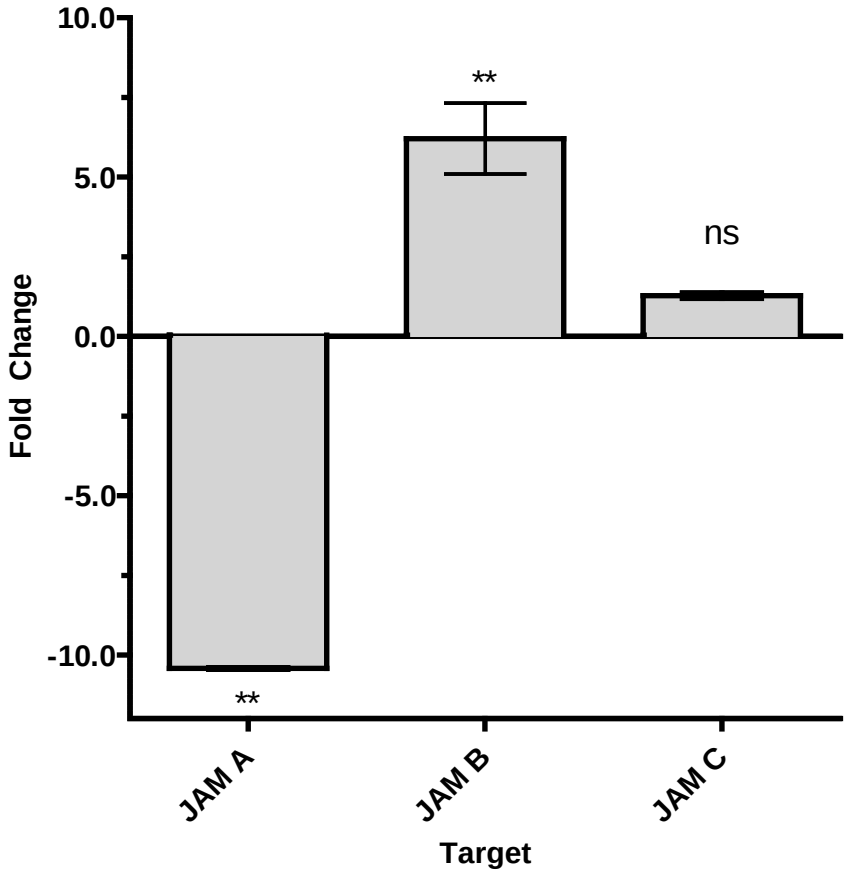

Figure 3.14: Normalized gene expression ($2^{-\Delta\Delta CT}$) of Junctional Adhesion Molecule A, B and C in HepG2$^{CLDN-1+}$ cells. HepG2$^{CLDN-1+}$ and HepG2$^{pCMV-ve}$ cells were cultured for 72 hours prior to total RNA extraction. Amplification of Junctional Adhesion Molecule A, B and C was performed alongside GAPDH and beta-actin as reference genes using RT-PCR. Relative normalised gene expression was calculated using the $2^{-\Delta\Delta CT}$ method. Data presented is representative of mean fold change ±s.e.m from three biological replicates. Paired t-test was performed to determine statistical significance, ns – no significant change ** P≤0.01 .

Gene expression of JAM A was -10.42 fold decreased compared to HepG2$^{pCMV-ve}$ cells P=0.002. However, JAM B showed a significant 6.2 -fold increase (P=0.005) in gene expression. The change in JAM C expression was not significant (P=0.543).

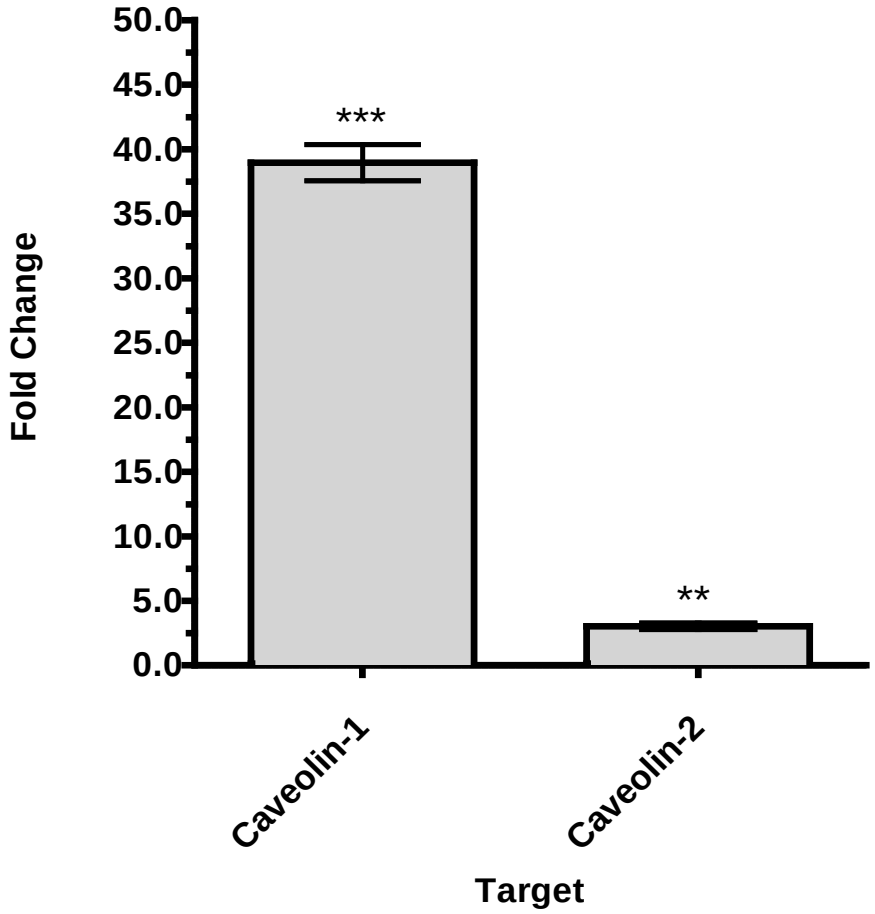

Figure 3.15: Normalized gene expression ($2^{-\Delta\Delta CT}$) of caveolin-1 and -2 in HepG2$^{CLDN-1+}$ cells. HepG2$^{CLDN-1+}$ and HepG2$^{pCMV-ve}$ cells were cultured for 72 hours prior to total RNA extraction. Amplification of caveolin-1 and -2 was performed alongside GAPDH and beta-actin as reference genes using RT-PCR. Relative normalised gene expression was calculated using the $2^{-\Delta\Delta CT}$ method. Data presented is representative of mean fold change ±s.e.m from three biological replicates. Paired t-test was performed to determine statistical significance, ** P≤0.01 *** P≤0.001 .

Both caveolin-1 and -2 were shown to be significantly increased in HepG2$^{CLDN-1+}$ cells compared to HepG2$^{pCMV-ve}$ ($P<0.0001$ and $P=0.009$). Caveolin-1 was increased by a massive 38.9 fold compared to control, whereas caveolin -2 was upregulated 3.0 fold.

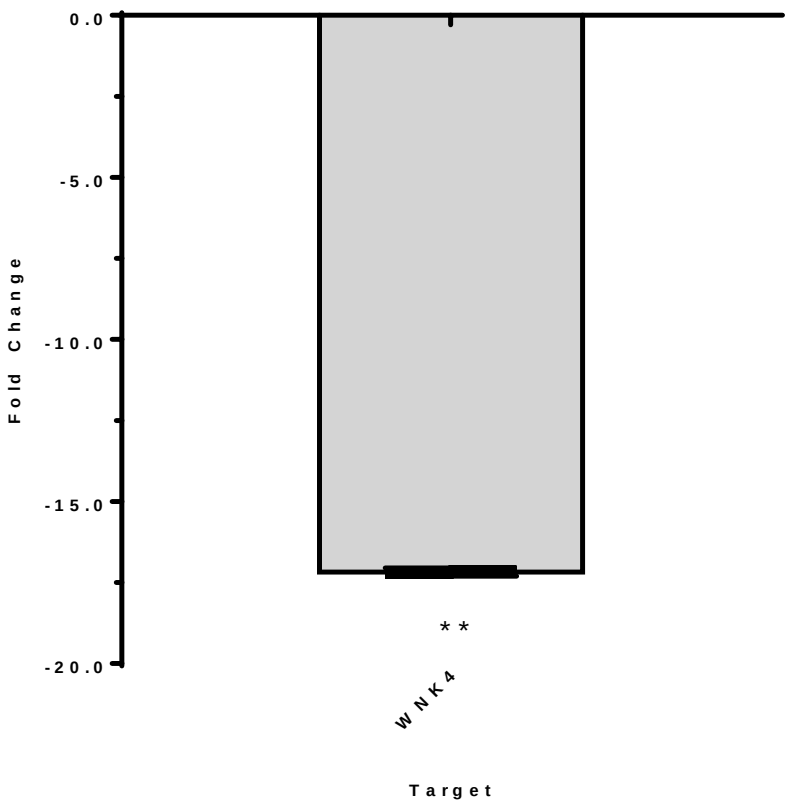

Figure 3.16: Normalized gene expression ($2^{-\Delta\Delta CT}$) of WNK4 in HepG2$^{CLDN-1+}$ cells. HepG2$^{CLDN-1+}$ and HepG2$^{pCMV-ve}$ cells were cultured for 72 hours prior to total RNA extraction. Amplification of WNK4 was performed alongside GAPDH and beta-actin as reference genes using RT-PCR. Relative normalised gene expression was calculated using the $2^{-\Delta\Delta CT}$ method. Data presented is representative of mean fold change ±s.e.m from three biological replicates. Paired t-test was performed to determine statistical significance, ** P≤0.01.

The expression of WNK4 was massively decreased in HepG2$^{CLDN-1+}$ cells compared to HepG2$^{pCMV-ve}$, this was represented by a -17.1 fold decrease(P=0.001).

3.6.2 Expression of tight junctional and associated genes in claudin-1 silenced HepG2 cells

The overexpression of claudin-1 in HepG2 cells appears to produce a junctional profile similar to that observed in invasive HCC cases (Holczbauer et al 2013). The expression profile of these junctional genes was then investigated in the claudin-1 silenced HepG2 cell to determine if these cells also displayed this pattern linked to invasive characteristics.

Target	Sample	Expression ($2^{-\Delta\Delta CT}$)	Expression ($2^{-\Delta\Delta CT}$) Standard Deviation	Compared to Regulation Threshold	P-Value	Exceeds P-Value Threshold (0.05)
Glyceraldehyde 3-phosphate dehydrogenase	HepG2 CLDN-1 siRNA	1.189	0.155	No change	0.312	Yes
Beta-actin	HepG2 CLDN-1 siRNA	1.009	0.148	No change	0.887	Yes
Caveolin-1	HepG2 CLDN-1 siRNA	2.656	0.066	Up Regulated	0.008	No
Caveolin-2	HepG2 CLDN-1 siRNA	3.165	0.164	Up Regulated	0.010	No
Claudin-1	HepG2 CLDN-1 siRNA	-8.937	0.010	Down Regulated	0.001	No
Claudin-2	HepG2 CLDN-1 siRNA	2.906	0.074	Up Regulated	0.010	No
Claudin-3	HepG2 CLDN-1 siRNA	1.514	0.090	Up Regulated	0.009	No
Claudin-4	HepG2 CLDN-1 siRNA	-1.451	0.055	Down Regulated	0.008	No
Claudin-5	HepG2 CLDN-1 siRNA	-1.719	0.024	Down Regulated	0.008	No

Claudin-7	HepG2 CLDN-1 siRNA	1.007	0.039	No change	0.499	Yes
Claudin-8	HepG2 CLDN-1 siRNA	-1.693	0.014	Down Regulated	0.001	No
Claudin-11	HepG2 CLDN-1 siRNA	4.779	0.039	Up Regulated	0.001	No
ZONAB	HepG2 CLDN-1 siRNA	4.913	0.111	Up Regulated	0.002	No
Junctional adhesion molecule A	HepG2 CLDN-1 siRNA	2.754	0.047	Up Regulated	0.014	No
Junctional adhesion molecule B	HepG2 CLDN-1 siRNA	1.077	0.141	No change	0.112	Yes
Junctional adhesion molecule C	HepG2 CLDN-1 siRNA	-1.358	0.035	Down Regulated	0.041	No
Afadin (AF6)	HepG2 CLDN-1 siRNA	-2.174	0.016	Down Regulated	0.020	No
Occludin	HepG2 CLDN-1 siRNA	-30.826	0.021	Down Regulated	0.002	No
Nectin-1	HepG2 CLDN-1 siRNA	-2.120	0.026	Down Regulated	0.001	No
Sp1 Transcription Factor	HepG2 CLDN-1 siRNA	3.567	0.117	Up Regulated	0.001	No
Zonula occludens-1 (ZO-1)	HepG2 CLDN-1 siRNA	-1.603	0.081	Down Regulated	0.003	No
Zonula occludens-2 (ZO-2)	HepG2 CLDN-1 siRNA	-2.979	0.012	Down Regulated	0.004	No
Zonula occludens-3 (ZO-3)	HepG2 CLDN-1 siRNA	-5.376	0.003	Down Regulated	0.036	No

Serine/Threonine-Protein Kinase WNK4	HepG2 CLDN-1 siRNA	-1.516	0.005	Down Regulated	0.001	No

Table 3.2: Normalised gene expression ($2^{-\Delta\Delta CT}$) of tight junctional and associated genes in claudin-1 silenced HepG2 cells. The table details the relative normalised gene expression of 24 tight junctional and associated genes in $HepG2^{CLDN\text{-}1-}$ cells. $HepG2^{scambled\text{-}ve}$ cells were used as the control. $HepG2^{CLDN\text{-}1-}$ and $HepG2^{scambled\text{-}ve}$ cells were cultured for 72 hours prior to total RNA extraction. Amplification of the genes outlined in Table 3.2 was performed alongside GAPDH and Beta-actin as the reference genes using RT-PCR. Relative normalised gene expression was calculated using the $2^{-\Delta\Delta CT}$ method. Data presented is representative of mean fold change ±s.e.m from three biological replicates. Paired t-test was performed to determine statistical significance. Statistical significance is indicated if the P value is lower than the 0.05 threshold.

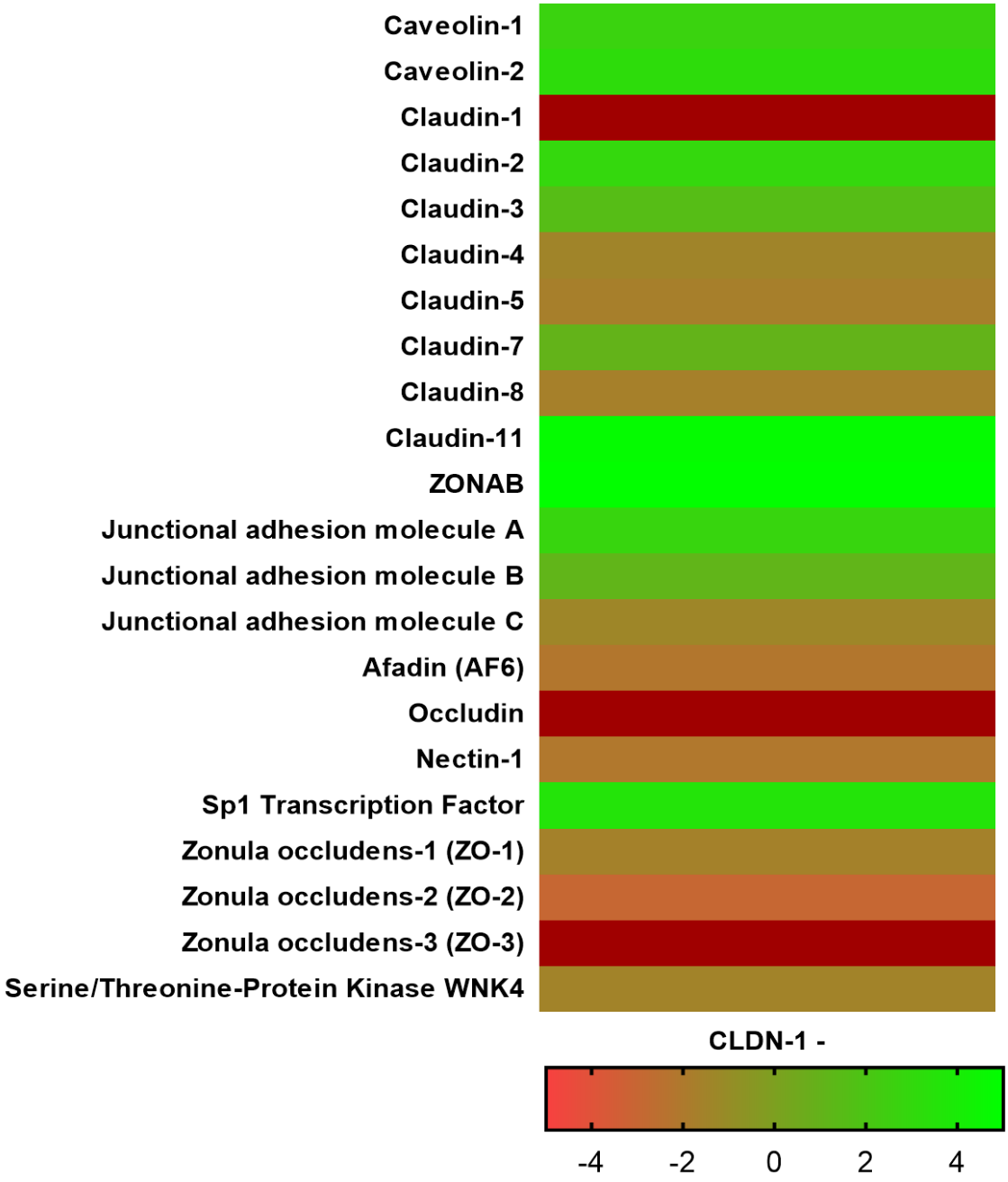

Figure 3.17: Heat map representing normalised gene expression ($2^{-\Delta\Delta CT}$) of tight junctional and associated genes in claudin-1 silenced HepG2 cells. Normalised gene expression values taken from Table 3.2 have been converted into a colorimetric scale outlined above to provide a visual representation of gene expression changes. Genes indicated by a green bar represent an upregulation in expression, whereas genes indicated by a red bar represent a down regulation in expression.

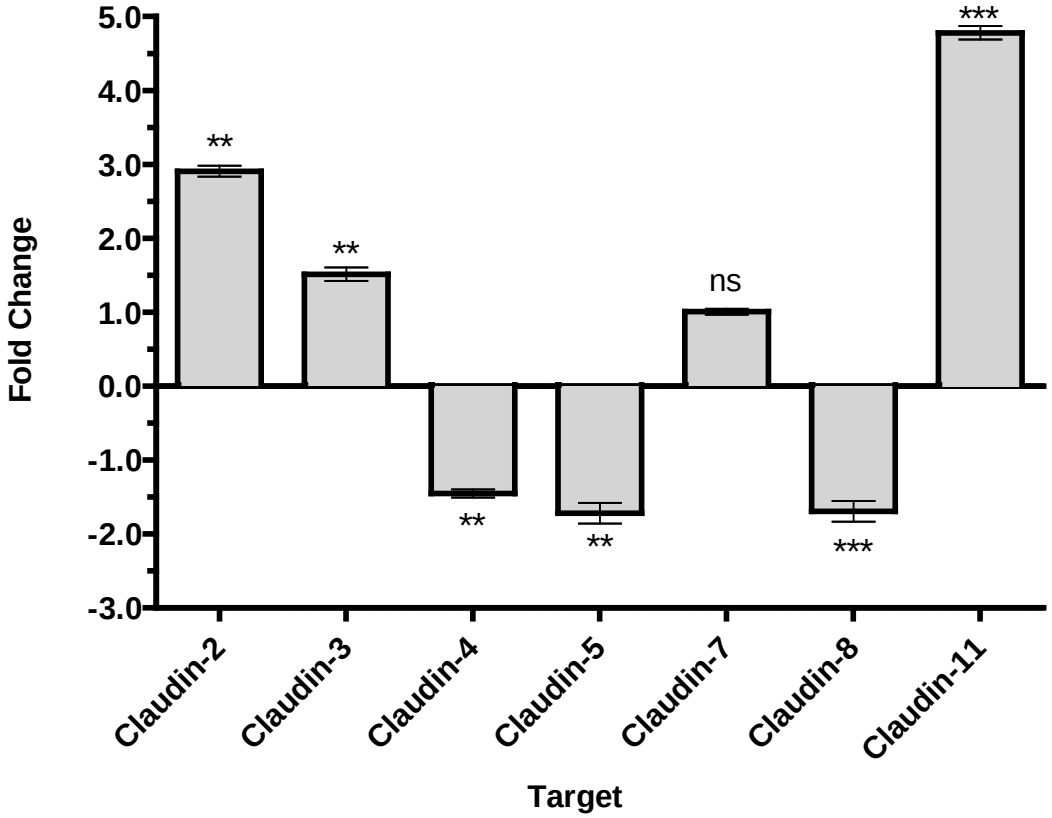

Figure 3.18: Normalized gene expression ($2^{-\Delta\Delta CT}$) of claudins-2, -3, -4, -5, -7, -8, and -11 in HepG2$^{CLDN-1-}$ cells. HepG2$^{CLDN-1-}$ and HepG2$^{scambled-ve}$ cells were cultured for 72 hours prior to total RNA extraction. Amplification of claudins-2, -3, -4, -5, -7, -8, and -11 was performed alongside GAPDH and Beta-actin as reference genes using RT-PCR. Relative normalised gene expression was calculated using the $2^{-\Delta\Delta CT}$ method. Data presented is representative of mean fold change ±s.e.m from three biological replicates. Paired t-test was performed to determine statistical significance, ns – no significant change ** P≤0.01 *** P≤0.001.

In response to silencing of claudin-1 the expression prolife of other claudin family members has changed. Large increases in expression of claudin 2 and 11, and a slight increase in claudin 3, was observed in HepG2$^{CLDN-1-}$ cells compared to control (P=0.009, 0.0010 and 0.008 respectively). Down regulation of claudin 4, 5 and 8 were also observed in HepG2$^{CLDN-1-}$ cells (P=0.007, P=0.007 and P<0.001 respectively). There was no significant

fold change in expression of claudin 7 (P=0.499). No expression of claudin-18 could be detected in either HepG2$^{CLDN-1-}$ or HepG2$^{scambled-ve}$ cells.

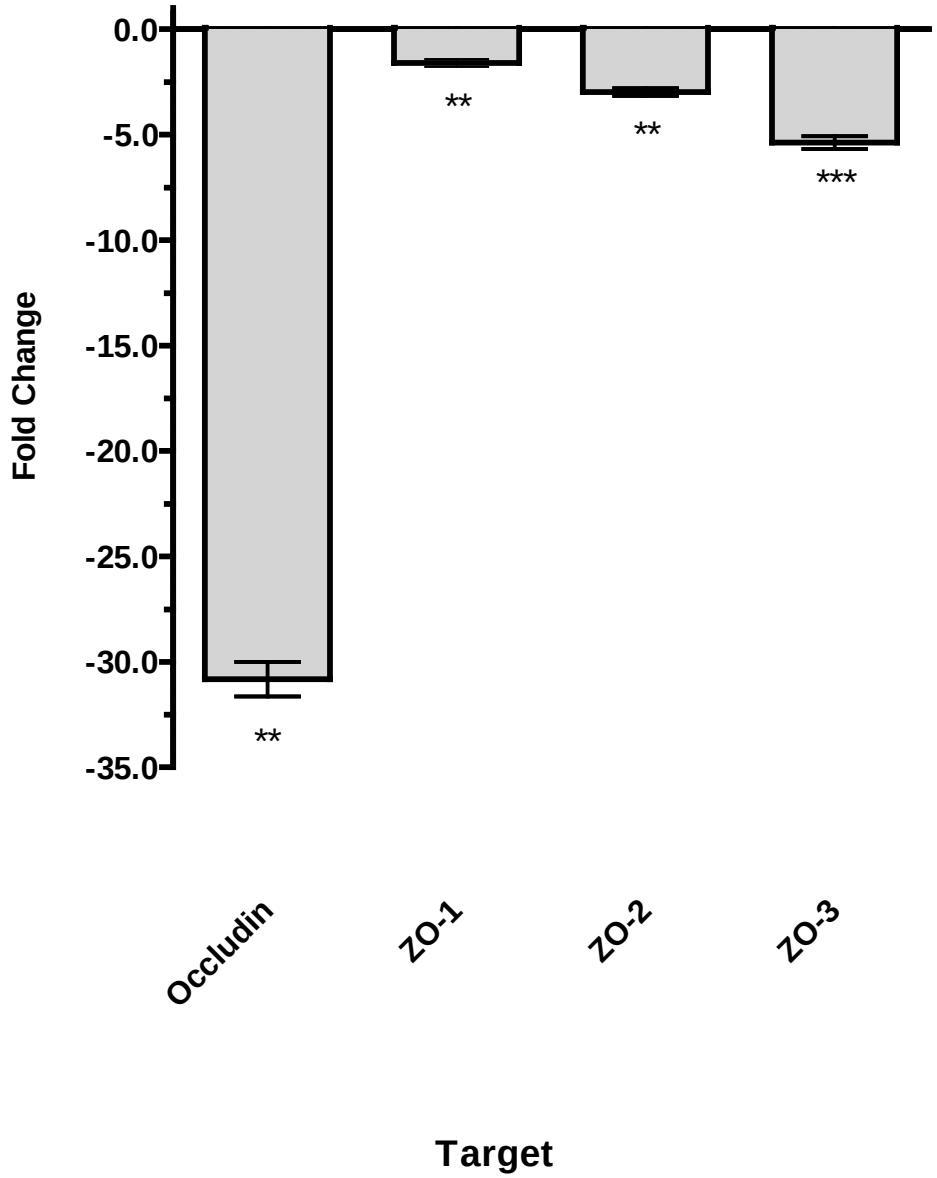

Figure 3.19: Normalized gene expression ($2^{-\Delta\Delta CT}$) of occludin, Zonula Occludens -1, -2 and -3 in HepG2$^{CLDN-1-}$ cells. HepG2$^{CLDN-1-}$ and HepG2$^{scambled-ve}$ cells were cultured for 72 hours prior to total RNA extraction. Amplification of occludin, zonula occludens -1, -2 and -3 was performed alongside GAPDH and Beta-actin as reference genes using RT-PCR. Relative normalised gene expression was calculated using the $2^{-\Delta\Delta CT}$ method. Data presented is representative of mean fold change ±s.e.m from three biological replicates. Paired t-test was performed to determine statistical significance, ** P≤0.01 *** P≤0.001.

The expression of occludin in HepG2$^{CLDN-1-}$ cells was decreased massively compared to HepG2$^{scambled-ve}$ represented by a -30.8 fold decrease. Statistical analysis indicated the decrease was significant (P=0.002). The expression of ZO -1, -2 and -3 was also shown to be significantly decreased in HepG2$^{CLDN-1-}$ cells compared to HepG2$^{scambled-ve}$ (P=0.003, P=0.004 and P<0.001 respectively).

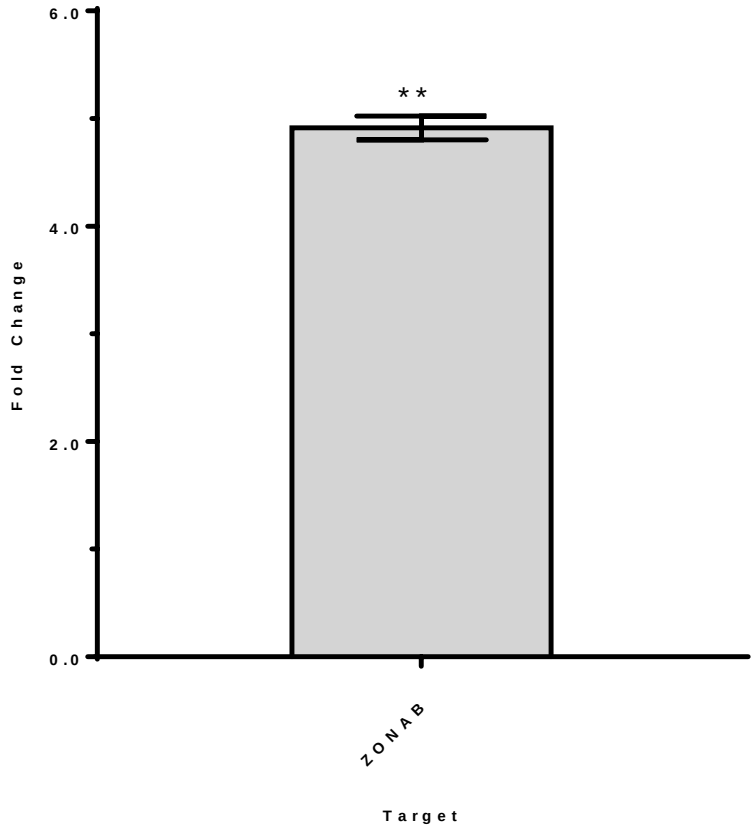

Figure 3.19: Normalized gene expression ($2^{-\Delta\Delta CT}$) of ZONAB in HepG2$^{CLDN-1-}$ cells. HepG2$^{CLDN-1-}$ and HepG2$^{scambled-ve}$ cells were cultured for 72 hours prior to total RNA extraction. Amplification of ZONAB was performed alongside GAPDH and Beta-actin as reference genes using RT-PCR. Relative normalised gene expression was calculated using the $2^{-\Delta\Delta CT}$ method. Data presented is representative of mean fold change ±s.e.m from three biological replicates. Paired t-test was performed to determine statistical significance, ** P≤0.01 *** P≤0.001.

The expression of transcription factor ZONAB was shown to be significantly increased by 4.9 fold in HepG2$^{CLDN-1-}$ cells (P=0.0017).

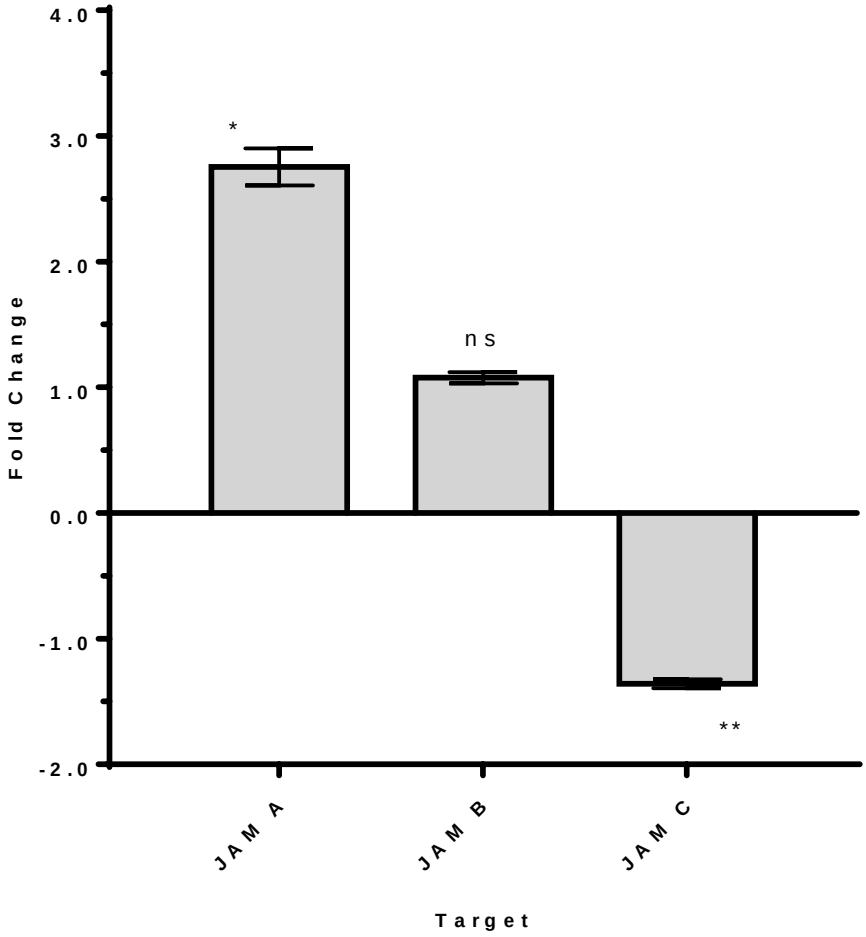

Figure 3.20: Normalized gene expression ($2^{-\Delta\Delta CT}$) of Junctional Adhesion Molecule A, B and C in HepG2$^{CLDN-1-}$ cells. HepG2$^{CLDN-1-}$ and HepG2$^{scambled-ve}$ cells were cultured for 72 hours prior to total RNA extraction. Amplification of Junctional Adhesion Molecule A, B and C was performed alongside GAPDH and Beta-actin as reference genes using RT-PCR. Relative normalised gene expression was calculated using the $2^{-\Delta\Delta CT}$ method. Data presented is representative of mean fold change ±s.e.m from three biological replicates. Paired t-test was performed to determine statistical significance, ns – no significant change * P≤0.05 ** P≤0.01

A significant 2.7-fold increase in JAM A expression was seen in HepG2$^{CLDN-1-}$ cells compared to control (P=0.014). The change in JAM B expression was not significant (P=0.11). The expression of JAM C was only slightly decreased in HepG2$^{CLDN-1-}$ compared to HepG2$^{scambled-ve}$, however it was significant (P=0.041).

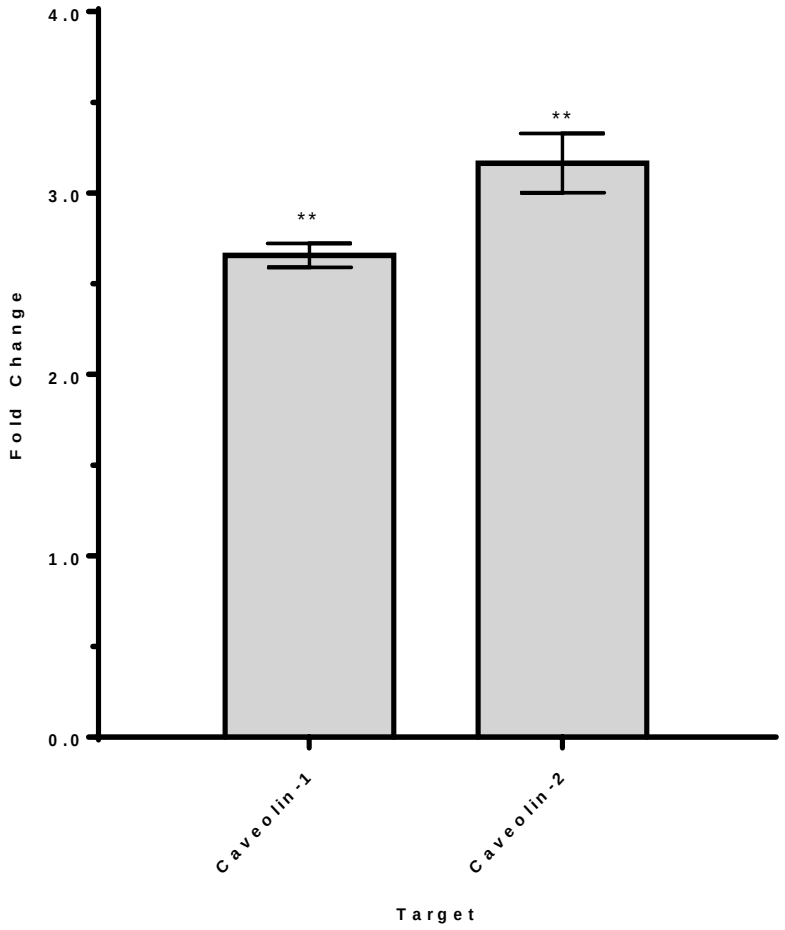

Figure 3.21: Normalized gene expression ($2^{-\Delta\Delta CT}$) of caveolin-1 and -2 in HepG2$^{CLDN-1-}$ cells. HepG2$^{CLDN-1-}$ and HepG2$^{scambled-ve}$ cells were cultured for 72 hours prior to total RNA extraction. Amplification of caveolin-1 and -2 was performed alongside GAPDH and Beta-actin as reference genes using RT-PCR. Relative normalised gene expression was calculated using the $2^{-\Delta\Delta CT}$ method. Data presented is representative of mean fold change ±s.e.m from three biological replicates. Paired t-test was performed to determine statistical significance, ** P≤0.01

The expression of both caveolin 1 and 2 was significantly increased in HepG2$^{CLDN-1-}$ cells compared to HepG2$^{scambled-ve}$. Statistical analysis indicated the increase in expression of both genes was significant (P=0.008, P=0.009).

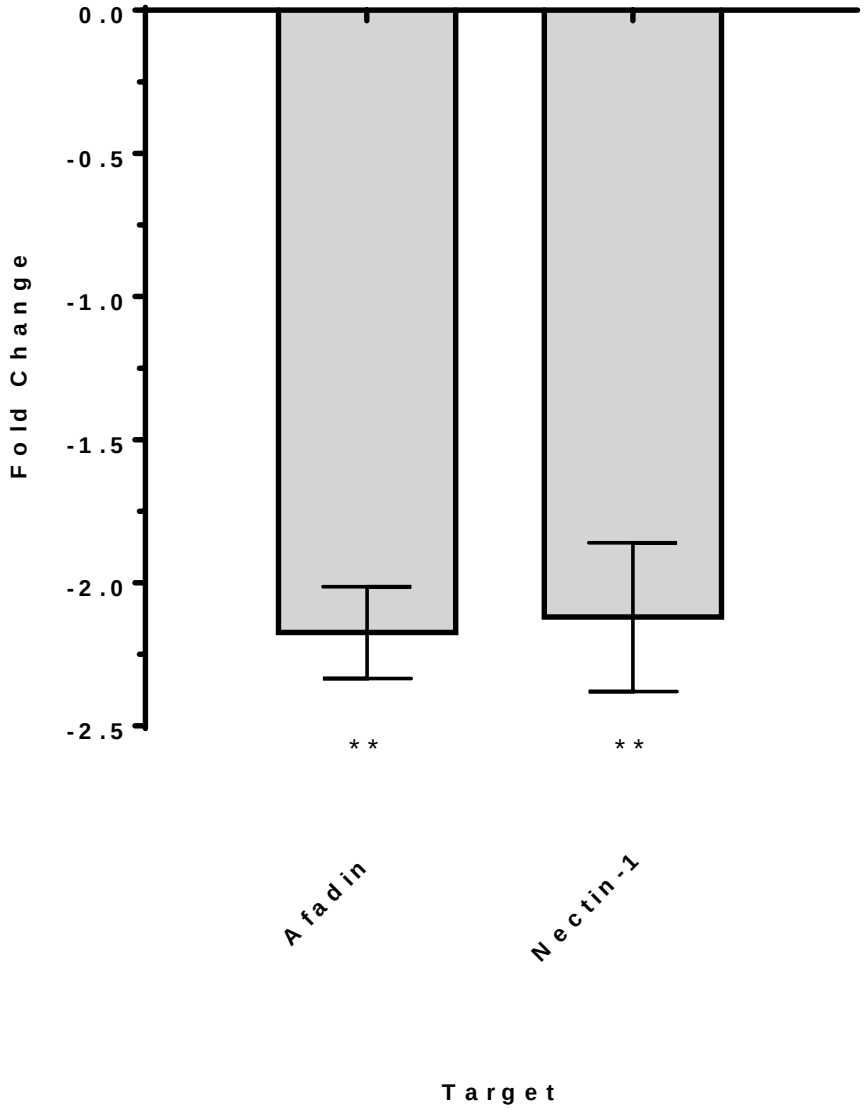

Figure 3.22: Normalized gene expression ($2^{-\Delta\Delta CT}$) of afadin and nectin-1 in HepG2$^{CLDN-1-}$ cells. HepG2$^{CLDN-1-}$ and HepG2$^{scambled-ve}$ cells were cultured for 72 hours prior to total RNA extraction. Amplification of afadin and nectin-1 was performed alongside GAPDH and Beta-actin as reference genes using RT-PCR. Relative normalised gene expression was calculated using the $2^{-\Delta\Delta CT}$ method. Data presented is representative of mean fold change ±s.e.m from three biological replicates. Paired t-test was performed to determine statistical significance, ** P≤0.01

The expression of both afadin and nectin-1 was significantly decreased in HepG2$^{CLDN-1-}$ cells compared to HepG2$^{scambled-ve}$. Statistical analysis indicated the decrease in expression of both genes was significant (P<0.001 and P<0.001).

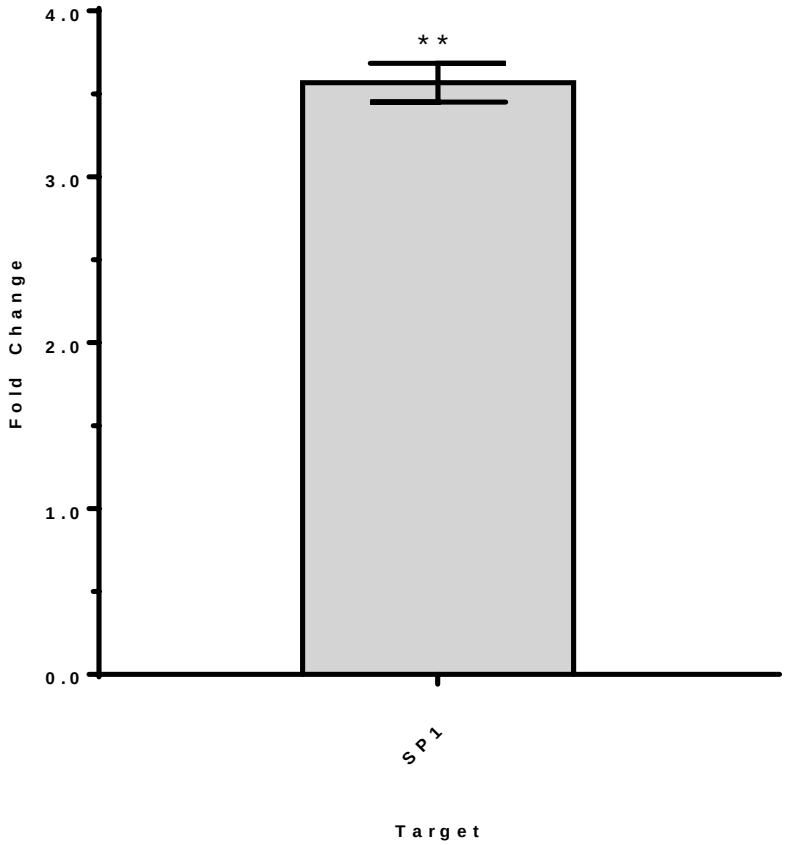

Figure 3.23: Normalized gene expression ($2^{-\Delta\Delta CT}$) of SP1 in HepG2$^{CLDN-1-}$ cells. HepG2$^{CLDN-1-}$ and HepG2$^{scambled-ve}$ cells were cultured for 72 hours prior to total RNA extraction. Amplification of SP1 was performed alongside GAPDH and Beta-actin as reference genes using RT-PCR. Relative normalised gene expression was calculated using the $2^{-\Delta\Delta CT}$ method. Data presented is representative of mean fold change ±s.e.m from three biological replicates. Paired t-test was performed to determine statistical significance, ** P≤0.01

The expression of SP1 in HepG2$^{CLDN-1-}$ cells was increased compared to HepG2$^{scambled-ve}$ represented by a 3.5-fold change. Statistical analysis indicated the increase was significant (P=0.001).

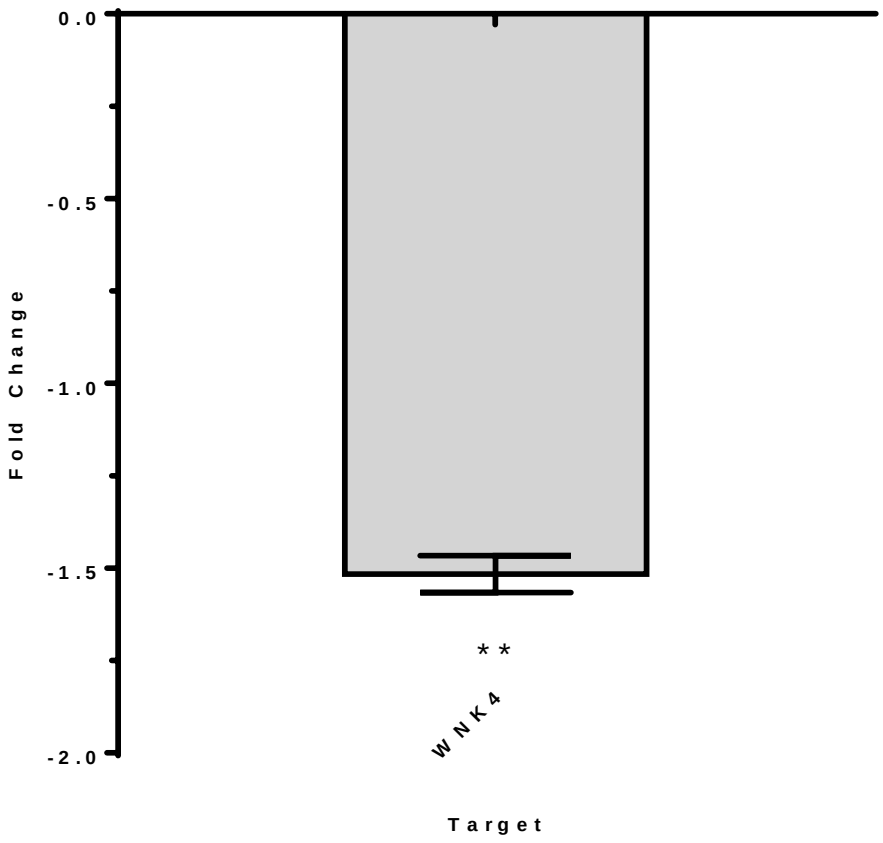

Figure 3.24: Normalized gene expression ($2^{-\Delta\Delta CT}$) of WNK4 in HepG2$^{CLDN-1-}$ cells. HepG2$^{CLDN-1-}$ and HepG2$^{scambled-ve}$ cells were cultured for 72 hours prior to total RNA extraction. Amplification of WNK4 was performed alongside GAPDH and Beta-actin as reference genes using RT-PCR. Relative normalised gene expression was calculated using the $2^{-\Delta\Delta CT}$ method. Data presented is representative of mean fold change ±s.e.m from three biological replicates. Paired t-test was performed to determine statistical significance, ** P≤0.01

The expression of WNK4 in HepG2$^{CLDN-1-}$ cells was decreased compared to HepG2$^{scambled-ve}$ represented by a -1.5 fold change. Statistical analysis indicated the decrease was significant (P=0.001).

Although there are a number of differences, it appears that both the over and under expression of claudin-1 in HepG2 cells produce similar patterns of expression of tight junctional and associated genes. As this pattern of expression has been documented with patients with invasive HCC, it is important to see if the overexpression or silencing of claudin-1 in HepG2 cells also displays these phenotypic changes in vitro (Holczbauer et al 2013).

3.7 Effect of claudin-1 on *in vitro* cell migration in HepG2 cells

Cases of HCC with aberrant levels of claudin-1 have been observed to have an increased metastatic potential. Observations when culturing $HepG2^{CLDN\text{-}1+}$ and $HepG2^{CLDN\text{-}1-}$ cells have suggested that these cell lines migrate at an increased rate compared to their respective controls. It was important to establish whether these cells migrated in a similar way to HCC cases reported in the literature. Migration assays were performed on $HepG2^{CLDN\text{-}1+}$, $HepG2^{CLDN\text{-}1-}$, $HepG2^{pCMV\text{-}ve}$ and $HepG2^{scambled\text{-}ve}$ cells to determine if an increase or decrease in claudin-1 changed the migratory capacity of HepG2 cells. Measurements of gap closure were taken every 12 hours or until complete closure. All migration assays were replicated a minimum of 6 times per cell line.

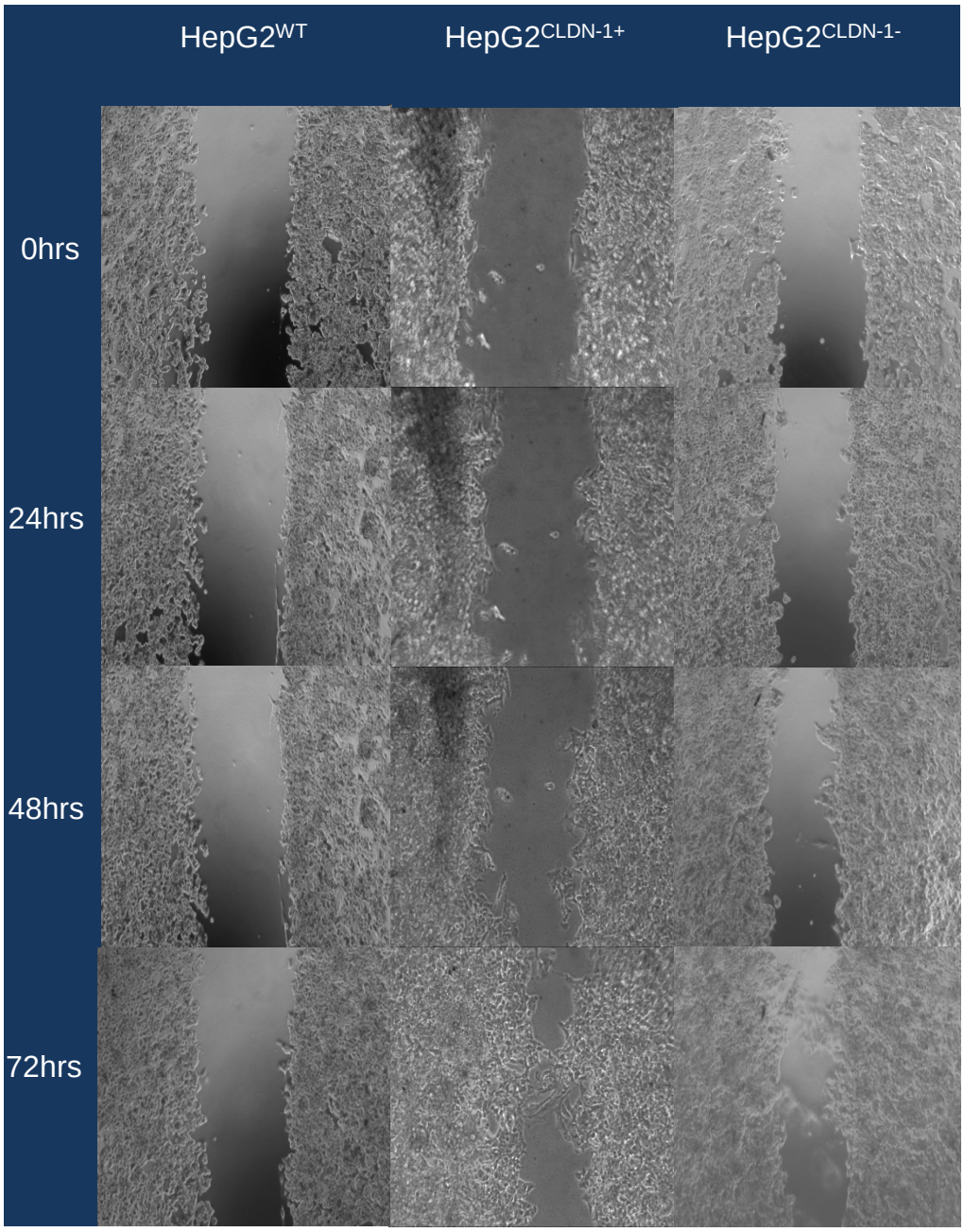

Figure 3.25: Sample migration assay images of HepG2$^{CLDN-1+}$, HepG2$^{CLDN-1-}$ and HepG2^{WT} cells over 72hrs. The images in figure 3.26 are representative of HepG2$^{CLDN-1+}$, HepG2$^{CLDN-1-}$ and HepG2^{WT} migration assays at their respective time points. Images were taken using an inverted light microscope at x10 magnification using a Jenoptik Rigel camera and Gryphax image capture software.

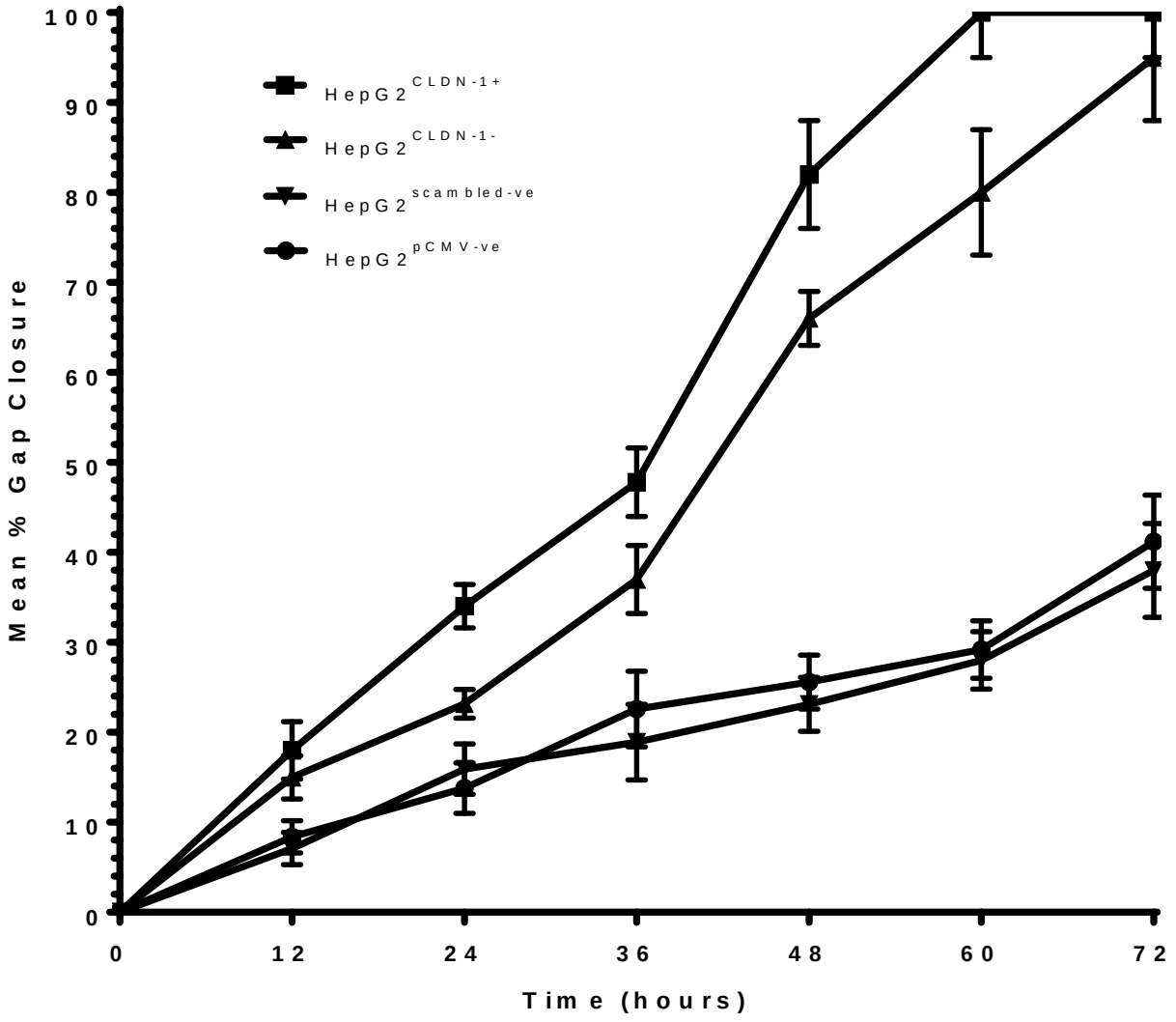

Figure 3.26: Average cell migration of HepG2$^{CLDN-1+}$, HepG2$^{CLDN-1-}$ and the respective controls HepG2$^{pCMV-ve}$ and HepG2$^{scambled-ve}$ cells over 72hrs. Measurements of gap closure were taken at hour 0 and every 12 hours after or until complete gap closure. Images were taken using a Jenoptik Rigel camera and Gryphax image capture software. Gap closure was analysed using Image J. Data presented is representative of mean fold change ±s.e.m from six biological replicates.

The initial increase in migration over the first 12 hours was not statistically significant for either HepG2$^{CLDN-1+}$ or HepG2$^{CLDN-1-}$ compared to the respective controls HepG2$^{pCMV-ve}$ and HepG2$^{scambled-ve}$ (P=0.143 and P=0.211 respectively). However, over 72 hours both HepG2$^{CLDN-1+}$and HepG2$^{CLDN-1-}$ displayed increased migration compared to HepG2$^{pCMV-ve}$ and HepG2$^{scambled-ve}$ (P=0.003 and P=0.012 respectively). HepG2$^{CLDN-1+}$ also displayed increased migratory capacity compared to HepG2$^{CLDN-1-}$ over 72 hours (P= 0.017).

HepG2$^{CLDN-1+}$ was the only sample to show complete gap closure over 72 hours, in every repeat experiment. HepG2$^{CLDN-1-}$ samples displayed complete gap closure in 50% of experiments after 72 hours. However, none of the controls HepG2$^{pCMV-ve}$, HepG2$^{scambled-ve}$ and HepG2^{WT} displayed complete gap closure.

An increased migratory capacity, as seen in both claudin-1 overexpressing and silenced cells, is a hallmark of metastatic disease. Cancer cells that display this property often exploit genes associated with epithelial to mesenchymal transition which drive disease progression. Therefore, the expression of these genes was determined in an attempt to investigate and explain the increased migratory capacity observed.

3.8 Determining the expression of epithelial to mesenchymal transition genes in claudin-1 overexpressing and claudin-1 silenced HepG2 cells

The increased migratory capacity of claudin-1 overexpressing and claudin-1 silenced HepG2 cells, indicates possible involvement of epithelial to mesenchymal transition or related mechanisms. Changes in tight junction expression are needed to alter barrier function and enable subsequent metastasis of cancer cells. Apart from maintenance of mechanical barriers, tight junctions have been documented to be involved in signal transduction and activation of pathways involved in accusation of an invasive phenotype. It could therefore be possible for changes in tight junction expression to be linked to the activation or upregulation of genes associated with of epithelial to mesenchymal transition or related mechanisms.

To explore this, claudin-1 overexpressing and claudin-1 silenced HepG2 cells were analysed to determine the expression of epithelial to mesenchymal transition genes using a PCR panel of 37 target and housekeeping genes.

3.8.1 Expression of epithelial to mesenchymal transition genes in claudin-1 overexpressing HepG2 cells

Target	Sample	Expression (2−ΔΔCT)	Expression (2−ΔΔCT) Standard Deviation	Compared to Regulation Threshold	P-Value	Exceeds P-Value Threshold (0.05)
Glyceraldehyde 3-phosphate dehydrogenase	HepG2 CLDN-1+	1.055	0.319	No Change	0.165	Yes
Beta-actin	HepG2 CLDN-1+	0.9769	0.445	No Change	0.354	Yes
Calcium/calmodulin-dependent protein kinase II inhibitor 1	HepG2 CLDN-1+	-20.704	0.021	Down Regulated	0.001	No
E-cadherin	HepG2 CLDN-1+	-6.112	0.004	Down Regulated	0.008	No
N-cadherin	HepG2 CLDN-1+	-6.169	0.105	Down Regulated	0.015	No
Alpha-catenin	HepG2 CLDN-1+	-3.307	0.193	Down Regulated	0.005	No
β-catenin	HepG2 CLDN-1+	3.484	0.522	Up Regulated	0.007	No
Desmocollin-2	HepG2 CLDN-1+	-3.281	0.154	Down Regulated	0.015	No
Desmoplakin	HepG2 CLDN-1+	-3.651	0.107	Down Regulated	0.027	No
Receptor tyrosine-protein kinase erbB-3	HepG2 CLDN-1+	-23.585	0.028	Down Regulated	0.003	No
Fibronectin	HepG2 CLDN-1+	-4.053	0.071	Down Regulated	0.001	No

Forkhead box protein C2	HepG2 CLDN-1+	2.641	0.294	Up Regulated	0.015	No
Frizzled-7	HepG2 CLDN-1+	2.908	0.641	Up Regulated	0.036	No
Homeobox protein Goosecoid	HepG2 CLDN-1+	1.938	0.205	Up Regulated	0.002	No
Jagged-1	HepG2 CLDN-1+	-19.305	0.045	Down Regulated	0.001	No
Lymphoid enhancer-binding factor-1	HepG2 CLDN-1+	6.495	0.402	Up Regulated	0.002	No
Metadherin	HepG2 CLDN-1+	2.208	0.019	Up Regulated	0.004	No
Notch-1	HepG2 CLDN-1+	1.255	0.113	Up Regulated	0.049	No
Nudix Hydrolase 13	HepG2 CLDN-1+	-3.226	0.244	Down Regulated	0.013	No
Beta-type platelet-derived growth factor receptor	HepG2 CLDN-1+	2.266	0.148	Up Regulated	0.003	No
Ras-related C3 botulinum toxin substrate 1	HepG2 CLDN-1+	2.375	0.978	Up Regulated	0.016	No
Zinc finger protein SNAI1 (SNAIL)	HepG2 CLDN-1+	6.870	0.371	Up Regulated	0.026	No
Zinc finger protein SNAI2 (SNAIL2)	HepG2 CLDN-1+	20.626	1.251	Up Regulated	0.006	No
Zinc finger protein SNAI3 (SNAIL3)	HepG2 CLDN-1+	-1.364	0.483	Down Regulated	0.459	Yes
Transcription Factor SOX-10	HepG2 CLDN-1+	2.882	0.649	Up Regulated	0.012	No

Transcription Factor 7	HepG2 CLDN-1+	3.734	0.035	Up Regulated	0.021	No
Transcription Factor 7 Like 1	HepG2 CLDN-1+	28.610	5.793	Up Regulated	0.005	No
Transcription Factor 7 Like 2	HepG2 CLDN-1+	26.572	1.503	Up Regulated	0.003	No
Tetraspanin-13	HepG2 CLDN-1+	3.133	0.196	Up Regulated	0.005	No
Twist Family BHLH Transcription Factor 1	HepG2 CLDN-1+	5.361	0.286	Up Regulated	0.003	No
Versican	HepG2 CLDN-1+	3.258	0.175	Up Regulated	0.008	No
Vimentin	HepG2 CLDN-1+	29.374	0.401	Up Regulated	0.007	No
Wnt Family Member 11	HepG2 CLDN-1+	-5.003	0.122	Down Regulated	0.017	No
Wnt Family Member 5a	HepG2 CLDN-1+	45.446	1.950	Up Regulated	0.001	No
Wnt Family Member 5b	HepG2 CLDN-1+	47.012	6.958	Up Regulated	0.002	No
Zinc Finger E-Box Binding Homeobox 1	HepG2 CLDN-1+	3.745	0.661	Up Regulated	0.015	No
Zinc Finger E-Box Binding Homeobox 2	HepG2 CLDN-1+	2.598	0.735	Up Regulated	0.015	No

Table 3.3: Normalised gene expression ($2^{-\Delta\Delta CT}$) of epithelial to mesenchymal transition genes in claudin-1 overexpressing HepG2 cells. The table details the relative normalised gene expression of 37 epithelial to mesenchymal transition and associated genes in $HepG2^{CLDN\text{-}1+}$ cells, $HepG2^{pCMV\text{-}ve}$ cells were used as the control. $HepG2^{CLDN\text{-}1+}$ and $HepG2^{pCMV\text{-}ve}$ cells were cultured for 72 hours prior to total RNA extraction. Amplification of the genes outlined in Table 3.3 was performed alongside GAPDH and beta-actin as the reference genes using RT-PCR. Relative normalised gene expression was calculated using the $2^{-\Delta\Delta CT}$ method. Data presented is representative of mean fold change

±s.e.m from three biological replicates. Paired t-test was performed to determine statistical significance. Statistical significance is indicated if the P value is lower than the 0.05 threshold.

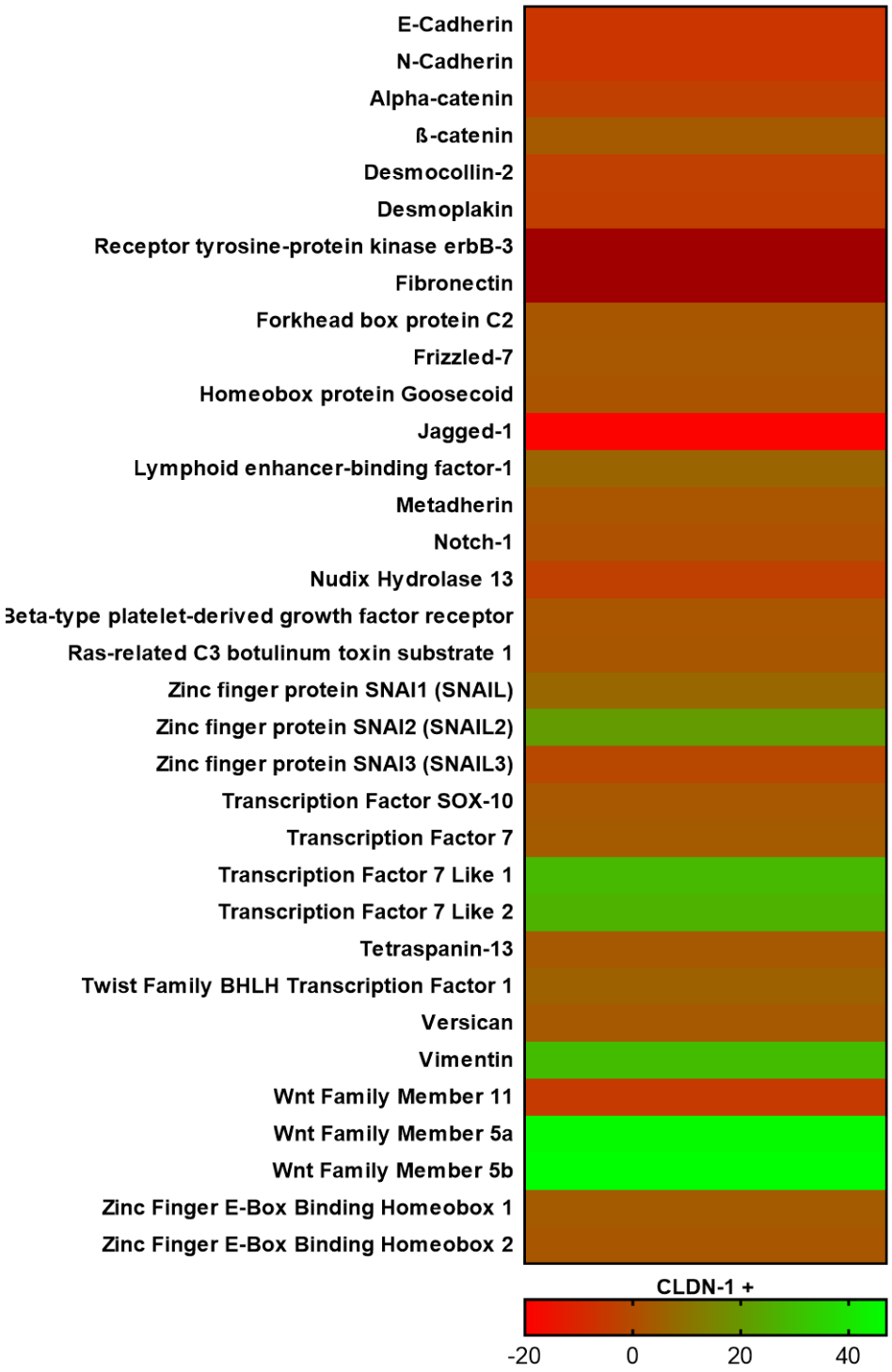

Figure 3.27: Heat map representing normalised gene expression ($2^{-\Delta\Delta CT}$) of epithelial to mesenchymal transition genes in claudin-1 overexpressing HepG2 cells. Normalised gene expression values taken from Table 3.3 have been converted into a colorimetric scale outlined above to provide a visual representation of large-scale changes. Genes indicated by a green bar represent an upregulation in expression, whereas genes indicated by a red bar represent a down regulation in expression.

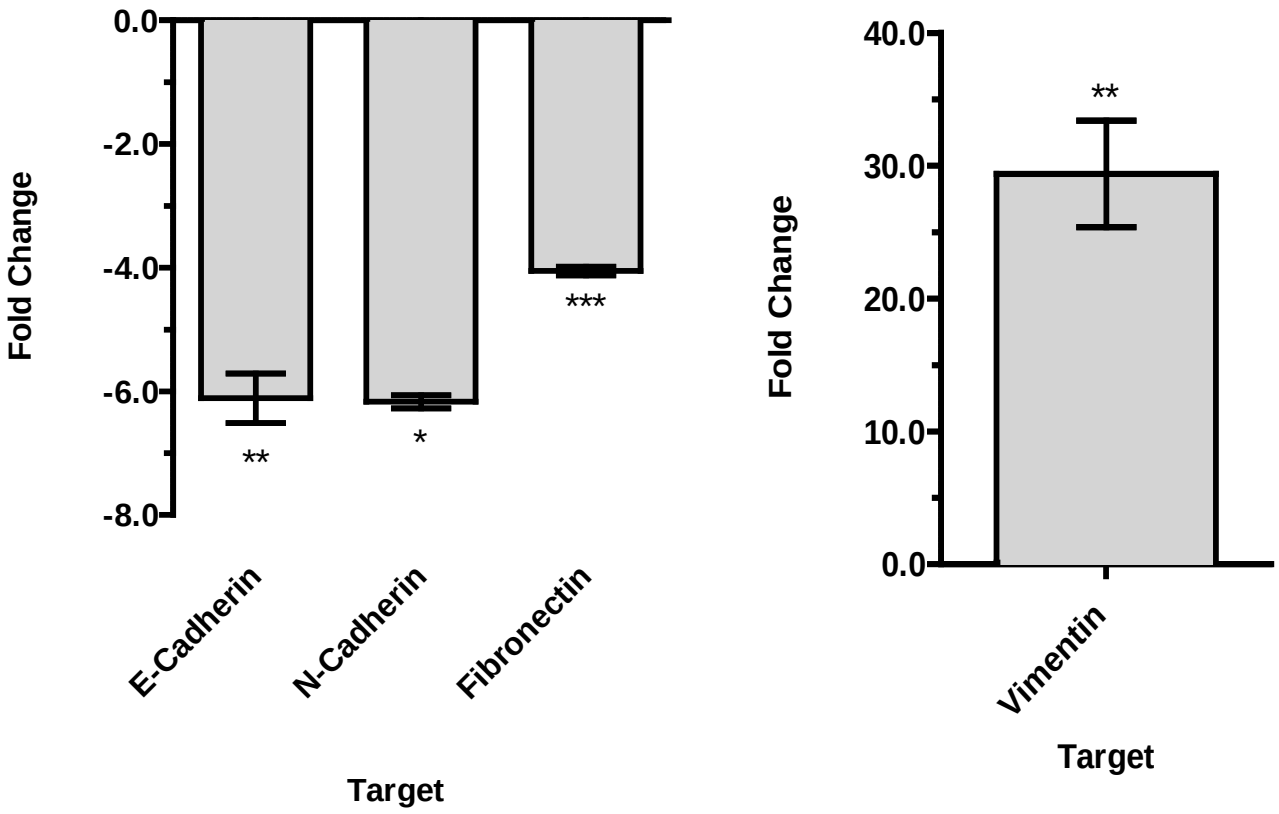

Figure 3.29: Normalized gene expression ($2^{-\Delta\Delta CT}$) of E-cadherin, N-cadherin, fibronectin and vimentin in HepG2$^{CLDN-1+}$ cells. HepG2$^{CLDN-1+}$ and HepG2$^{pCMV-ve}$ cells were cultured for 72 hours prior to total RNA extraction. Amplification of E-cadherin, N-cadherin, Fibronectin and vimentin was performed alongside GAPDH and Beta-actin as reference genes using RT-PCR. Relative normalised gene expression was calculated using the $2^{-\Delta\Delta CT}$ method. Data presented is representative of mean fold change ±s.e.m from three biological replicates. Paired t-test was performed to determine statistical significance, * P≤0.05 ** P≤0.01 *** P≤0.001.

Epithelial marker E-cadherin was significantly decreased in HepG2$^{CLDN-1+}$ cells compared to control HepG2$^{pCMV-ve}$, represented by a -6.1 fold decrease (P=0.007). Mesenchymal marker vimentin was massively increased by 29 fold in HepG2$^{CLDN-1+}$ cells (P=0.006). Interestingly, other markers of mesenchymal cells, N-cadherin and fibronectin were found to be significantly decreased by -6.1 and -4.0 fold respectively (P=0.014 and P<0.001).

E-cadherin and vimentin are classic markers of EMT initiation in cancer cell progression. The down regulation of the epithelial marker E-cadherin and the upregulation of the

mesenchymal marker vimentin are hallmarks of the transition. The large fold changes in these markers seen as a result of claudin-1 overexpression provide strong evidence that EMT is occurring in these cells.

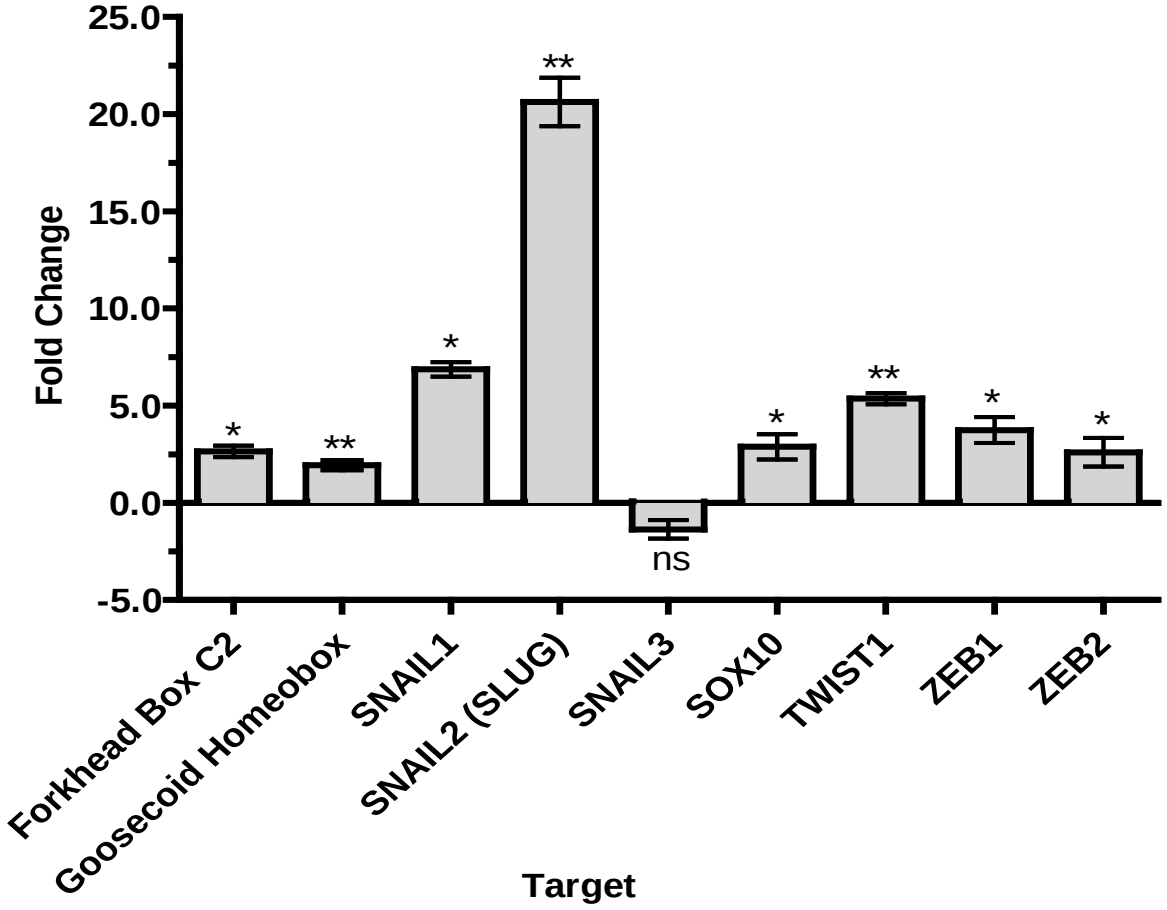

Figure 3.30: Normalized gene expression ($2^{-\Delta\Delta CT}$) of EMT associated transcription factors in HepG2$^{CLDN-1+}$ cells. HepG2$^{CLDN-1+}$ and HepG2$^{pCMV-ve}$ cells were cultured for 72 hours prior to total RNA extraction. Amplification of Forkhead box C2, Goosecoid homeobox, SNAIL1, SNAIL2, SNAIL3, SOX10, TWIST1, ZEB1 and ZEB2 was performed alongside GAPDH and Beta-actin as reference genes using RT-PCR. Relative normalised gene expression was calculated using the $2^{-\Delta\Delta CT}$ method. Data presented is representative of mean fold change ±s.e.m from three biological replicates. Paired t-test was performed to determine statistical significance, ns – not significant * P≤0.05 ** P≤0.01 *** P≤0.001.

Classic EMT inducing transcription factors TWIST1, ZEB1 and ZEB2 were all significantly increased by 5.3, 2.7 and 2.5 fold respectively (P=0.003, P=0.014 and P= 0.015). SNAIL2, otherwise known as SLUG, represented the largest increase in gene expression with a 20-

fold change, followed by SNAIL1 with a 6.8-fold increase (P=0.005, P=0.025 respectively). However, there was no significant change in express of SNAIL 3 (P=0.458). Other EMT inducing transcription factors Forkhead Box C2, Goosecoid Homeobox, and SOX10 all displayed increased expression by 2.6, 1.9, and 2.8 fold respectively (P=0.014, P=0.002 P=0.012)

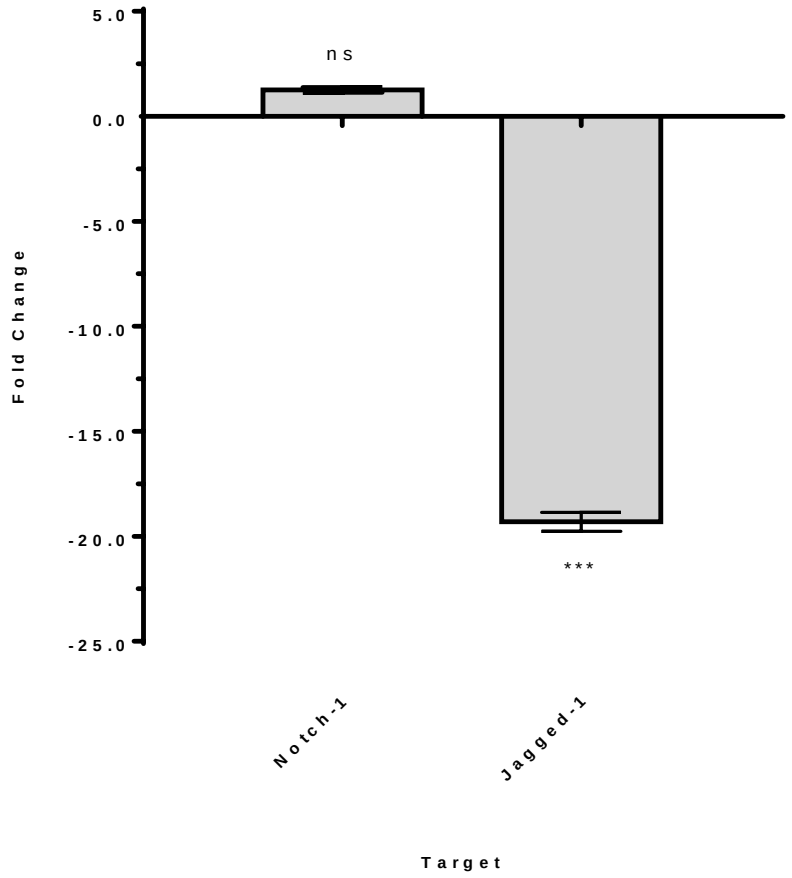

Figure 3.31: Normalized gene expression ($2^{-\Delta\Delta CT}$) of NOTCH associated genes in HepG2$^{CLDN-1+}$ cells. HepG2$^{CLDN-1+}$ and HepG2$^{pCMV-ve}$ cells were cultured for 72 hours prior to total RNA extraction. Amplification of notch-1 and jagged-1 was performed alongside GAPDH and Beta-actin as reference genes using RT-PCR. Relative normalised gene expression was calculated using the $2^{-\Delta\Delta CT}$ method. Data presented is representative of mean fold change ±s.e.m from three biological replicates. Paired t-test was performed to determine statistical significance, ns – not significant *** P≤0.001.

The gene expression of notch-1 appeared to be increased 1.25 fold compared to control. However, the increase was not significant as the P value exceeded the threshold, represented by P=0.078. The expression of jagged-1 was massively decreased,

represented by a -19.3 fold change. Statistical analysis determined that the change in expression was significant (P<0.001).

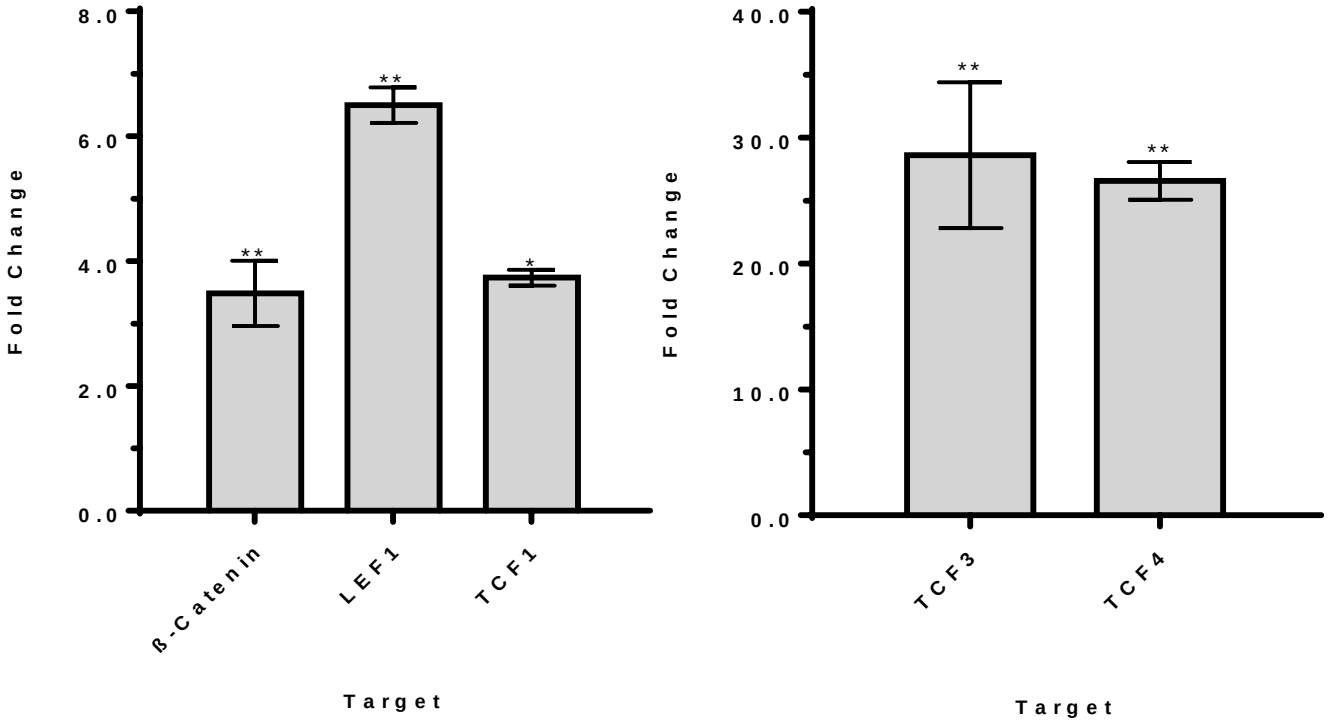

Figure 3.32: Normalized gene expression ($2^{-\Delta\Delta CT}$) of WNT / β-catenin target genes in HepG2$^{CLDN-1+}$ cells. HepG2$^{CLDN-1+}$ and HepG2$^{pCMV-ve}$ cells were cultured for 72 hours prior to total RNA extraction. Amplification of β-catenin, LEF1, TCF1, TCF3 and TCF4 was performed alongside GAPDH and Beta-actin as reference genes using RT-PCR. Relative normalised gene expression was calculated using the $2^{-\Delta\Delta CT}$ method. Data presented is representative of mean fold change ±s.e.m from three biological replicates. Paired t-test was performed to determine statistical significance, * P≤0.05 ** P≤0.01

The expression of β-catenin was significantly increased by 3.5 fold in HepG2$^{CLDN-1+}$ compared to HepG2$^{pCMV-ve}$ (P=0.006). Associated WNT / β-catenin transcription factors LEF1 and TCF1 were also increased HepG2$^{CLDN-1+}$ cells by 6.5 and 3.7 fold respectively (P=0.002 and P=0.022). The largest increase in expression of WNT / β-catenin target genes was transcription factors TCF3 and TCF4 which displayed 28 and 26 fold increases in expression (P=0.0051 and P=0.003).

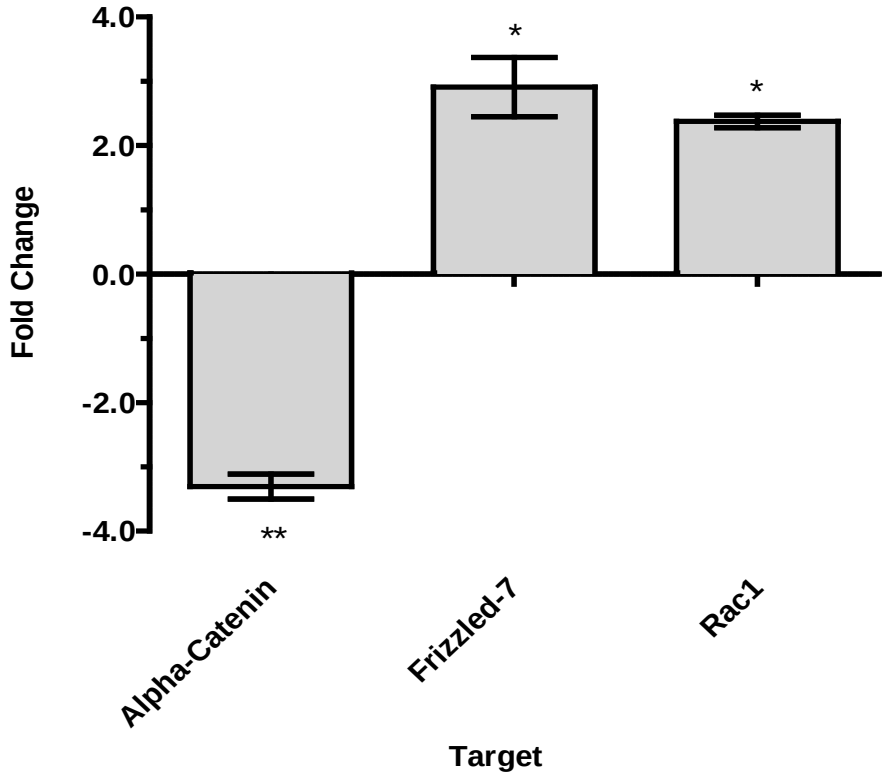

Figure 3.33: Normalized gene expression ($2^{-\Delta\Delta CT}$) of associated WNT/β-catenin target genes in HepG2$^{CLDN-1+}$ cells. HepG2$^{CLDN-1+}$ and HepG2$^{pCMV-ve}$ cells were cultured for 72 hours prior to total RNA extraction. Amplification of alpha-catenin, frizzled-7 and rac1 was performed alongside GAPDH and Beta-actin as reference genes using RT-PCR. Relative normalised gene expression was calculated using the $2^{-\Delta\Delta CT}$ method. Data presented is representative of mean fold change ±s.e.m from three biological replicates. Paired t-test was performed to determine statistical significance, * P≤0.05 ** P≤0.01

The expression of alpha-catenin was significant decreased by -3.3 fold in HepG2$^{CLDN-1+}$ cells compared to control (P=0.004). Expression of frizzled-7 and rac1 was increased in HepG2$^{CLDN-1+}$ cells by 2.9 and 2.3 fold respectively (P=0.035 and P=0.015)

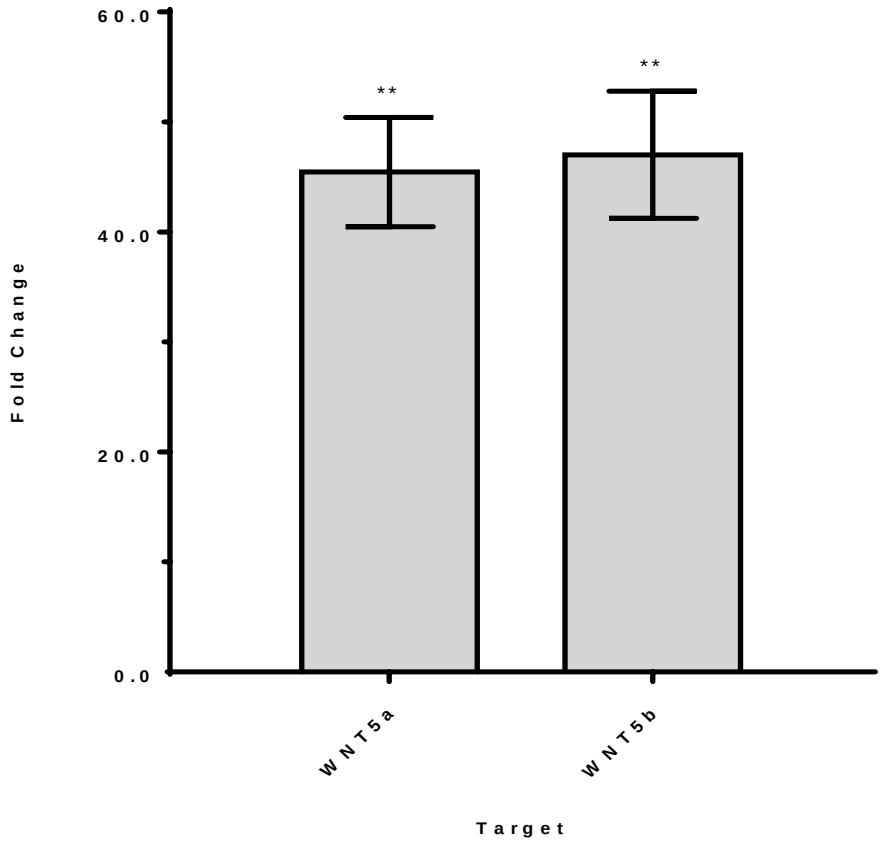

Figure 3.34: Normalized gene expression ($2^{-\Delta\Delta CT}$) of WNT5a and WNT5b in HepG2$^{CLDN-1+}$ cells. HepG2$^{CLDN-1+}$ and HepG2$^{pCMV-ve}$ cells were cultured for 72 hours prior to total RNA extraction. Amplification of WNT5a and WNT5b was performed alongside GAPDH and Beta-actin as reference genes using RT-PCR. Relative normalised gene expression was calculated using the $2^{-\Delta\Delta CT}$ method. Data presented is representative of mean fold change ±s.e.m from three biological replicates. Paired t-test was performed to determine statistical significance, ** P≤0.01

Both WNT5a and WNT5b displayed a large significant increase of 45 and 47 fold respectively in HepG2$^{CLDN-1+}$ cells compared to control. Statistical analysis indicated the increase in expression of both genes was significant (P=0.001, P=0.002).

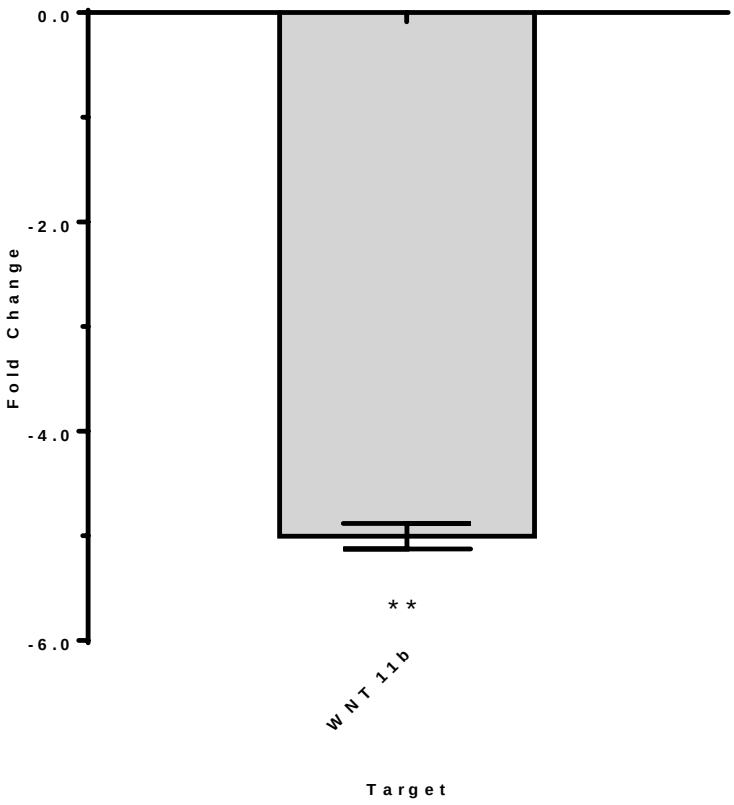

Figure 3.35: Normalized gene expression ($2^{-\Delta\Delta CT}$) of WNT11a in HepG2$^{CLDN-1+}$ cells. HepG2$^{CLDN-1+}$ and HepG2$^{pCMV-ve}$ cells were cultured for 72 hours prior to total RNA extraction. Amplification of WNT11a was performed alongside GAPDH and Beta-actin as reference genes using RT-PCR. Relative normalised gene expression was calculated using the $2^{-\Delta\Delta CT}$ method. Data presented is representative of mean fold change ±s.e.m from three biological replicates. Paired t-test was performed to determine statistical significance, ** P≤0.01

The expression of WNT11a in HepG2$^{CLDN-1+}$ cells was decreased compared to control represented by a 0.65-fold change. Statistical analysis indicated the decrease was significant (P=0.001).

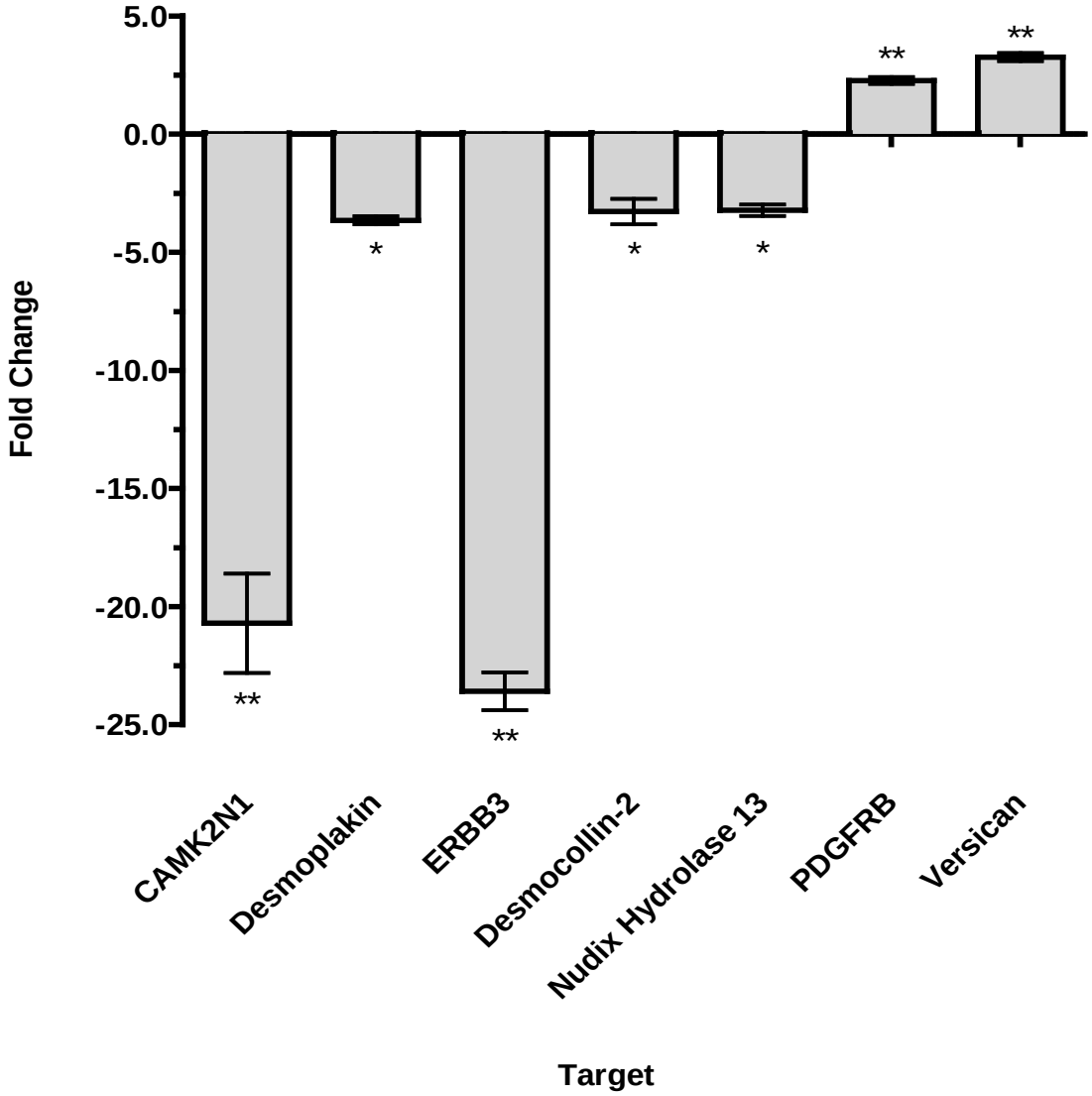

Figure 3.36: Normalized gene expression ($2^{-\Delta\Delta CT}$) of other associated EMT target genes in HepG2$^{CLDN-1+}$ cells . HepG2$^{CLDN-1+}$ and HepG2$^{pCMV-ve}$ cells were cultured for 72 hours prior to total RNA extraction. Amplification of CAMK2N1, desmoplakin, ERBB3, desmocollin-2, Nudix hydrolase 13, PDGFRB and versican was performed alongside GAPDH and Beta-actin as reference genes using RT-PCR. Relative normalised gene expression was calculated using the $2^{-\Delta\Delta CT}$ method. Data presented is representative of mean fold change ±s.e.m from three biological replicates. Paired t-test was performed to determine statistical significance, * P≤0.05 ** P≤0.01

CAMK2N1 and ERBB3 represented the largest decrease of associated EMT target genes, represented by a -20.7 and -23.5 fold change (P=0.001, P=0.002). Desmoplakin, Desmocollin-2, and Nudix Hydrolase 13 were also significantly decreased by -3.6, -3.2 and -3.2 fold change respectively (P=0.026, P=0.014, and P=0.012). The expression of

PDGFRB and Versican was significantly increased compared to control in HepG2$^{CLDN-1+}$ cells by 2.26 and 3.35 fold respectively (P=0.0027 and P=0.0079).

3.8.2 Expression of epithelial to mesenchymal transition genes in claudin-1 silenced HepG2 cells.

Significant upregulation of EMT transcription factors and vimentin provide strong evidence of EMT initiation in claudin-1 overexpressing HepG2 cells. EMT initiation is often associated with an increase in migratory capacity (Karlsson et al 2017). It is therefore likely that the increase is EMT markers is linked to the increased migratory capacity observed in these cells. As the migratory capacity of claudin-1 silenced HepG2 cells was also significantly increased it is important to determine the expression of EMT genes in these cells to examine if the same link existed.

Target	Sample	Expression ($2^{-\Delta\Delta CT}$)	Expression ($2^{-\Delta\Delta CT}$) Standard Deviation	Compared to Regulation Threshold	P-Value	Exceeds P-Value Threshold (0.05)
Glyceraldehyde 3-phosphate dehydrogenase	HepG2 CLDN-1 siRNA	1.035	0.009	No Change	0.000	No
Beta-actin	HepG2 CLDN-1 siRNA	-1.343	0.032	No Change	0.003	No
α-Catenin	HepG2 CLDN-1 siRNA	1.376	0.077	Up Regulation	0.025	No
E-cadherin	HepG2 CLDN-1 siRNA	-1.529	0.001	Down Regulated	0.017	No
N-cadherin	HepG2 CLDN-1 siRNA	1.484	0.068	Up Regulated	0.022	No

β-catenin	HepG2 CLDN-1 siRNA	1.397	0.110	Up Regulated	0.022	No
Desmocollin-2	HepG2 CLDN-1 siRNA	1.685	0.099	Up Regulated	0.015	No
Desmoplakin	HepG2 CLDN-1 siRNA	1.922	0.041	Up Regulated	0.004	No
Epidermal Growth Factor Receptor	HepG2 CLDN-1 siRNA	1.767	0.106	Up Regulated	0.009	No
Fibronectin	HepG2 CLDN-1 siRNA	2.042	0.003	Up Regulated	0.013	No
Forkhead box protein C2	HepG2 CLDN-1 siRNA	4.813	0.168	Up Regulated	0.002	No
Frizzled-7	HepG2 CLDN-1 siRNA	2.508	0.041	Up Regulated	0.002	No
Homeobox protein Goosecoid	HepG2 CLDN-1 siRNA	2.591	0.152	Up Regulated	0.007	No
Jagged-1	HepG2 CLDN-1 siRNA	3.110	0.170	Up Regulated	0.003	No
Lymphoid enhancer-binding factor-1	HepG2 CLDN-1 siRNA	-1.138	0.012	Down Regulated	0.025	No
Microtubule Associated Protein 1B	HepG2 CLDN-1 siRNA	1.846	0.087	Up Regulated	0.004	No
Moesin	HepG2 CLDN-1 siRNA	8.302	0.664	Up Regulated	0.000	No
Notch-1	HepG2 CLDN-1 siRNA	3.572	0.231	Up Regulated	0.002	No
Nudix Hydrolase 13	HepG2 CLDN-1 siRNA	-26.455	0.005	Down Regulated	0.003	No
Ras-Related C3 Botulinum Toxin Substrate 1	HepG2 CLDN-1 siRNA	-1.783	0.020	Down Regulated	0.014	No

Zinc finger protein SNAI1 (SNAIL)	HepG2 CLDN-1 siRNA	1.511	0.014	Up Regulated	0.028	No
Zinc finger protein SNAI2 (SNAIL2)	HepG2 CLDN-1 siRNA	-7.138	0.005	Down Regulated	0.006	No
Zinc finger protein SNAI3 (SNAIL3)	HepG2 CLDN-1 siRNA	-8.929	0.005	Down Regulated	0.007	No
Transcription Factor SOX-10	HepG2 CLDN-1 siRNA	-5.274	0.006	Down Regulated	0.004	No
Transcription Factor 7	HepG2 CLDN-1 siRNA	3.112	0.126	Up Regulated	0.003	No
Transcription Factor 7 Like 1	HepG2 CLDN-1 siRNA	1.848	0.014	Up Regulated	0.021	No
Transcription Factor 7 Like 2	HepG2 CLDN-1 siRNA	1.304	0.022	Up Regulated	0.057	No
Twist Family BHLH Transcription Factor 1	HepG2 CLDN-1 siRNA	2.418	0.134	Up Regulated	0.002	No
Vimentin	HepG2 CLDN-1 siRNA	5.351	0.259	Up Regulated	0.002	No
Wnt Family Member 5a	HepG2 CLDN-1 siRNA	-2.141	0.106	Down Regulated	0.013	No
Wnt Family Member 5b	HepG2 CLDN-1 siRNA	-1.017	0.052	Down Regulated	0.213	Yes
Wnt Family Member 11	HepG2 CLDN-1 siRNA	-1.072	0.047	Down Regulated	0.165	Yes
Zinc Finger E-Box Binding Homeobox 1	HepG2 CLDN-1 siRNA	1.021	0.005	No Change	0.153	Yes
Zinc Finger E-Box Binding Homeobox 2	HepG2 CLDN-1 siRNA	2.662	0.137	Up Regulated	0.011	No

Table 3.4: Normalised gene expression ($2^{-\Delta\Delta CT}$) of epithelial to mesenchymal transition genes in claudin-1 silenced HepG2 cells. The table details the relative normalised gene expression of 24 tight junctional and associated genes in $HepG2^{CLDN\text{-}1-}$ cells. $HepG2^{scambled\text{-}ve}$ cells were used as the control. $HepG2^{CLDN\text{-}1-}$ and $HepG2^{scambled\text{-}ve}$ cells were cultured for 72 hours prior to total RNA extraction. Amplification of the genes outlined in Table 3.4 was performed alongside GAPDH and Beta-actin as the reference genes using RT-PCR. Relative normalised gene expression was calculated using the $2^{-\Delta\Delta CT}$ method. Data presented is representative of mean fold change ±s.e.m from three biological replicates. Paired t-test was performed to determine statistical significance. Statistical significance is indicated if the P value is lower than the 0.05 threshold.

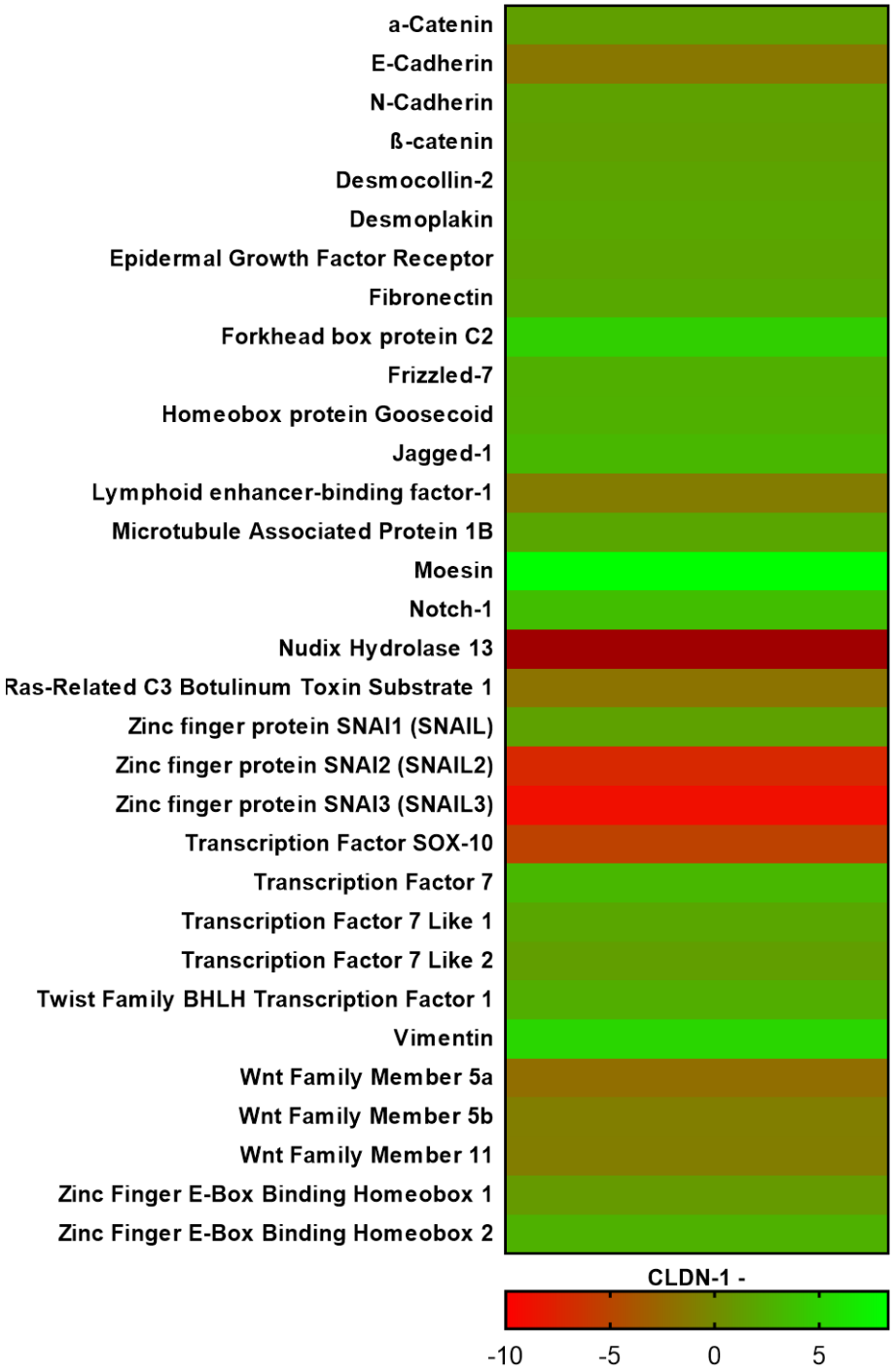

Figure 3.37: Heat map representing normalised gene expression ($2^{-\Delta\Delta CT}$) of epithelial to mesenchymal transition genes in claudin-1 silenced HepG2 cells. Normalised gene expression values taken from Table 3.1 have been converted into a colorimetric scale outlined above to provide a visual representation of large scale changes. Genes indicated by a green bar represent an upregulation in expression, whereas genes indicated by a red bar represent a down regulation in expression.

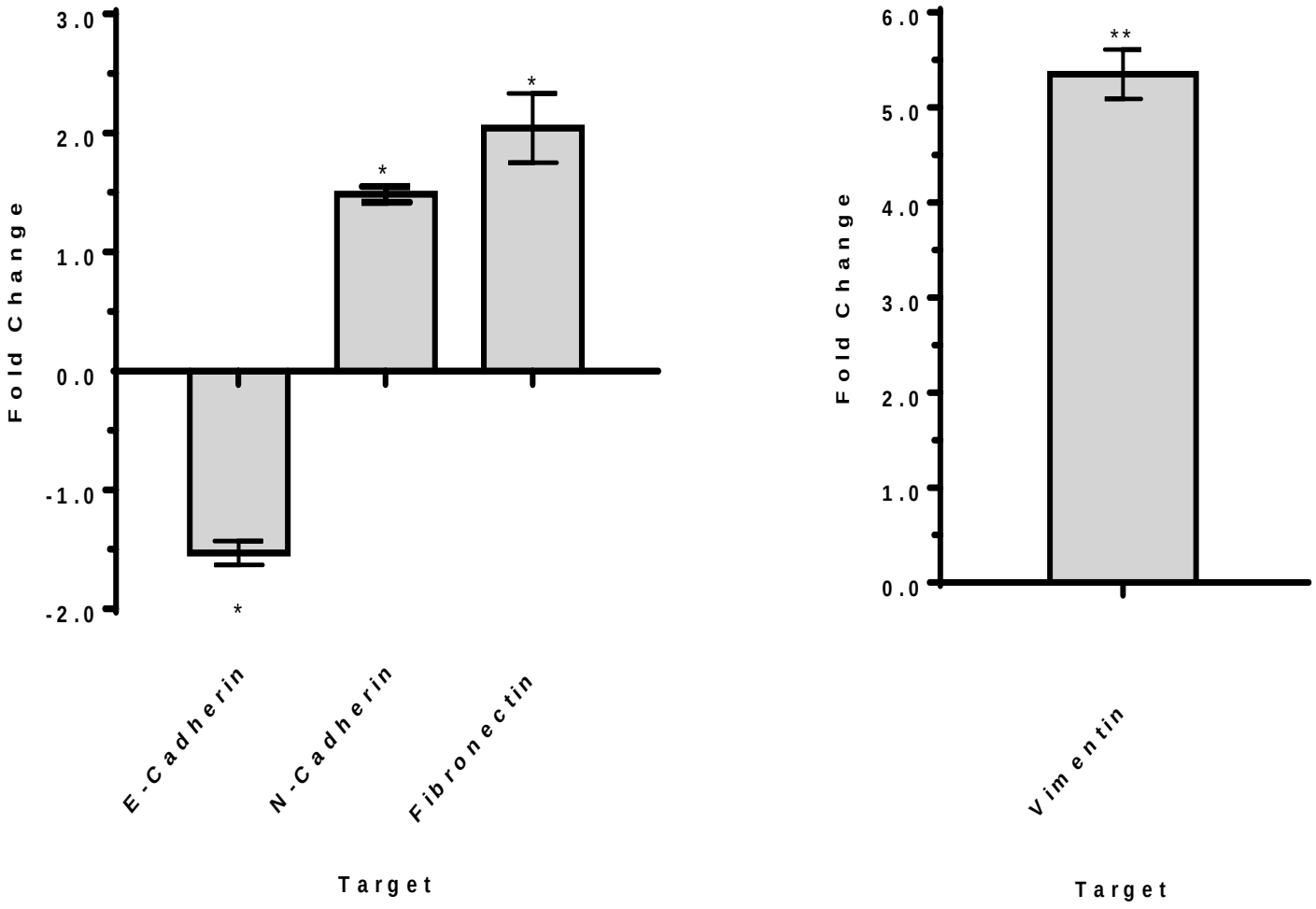

Figure 3.38: Normalized gene expression ($2^{-\Delta\Delta CT}$) of E-cadherin, N-cadherin, and fibronectin, and vimentin in HepG2$^{CLDN-1-}$ cells. HepG2$^{CLDN-1-}$ and HepG2$^{scambled-ve}$ cells were cultured for 72 hours prior to total RNA extraction. Amplification of E-cadherin, N-cadherin, and fibronectin, and vimentin was performed alongside GAPDH and beta-actin as reference genes using RT-PCR. Relative normalised gene expression was calculated using the $2^{-\Delta\Delta CT}$ method. Data presented is representative of mean fold change ±s.e.m from three biological replicates. Paired t-test was performed to determine statistical significance, * P≤0.05 ** P≤0.01

Epithelial marker E-cadherin displayed a decrease in HepG2$^{CLDN-1-}$ cells compared to control HepG2$^{scambled-ve}$, represented by a -1.5 fold change. Statistical analysis determined the fold change significant (P=0.017). The mesenchymal marker vimentin was increased by 5.3 fold in HepG2$^{CLDN-1+}$ cells (P=0.002). Other markers of mesenchymal cells, N-cadherin and Fibronectin were found to be significantly increased by 1.48 fold 2.04 fold (P=0.021 and P=0.0126).

E-cadherin and vimentin are classic markers of EMT initiation in cancer cell progression. The down regulation of the epithelial marker E-cadherin and the upregulation of the mesenchymal marker vimentin are hallmarks of the transition. Interestingly in claudin-1 silenced cells there is a large increase in vimentin expression, but only a small decrease in E-cadherin. This suggests these cells still express both epithelial and mesenchymal markers.

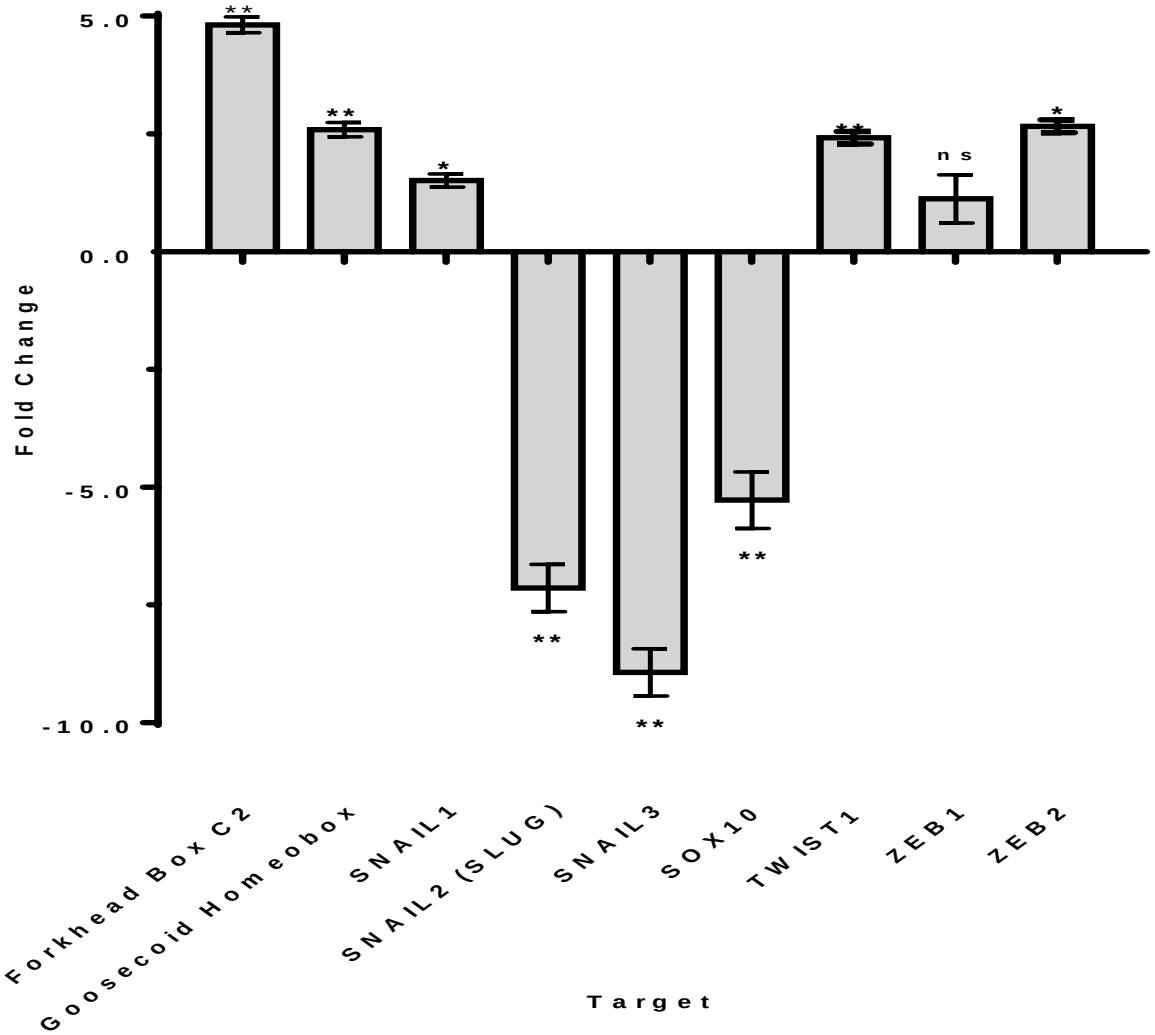

Figure 3.39: Normalized gene expression ($2^{-\Delta\Delta CT}$) of EMT associated transcription factors in HepG2$^{CLDN-1-}$ cells. HepG2$^{CLDN-1-}$ and HepG2$^{scambled-ve}$ cells were cultured for 72 hours prior to total RNA extraction. Amplification of Forkhead box C2, Goosecoid homeobox, SNAIL1, SNAIL2, SNAIL3, SOX10, TWIST1, ZEB1 and ZEB2 was performed alongside GAPDH and beta-actin as reference genes using RT-PCR. Relative normalised gene expression was calculated using the $2^{-\Delta\Delta CT}$ method. Data presented is representative of mean fold change ±s.e.m from three biological replicates. Paired t-test was performed to determine statistical significance, ns – not significant * P≤0.05 ** P≤0.01

Classic EMT inducing transcription factors TWIST1 and ZEB2 were significantly increased by 2.42 and 2.66 fold respectively (P=0.002, P=0.010). Interestingly, ZEB1 was only very slightly increased but the change in expression was not significant (P=0.152). SNAIL1 was the only member of the SNAIL family transcription factors to show an increase in expression, represented by a 1.51-fold change (P=0.028). Other members, SNAIL2 and 3

both decrease significantly by -7.1 and -8.9-fold change (P=0.005, P=0.006 respectively). The expression of SOX10 also significantly decreased, represented by a -5.27 fold change (P=0.003). Other EMT inducing transcription factors Forkhead Box C2 and Goosecoid Homeobox displayed increased expression by 4.8 and 2.6 fold respectively (P=0.002 and P=0.006)

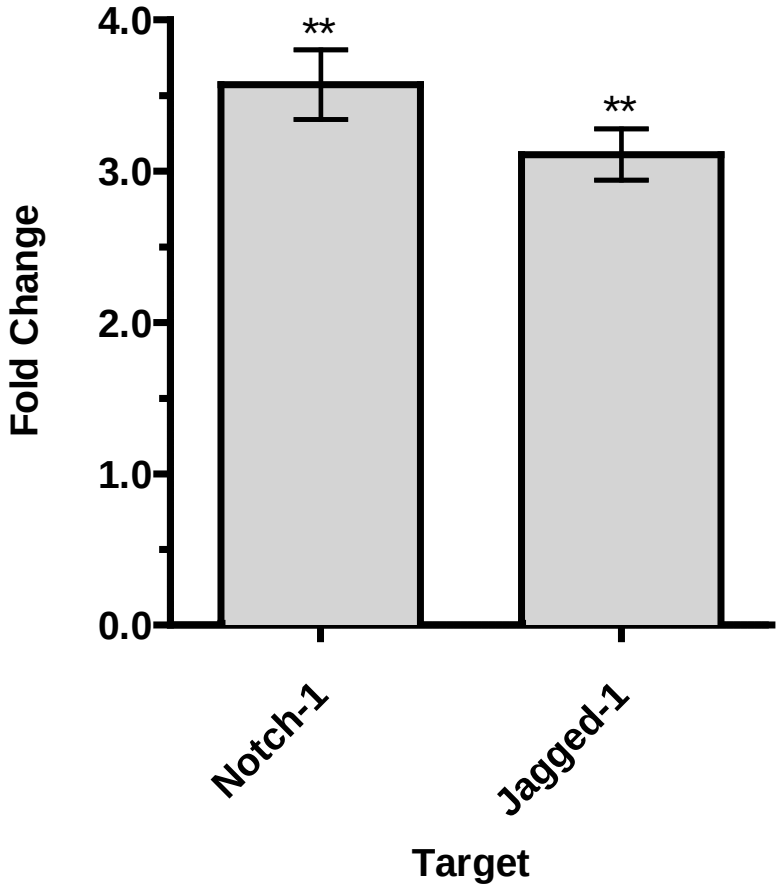

Figure 3.40: Normalized gene expression ($2^{-\Delta\Delta CT}$) of NOTCH associated genes in HepG2$^{CLDN-1-}$ cells. HepG2$^{CLDN-1-}$ and HepG2$^{scambled-ve}$ cells were cultured for 72 hours prior to total RNA extraction. Amplification of notch-1 and jagged-1 was performed alongside GAPDH and beta-actin as reference genes using RT-PCR. Relative normalised gene expression was calculated using the $2^{-\Delta\Delta CT}$ method. Data presented is representative of mean fold change ±s.e.m from three biological replicates. Paired t-test was performed to determine statistical significance, ** P≤0.01

Both NOTCH-1 and JAGGED-1 displayed significantly increased expression, 3.57 and 3.11 fold respectively in HepG2$^{CLDN-1-}$ cells compared to control. Statistical analysis indicated the increase in expression of both genes was significant (P=0.002, P=0.003).

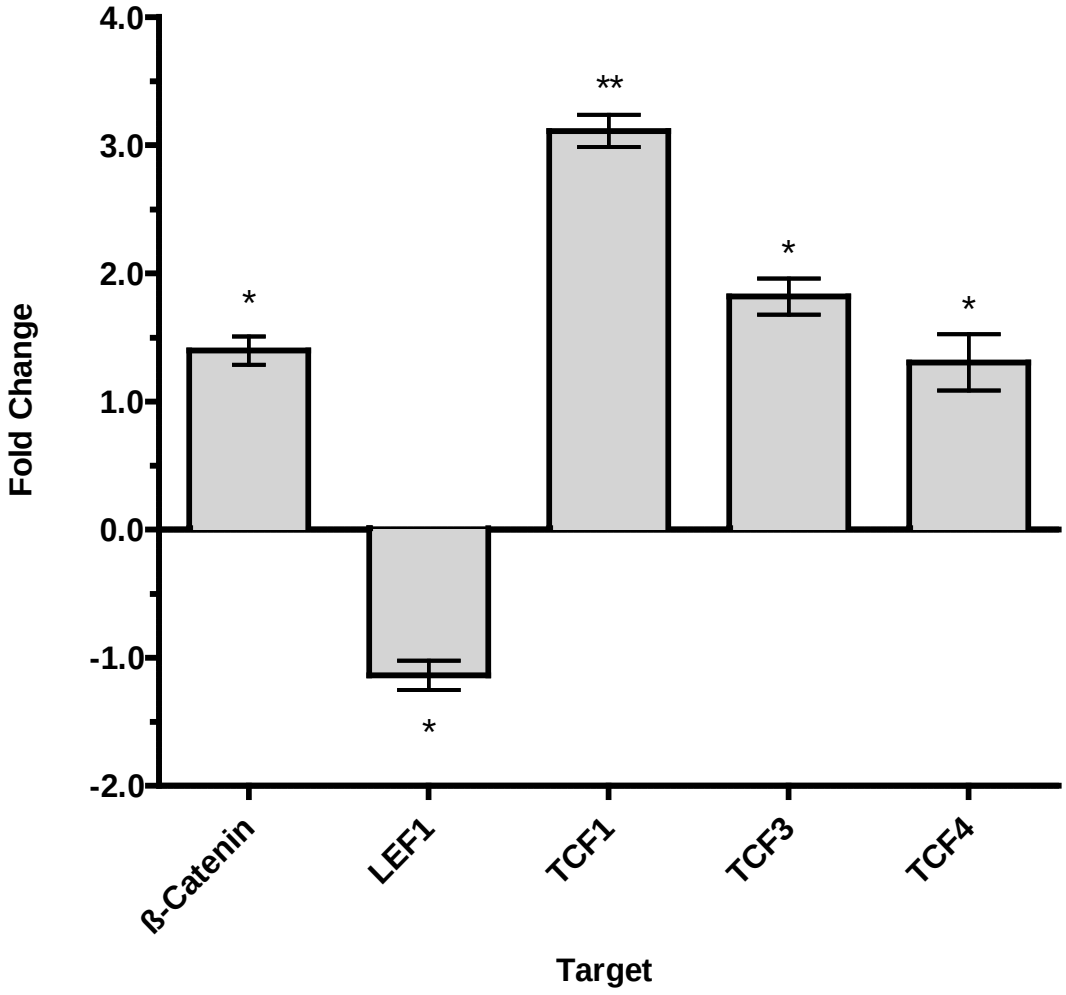

Figure 3.41: Normalized gene expression ($2^{-\Delta\Delta CT}$) of WNT / β-catenin target genes in HepG2$^{CLDN-1-}$ cells. HepG2$^{CLDN-1-}$ and HepG2$^{scambled-ve}$ cells were cultured for 72 hours prior to total RNA extraction. Amplification of β-catenin, LEF1, TCF1, TCF3 and TCF4 was performed alongside GAPDH and beta-actin as reference genes using RT-PCR. Relative normalised gene expression was calculated using the $2^{-\Delta\Delta CT}$ method. Data presented is representative of mean fold change ±s.e.m from three biological replicates. Paired t-test was performed to determine statistical significance, * P≤0.05 ** P≤0.01

The expression of β-catenin was slightly increased in HepG2$^{CLDN-1-}$ cells compared to control HepG2$^{scambled-ve}$, represented by a 1.4-fold change. Statistical analysis determined the fold change significant (P=0.022). Expression of LEF1 was found to be slightly

decreased, however the change in expression was significant (P=0.02). The expression of TCF1, TCF3 and TCF4 were all found to have increased expression in in HepG2$^{CLDN-1-}$ cells compared to control HepG2$^{scambled-ve}$ by 3.11, 1.84 and 1.30-fold change respectively. The change in expression of TCF1 and 3 was found to be significant but the change in expression of TCF4 was not (P=0.003, P=0.021 and P=0.057 respectively)

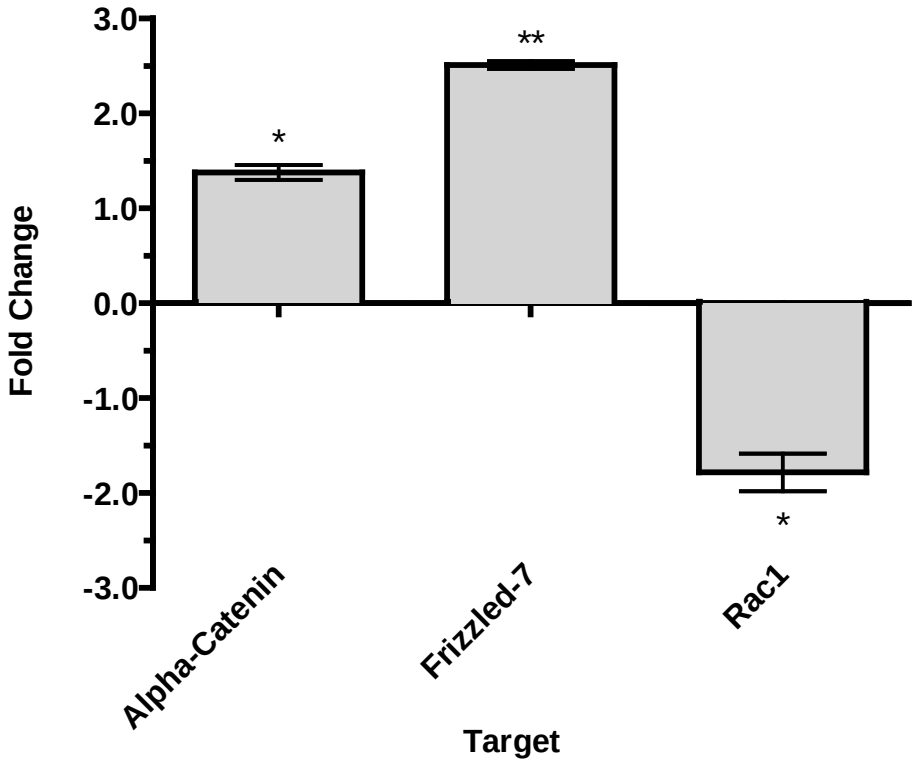

Figure 3.42: Normalized gene expression ($2^{-\Delta\Delta CT}$) of associated WNT / β-catenin target genes in HepG2$^{CLDN-1-}$ cells. HepG2$^{CLDN-1-}$ and HepG2$^{scambled-ve}$ cells were cultured for 72 hours prior to total RNA extraction. Amplification of alpha-catenin, frizzled-7 and rac1 was performed alongside GAPDH and beta-actin as reference genes using RT-PCR. Relative normalised gene expression was calculated using the $2^{-\Delta\Delta CT}$ method. Data presented is representative of mean fold change ±s.e.m from three biological replicates. Paired t-test was performed to determine statistical significance, * P≤0.05 ** P≤0.01

The expression of α-Catenin and frizzled-7 was significantly increased by 1.37 and 2.5 fold respectively in HepG2$^{CLDN-1-}$ cells compared to control (P=0.024 and P=0.002). Expression of Rac1 was significantly in HepG2$^{CLDN-1-}$ cells -1.78-fold change (P=0.013)

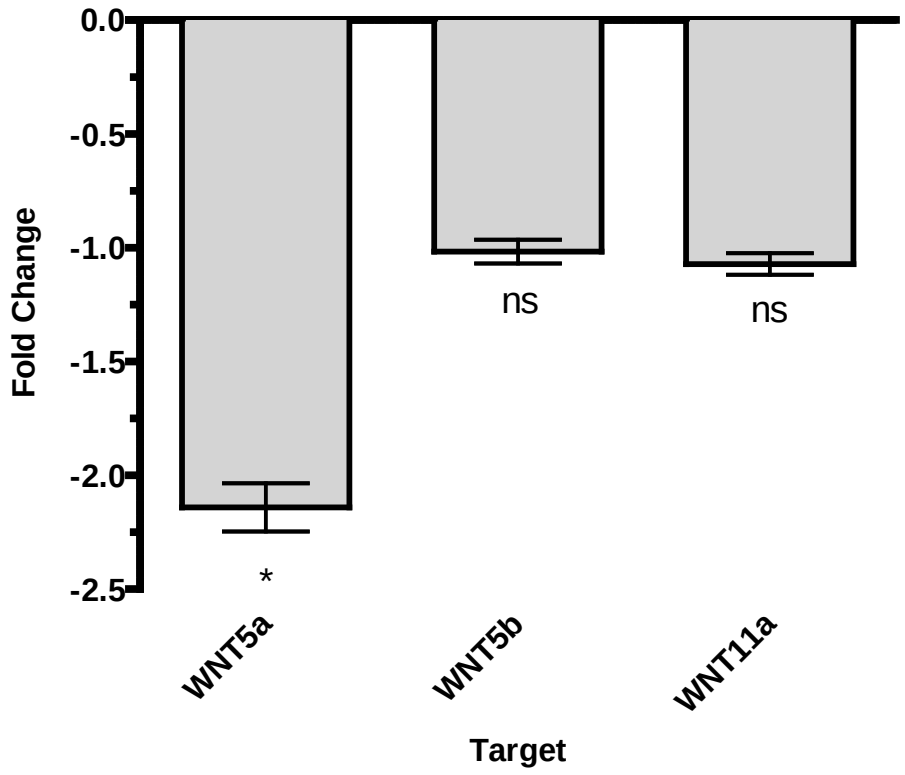

Figure 3.43: Normalized gene expression ($2^{-\Delta\Delta CT}$) of WNT5a, WNT5b and WNT11a in HepG2$^{CLDN-1-}$ cells. HepG2$^{CLDN-1-}$ and HepG2$^{scambled-ve}$ cells were cultured for 72 hours prior to total RNA extraction. Amplification of WNT5a, WNT5b and WNT11a was performed alongside GAPDH and beta-actin as reference genes using RT-PCR. Relative normalised gene expression was calculated using the $2^{-\Delta\Delta CT}$ method. Data presented is representative of mean fold change ±s.e.m from three biological replicates. Paired t-test was performed to determine statistical significance, ns – not significant * P≤0.05

The expression of WNT5a, WNT5b and WNT11a were all decreased in HepG2$^{CLDN-1-}$ cells compared to control by -2.14, -1.01- and -1.07-fold change respectively. Statistical analysis revealed only the change in expression of WNT5a was significant (P=0.013, P=0.912 and P=0.165)

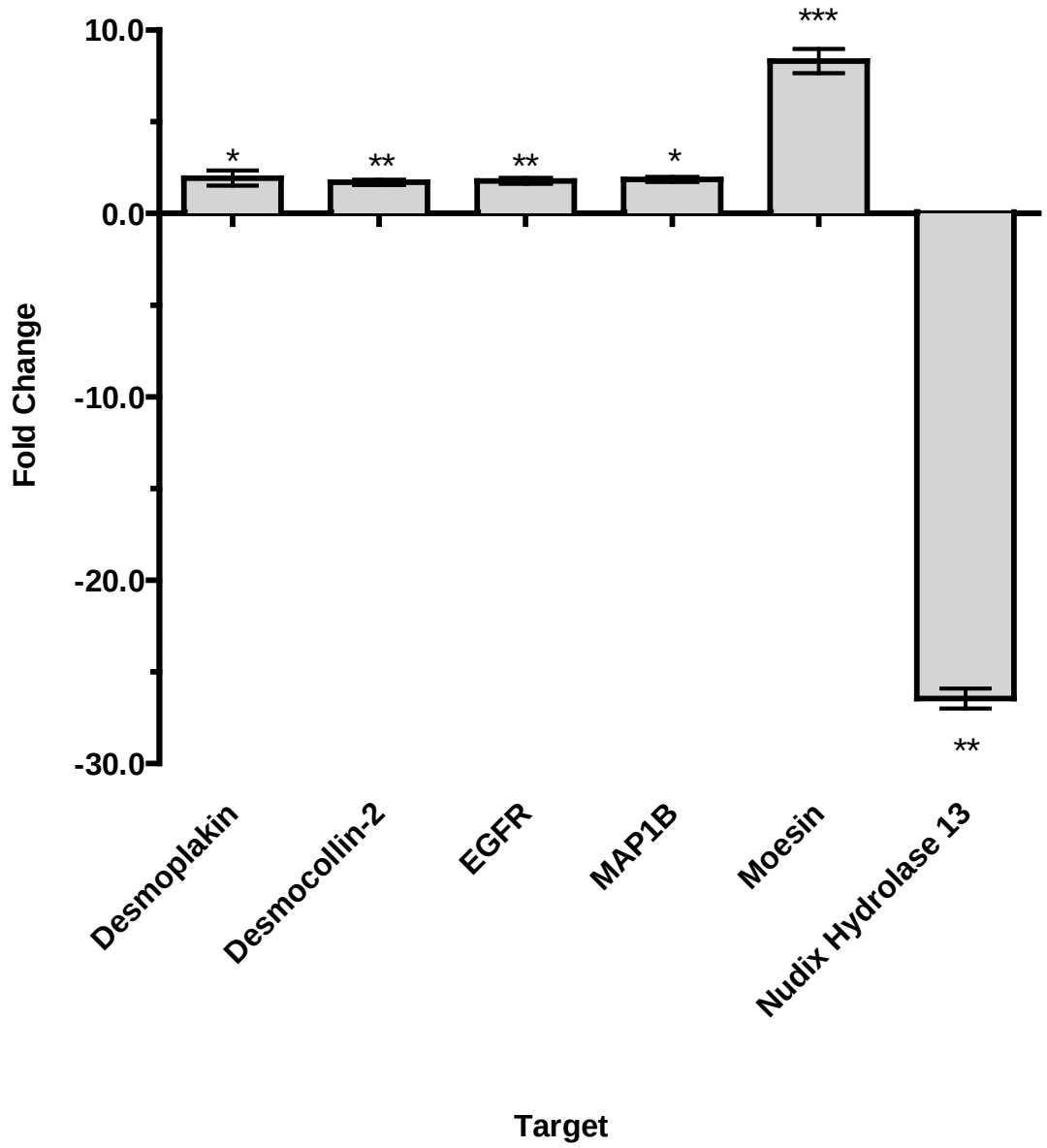

Figure 3.44: Normalized gene expression ($2^{-\Delta\Delta CT}$) of other associated EMT target genes in HepG2$^{CLDN-1-}$ cells. HepG2$^{CLDN-1-}$ and HepG2$^{scambled-ve}$ cells were cultured for 72 hours prior to total RNA extraction. Amplification of desmoplakin, desmocollin-2, EGFR, MAP1B, moesin and nudix hydrolase 13 was performed alongside GAPDH and beta-actin as reference genes using RT-PCR. Relative normalised gene expression was calculated using the $2^{-\Delta\Delta CT}$ method. Data presented is representative of mean fold change ±s.e.m from three biological replicates. Paired t-test was performed to determine statistical significance, * P≤0.05 ** P≤0.01

The expression of Desmoplakin, Desmocollin-2, EGFR, MAP1b and Moesin were all increased in HepG2$^{CLDN-1-}$ cells compared to control. Statistical analysis of these genes revealed that the increased expression was significant (P=0.015, P=0.004, P=0.009,

P=0.004 and P<0.001). The expression of Nudix Hydrolase 13 was significantly decreased in HepG2$^{CLDN-1-}$ cells compared to control by -26.45 fold (P=0.003).

Although there are a number of differences, it appears that both over and under expression of claudin-1 in HepG2 cells produce similar patterns of expression of EMT genes. A number of these genes, particularly EMT transcription factors, are able to mediate groups of tumour metastasis genes capable of remodelling the tumour microenvironment and ultimately orchestrating an invasive and metastatic phenotype (Karlsson et al 2017). It is important to determine the expression of these genes in claudin-1 overexpressing and silenced cells as it could give an indication of the metastatic potential in these cells and how HCC tumours presenting with the same molecular profile might behave *in vivo*.

3.9 Expression of β-catenin in claudin-1 overexpressed and claudin-1 silenced HepG2 cells

The gene expression of β-catenin was shown to be significantly increased both HepG2$^{CLDN-1+}$ and HepG2$^{CLDN-1-}$ cells by 3.6 fold and 1.4 fold respectively. The role of β-catenin in the initiation of EMT is complex, but initiation relies on stabilisation of the protein. Unless stabilised, β-catenin is ubiquitinatised and targeted for proteosomal degradation by the β-catenin destruction complex (MacDonald et al 2009). PCR data has revealed the that both claudin-1 overexpression and silencing influences the expression of β-catenin and several WNT/β-catenin target genes. However, the protein level of β-catenin needed to be quantified to determine if the increased levels of mRNA seen in PCR were translated to protein, and if that protein was stabilised or targeted for degradation.

The protein expression of β-catenin was determined in HepG2$^{CLDN-1+}$, HepG2$^{CLDN-1-}$ and their respective controls HepG2$^{pCMV-ve}$, HepG2$^{scambled-ve}$ via western blotting.

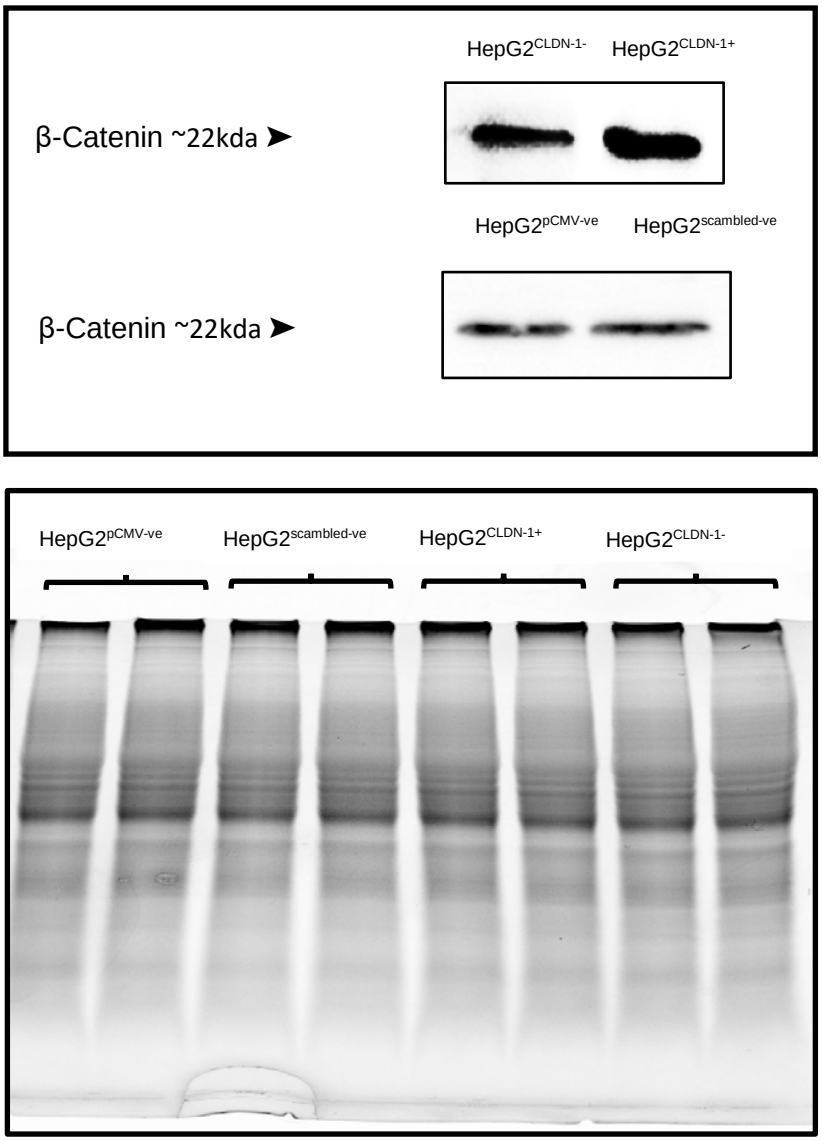

Figure 3.45: β-catenin protein expression in HepG2$^{CLDN-1+}$, HepG2$^{CLDN-1-}$ and the respective controls HepG2$^{pCMV-ve}$ and HepG2$^{scambled-ve}$ cells. HepG2$^{CLDN-1+}$, HepG2$^{CLDN-1-}$ and their respective controls HepG2$^{pCMV-ve}$, HepG2$^{scambled-ve}$ were cultured for 72 hours prior to cell lysis and extraction using TRIsure. Protein concentration was determined using a nanodrop spectrophotometer. Cell lysates were denatured and subjected to SDS-PAGE and immunoblot to determine the protein expression of β-catenin. The first image (above) represents an immunoblot which has been probed using a β-catenin Rabbit monoclonal antibody (Cell Signalling #8480) on samples HepG2$^{CLDN-1+}$, HepG2$^{CLDN-1-}$ and HepG2$^{pCMV-ve}$, HepG2$^{scambled-ve}$. The second image (below) represents a stain-free gel used as a loading control. Normalised expression was calculated using Bio-Rad Stain Free Technology and Lab Manager software. Data presented is representative of mean fold change ±s.e.m from three biological replicates. Paired t-test was performed to determine statistical significance.

Normalisation using stain-free technology determined that HepG2$^{CLDN-1+}$ cells contained a 4.5-fold increase in β-catenin protein compared to HepG2$^{pCMV-ve}$ cells. HepG2$^{CLDN-1+}$showed a 2-fold increase compared to HepG2$^{scambled-ve}$ cells. This indicates that the β-catenin expression is increased in both HepG2$^{CLDN-1+}$ and HepG2$^{CLDN-1+}$ cells and is not being targeted for destruction.

3.10 Determining the expression of tumour metastasis related genes in claudin-1 overexpressing and claudin-1 silenced HepG2 cells

Epithelial–mesenchymal transition (EMT) is an important initiation step for several cancers in the early stages of metastasis. Increased motility and reduced intercellular adhesion associated with EMT increase the metastatic capacity of cancer cells, but other processes that enable invasion and colonisation need to be activated for successful cancer migration. The expression of genes associated with tumour metastasis can be influenced by a number of mechanisms and mutations including those responsible for EMT. Screening of the expression of tumour metastasis and associated oncogenes provide valuable prognostic markers and predictions of the migratory capacity of those cells.

Claudin-1 overexpressing and claudin-1 silenced HepG2 cells were analysed to determine the expression of genes associated with tumour metastasis using a PCR panel of 26 target and housekeeping genes (GAPDH/Beta-actin)

3.10.1 Expression of tumour metastasis related genes in claudin-1 overexpressing HepG2 cells

Target	Sample	Expression ($2^{-\Delta\Delta CT}$)	Expression ($2^{-\Delta\Delta CT}$) Standard Deviation	Compared to Regulation Threshold	P-Value	Exceeds P-Value Threshold (0.05)
Glyceraldehyde 3-phosphate dehydrogenase	HepG2 CLDN-1+	1.033	0.135	No Change	0.256	Yes
Beta-actin	HepG2 CLDN-1+	-1.004	0.306	No Change	0.732	Yes
Cathepsin-K	HepG2 CLDN-1+	2.556	0.158	Up Regulated	0.004	No
Cathepsin-L	HepG2 CLDN-1+	2.402	0.146	Up Regulated	0.003	No
CD44 Molecule	HepG2 CLDN-1+	-6.452	0.102	Down Regulated	0.009	No
C-X-C motif chemokine-12	HepG2 CLDN-1+	36.603	5.729	Up Regulated	0.003	No
C-X-C chemokine receptor type-4	HepG2 CLDN-1+	2.577	0.565	Up Regulated	0.015	No
Ephrin Type-B receptor-2	HepG2 CLDN-1+	65.314	2.632	Up Regulated	0.003	No
Dysadherin	HepG2 CLDN-1+	39.297	1.560	Up Regulated	0.005	No
Kisspeptin-1	HepG2 CLDN-1+	-4.885	0.144	Down Regulated	0.002	No
Kisspeptin Receptor	HepG2 CLDN-1+	-3.386	0.026	Down Regulated	0.002	No
Cytokeratin-7	HepG2 CLDN-1+	-1.894	0.112	Down Regulated	0.015	No
Cytokeratin-14	HepG2 CLDN-1+	-2.196	0.025	Down Regulated	0.041	No
Cytokeratin-19	HepG2 CLDN-1+	-24.331	0.910	Down Regulated	0.002	No
Matrix Metalloproteinase-2	HepG2 CLDN-1+	54.839	1.745	Up Regulated	0.003	No
Matrix Metalloproteinase-3	HepG2 CLDN-1+	-57.657	0.012	Down Regulated	0.001	No
Matrix Metalloproteinase-7	HepG2 CLDN-1+	-61.923	0.064	Down Regulated	0.019	No

Matrix Metalloproteinase-9	HepG2 CLDN-1+	2.865	0.261	Up Regulated	0.001	No
Matrix Metalloproteinase-10	HepG2 CLDN-1+	2.811	0.307	Up Regulated	0.010	No
Matrix Metalloproteinase-11	HepG2 CLDN-1+	1.210	0.491	No Change	0.455	Yes
Matrix Metalloproteinase-13	HepG2 CLDN-1+	10.864	0.437	Up Regulated	0.003	No
Tissue Inhibitor of Metalloproteinases-1	HepG2 CLDN-1+	-1.480	0.056	Down Regulated	0.002	No
Tissue Inhibitor of Metalloproteinases-2	HepG2 CLDN-1+	-3.096	0.129	Down Regulated	0.002	No
Tissue Inhibitor of Metalloproteinases-3	HepG2 CLDN-1+	-4.880	0.034	Down Regulated	0.005	No
Tissue Inhibitor of Metalloproteinases-4	HepG2 CLDN-1+	-17.391	0.023	Down Regulated	0.003	No
TRAIL (Tumor Necrosis Factor Superfamily Member 10)	HepG2 CLDN-1+	-7.616	0.262	Down Regulated	0.004	No

Table 3.5: Normalised gene expression ($2^{-\Delta\Delta CT)}$ of tumour metastasis related genes in claudin-1 overexpressing HepG2 cells. The table details the relative normalised gene expression of 26 tumour metastasis related genes in $HepG2^{CLDN-1+}$ cells, $HepG2^{pCMV-ve}$ cells were used as the control. $HepG2^{CLDN-1+}$ and $HepG2^{pCMV-ve}$ cells were cultured for 72 hours prior to total RNA extraction. Amplification of the genes outlined in Table 3.5 was performed alongside GAPDH and beta-actin as the reference genes using RT-PCR. Relative normalised gene expression was calculated using the $2^{-\Delta\Delta CT}$ method. Data presented is representative of mean fold change ±s.e.m from three biological replicates. Paired t-test was performed to determine statistical significance. Statistical significance is indicated if the P value is lower than the 0.05 threshold.

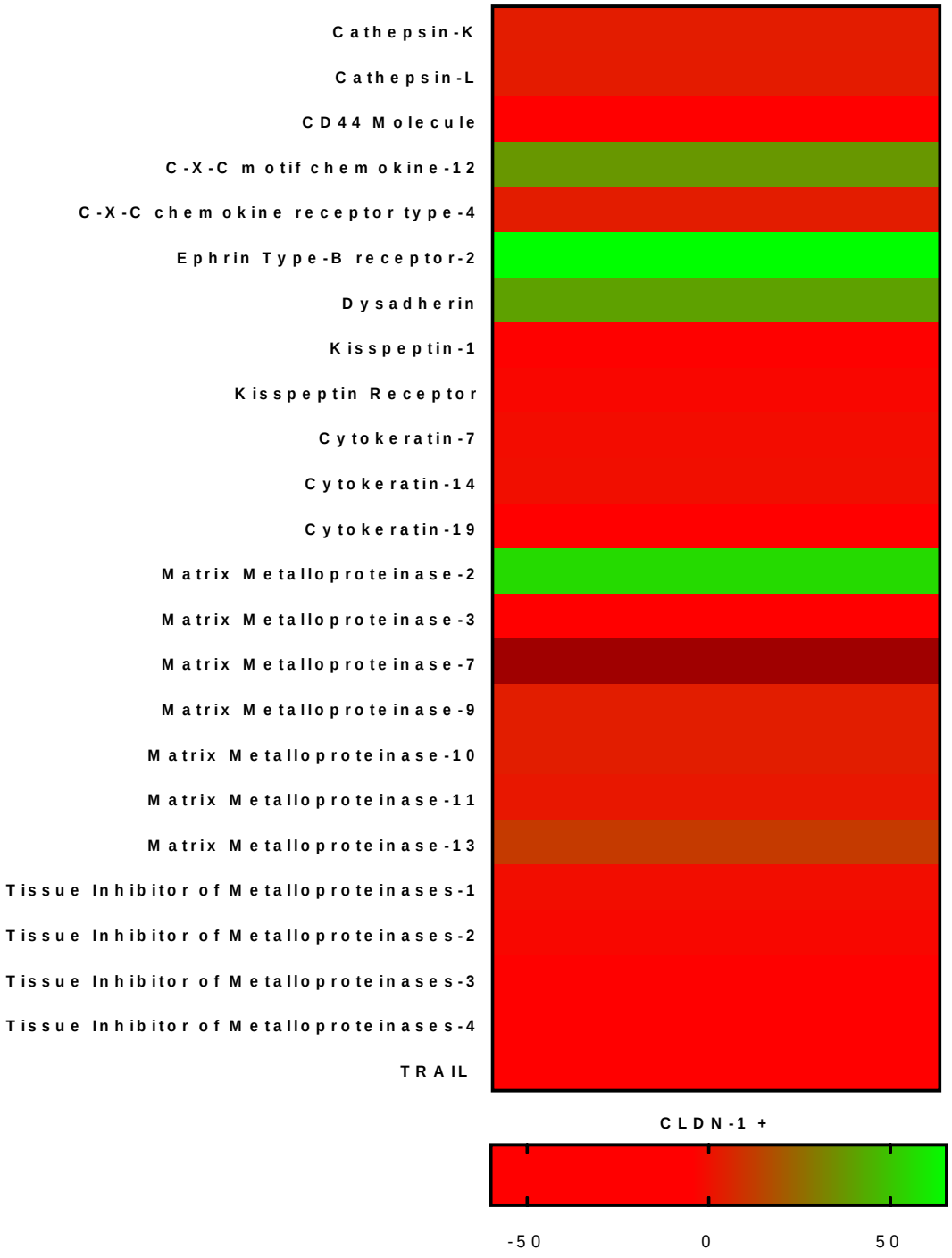

Figure 3.46: Heat map representing normalised gene expression ($2^{-\Delta\Delta CT}$) of tumour metastasis related genes in claudin-1 overexpressing HepG2 cells. Normalised gene expression values taken from Table 3.3 have been converted into a colorimetric scale outlined above to provide a visual representation of large scale changes. Genes indicated by a green bar represent an upregulation in expression, whereas genes indicated by a red bar represent a down regulation in expression.

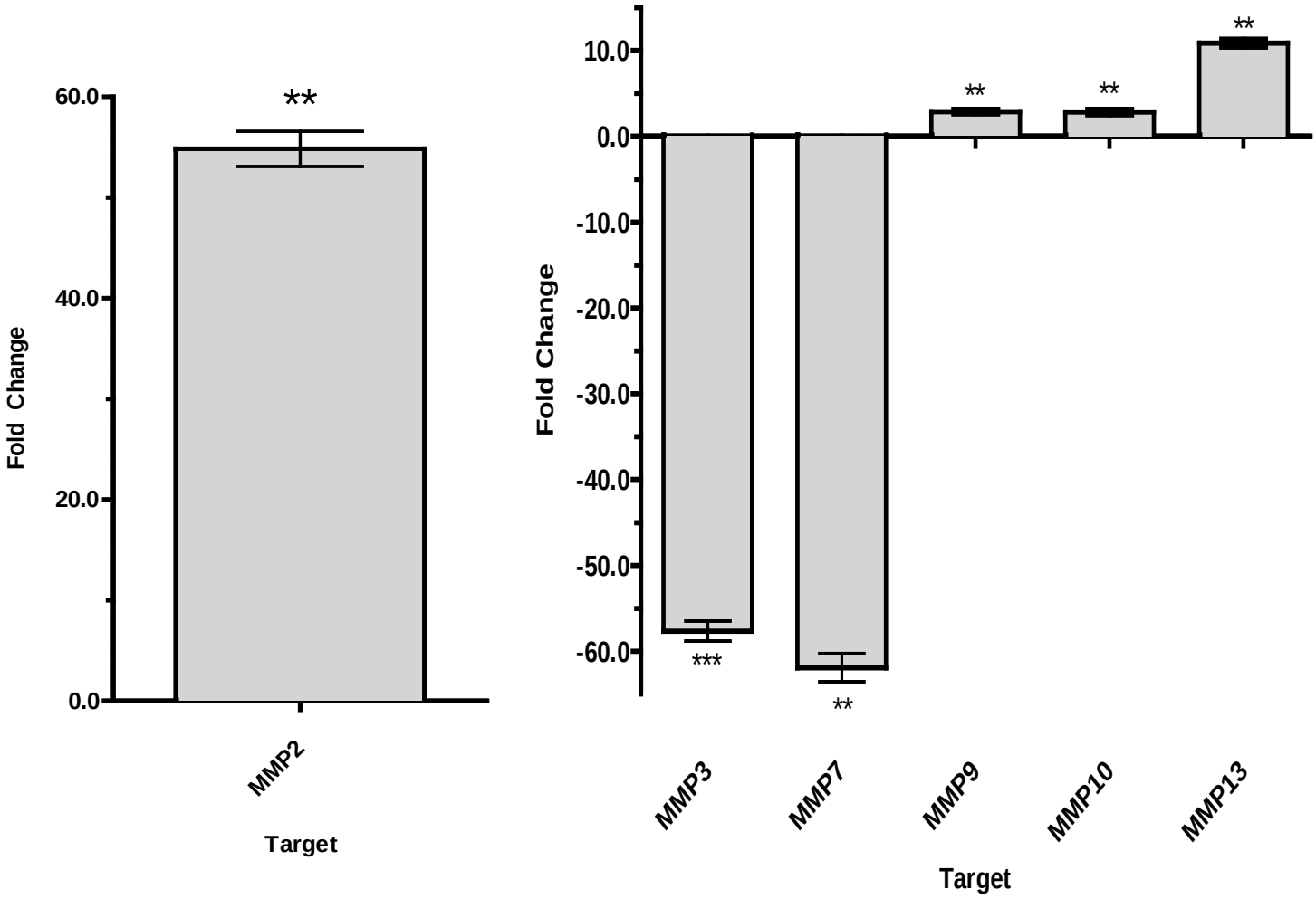

Figure 3.47: Normalized gene expression ($2^{-\Delta\Delta CT}$) of Matrix Metalloproteinases in HepG2$^{CLDN-1+}$ cells. HepG2$^{CLDN-1+}$ and HepG2$^{pCMV-ve}$ cells were cultured for 72 hours prior to total RNA extraction. Amplification of MMP2, MMP3, MMP7, MMP9, MMP10 and MMP13 was performed alongside GAPDH and beta-actin as reference genes using RT-PCR. Relative normalised gene expression was calculated using the $2^{-\Delta\Delta CT}$ method. Data presented is representative of mean fold change ±s.e.m from three biological replicates. Paired t-test was performed to determine statistical significance, * P≤0.05 ** P≤0.01 *** P≤0.001 .

The expression of MMP2 was massively increased in HepG2$^{CLDN-1+}$ cells compared to HepG2$^{pCMV-ve}$, represented by a significant 54.8-fold change (P=0.002). The second largest increase was MMP13 with a significant 10.8-fold increase (P=0.003). MMP's 9, 10 and 11 were also increased by 2.8, 2.8 and 1.2 fold respectively. Statistical analysis indicated MMP9 and 10 was significantly increased (P=0.001, P=0.009). MMP11 exceeded the P-value threshold (P=0.45). MMP3 and 7 decreased in HepG2$^{CLDN-1+}$ cells compared to

control, represented by a significant -57.6 and -61.9 fold change, respectively (P=0.0008 and 0.019).

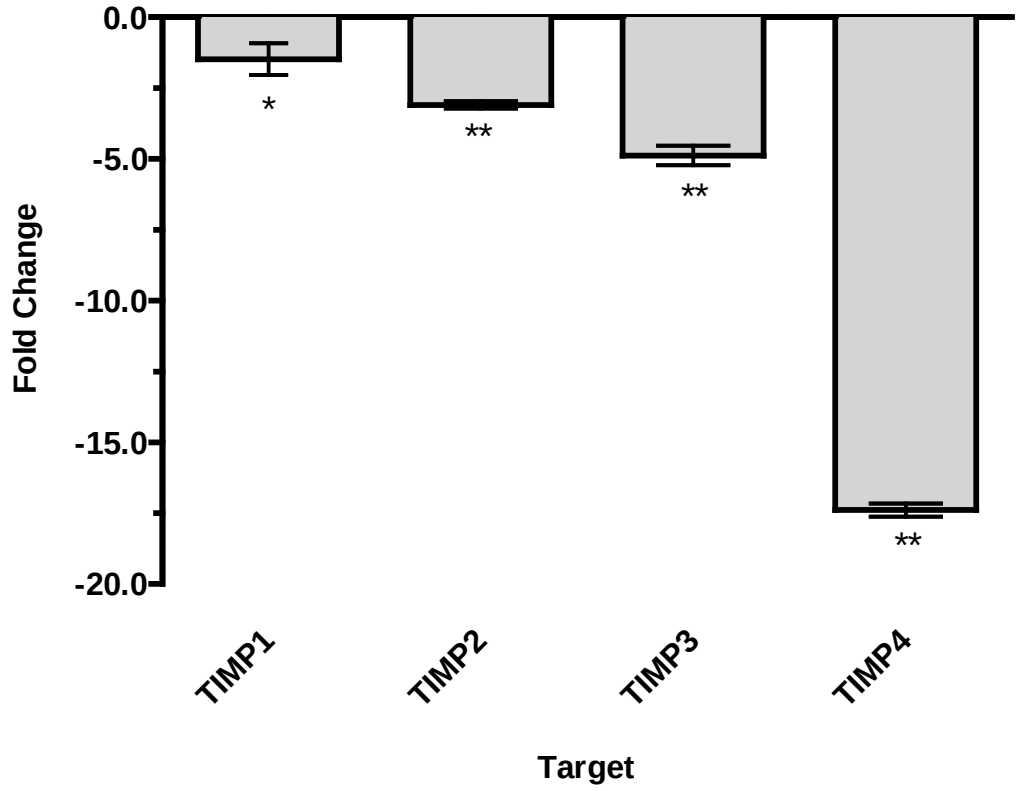

Figure 3.48: Normalized gene expression ($2^{-\Delta\Delta CT}$) of TIMP -1, -2, -3 and -4 in HepG2$^{CLDN-1+}$ cells. HepG2$^{CLDN-1+}$ and HepG2$^{pCMV-ve}$ cells were cultured for 72 hours prior to total RNA extraction. Amplification of TIMP -1, -2, -3 and -4 was performed alongside GAPDH and beta-actin as reference genes using RT-PCR. Relative normalised gene expression was calculated using the $2^{-\Delta\Delta CT}$ method. Data presented is representative of mean fold change ±s.e.m from three biological replicates. Paired t-test was performed to determine statistical significance, * P≤0.05 ** P≤0.01

Expression of TIMP family members 1-4 were decreased in HepG2$^{CLDN-1+}$ cells compared to HepG2$^{pCMV-ve}$ represented by a -1.5, -3.1, -4.9- and -17.5 fold change, respectively. Statistical analysis indicated changes in expression of all TIMPS 1-4 was significant (P=0.002, P=0.002, P=0.010 and P=0.003)

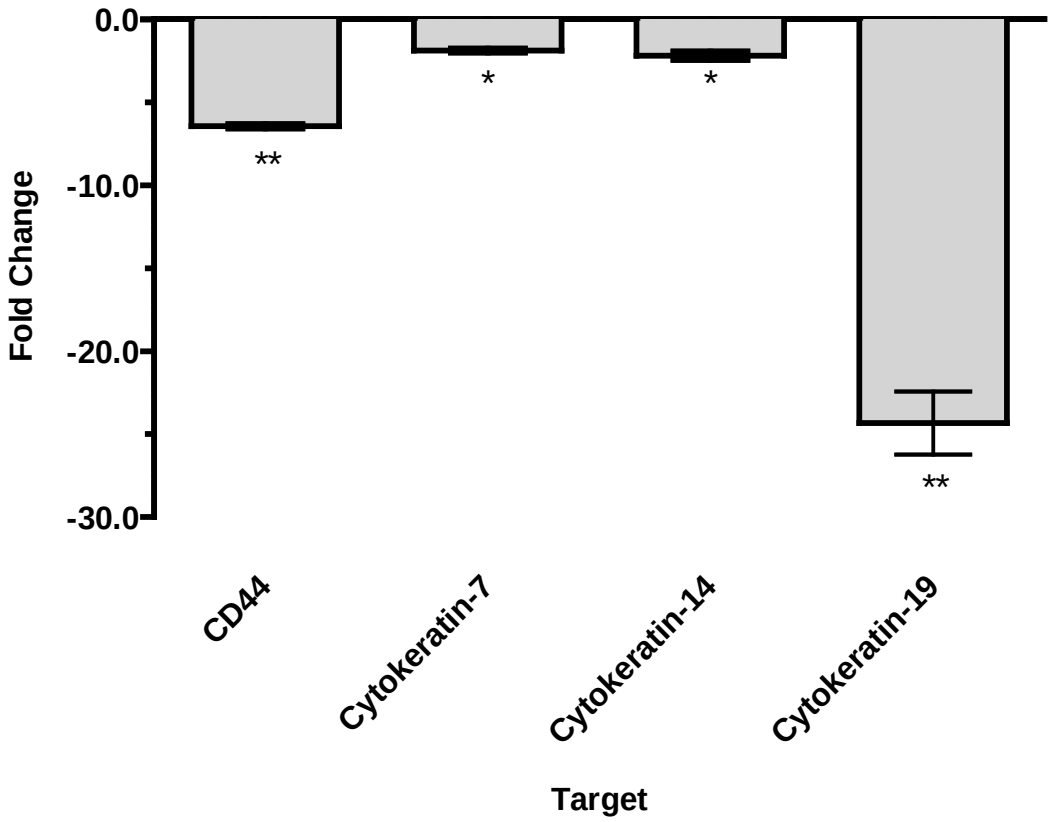

Figure 3.49: Normalized gene expression ($2^{-\Delta\Delta CT}$) of cancer stem cell markers in HepG2$^{CLDN-1+}$ cells. HepG2$^{CLDN-1+}$ and HepG2$^{pCMV-ve}$ cells were cultured for 72 hours prior to total RNA extraction. Amplification of CD44, cytokeratin-7, cytokeratin-14 and cytokeratin-19 was performed alongside GAPDH and beta-actin as reference genes using RT-PCR. Relative normalised gene expression was calculated using the $2^{-\Delta\Delta CT}$ method. Data presented is representative of mean fold change ±s.e.m from three biological replicates. Paired t-test was performed to determine statistical significance, * P≤0.05 ** P≤0.01

The expression of cancer stem cell markers CD44 and cytokeratins -7, -14 and -19 were decreased in HepG2$^{CLDN-1+}$ cells compared to HepG2$^{pCMV-ve}$, represented by a -6.45, -1.9, -1.2 and -24.3 fold change respectively. Statistical analysis indicated that the decrease in expression of CD44 and Cytokeratin members was significant (P= 0.009, P= 0.015, P= 0.041 and P=0.002)

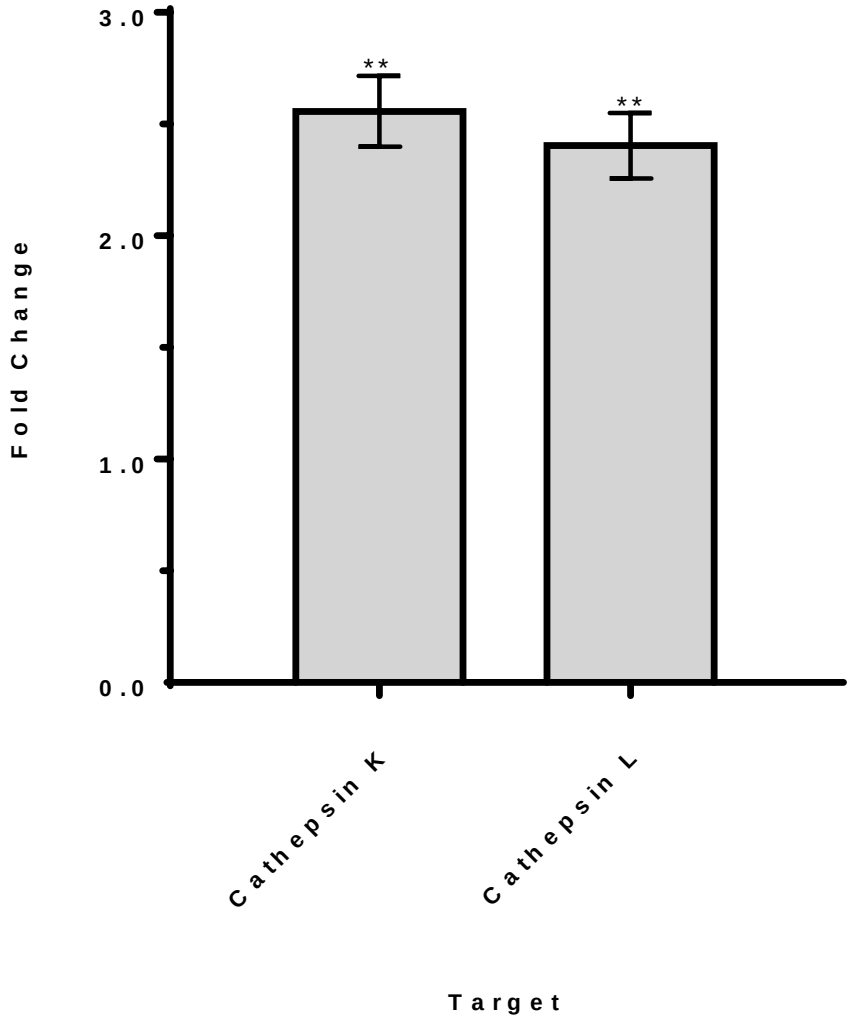

Figure 3.50: Normalized gene expression ($2^{-\Delta\Delta CT}$) of cathepsin K and L in HepG2$^{CLDN-1+}$ cells. HepG2$^{CLDN-1+}$ and HepG2$^{pCMV-ve}$ cells were cultured for 72 hours prior to total RNA extraction. Amplification of cathepsin K and L was performed alongside GAPDH and beta-actin as reference genes using RT-PCR. Relative normalised gene expression was calculated using the $2^{-\Delta\Delta CT}$ method. Data presented is representative of mean fold change ±s.e.m from three biological replicates. Paired t-test was performed to determine statistical significance, ** P≤0.01

Both cathepsin K and L displayed significantly increased expression, 2.55 and 2.40 fold respectively in HepG2$^{CLDN-1+}$ cells compared to control. Statistical analysis indicated the increase in expression of both genes was significant (P=0.004, P=0.003).

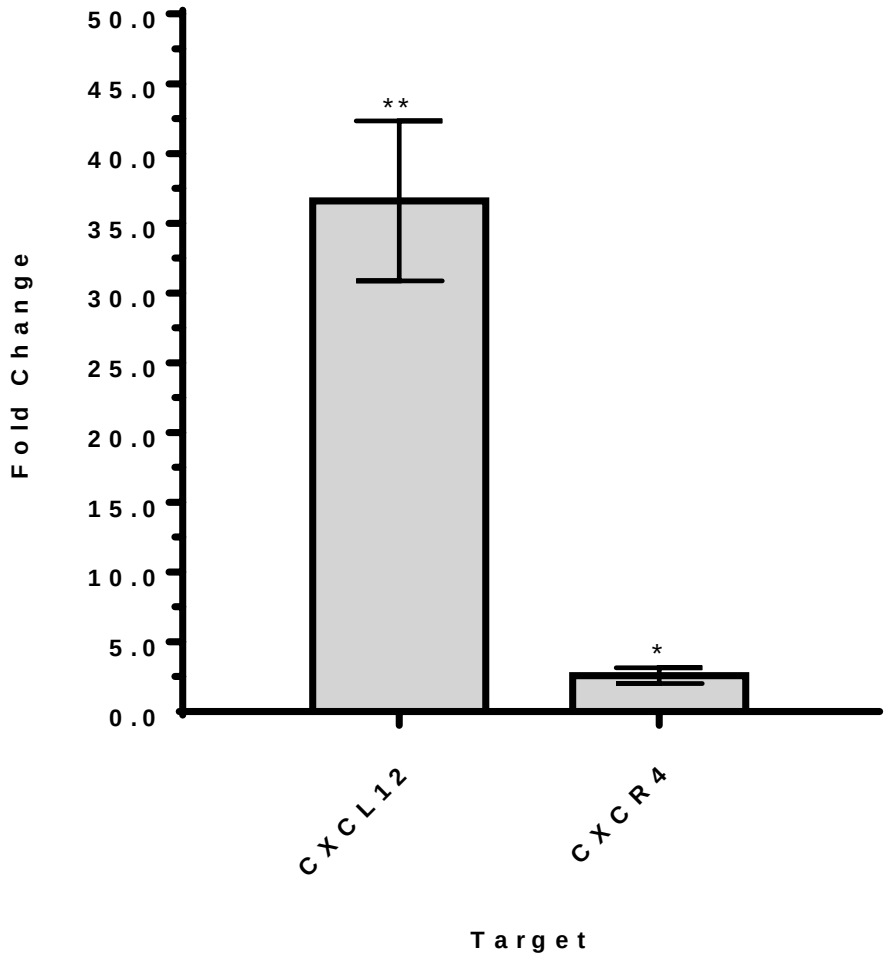

Figure 3.51: Normalized gene expression ($2^{-\Delta\Delta CT}$) of CXCL12 and CXCR4 in HepG2$^{CLDN\text{-}1+}$ cells. HepG2$^{CLDN\text{-}1+}$ and HepG2$^{pCMV\text{-}ve}$ cells were cultured for 72 hours prior to total RNA extraction. Amplification of CXCL12 and CXCR4 was performed alongside GAPDH and beta-actin as reference genes using RT-PCR. Relative normalised gene expression was calculated using the $2^{-\Delta\Delta CT}$ method. Data presented is representative of mean fold change ±s.e.m from three biological replicates. Paired t-test was performed to determine statistical significance, * P≤0.05 ** P≤0.01

Both C-X-C motif chemokine-12 and C-X-C chemokine receptor type-4 displayed significantly increased expression, 36.6 and 2.6 fold respectively in HepG2$^{CLDN\text{-}1+}$ cells compared to control. Statistical analysis indicated the increase in expression of both genes was significant (P=0.002, P=0.014).

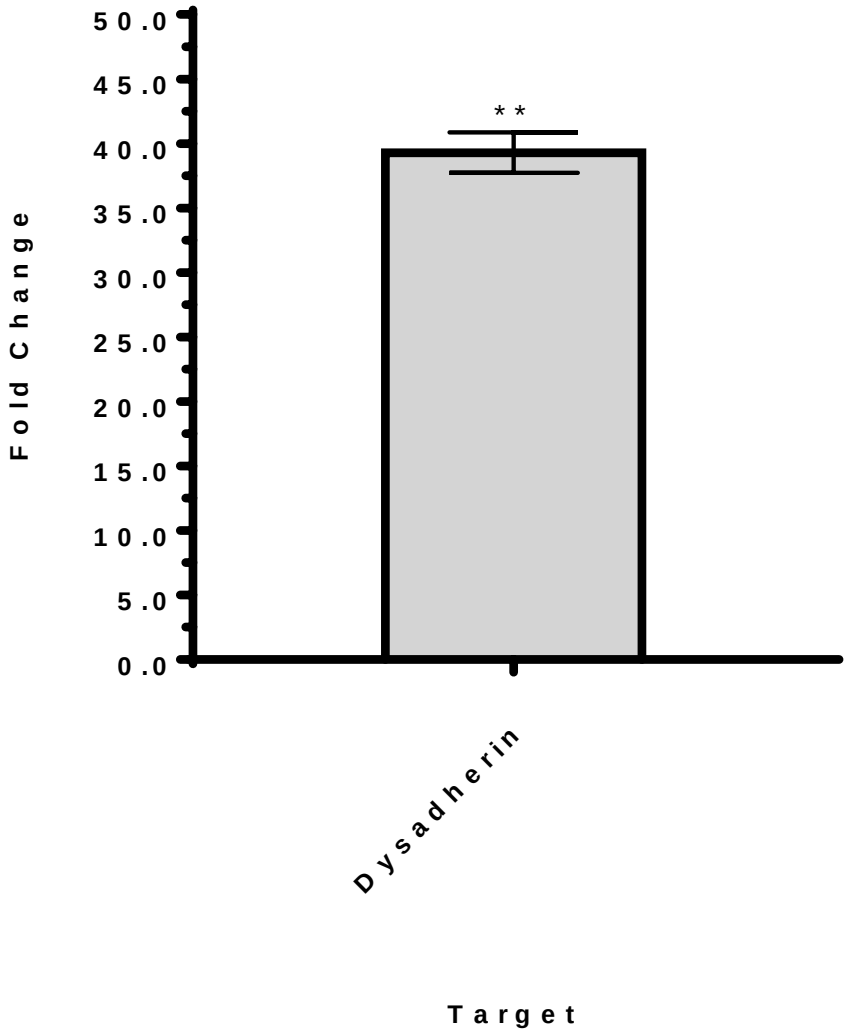

Figure 3.52: Normalized gene expression ($2^{-\Delta\Delta CT}$) of dysadherin in HepG2$^{CLDN-1+}$ cells. HepG2$^{CLDN-1+}$ and HepG2$^{pCMV-ve}$ cells were cultured for 72 hours prior to total RNA extraction. Amplification of dysadherin was performed alongside GAPDH and beta-actin as reference genes using RT-PCR. Relative normalised gene expression was calculated using the $2^{-\Delta\Delta CT}$ method. Data presented is representative of mean fold change ±s.e.m from three biological replicates. Paired t-test was performed to determine statistical significance, ** P≤0.01

The expression of Dysadherin was increased considerably in HepG2$^{CLDN-1+}$ cells compared to control represented by a 39.3-fold change. Statistical analysis indicated the increase in expression was significant (P=0.004).

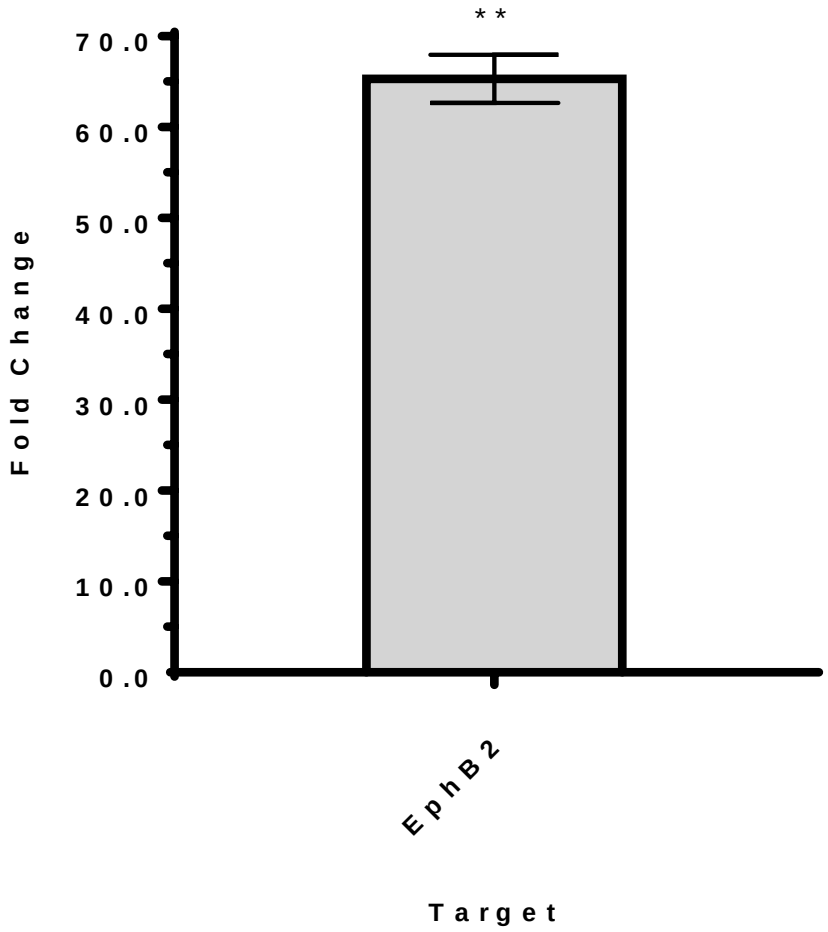

Figure 3.53: Normalized gene expression ($2^{-\Delta\Delta CT}$) of EphB2 in HepG2$^{CLDN-1+}$ cells. HepG2$^{CLDN-1+}$ and HepG2$^{pCMV-ve}$ cells were cultured for 72 hours prior to total RNA extraction. Amplification of EphB2 was performed alongside GAPDH and beta-actin as reference genes using RT-PCR. Relative normalised gene expression was calculated using the $2^{-\Delta\Delta CT}$ method. Data presented is representative of mean fold change ±s.e.m from three biological replicates. Paired t-test was performed to determine statistical significance, ** P≤0.01

The expression of EphB2 was increased considerably in HepG2$^{CLDN-1+}$ cells compared to control represented by a 65.3-fold change. Statistical analysis indicated the increase in expression was significant (P=0.0027).

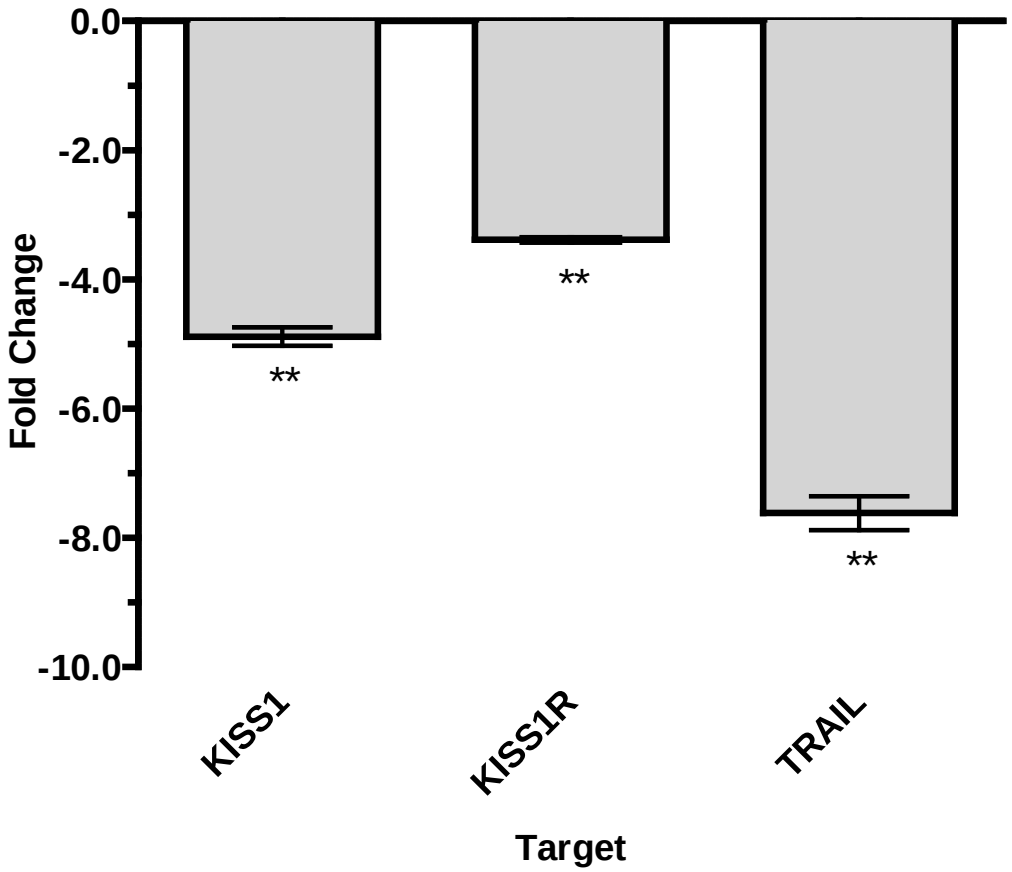

Figure 3.54: Normalized gene expression ($2^{-\Delta\Delta CT}$) of KISS1, KISS1R and TRAIL in HepG2$^{CLDN-1+}$ cells. HepG2$^{CLDN-1+}$ and HepG2$^{pCMV-ve}$ cells were cultured for 72 hours prior to total RNA extraction. Amplification of KISS1, KISS1R and TRAIL was performed alongside GAPDH and beta-actin as reference genes using RT-PCR. Relative normalised gene expression was calculated using the $2^{-\Delta\Delta CT}$ method. Data presented is representative of mean fold change ±s.e.m from three biological replicates. Paired t-test was performed to determine statistical significance, ** P≤0.01

Expression of KISS1 and KISS1R decreased in HepG2$^{CLDN-1+}$ cells compared to control represented by a -4.9 and -3.4 fold change. Statistical analysis indicated changes in expression of KISS1 and KISS1R was significant (P=0.001 and P=0.002 respectively). The expression of TRAIL also significantly decreased in HepG2$^{CLDN-1+}$ cells by -7.6 fold (P=0.004).

Large increases in expression of several tumour metastasis related genes provides further evidence for the acquisition of and invasive phenotype during claudin-1 overexpression in

HepG2 cells. The expression of these genes was also determined in claudin-1 silenced HepG2 cells to examine they too are associated with the same phenotypic changes.

3.10.2 Expression of tumour metastasis related genes in claudin-1 silenced HepG2 cells

Large increases in expression of several tumour metastasis related genes provides further evidence for the acquisition of and invasive phenotype during claudin-1 overexpression in HepG2 cells. The expression of these genes was also determined in claudin-1 silenced HepG2 cells to examine they too are associated with the same phenotypic changes.

Target	Sample	Expression ($2^{-\Delta\Delta CT}$)	Expression ($2^{-\Delta\Delta CT}$) Standard Deviation	Expression in Comparison to Control	P-Value	Exceeds P-Value Threshold (0.05)
Glyceraldehyde 3-phosphate dehydrogenase	HepG2 CLDN-1 siRNA	1.108	0.115	No Change	0.003	No
Beta-actin	HepG2 CLDN-1 siRNA	-1.093	0.199	No Change	0.002	No
CD44 Molecule	HepG2 CLDN-1 siRNA	3.514	0.278	Up Regulation	0.002	No
Dysadherin	HepG2 CLDN-1 siRNA	-0.336	0.268	Up Regulation	0.001	No
Kisspeptin-1	HepG2 CLDN-1 siRNA	-1.550	0.015	Down Regulation	0.010	No
Kisspeptin Receptor	HepG2 CLDN-1 siRNA	-2.020	0.019	Down Regulation	0.002	No

Cytokeratin-7	HepG2 CLDN-1 siRNA	3.081	0.142	Up Regulated	0.003	No
Cytokeratin-14	HepG2 CLDN-1 siRNA	3.649	0.136	Up Regulated	0.001	No
Cytokeratin-19	HepG2 CLDN-1 siRNA	4.525	0.250	Up Regulated	0.007	No
Matrix Metalloproteinase-2	HepG2 CLDN-1 siRNA	14.781	0.823	Up Regulation	0.000	No
Matrix Metalloproteinase-3	HepG2 CLDN-1 siRNA	1.171	0.074	Up Regulation	0.388	Yes
Matrix Metalloproteinase-7	HepG2 CLDN-1 siRNA	1.728	0.257	Up Regulation	0.025	No
Matrix Metalloproteinase-9	HepG2 CLDN-1 siRNA	2.818	0.129	Up Regulation	0.003	No
Matrix Metalloproteinase-10	HepG2 CLDN-1 siRNA	1.020	0.082	Up Regulation	0.145	Yes
Matrix Metalloproteinase-11	HepG2 CLDN-1 siRNA	-1.117	0.042	Down Regulation	0.673	Yes
Matrix Metalloproteinase-13	HepG2 CLDN-1 siRNA	3.052	0.073	Up Regulation	0.004	No
Metastasis suppressor-1	HepG2 CLDN-1 siRNA	-1.634	0.045	Down Regulation	0.015	No
Plasminogen activator inhibitor-1	HepG2 CLDN-1 siRNA	7.357	0.162	Up Regulation	0.007	No
Tissue Inhibitor of Metalloproteinases-1	HepG2 CLDN-1 siRNA	-1.269	0.062	Down Regulation	0.018	No
Tissue Inhibitor of Metalloproteinases-2	HepG2 CLDN-1 siRNA	-1.905	0.128	Down Regulation	0.008	No

Tissue Inhibitor of Metalloproteinases-3	HepG2 CLDN-1 siRNA	-1.285	0.057	Down Regulation	0.012	No
Tissue Inhibitor of Metalloproteinases-4	HepG2 CLDN-1 siRNA	-1.091	0.065	Down Regulation	0.180	Yes

Table 3.6: Normalised gene expression ($2^{-\Delta\Delta CT}$) of tumour metastasis related genes in claudin-1 silenced HepG2 cells. The table details the relative normalised gene expression of 22 tumour metastasis related genes in $HepG2^{CLDN\text{-}1\text{-}}$ cells. $HepG2^{scambled\text{-}ve}$ cells were used as the control. $HepG2^{CLDN\text{-}1\text{-}}$ and $HepG2^{scambled\text{-}ve}$ cells were cultured for 72 hours prior to total RNA extraction. Amplification of the genes outlined in Table 3.6 was performed alongside GAPDH and Beta-actin as the reference genes using RT-PCR. Relative normalised gene expression was calculated using the $2^{-\Delta\Delta CT}$ method. Data presented is representative of mean fold change ±s.e.m from three biological replicates. Paired t-test was performed to determine statistical significance. Statistical significance is indicated if the P value is lower than the 0.05 threshold.

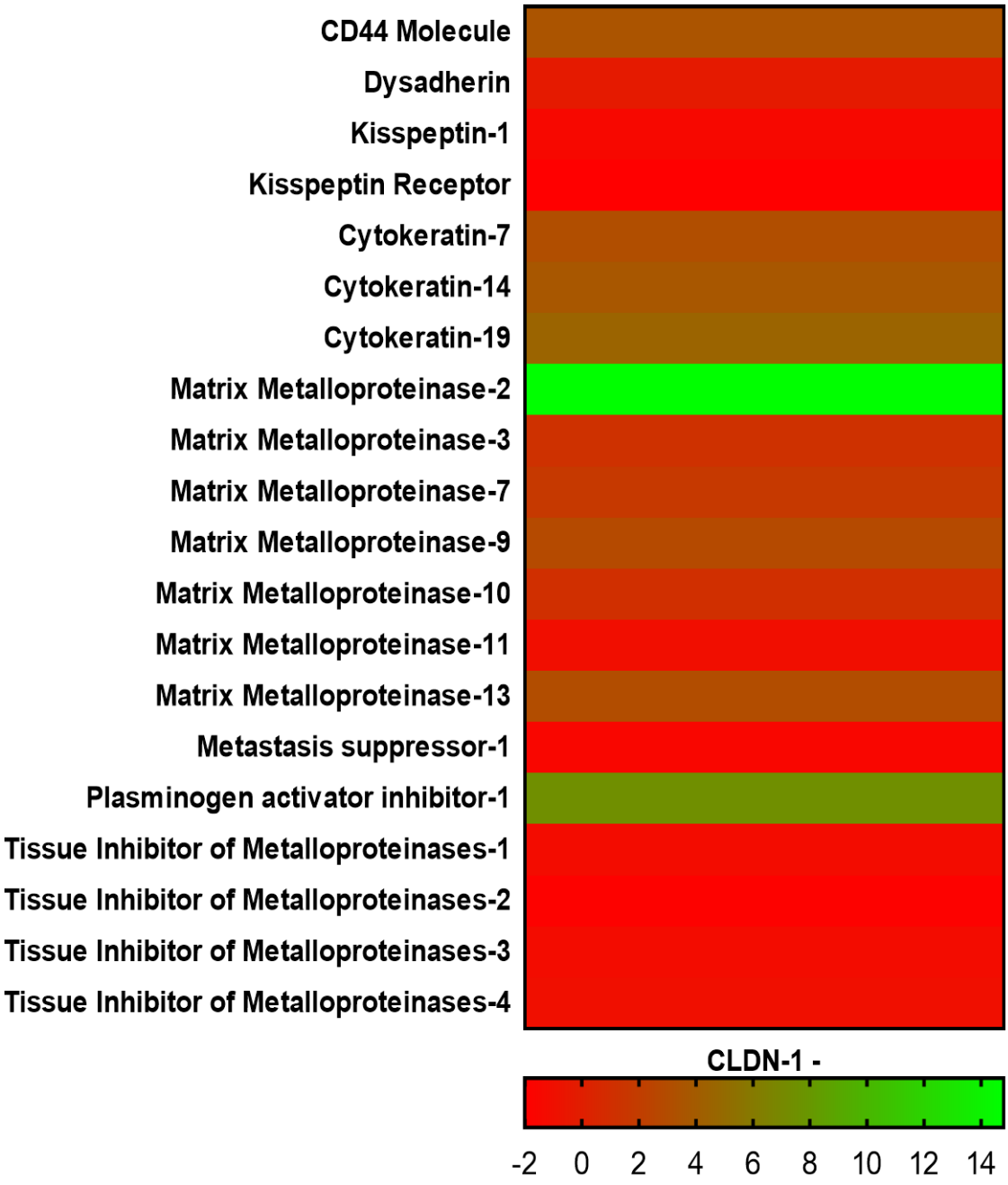

Figure 3.55: Heat map representing normalised gene expression ($2^{-\Delta\Delta CT}$) of tumour metastasis related genes in claudin-1 silenced HepG2 cells. Normalised gene expression values taken from Table 3.1 have been converted into a colorimetric scale outlined above to provide a visual representation of large-scale changes. Genes indicated by a green bar represent an upregulation in expression, whereas genes indicated by a red bar represent a down regulation in expression.

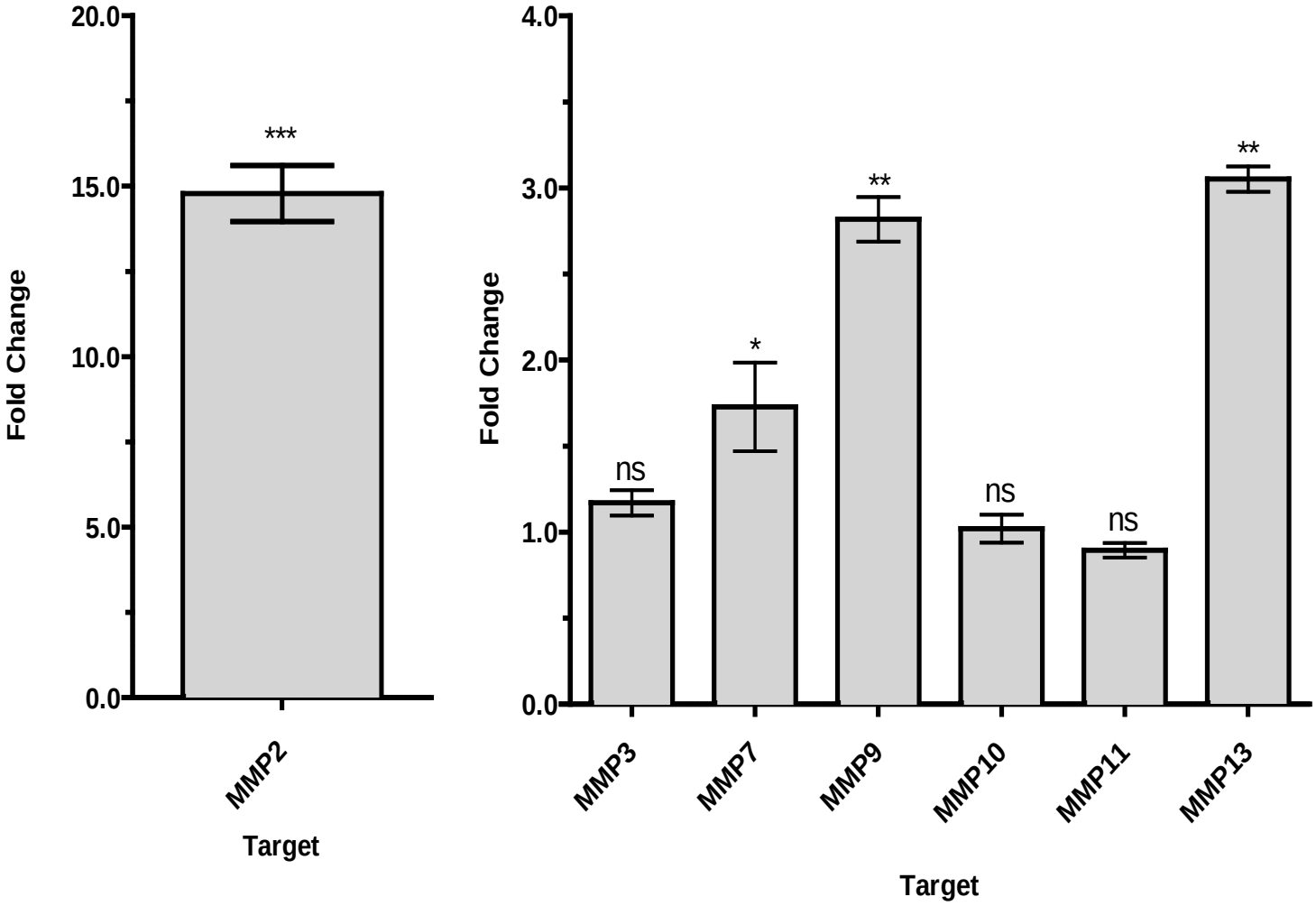

Figure 3.56: Normalized gene expression ($2^{-\Delta\Delta CT}$) of Matrix Metalloproteinases in HepG2$^{CLDN-1-}$ cells. HepG2$^{CLDN-1-}$ and HepG2$^{scambled-ve}$ cells were cultured for 72 hours prior to total RNA extraction. Amplification of MMP2, MMP3, MMP7, MMP9, MMP10, MMP11 and MMP13 was performed alongside GAPDH and Beta-actin as reference genes using RT-PCR. Relative normalised gene expression was calculated using the $2^{-\Delta\Delta CT}$ method. Data presented is representative of mean fold change ±s.e.m from three biological replicates. Paired t-test was performed to determine statistical significance, ns – not significant * P≤0.05 ** P≤0.01 *** P≤0.001.

The expression of MMP2 was massively increased in HepG2$^{CLDN-1-}$ cells compared to control, represented by a significant 14.8-fold change (P<0.001). MMP 7, 9, and 13 also presented with increased expression represented by 1.73, 2.82, and 3.05-fold change. Statistical analysis indicated MMP 7, 9, and 13 were significantly increased (P= P=0.025,0.003 and P=0.004 respectively). Statistical analysis of MMP 3, 10 and 11 was found not to be significant as the P-values exceeded the threshold (P=0.388, P=0.145, and P=0.673 respectively)

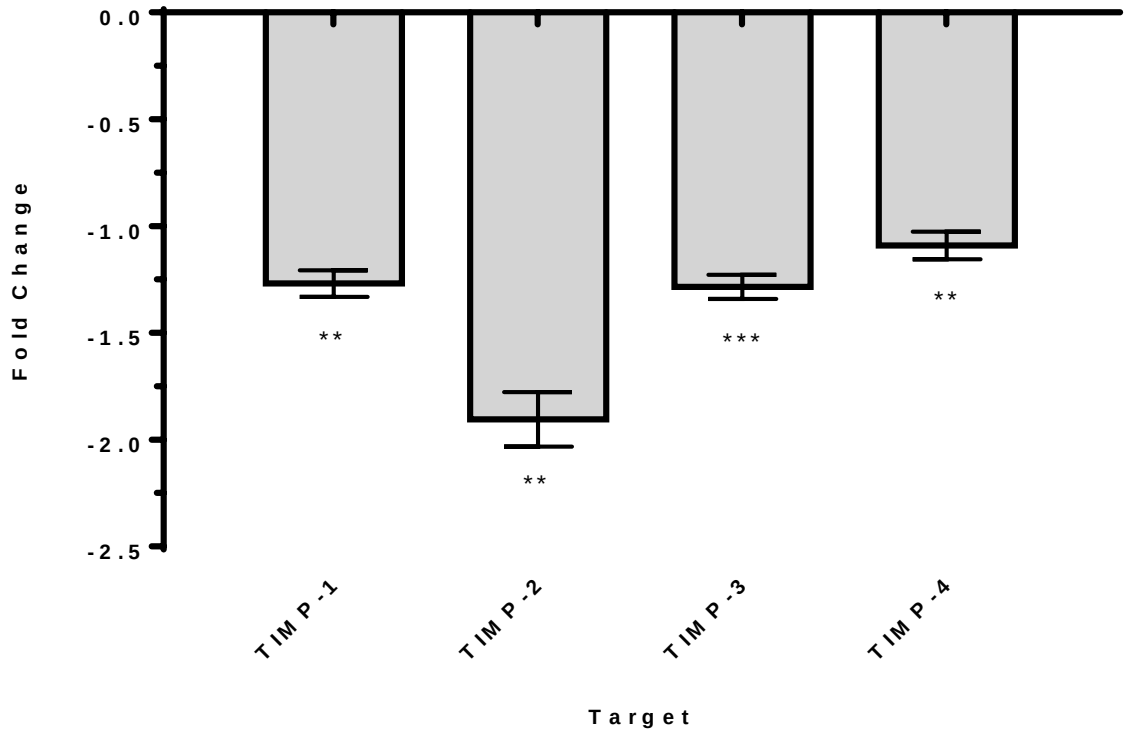

Figure 3.57: Normalized gene expression ($2^{-\Delta\Delta CT}$) of TIMP -1, -2, -3 and -4 in HepG2$^{CLDN-1-}$ cells. HepG2$^{CLDN-1-}$ and HepG2$^{scambled-ve}$ cells were cultured for 72 hours prior to total RNA extraction. Amplification of TIMP -1, -2, -3 and -4 was performed alongside GAPDH and Beta-actin as reference genes using RT-PCR. Relative normalised gene expression was calculated using the $2^{-\Delta\Delta CT}$ method. Data presented is representative of mean fold change ±s.e.m from three biological replicates. Paired t-test was performed to determine statistical significance, ** P≤0.01 *** P≤0.001.

Expression of TIMP family members 1-4 were decreased in HepG2$^{CLDN-1-}$ cells compared to control, represented by a -1.3, -1.9, -1.3 and -1.1 fold change, respectively. Statistical analysis indicated changes in expression of TIMPS 1-3 was significant (P=0.018, P=0.008 and P=0.011). The change in expression of TIMP4 in HepG2$^{CLDN-1-}$ cells was not significant as the P-value exceeded the threshold.

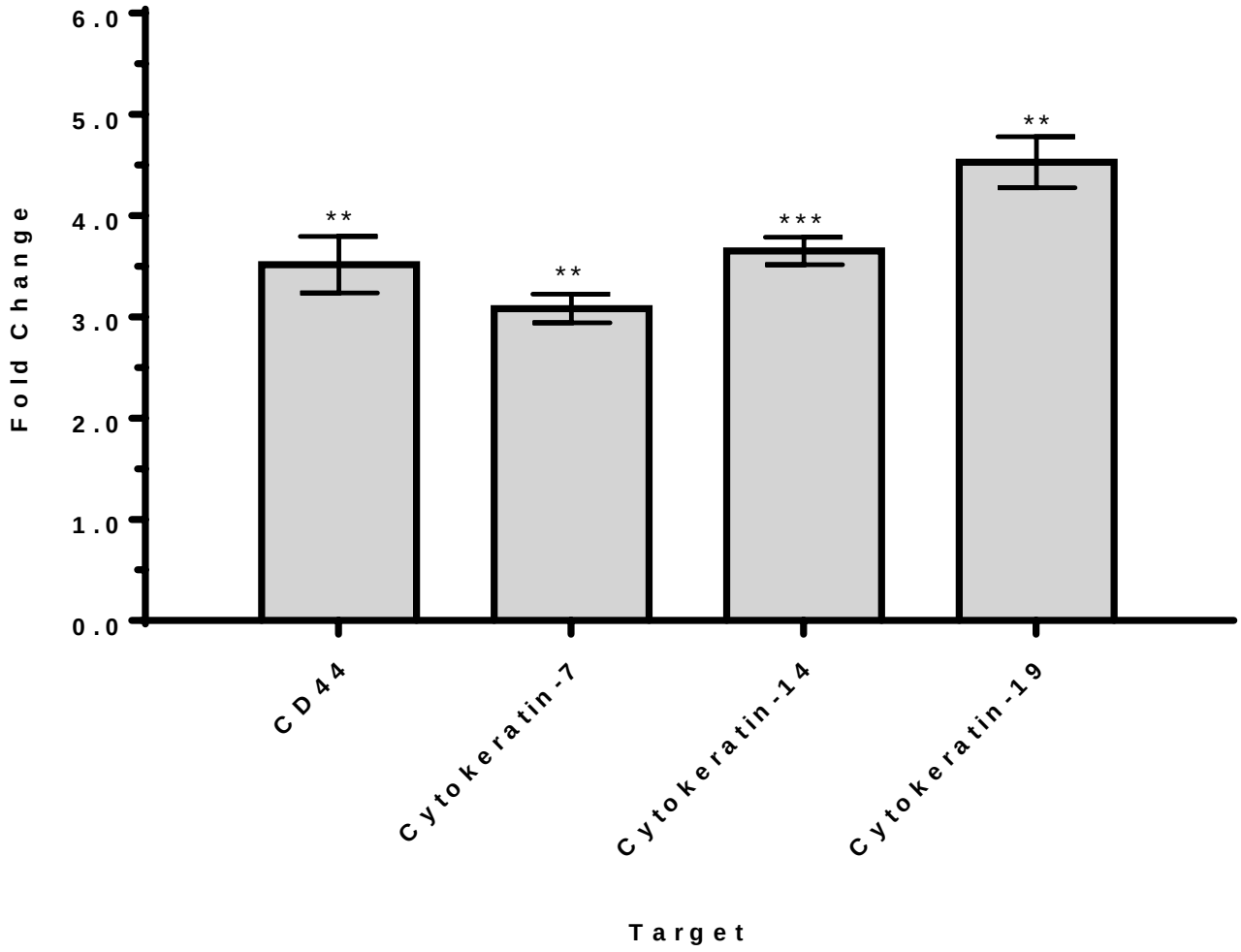

Figure 3.58: Normalized gene expression ($2^{-\Delta\Delta CT}$) of cancer stem cell markers in HepG2$^{CLDN-1-}$ cells. HepG2$^{CLDN-1-}$ and HepG2$^{scambled-ve}$ cells were cultured for 72 hours prior to total RNA extraction. Amplification of CD44, cytokeratin-7, cytokeratin-14 and cytokeratin-19 was performed alongside GAPDH and Beta-actin as reference genes using RT-PCR. Relative normalised gene expression was calculated using the $2^{-\Delta\Delta CT}$ method. Data presented is representative of mean fold change ±s.e.m from three biological replicates. Paired t-test was performed to determine statistical significance, ** P≤0.01 *** P≤0.001.

The expression of cancer stem cell markers CD44 and Cytokeratins -7, -14, and -19 were increased HepG2$^{CLDN-1-}$ cells compared to HepG2$^{scambled-ve}$, represented by a 3.51, 3.08, 3.64, and 4.52-fold change respectively. Statistical analysis indicated that the increase in expression of CD44 and Cytokeratin members was significant (P=0.002, P=0.003, P=<0.001, and P=0.006)

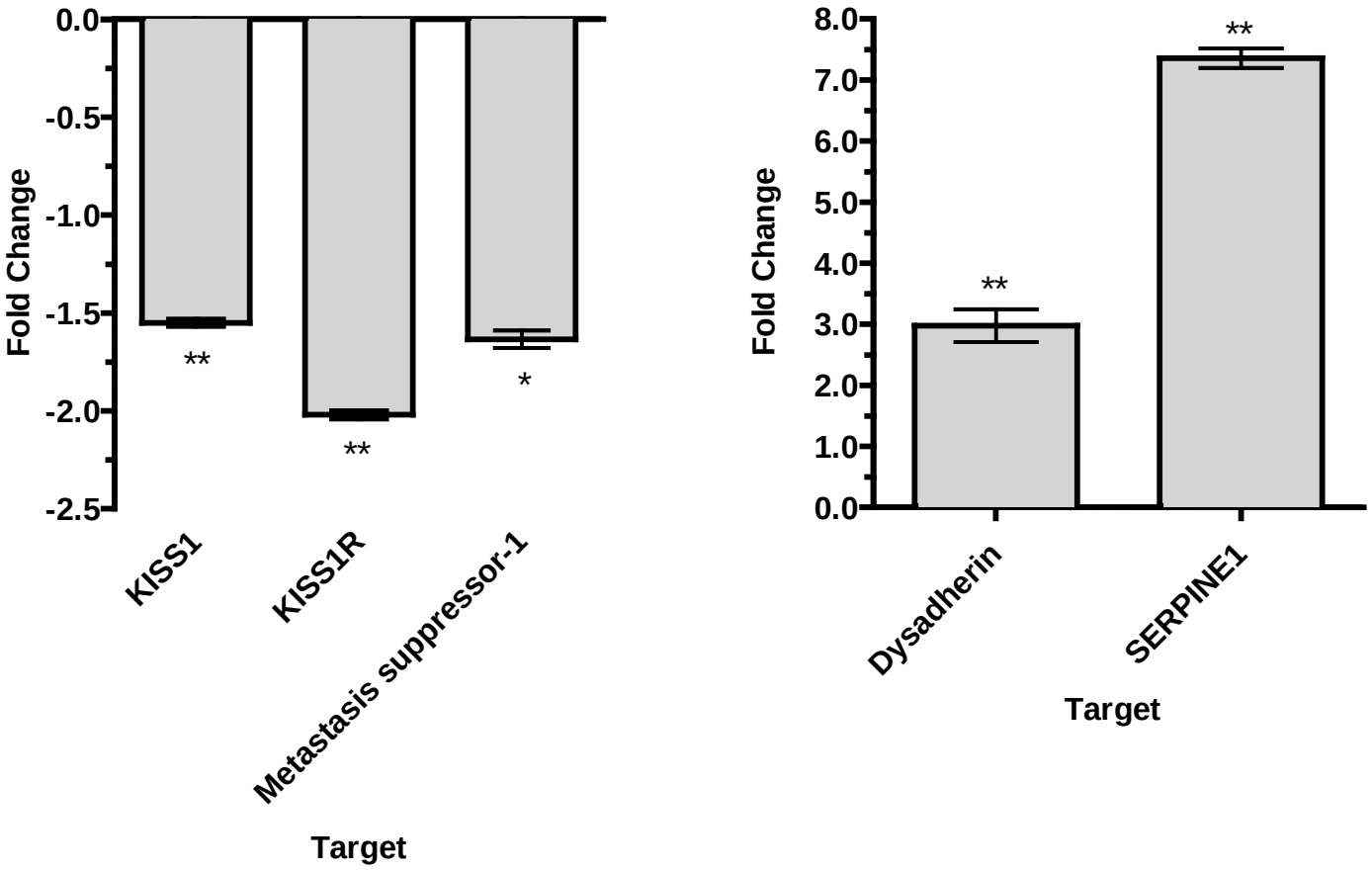

Figure 3.59: Normalized gene expression ($2^{-\Delta\Delta CT}$) of other associated tumour metastasis target genes in HepG2$^{CLDN\text{-}1-}$ cells. HepG2$^{CLDN\text{-}1-}$ and HepG2$^{scambled\text{-}ve}$ cells were cultured for 72 hours prior to total RNA extraction. Amplification of CD44, cytokeratin-7, cytokeratin-14 and cytokeratin-19 was performed alongside GAPDH and beta-actin as reference genes using RT-PCR. Relative normalised gene expression was calculated using the $2^{-\Delta\Delta CT}$ method. Data presented is representative of mean fold change ±s.e.m from three biological replicates. Paired t-test was performed to determine statistical significance, ** P≤0.01 *** P≤0.001.

Expression of KISS1 and KISS1R was decreased in HepG2$^{CLDN\text{-}1-}$ cells compared to control, represented by a -1.6- and -2.0 fold change. Statistical analysis indicated changes in expression of KISS1 and KISS1R was significant (P=0.009 and P=0.002 respectively). The expression of Metastasis suppressor-1 was also significantly decreased in HepG2$^{CLDN\text{-}1+}$ cells by -1.6 fold (P=0.014). Both Dysadherin and (Plasminogen activator inhibitor-1) presented with increased expression, 2.98 and 7.36 fold respectively in HepG2$^{CLDN\text{-}1+}$ cells

compared to control. Statistical analysis indicated the increase in expression of both genes was significant (P=0.001, P=0.007).

Both claudin-1 overexpressing and silenced HepG2 cells show similar expression patterns of tumour metastasis genes. Large increases in the expression of genes such as matrix metalloproteinases are often seen in invasive neoplasms, indicating that both groups of cells display hallmarks of increased metastatic potential (Deryugina & Quigley 2006). However, an important difference between these groups is claudin-1 silenced HepG2 cells show an increase in markers such as CD44, CK14 and CK19 usually seen on hepatic stem cells, whereas claudin-1 overexpressing cells do not. (Li et al 2013).

3.11 Comparison of gene expression data from tight junctional, EMT and tumour metastasis genes in claudin-1 overexpressing and silenced HepG2 cells

3.11.1 Comparison of tight junctional gene expression

The comparison of the expression of claudin members would suggest there are similarities between claudin-1 overexpressing and silenced HepG2 cells. Both groups of cells expressed increased levels of claudin-2 and decreased levels of claudin-4 and -5. They also both displayed small increases of claudin-3 and claudin-8, however the change in expression of claudin-8 was found not to be significant in claudin-1 overexpressing cells. Differences between the two groups of cells include a significant increase in claudin-7 during claudin-1 overexpression, which is absent in claudin-1 silenced cells, and a significant increase in claudin-11 in claudin-1 silenced cells, which is absent in claudin-1 overexpressing cells.

Claudin-1 overexpressing and silenced cells also show a similar pattern of

expression of occludin, zona occludens and ZONAB. In both cell groups the gene expression of occludin and zona occludens was decreased and the expression of ZONAB was increased. However, in claudin-1 silenced cells the level of expression of occludin was significantly lower than in claudin-1 overexpressing cells. Whereas, the expression level of zona occludens, ZO-2 in particular, was significantly lower in in claudin-1 overexpressing cells. As there is a close association between occludin and zona occludin this inverse pattern could provide evidence of compensatory mechanisms.

The pattern of expression of junctional adhesion molecules displayed clear differences between claudin-1 overexpressing and silenced cells. JAM A was significantly decreased in claudin-1 overexpressing cells, but significantly increased in silenced cells. The expression of JAM B was significantly increased in claudin-1 overexpressing cells, however there was no significant change in silenced cells.

The expression of caveolin-1 and -2 were significantly increased in both claudin-1 overexpressing and silenced cells. However, the increase observed in claudin-1 overexpressing cells was significantly higher than silenced cells. Caveolin-1 represented one of the highest increases in expression of the genes tested, indicating its potential as a contributor to the phenotype observed.

The expression of WNK4 was down related in both claudin-1 overexpressing and silenced cells, however the decrease in expression was more significant in claudin-1 silenced cells.

3.11.2 Comparison of epithelial to mesenchymal transition genes expression

The expression of the classical epithelial marker e-cadherin was significantly decreased in claudin-1 overexpressing and silenced cells. However, the level of down regulation was significantly higher in claudin-1 overexpressing cells. The pattern of expression of N-cadherin and fibronectin was inversed in the two cell groups, with a decrease in expression

observed in claudin-1 overexpressing cells and an increase in expression observed in claudin-1 silenced cells. The classical mesenchymal marker vimentin displayed increased expression in both claudin-1 overexpressing cells and silenced cells, although the increased expression was significantly higher in claudin-1 overexpressing cells. EMT transcription factors are key regulators in orchestrating the transition, their expression often gives an indication of how EMT is initiated and sustained. Claudin-1 overexpressing cells displayed increased expression of SNAIL -1, -2, -3 and TWIST, with SNAIL 2 showing the largest increase. Claudin-1 silenced cells also displayed and increase in TWIST expression; however, the expression of SNAIL 1 was only slightly increased and the levels of SNAIL-2 and -3 were significantly decreased. The largest increases in EMT-TFs in claudin-1 silenced cells were forkhead box C2 and homeobox goosecoid suggesting any EMT involvement in these cells would be more likely be orchestrated by these transcription factors. While forkhead box C2 and homeobox goosecoid were slightly overexpressed in claudin-1 overexpressing cells, it is more likely SNAIL-1 and -2 are involved in EMT initiation in these cells. These differences could indicate the phenotypes observed in these cells are regulated by different mechanisms.

Notch and jagged-1 expression was significantly increased in claudin-1 silenced cells indicating the potentially involvement of notch-jagged signalling in these cells. Claudin-1 overexpressing cells however, displayed a slight increase in notch expression and a significant decrease in jagged expression, making notch-jagged signalling unlikely in these cells.

The expression of β-catenin and associated genes TCF1, LEF1, TCF3 and TCF4 was significantly increased in claudin-1 overexpressing cells TCF3 and TCF4 were particularly increased in these cells. The expression of these genes with the exception of LEF1 were slightly increased in claudin-1 silenced cells. However, the small increases

make it unlikely β-catenin is participating in the phenotypic changes observed in these cells.

Other genes associated with β-catenin such as α-catenin, frizzled-7 and rac-1displayed different patterns of expression in both claudin-1 overexpressing and silenced cells. The expression of α-catenin was significantly increased in claudin-1 overexpressing cells, but slight increased during claudin-1 silencing. Frizzled-7 displayed increased expression in both cell groups. Whereas, rac-1 increased in claudin-1 overexpressing cells but decreased in silenced cells.

Claudin-1 overexpressing cells displayed large increases in WNT5a and WNT5b providing further evidence of the involvement of WNT/β-catenin involvement. Claudin-1 silenced cells displayed decreased expression of WNT5a and no significant change in WNT5b expression, making the involvement unlikely involvement of WNT/β-catenin in these cells. WNT11a was decreased in claudin-1 overexpressing cells and displayed no significant change in expression in claudin-1 silenced cells.

3.11.3 Comparison of tumour metastasis gene expression

Claudin-1 overexpressing and silenced cells displayed a similar pattern of expression of matrix metalloproteases with significant increases in expression of MMP-2, -9 and -13. Differences include an increase in expression of MMP-10 in claudin-1 overexpressing cells and a slight increase in MMP-7 in claudin-1 silenced cells. Claudin-1 overexpressing cells also displayed decreased expression of MMP-3 and MMP-7.

The expression of TIMPS 1-4 in both claudin-1 overexpressing and silenced cells was significantly decreased. The exception to this was the slight decrease in expression of TIMP-4 in claudin-1 silenced cells which was found not to be significant. The decrease in expression in TIMPS 1-4 was significantly larger in claudin-1 overexpressing compared with claudin-1 silenced cells.

The expression of CD44, and cytokeratins -7, -14 -19 were all significantly

decreased in claudin-1 overexpressing cells, but significantly increased in claudin-1 silenced cells. Cytokeratins are markers of an epithelial phenotype, interestingly claudin-1 silenced cells display co-express both epithelial and mesenchymal markers.

3.11 Determining the miRNA expression profile of claudin-1 overexpressing and claudin-1 silenced HepG2 cells

MicroRNAs are highly conserved, small non-coding RNA molecules that function as post-transcriptional regulators of gene expression. MicroRNAs have been documented to be dysregulated in human cancers. MicroRNAs are known to act as both oncogenes activators and tumour suppressors. Their influence on gene expression has been shown to directly modulate cellular mechanisms such as proliferation, invasion and metastasis. The MicroRNA expression profile in some cancers can define tumour types and predict progression, prognosis and response to treatment (Hayes et al 2014). Profiling the expression of miRNAs in claudin-1 overexpressing and claudin-1 silenced HepG2 cells will aid in the understanding of the gene regulation in these cells. A number of tight junctional, EMT and tumour metastasis genes are directly regulated by miRNAs. The expression of which can give us further understanding of signalling pathways and outline possible biomarkers associated with the invasive phenotype (Ma & Weinberg 2008).

Claudin-1 overexpressing and claudin-1 silenced HepG2 cells were analysed to determine the expression mature MicroRNAs using a PCR array of 69 target and housekeeping genes (U6, RNU44 and RNU48)

3.11.1 miRNA expression profile of claudin-1 overexpressing HepG2 cells

Target	Sample	Expression ($2^{-\Delta\Delta CT}$)	Expression ($2^{-\Delta\Delta CT}$) Standard Deviation	Expression in Comparison to Control	P-Value	Exceeds P-Value Threshold (0.05)
U6 snRNA	HepG2 CLDN-1+	1.001	0.250	No Change	0.002	No
RNU44	HepG2 CLDN-1+	1.063	0.030	No Change	0.001	No
RNU48	HepG2 CLDN-1+	-1.011	0.050	No Change	0.005	No
miR-10a	HepG2 CLDN-1+	119.235	5.635	Up Regulated	0.013	No
miR-9	HepG2 CLDN-1+	75.362	4.173	Up Regulated	0.018	No
miR-147	HepG2 CLDN-1+	46.643	2.125	Up Regulated	0.008	No
miR-10b	HepG2 CLDN-1+	44.758	2.512	Up Regulated	0.007	No
miR-95	HepG2 CLDN-1+	44.306	1.502	Up Regulated	0.003	No
miR-423-5p	HepG2 CLDN-1+	43.776	2.113	Up Regulated	0.001	No
miR-433	HepG2 CLDN-1+	42.992	1.087	Up Regulated	0.001	No
miR-15a	HepG2 CLDN-1+	41.534	2.124	Up Regulated	0.002	No
miR-598	HepG2 CLDN-1+	21.962	1.880	Up Regulated	0.001	No
miR-489	HepG2 CLDN-1+	21.925	0.980	Up Regulated	0.002	No
miR-328	HepG2 CLDN-1+	21.026	0.058	Up Regulated	0.001	No
miR-542-5p	HepG2 CLDN-1+	11.169	0.333	Up Regulated	0.085	No
miR-542-3p	HepG2 CLDN-1+	5.538	0.516	Up Regulated	0.003	No
miR-181a	HepG2 CLDN-1+	2.771	0.242	Up Regulated	0.002	No
miR-181c	HepG2 CLDN-1+	2.746	0.080	Up Regulated	0.000	No

miR-545	HepG2 CLDN-1+	2.695	0.751	Up Regulated	0.003	No
miR-324-5p	HepG2 CLDN-1+	2.462	0.192	Up Regulated	0.003	No
miR-221	HepG2 CLDN-1+	2.385	0.355	Up Regulated	0.005	No
miR-494	HepG2 CLDN-1+	2.290	0.278	Up Regulated	0.015	No
miR-18b	HepG2 CLDN-1+	2.283	0.133	Up Regulated	0.007	No
miR-18a	HepG2 CLDN-1+	2.009	0.323	Up Regulated	0.002	No
miR-339-5p	HepG2 CLDN-1+	-1.402	0.022	Down Regulated	0.020	No
miR-532	HepG2 CLDN-1+	-1.404	0.055	Down Regulated	0.001	No
miR-345	HepG2 CLDN-1+	-1.409	0.144	Down Regulated	0.022	No
miR-532-3p	HepG2 CLDN-1+	-1.438	0.170	Down Regulated	0.040	No
miR-140-3p	HepG2 CLDN-1+	-1.549	0.033	Down Regulated	0.014	No
miR-223	HepG2 CLDN-1+	-1.710	0.012	Down Regulated	0.004	No
miR-320	HepG2 CLDN-1+	-1.785	0.018	Down Regulated	0.022	No
miR-30b	HepG2 CLDN-1+	-1.812	0.031	Down Regulated	0.005	No
miR-26a	HepG2 CLDN-1+	-2.400	0.127	Down Regulated	0.008	No
miR-365	HepG2 CLDN-1+	-2.523	0.038	Down Regulated	0.008	No
miR-491	HepG2 CLDN-1+	-2.815	0.040	Down Regulated	0.011	No
miR-425-5p	HepG2 CLDN-1+	-3.481	0.037	Down Regulated	0.003	No
miR-636	HepG2 CLDN-1+	-3.639	0.017	Down Regulated	0.005	No
miR-185	HepG2 CLDN-1+	-3.759	0.027	Down Regulated	0.030	No
miR-29c	HepG2 CLDN-1+	-3.798	0.057	Down Regulated	0.015	No
miR-148a	HepG2 CLDN-1+	-3.821	0.046	Down Regulated	0.001	No

miR-518b	HepG2 CLDN-1+	-3.865	0.192	Down Regulated	0.004	No
miR-26b	HepG2 CLDN-1+	-4.177	0.042	Down Regulated	0.030	No
miR-28-3p	HepG2 CLDN-1+	-4.936	0.068	Down Regulated	0.001	No
miR-193b	HepG2 CLDN-1+	-5.787	0.112	Down Regulated	0.004	No
miR-138	HepG2 CLDN-1+	-6.028	0.042	Down Regulated	0.002	No
miR-29a	HepG2 CLDN-1+	-10.753	0.070	Down Regulated	0.001	No
miR-202	HepG2 CLDN-1+	-12.121	0.199	Down Regulated	0.001	No
miR-200c	HepG2 CLDN-1+	-12.953	0.032	Down Regulated	0.001	No
miR-361	HepG2 CLDN-1+	-24.038	0.014	Down Regulated	0.008	No
miR-122	HepG2 CLDN-1+	-24.096	0.016	Down Regulated	0.003	No
miR-548b	HepG2 CLDN-1+	-24.155	0.013	Down Regulated	0.004	No
miR-376c	HepG2 CLDN-1+	-24.631	0.020	Down Regulated	0.003	No
miR-152	HepG2 CLDN-1+	-24.814	0.181	Down Regulated	0.008	No
miR-431	HepG2 CLDN-1+	-25.126	0.176	Down Regulated	0.004	No
miR-192	HepG2 CLDN-1+	-33.898	0.618	Down Regulated	0.001	No
miR-486-3p	HepG2 CLDN-1+	-47.393	0.132	Down Regulated	0.033	No
miR-455-3p	HepG2 CLDN-1+	-97.087	0.035	Down Regulated	0.020	No
miR-28	HepG2 CLDN-1+	-98.039	0.696	Down Regulated	0.003	No
miR-381	HepG2 CLDN-1+	-100.000	0.474	Down Regulated	0.002	No
miR-194	HepG2 CLDN-1+	-103.093	0.723	Down Regulated	0.001	No
miR-130a	HepG2 CLDN-1+	-113.636	1.100	Down Regulated	0.008	No
miR-150	HepG2 CLDN-1+	-123.457	0.092	Down Regulated	0.002	No

miR-486	HepG2 CLDN-1+	-192.308	3.850	Down Regulated	0.003	No
miR-200a	HepG2 CLDN-1+	-192.308	1.120	Down Regulated	0.009	No
miR-145	HepG2 CLDN-1+	-192.308	4.450	Down Regulated	0.001	No
miR-34a	HepG2 CLDN-1+	-192.308	3.740	Down Regulated	0.004	No
miR-372	HepG2 CLDN-1+	-384.615	0.046	Down Regulated	0.001	No
miR-200b	HepG2 CLDN-1+	-769.231	4.520	Down Regulated	0.002	No
miR-146a	HepG2 CLDN-1+	-1666.667	0.007	Down Regulated	0.004	No

Table 3.7: Normalised gene expression ($2^{-\Delta\Delta CT}$) profile of miRNAs in claudin-1 overexpressing HepG2 cells. The table details the relative normalised gene expression of 69 miRNAs in $HepG2^{CLDN-1+}$ cells, $HepG2^{pCMV-ve}$ cells were used as the control. $HepG2^{CLDN-1+}$ and $HepG2^{pCMV-ve}$ cells were cultured for 72 hours prior to total RNA extraction. Amplification of the genes outlined in Table 3.7 was performed alongside U6, RNU44 and RNU48 as the reference genes using RT-PCR. Relative normalised gene expression was calculated using the $2^{-\Delta\Delta CT}$ method. Data presented is representative of mean fold change ±s.e.m from three biological replicates. Paired t-test was performed to determine statistical significance. Statistical significance is indicated if the P value is lower than the 0.05 threshold.

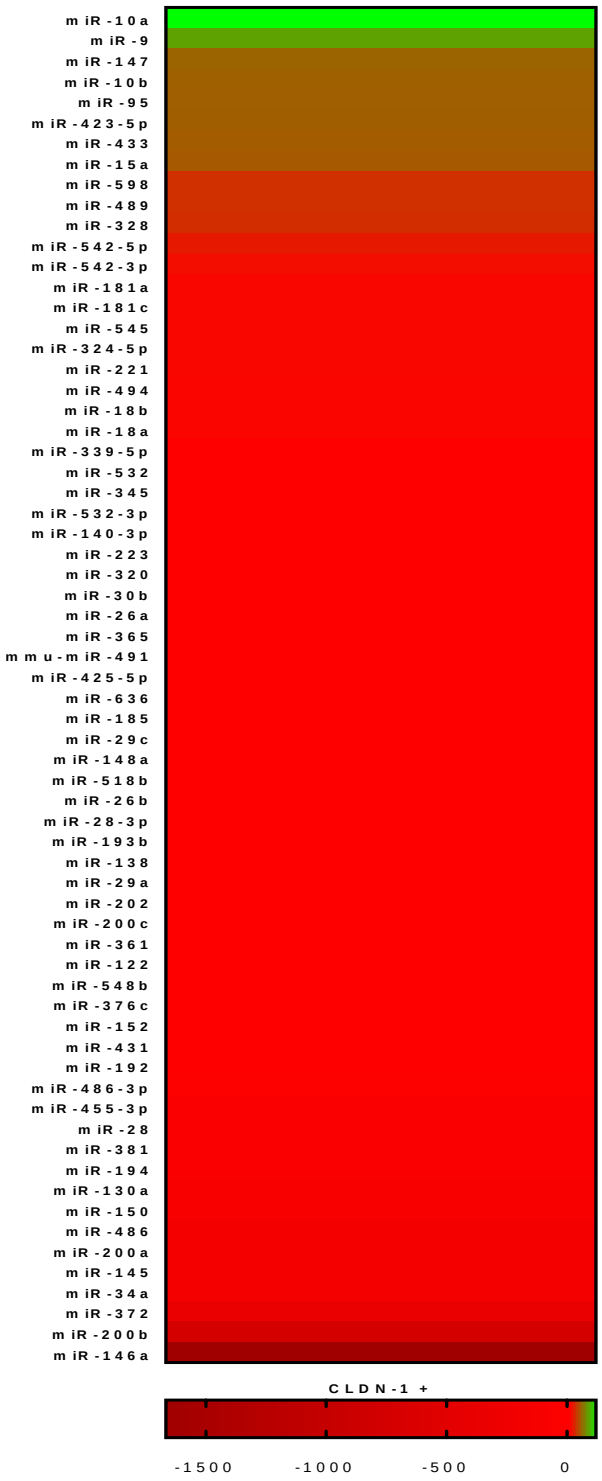

Figure 3.60: Heat map representing normalised gene expression profile ($2^{-\Delta\Delta CT}$) of miRNAs in claudin-1 overexpressing HepG2 cells. Normalised gene expression values taken from Table 3.7 have been converted into a colorimetric scale outlined above to provide a visual representation of large-scale changes. Genes indicated by a green bar represent an upregulation in expression, whereas genes indicated by a red bar represent a down regulation in expression.

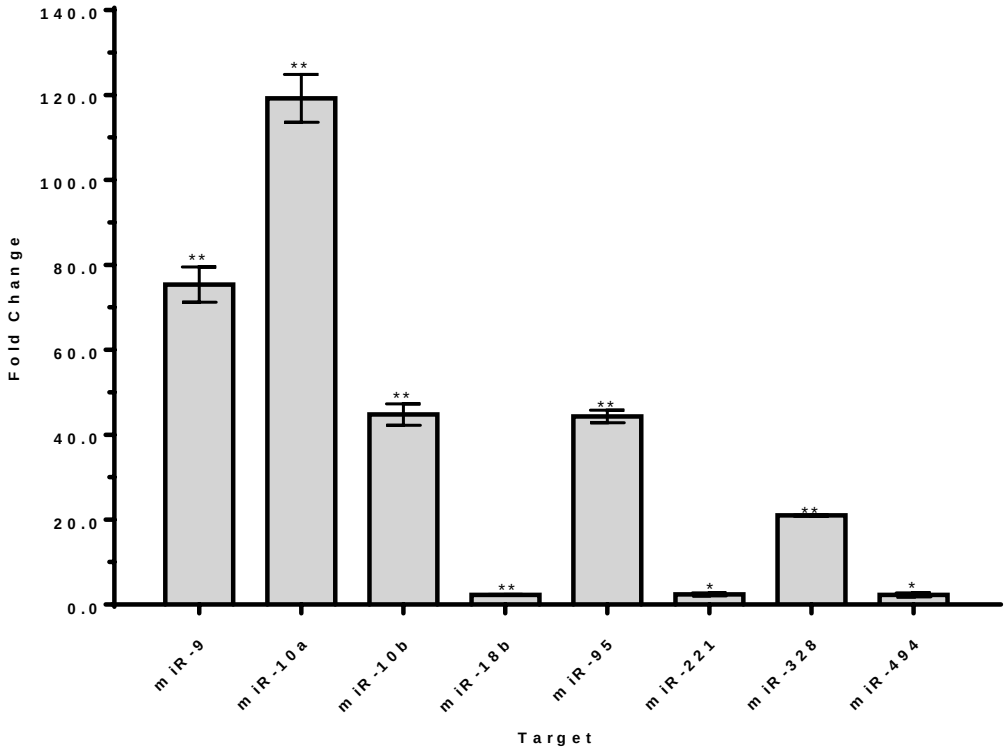

Figure 3.61: Normalised gene expression profile ($2^{-\Delta\Delta CT}$) of miRNAs in HepG2$^{CLDN-1+}$ cells which are associated with a poor prognosis in HCC. HepG2$^{CLDN-1+}$ and HepG2$^{pCMV-ve}$ cells were cultured for 72 hours prior to total RNA extraction. Amplification of miR-9, -10a, -10b, -18b, -95, -221, -328 and -494 was performed alongside U6, RNU44 and RNU48 as reference genes using RT-PCR. Relative normalised gene expression was calculated using the $2^{-\Delta\Delta CT}$ method. Data presented is representative of mean fold change ±s.e.m from three biological replicates. Paired t-test was performed to determine statistical significance, * P≤0.05 ** P≤0.01

The expression of miRNAs -9, -10a, -10b, -18b, -95, -221, -328 and 493 were all increased HepG2$^{CLDN-1+}$ cells compared to HepG2$^{pCMV-ve}$, represented by a 75.4, 119.2, 44.8, 2.3, 44.3, 2.34, 21.0 and 2.3 fold change respectively. Statistical analysis indicated that the increase in expression of these miRNA members was significant (P=0.001, P=0.001, P=0.007, P=0.006, P=0.003, P=0.045, P=0.001, P=0.015)

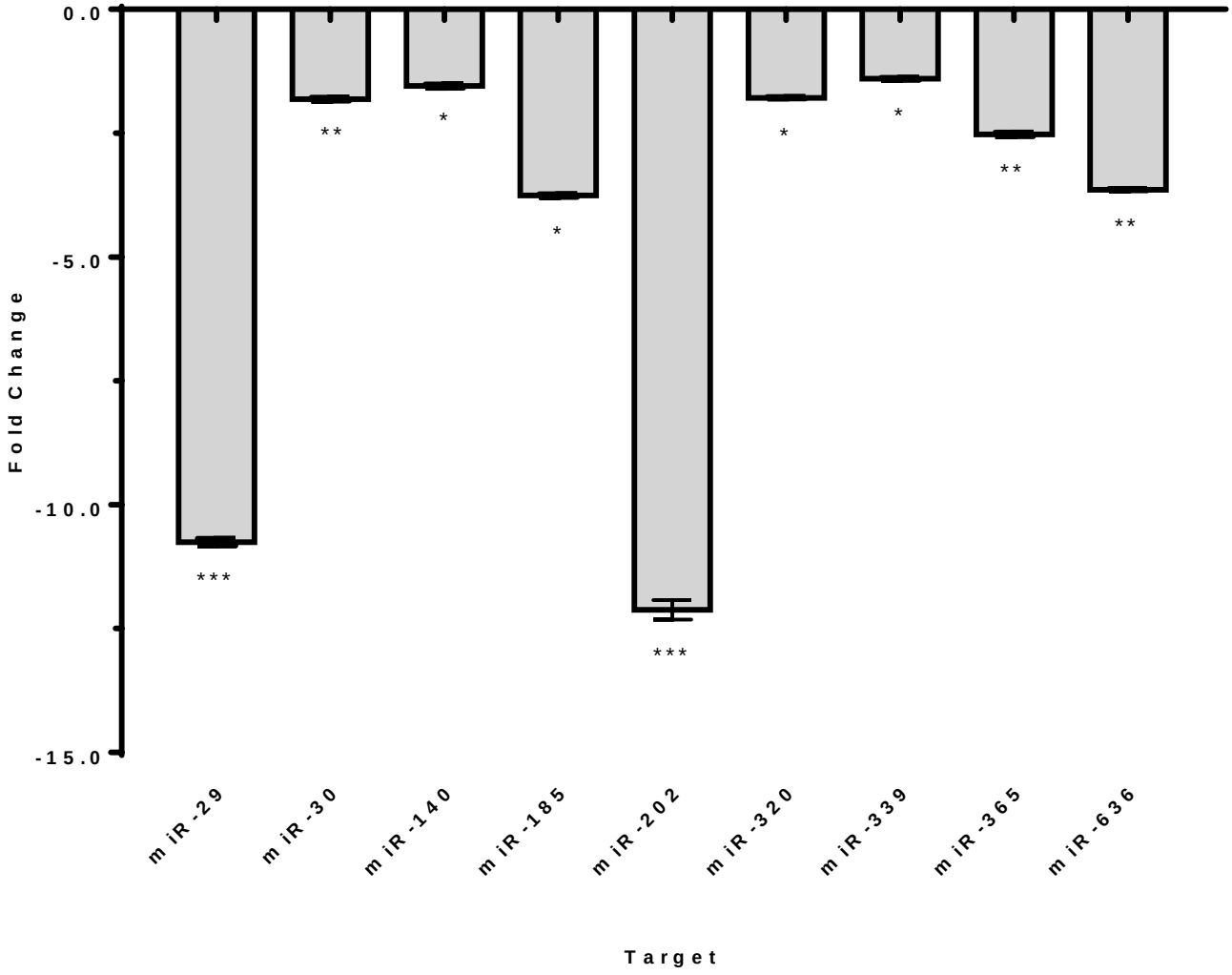

Figure 3.62: Normalised gene expression profile ($2^{-\Delta\Delta CT}$) of miRNAs in HepG2$^{CLDN-1+}$ cells which are known tumour suppressors in HCC. HepG2$^{CLDN-1+}$ and HepG2$^{pCMV-ve}$ cells were cultured for 72 hours prior to total RNA extraction. Amplification of miR-29, -30b, -140, -185, -202, -320, -339, -365 and -636 was performed alongside U6, RNU44 and RNU48 as reference genes using RT-PCR. Relative normalised gene expression was calculated using the $2^{-\Delta\Delta CT}$ method. Data presented is representative of mean fold change ±s.e.m from three biological replicates. Paired t-test was performed to determine statistical significance, * P≤0.05 ** P≤0.01 *** P≤0.01

The expression of miRNAs -29, -30b, -140, -185, -202, -320, -339, -365 and -636 were all decreased HepG2$^{CLDN-1+}$ cells compared to HepG2$^{pCMV-ve}$, represented by a -10.8, -1.8, -1.5, -3.8, -12.1, -1.8, -1.4, -2.5 and -3.6 change respectively. Statistical analysis indicated that the increase in expression of these miRNA members was significant (P=0.001, P=0.005, P=0.014, P=0.03, P=0.001, P=0.022, P=0.02 P=0.0077 P=0.0049)

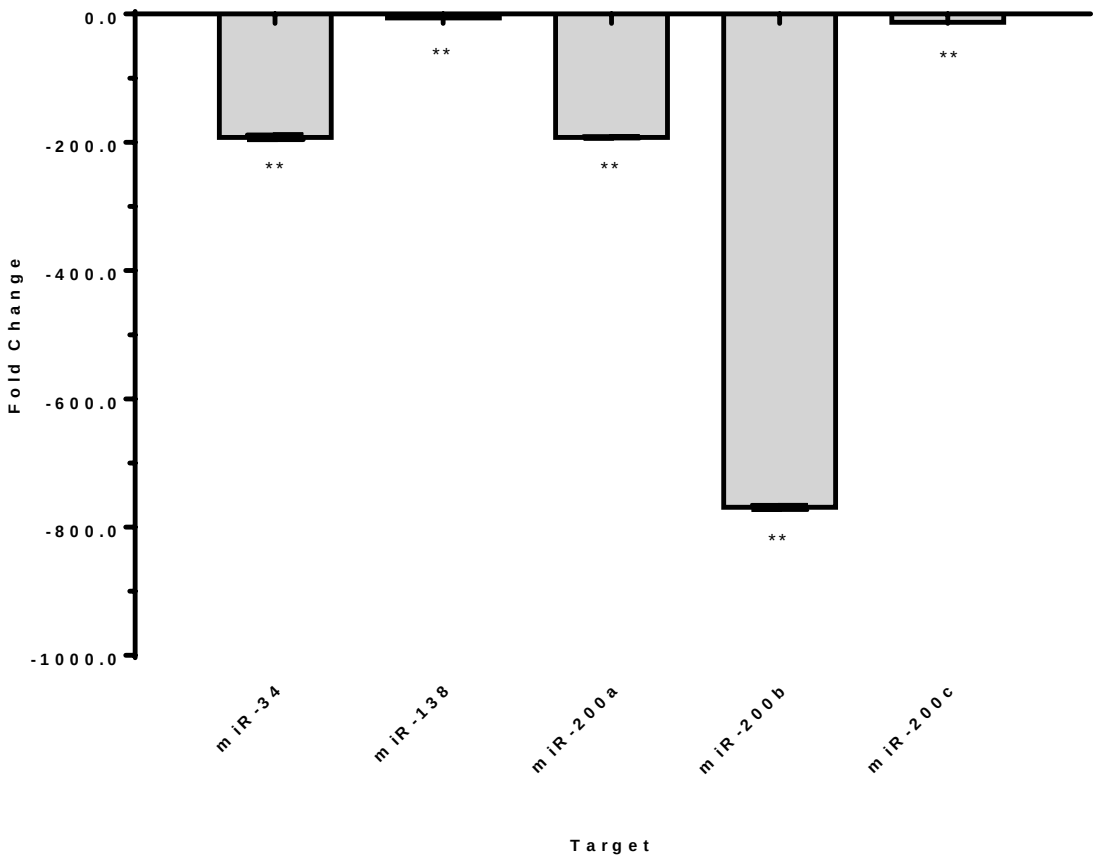

Figure 3.63: Normalised gene expression profile ($2^{-\Delta\Delta CT}$) of miRNAs in HepG2$^{CLDN-1+}$ cells which supress EMT in HCC. HepG2$^{CLDN-1+}$ and HepG2$^{pCMV-ve}$ cells were cultured for 72 hours prior to total RNA extraction. Amplification of miR-34, -138, -200a, -200b and -200c was performed alongside U6, RNU44 and RNU48 as reference genes using RT-PCR. Relative normalised gene expression was calculated using the $2^{-\Delta\Delta CT}$ method. Data presented is representative of mean fold change ±s.e.m from three biological replicates. Paired t-test was performed to determine statistical significance, * P≤0.05 ** P≤0.01

The expression of miRNAs -34, -138, -200a, -200b and -200c were all decreased HepG2$^{CLDN-1+}$ cells compared to HepG2$^{pCMV-ve}$, represented by a -192.3, -6.0, -192.3, -769.2 and -12.9 change respectively. Statistical analysis indicated that the increase in expression of these miRNA members was significant (P=0.004, P=0.002, P=0.009, P=0.002, P=0.001)

miRNAs are critical for transcriptional repression of genes involved initiating an invasive phenotype, as such they represent a vital milestone cancer must overcome to gain the characteristics needed to metastasise (Israel et al 2009). Since miRNAs target gene transcripts for destruction, it is common to see a decrease in expression of a number of regulatory miRNAs as cancer cells obtain an invasive phenotype. The genes in which miRNAs repress are then able to be expressed in their absence (Chu et al 2014). Several miRNAs in claudin-1 overexpressing HepG2 cells have been associated with tumour suppression and EMT suppression in hepatocellular carcinoma. Their decreased expression in these cells would suggest that claudin-1 overexpression removes the miRNA suppressive capacity allowing these cells to upregulated genes associated with tumour progression and EMT initiation. The miRNA expression profile of claudin-1 silenced HepG2 cells was also performed to determine if these cells are regulated by the same mechanisms.

3.11.2 miRNA expression profile of claudin-1 silenced HepG2 cells

Target	Sample	Expression ($2^{-\Delta\Delta CT}$)	Expression ($2^{-\Delta\Delta CT}$) Standard Deviation	Expression in Comparison to Control	P-Value	Exceeds P-Value Threshold (0.05)
U6 snRNA	HepG2 CLDN-1 siRNA	1.033	0.250	No Change	0.0018	No
RNU44	HepG2 CLDN-1 siRNA	1.029	0.030	No Change	0.0001	No
RNU48	HepG2 CLDN-1 siRNA	1.100	0.050	No Change	0.0046	No

miR-27a	HepG2 CLDN-1 siRNA	82.455	1.774	Up Regulated	0.0082	No
miR-142-3p	HepG2 CLDN-1 siRNA	35.274	1.530	Up Regulated	0.0065	No
miR-139-5p	HepG2 CLDN-1 siRNA	34.781	2.535	Up Regulated	0.0053	No
miR-331-5p	HepG2 CLDN-1 siRNA	34.549	2.331	Up Regulated	0.0053	No
miR-532	HepG2 CLDN-1 siRNA	34.101	0.527	Up Regulated	0.0050	No
miR-429	HepG2 CLDN-1 siRNA	9.091	0.686	Up Regulated	0.0038	No
miR-362	HepG2 CLDN-1 siRNA	7.143	0.419	Up Regulated	0.0027	No
miR-660	HepG2 CLDN-1 siRNA	6.916	0.301	Up Regulated	0.0004	No
miR-135a	HepG2 CLDN-1 siRNA	6.904	0.387	Up Regulated	0.0040	No
miR-18b	HepG2 CLDN-1 siRNA	6.654	0.447	Up Regulated	0.0075	No
miR-150	HepG2 CLDN-1 siRNA	6.537	0.472	Up Regulated	0.0077	No
miR-501	HepG2 CLDN-1 siRNA	5.262	0.035	Up Regulated	0.0009	No
miR-210	HepG2 CLDN-1 siRNA	3.351	0.025	Up Regulated	0.0012	No
miR-182	HepG2 CLDN-1 siRNA	2.478	0.052	Up Regulated	0.0053	No

miR-20b	HepG2 CLDN-1 siRNA	1.997	0.863	Up Regulated	0.0010	No
mmu-miR-374-5p	HepG2 CLDN-1 siRNA	1.975	0.019	Up Regulated	0.0002	No
miR-365	HepG2 CLDN-1 siRNA	1.971	0.049	Up Regulated	0.0001	No
miR-99b	HepG2 CLDN-1 siRNA	1.956	0.027	Up Regulated	0.0028	No
miR-331	HepG2 CLDN-1 siRNA	1.942	0.066	Up Regulated	0.0082	No
let-7e	HepG2 CLDN-1 siRNA	1.923	0.047	Up Regulated	0.0011	No
miR-29a	HepG2 CLDN-1 siRNA	1.918	0.093	Up Regulated	0.0011	No
miR-146b	HepG2 CLDN-1 siRNA	1.910	0.787	Up Regulated	0.0023	No
miR-885-5p	HepG2 CLDN-1 siRNA	1.892	0.059	Up Regulated	0.0022	No
miR-222	HepG2 CLDN-1 siRNA	1.879	0.011	Up Regulated	0.0130	No
miR-532-3p	HepG2 CLDN-1 siRNA	1.800	0.053	Up Regulated	0.0033	No
miR-135b	HepG2 CLDN-1 siRNA	1.799	0.076	Up Regulated	0.0020	No
let-7g	HepG2 CLDN-1 siRNA	1.769	0.018	Up Regulated	0.0009	No
miR-146a	HepG2 CLDN-1 siRNA	1.765	0.072	Up Regulated	0.0039	No

miR-200c	HepG2 CLDN-1 siRNA	-1.342	0.038	Down Regulated	0.0039	No
miR-29c	HepG2 CLDN-1 siRNA	-1.346	0.065	Down Regulated	0.0000	No
miR-186	HepG2 CLDN-1 siRNA	-1.364	0.013	Down Regulated	0.0060	No
miR-452	HepG2 CLDN-1 siRNA	-1.369	0.070	Down Regulated	0.0006	No
miR-140-3p	HepG2 CLDN-1 siRNA	-1.431	0.030	Down Regulated	0.0011	No
miR-455	HepG2 CLDN-1 siRNA	-1.536	0.067	Down Regulated	0.0016	No
miR-335	HepG2 CLDN-1 siRNA	-1.629	0.023	Down Regulated	0.0125	No
miR-484	HepG2 CLDN-1 siRNA	-1.661	0.088	Down Regulated	0.0020	No
miR-28	HepG2 CLDN-1 siRNA	-1.689	0.046	Down Regulated	0.0200	No
miR-374	HepG2 CLDN-1 siRNA	-1.692	0.011	Down Regulated	0.0320	No
miR-342-3p	HepG2 CLDN-1 siRNA	-1.792	0.043	Down Regulated	0.0070	No
miR-28-3p	HepG2 CLDN-1 siRNA	-1.918	0.066	Down Regulated	0.0013	No
miR-200b	HepG2 CLDN-1 siRNA	-2.006	0.048	Down Regulated	0.0019	No
miR-26a	HepG2 CLDN-1 siRNA	-2.078	0.066	Down Regulated	0.0012	No

miR-192	HepG2 CLDN-1 siRNA	-2.110	0.078	Down Regulated	0.0054	No
miR-30b	HepG2 CLDN-1 siRNA	-2.130	0.076	Down Regulated	0.0011	No
miR-183	HepG2 CLDN-1 siRNA	-2.167	0.016	Down Regulated	0.0097	No
miR-744	HepG2 CLDN-1 siRNA	-2.180	0.093	Down Regulated	0.0018	No
miR-200a	HepG2 CLDN-1 siRNA	-2.793	0.077	Down Regulated	0.0014	No
miR-138	HepG2 CLDN-1 siRNA	-2.795	0.084	Down Regulated	0.0059	No
miR-339-5p	HepG2 CLDN-1 siRNA	-2.918	0.013	Down Regulated	0.0089	No
miR-132	HepG2 CLDN-1 siRNA	-3.249	0.015	Down Regulated	0.0034	No
miR-628-5p	HepG2 CLDN-1 siRNA	-3.412	0.011	Down Regulated	0.0019	No
miR-145	HepG2 CLDN-1 siRNA	-3.720	0.027	Down Regulated	0.0013	No
miR-190	HepG2 CLDN-1 siRNA	-3.747	0.019	Down Regulated	0.0027	No
miR-324-5p	HepG2 CLDN-1 siRNA	-3.817	0.047	Down Regulated	0.0020	No
miR-340	HepG2 CLDN-1 siRNA	-3.870	0.061	Down Regulated	0.0001	No
miR-376c	HepG2 CLDN-1 siRNA	-3.870	0.031	Down Regulated	0.0001	No

miR-148a	HepG2 CLDN-1 siRNA	-3.880	0.016	Down Regulated	0.0084	No
miR-212	HepG2 CLDN-1 siRNA	-3.883	0.024	Down Regulated	0.0001	No
miR-130a	HepG2 CLDN-1 siRNA	-3.956	0.076	Down Regulated	0.0018	No
miR-9	HepG2 CLDN-1 siRNA	-6.588	0.022	Down Regulated	0.0001	No
miR-101	HepG2 CLDN-1 siRNA	-7.479	0.066	Down Regulated	0.0002	No
miR-193a-5p	HepG2 CLDN-1 siRNA	-7.599	0.012	Down Regulated	0.0003	No
miR-636	HepG2 CLDN-1 siRNA	-7.610	0.045	Down Regulated	0.0016	No
miR-128a	HepG2 CLDN-1 siRNA	-7.675	0.065	Down Regulated	0.0021	No
miR-181a	HepG2 CLDN-1 siRNA	-7.855	0.056	Down Regulated	0.0029	No
miR-34a	HepG2 CLDN-1 siRNA	-8.019	0.014	Down Regulated	0.0042	No
let-7a	HepG2 CLDN-1 siRNA	-8.130	0.029	Down Regulated	0.0061	No
miR-486	HepG2 CLDN-1 siRNA	-8.818	0.015	Down Regulated	0.0021	No
miR-149	HepG2 CLDN-1 siRNA	-14.793	0.034	Down Regulated	0.0008	No
miR-455-3p	HepG2 CLDN-1 siRNA	-15.106	0.042	Down Regulated	0.0043	No

miR-99a	HepG2 CLDN-1 siRNA	-15.291	0.092	Down Regulated	0.0010	No
miR-100	HepG2 CLDN-1 siRNA	-181.818	0.048	Down Regulated	0.0004	No
miR-215	HepG2 CLDN-1 siRNA	-769.231	0.043	Down Regulated	0.0008	No

Table 3.8: Normalised gene expression profile ($2^{-\Delta\Delta CT}$) of miRNAs in claudin-1 silenced HepG2 cells. The table details the relative normalised gene expression of 76 miRNAs in $HepG2^{CLDN\text{-}1\text{-}}$ cells, $HepG2^{scambled\text{-}ve}$ cells were used as the control. $HepG2^{CLDN\text{-}1\text{-}}$ and $HepG2^{scambled\text{-}ve}$ cells were cultured for 72 hours prior to total RNA extraction. Amplification of the genes outlined in Table 3.7 was performed alongside U6, RNU44 and RNU48 as the reference genes using RT-PCR. Relative normalised gene expression was calculated using the $2^{-\Delta\Delta CT}$ method. Data presented is representative of mean fold change ±s.e.m from three biological replicates. Paired t-test was performed to determine statistical significance. Statistical significance is indicated if the P value is lower than the 0.05 threshold.

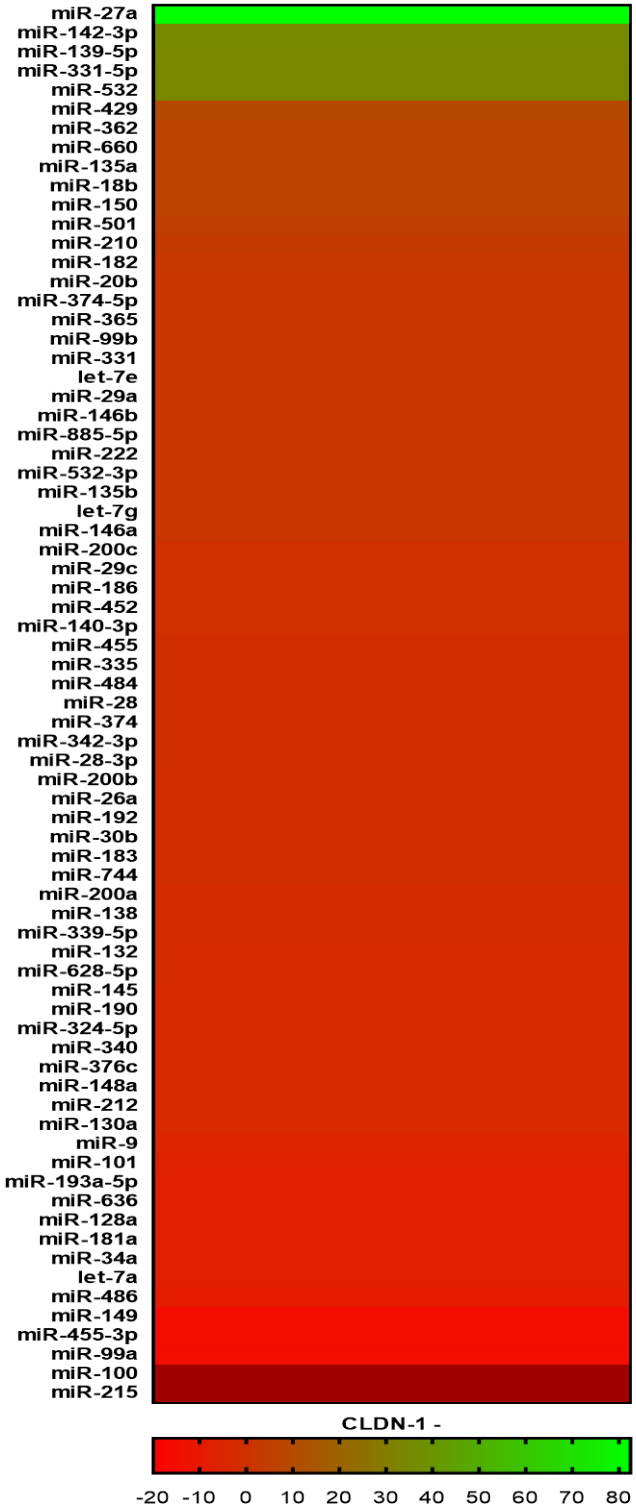

Figure 3.64: Heat map representing normalised gene expression profile ($2^{-\Delta\Delta CT}$) of miRNAs in claudin-1 silenced HepG2 cells. Normalised gene expression values taken from Table 3.8 have been converted into a colorimetric scale outlined above to provide a visual representation of large-scale changes. Genes indicated by a green bar represent an upregulation in expression, whereas genes indicated by a red bar represent a down regulation in expression.

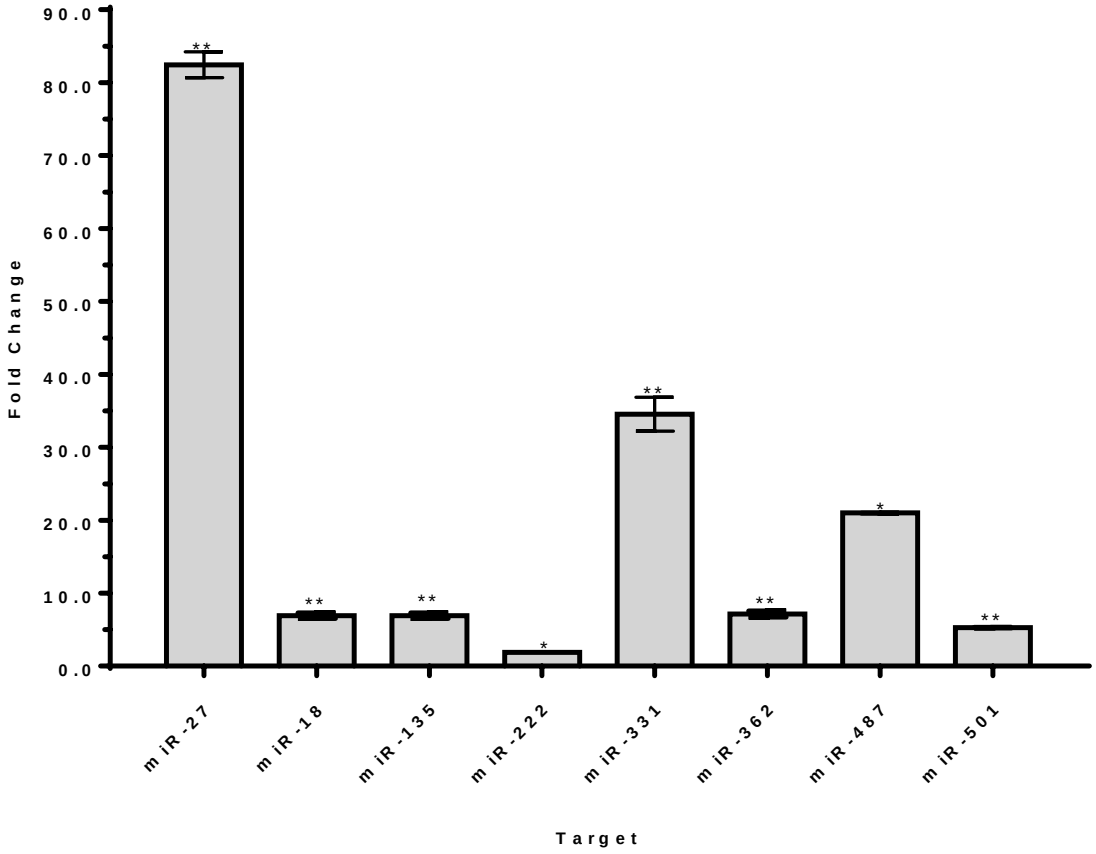

Figure 3.65: Normalised gene expression profile ($2^{-\Delta\Delta CT}$) of miRNAs in HepG2$^{CLDN-1-}$ cells which are associated with a poor prognosis in HCC. HepG2$^{CLDN-1-}$ and HepG2$^{scambled-ve}$ cells were cultured for 72 hours prior to total RNA extraction. Amplification of miR-27, -18, -135, -222, -331, -362, -487 and -501 was performed alongside U6, RNU44 and RNU48 as reference genes using RT-PCR. Relative normalised gene expression was calculated using the $2^{-\Delta\Delta CT}$ method. Data presented is representative of mean fold change ±s.e.m from three biological replicates. Paired t-test was performed to determine statistical significance, * P≤0.05 ** P≤0.01

The expression of miRNAs -27, -18, -135, -222, -331, -362, -487 and -501 were all increased HepG2$^{CLDN-1-}$ cells compared to HepG2$^{scambled-ve}$, represented by a 82.5, 1.8, 6.9, 6.9, 34.5, 7.1, 21.0 and 5.3 fold change respectively. Statistical analysis indicated that the increase in expression of these miRNA members was significant (P=0.008, P=0.004, P=0.004, P=0.013, P=0.005, P=0.003, P=0.011 , P=0.001)

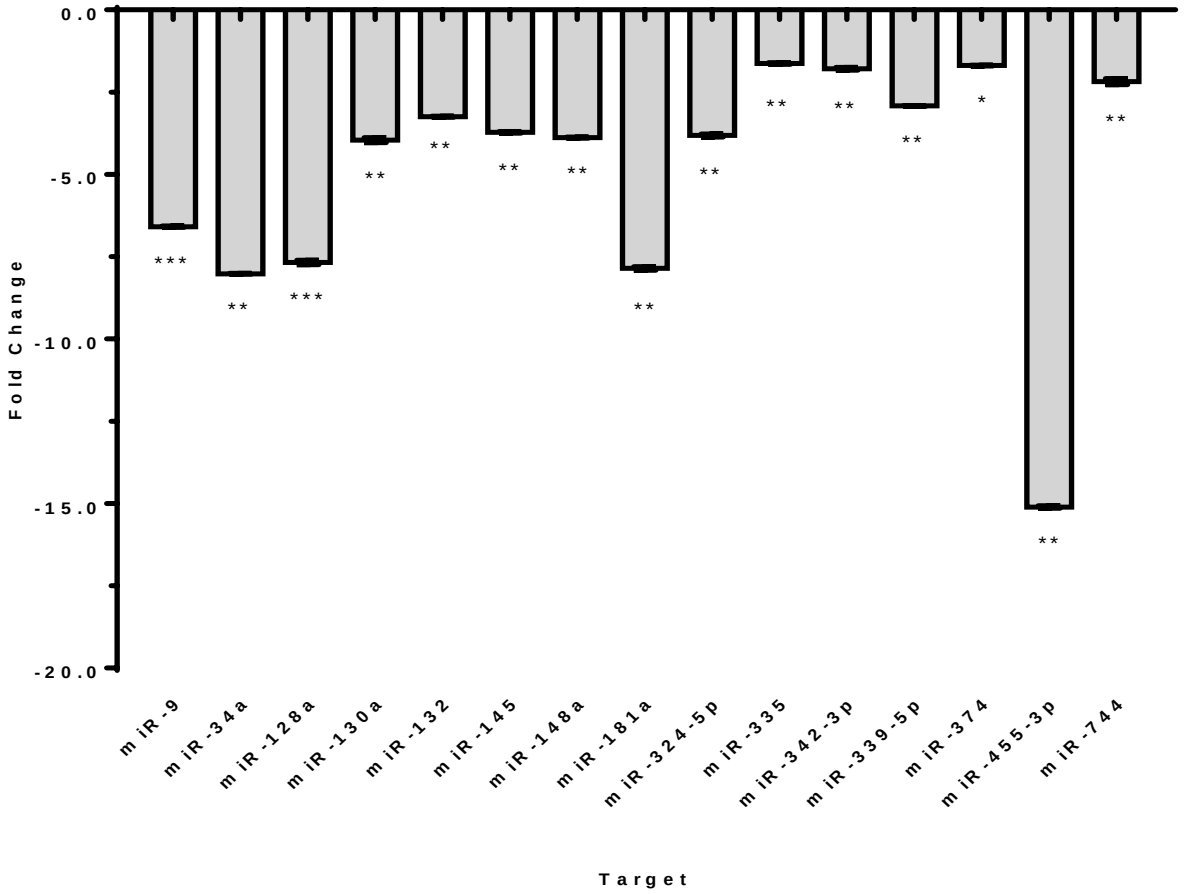

Figure 3.66: Normalised gene expression profile ($2^{-\Delta\Delta CT}$) of miRNAs in HepG2$^{CLDN-1-}$ cells which are known tumour suppressors in HCC. HepG2$^{CLDN-1-}$ and HepG2$^{scambled-ve}$ cells were cultured for 72 hours prior to total RNA extraction. Amplification of miR-9, -34a, -128a, -130a, -132, -145, -148a, -181a, -324-5p, -335, -342-3p, -339-5p, -374, -455-3p and 744 was performed alongside U6, RNU44 and RNU48 as reference genes using RT-PCR. Relative normalised gene expression was calculated using the $2^{-\Delta\Delta CT}$ method. Data presented is representative of mean fold change ±s.e.m from three biological replicates. Paired t-test was performed to determine statistical significance, * P≤0.05 ** P≤0.01 *** P≤0.001

The expression of miRNAs -9, -34a, -128a, -130a, -132, -145, -148a, -181a, -324-5p, -335, -342-3p, -339-5p, -374, -455-3p and 744were all decreased HepG2$^{CLDN-1-}$ cells compared to HepG2$^{scambled-ve}$, represented by a -6.6, -8.0, -7.7, -4.0, -3.2, -3.7, -3.9, -7.9, -3.8, -1.6, -1.8, -2.9, -1.7, -15.1 and -2.2 fold change respectively. Statistical analysis indicated that the increase in expression of these miRNA members was significant (P≤0.001, P=0.004, P≤0.001, P=0.002, P=0.003, P=0.001, P=0.008, P=0.003, P=0.002, P=0.01, P=0.007, P=0.009, P=0.032, P=0.004 P=0.002)

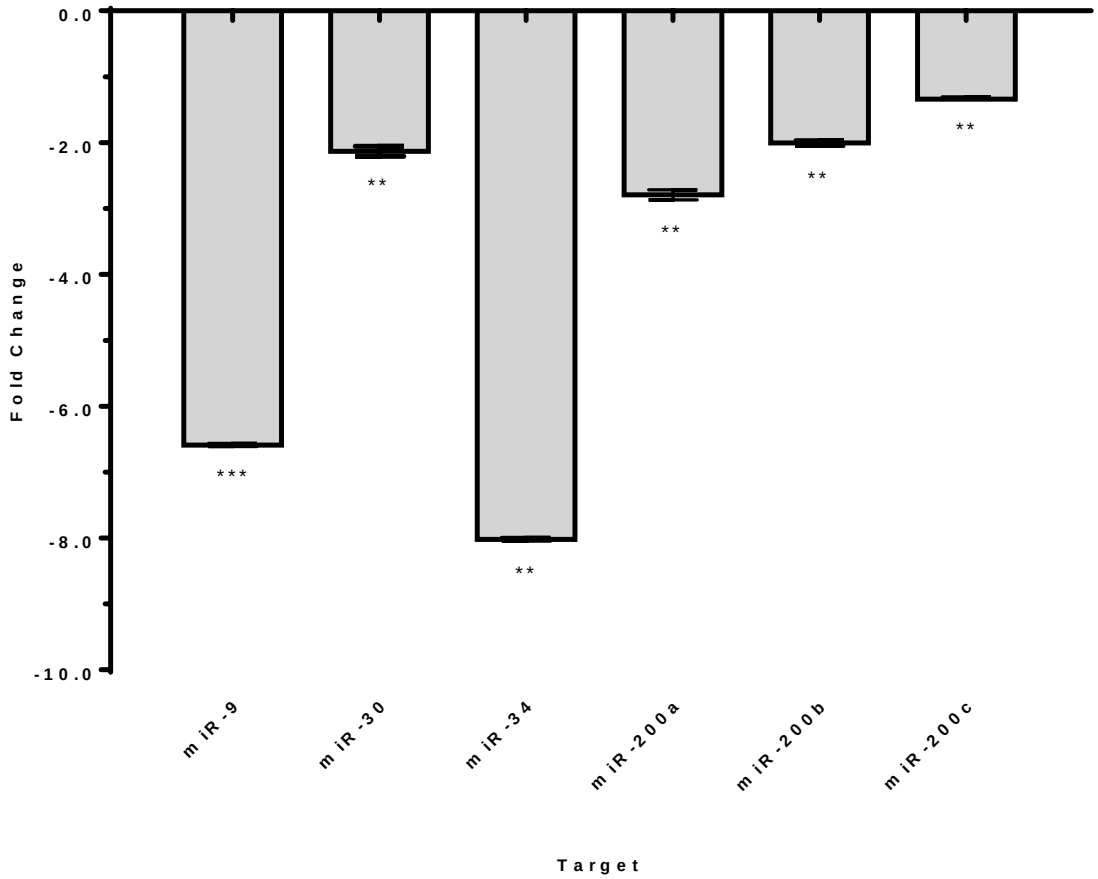

Figure 3.67: Normalised gene expression profile ($2^{-\Delta\Delta CT}$) of miRNAs in HepG2$^{CLDN-1-}$ cells which supress EMT in HCC. HepG2$^{CLDN-1-}$ and HepG2$^{scambled-ve}$ cells were cultured for 72 hours prior to total RNA extraction. Amplification of miR-9, -30, -34, -200a, -200b and -200c was performed alongside U6, RNU44 and RNU48 as reference genes using RT-PCR. Relative normalised gene expression was calculated using the $2^{-\Delta\Delta CT}$ method. Data presented is representative of mean fold change ±s.e.m from three biological replicates. Paired t-test was performed to determine statistical significance, * P≤0.05 ** P≤0.01 *** P≤0.001

The expression of miRNAs -9, -30, -34, -200a, -200b and -200c were all decreased in HepG2$^{CLDN-1-}$ cells compared to HepG2$^{scambled-ve}$, represented by an -6.6, -2.1, -8.0, -2.8, -2.0 and -1.3 fold change respectively. Statistical analysis indicated that the increase in expression of these miRNA members was significant (P≤0.001, P=0.001, P=0.004, P=0.001, P=0.001, P=0.0039)

By profiling the miRNA expression of both claudin-1 overexpressing and silenced HepG2 cells, it can be seen that generally the expression of many miRNAs decrease compared to control. The silencing of these miRNAs is expected as many of the genes in which they target are observed to be overexpressed in our qPCR studies. An important example of this is the miR200 family, which all members were significantly downregulated in both claudin-1 overexpressing and silenced cells. This family of miRNAs are master regulators of EMT that act by strongly repressing mesenchymal genes and inhibit the initiating steps of metastasis (Korpal & Kang 2008). The decrease in the miR200 family seen in these cells suggests an increase in metastasis potential and further provides evidence of the initiation of EMT.

Chapter 4: Discussion

4.1 General discussion

Investigating of the role of claudin-1 in the initiation and progression of HCC has direct clinical implications, especially as the characterisation of the molecular mechanisms involved may predict tumour precession and outline avenues of potential therapeutic intervention. The altered migratory capacity of cancer cells, driven by changes in molecular mechanisms, is what determines a cancers metastatic potential and ultimately the progression and prognosis of the disease. An important aim of this thesis was to investigate if the overexpressing and the silenced claudin-1 HepG2 cells would display the same documented increase in migratory capacity as in the literature. The results from the migration assay indicated that both claudin-1 overexpressing and silenced HepG2 cells displayed increased migration over 72 hours. These results therefore correspond with the increased migratory capacity observed in cases of HCC with aberrant levels of claudin-1 documented in the literature (Holczbauer et al 2013). As a result of the increased migratory capacity of these cells, further investigation took place to determine the molecular mechanisms in which contribute to this major tumour progressive property.

4.1.1 The expression of tight junctional and associated genes in claudin-1 overexpressing and silenced HepG2 cells

Tight junctional proteins such as claudins have a complex and tissue specific role across a range of human cancer types (Singh et al 2010). Aberrant cellular expression of claudins has been continually implicated in the initiation and subsequent progression of the disease and has a significant effect on the expression of many other cellular components. The expression pattern of claudin-1, -3, -4 and -5 in particular have been implicated as the key members

responsible for the acquisition of an invasive phenotype in HCC (Kwon 2013).

The expression of tight junction family members was determined in claudin-1 overexpressing and claudin-1 silenced HepG2 cells, to investigate if the change in gene expression had any effect on tight junction composition. Modulation of the tight junction is crucial for cancer cells to overcome cell-cell contact in the first steps of metastasis. Furthermore, it is well documented that HCCs often present with differential expression patterns of tight junction family members (Martin & Jiang 2009).

Overexpression of claudin-1 in HepG2 cells resulted in increased expression of claudin family members -2 and -7. claudins -4, -5 and -11 were significantly decreased, while the expression of claudins -3 and -8 remained unchanged. Silencing of claudin-1 in HepG2 cells resulted in increased expression of claudins -2, -3 and 11. Claudins -4, -5 and 8 were significantly decreased, while expression of claudin- 7 remained unchanged.

There is little supporting data linking claudin-2 in the progression of HCC, although it usually downregulated (Holczbauer et al 2013). It is therefore interesting to see that claudin-2 was increased in both overexpressing and silenced HepG2 cells. Claudin-2 is commonly overexpressed in colorectal cancer and correlates with poor prognosis. In vivo experiments overexpressing claudin-2 resulted in increased cell proliferation and anchorage-independent growth (Dhawan et al 2011). It is therefore possible for claudin-2 to be linked to the increased cell proliferation and migration of both claudin-1 overexpressing and silenced HepG2 cells. Experiments using fibroblasts lacking tight junctions, show that only claudin-1 and -2 are able to initiate the formation of tight junctional strands (Landy et al 2016). It is therefore possible that the upregulation of claudin-2 could be in response to junctional dysregulation in an attempt to restore tight junction integrity.

The expression of claudin-3 is commonly downregulated in HCC (Holczbauer et al 2013). Experiments involving forced expression of claudin-3 in HepG2 cells resulted in

decreased metastatic potential via downregulation of the WNT/β-catenin pathways (Jiang et al 2014). The increased expression of claudin-3 in claudin-1 silenced HepG2 cells may explain in part why β-catenin levels where higher in claudin-1 overexpressed, which would give these cells a proliferative and migratory advantage.

Claudin -4 and -5 are frequently decreased in HCC, with some reports indicating no detectable claudin-4 positivity (Holczbauer et al 2013). Claudin -4 and -5 have also been described as prognostic markers with higher expressions correlating with an increased prognosis (Bouchagier et al 2014). The decreased expression of claudin-4 and -5, combined with the increase in migratory capacity in both claudin-1 overexpressed and claudin-1 silenced cells correlates with findings in the literature. Claudin-7 presented with the largest increase in expression of all claudin family members during claudin-1 overexpression. However, no change in expression was detected in claudin-1 silenced cells. Claudin-7 is frequently overexpressed in HCC, although reports suggest that there is no significant correlation between the expression of claudin-7, tumour grade, or patient demographic data (Brokalaki et al 2012). Despite this, claudin-7 is considered as a possible stem cell marker due to the significantly increased levels during liver regeneration. It has been suggested that cells with and increased expression of claudin-7 may display increased stemness associated properties (Bouchagier et al 2014).

The expression of claudin-8 was decreased in both claudin-1 overexpressed and claudin-1 silenced HepG2 cells, although the change in expression in claudin-1 overexpressed HepG2 cells was not significant. Very little data exists regarding the expression of claudin-8 in HCC or its significance in progression of the disease. However, one study reported that the expression of claudin-8 was found to be downregulated (Ding & Chen 2013).

Claudin-11 was almost completely silenced in claudin-1 overexpressing HepG2 cells

but almost 5 fold increased in claudin-1 silenced cells. While little data exists on the levels or role of claudin-11 in HCC, one study describes the inverse link between miR-99 and claudin-11 levels in HCC, implying that a decrease in claudin-11 caused by miR-99 overexpression resulting in increased migration (Yang et al 2015). The decrease in claudin-11 combined with the increase in miR-99a may contribute to the increased migratory capacity of claudin-1 overexpressed cells. The increased expression of claudin-11 in claudin-1 silenced cells may contribute towards the difference in migratory capacity compared to claudin-1 overexpressed cells.

Occludin is another vital tight junction constituent that that is often dysregulated in a number of human cancers. Occludin is a potential tumour suppressor in cancer, with its expression inversely correlating with level of tumorigenicity in a number of malignancies (Osanai et al 2006). Studies have shown that occludin is frequently downregulated in HCC (Bouchagier et al 2014). Although no correlation was found between occludin expression and overall survival. Occludin was downregulated most frequently in poorly differentiated tumours and correlated with the decreased polarity of the cells (Orbán et al 2008). The decrease in expression seen in our experiments correlate with the literature. Occludin is downregulated in both claudin-1 overexpressed and claudin-1 silenced cells potentially aiding the increased migratory capacity.

The expression of Junctional Adhesion Molecule A (JAM A) was dysregulated in both claudin-1 overexpressed and claudin-1 silenced cells. Claudin-1 overexpression in HepG2 cells almost completely silenced JAM A. Little data is available regarding a role of JAM A, B or C in HCC, with no documented link to prognosis or survival. However, experiments silencing JAM A in HepG2 cells caused tight junction mislocalisation and prevented pseudocanaliculi formation, despite no alterations to the levels of claudin-1, occludin, and ZO-1. Our findings in response to claudin-1 overexpression produced similar changes in cell

morphology, i.e. decreased JAM A expression, reduction in cellular polarity, and absent pseudocanaliculi formation (Konoka et al 2007). The combination of our results with existing literature suggests that JAM A is important for hepatic cell polarity and its absence may contribute to cell dysregulation which might ultimately translate to a worse prognosis in HCC.

The expression of JAM A increased in claudin-1 silenced cells, and although there is no data indicating the clinicopathological significance of JAM A in HCC, reports of JAM A overexpression in other human cancers suggest its role in EMT induction via the PI3K/AKT pathway (Tian et al 2015).

Very little is known about the function of JAM B and C in any cancers, but it was interesting to observe a large increase in JAM B expression in claudin-1 overexpressing HepG2 cells. It is possible that JAM B is increased as a compensatory mechanism in an attempt to restore polarity, in a similar way claudin composition can be altered to maintain barrier function (Bojarski et al 2004).

Adherence junctions composed of afadin and nectin subunits form Ca^{2+} dependent, cadherin based cell-cell structures by dimerization. Afadin (AF6) is a structural intermediate between the actin cytoskeleton and transmembrane adhesion molecule nectin. Similar to tight junctions, adherence junctions function to maintain epithelial barrier function and to a varying degree polarity (Niessen 2007). The expression and localisation of adherence junctions are commonly dysregulated in human cancers. In breast cancer afadin is phosphorylated via the PI3K-AKT signalling pathway resulting in increased migration and outlining the pathophysiological significance of adherence junctions in cancer (Elloul et al 2014). Although there is little data regarding afadin and nectin in HCC, reduced expression is associated with a poor prognosis in breast, colon, pancreatic, and endometrial cancers. A recent study by Ma et al (2016) found that a decrease in expression of adherence junction molecules could activate AKT signalling increasing cell survival and apoptosis resistance in HCC. The

decreased expression of afadin and nectin observed in claudin-1 silenced HepG2 cells might indicate increased tumour progressive capacity and possible AKT signalling involvement.

SP1 is a highly conserved transcription factor that regulates the expression of a number of genes involved in proliferation, apoptosis, differentiation, and epigenetic silencing and promotion. Although the function of SP1 is often cancer and pathway specific, its upregulation is associated with increased invasiveness, greater metastatic potential, and overall poorer prognosis in gastric, pancreatic, and breast carcinomas (Beishline & Azizkhan-Clifford 2015). The expression of SP1 in HCC was reported to be increased, and its expression inversely correlating with prognosis (Huang et al 2015). The increase in SP1 expression in claudin-1 silenced HepG2 cells might indicate an increase in tumorigenicity with a reduction in claudin-1 expression.

WNK4 is a Serine/threonine-protein kinase involved in regulating SPAK/OSR1 and ion cotransporters. Little data exists about the role of WNK4 in cancer, but it is known to be involved in developmental and cellular processes and is often mutated or downregulated (Shimizu et al 2013). Experiments involving siRNA targeting of WNK4 has increased SMAD2/3-dependent transcriptional regulation and subsequently inhibiting SMAD2 and TGF-β signalling (Moniz & Jordan 2010). WNK4 is found almost exclusively in polarized epithelia and therefore its expression can indicate cellular polarity (Kahle et al 2004). Therefore, the decrease in expression of WNK4 in claudin-1 silenced and claudin-1 overexpressed HepG2 cells might be an indicator of reduced cellular polarity compared to control cells.

Scaffold proteins such as Zonula Occludens -1, -2 and -3 provide a linkage between membrane bound junctional proteins, such as claudins and occludin and the actin cytoskeleton (Lee & Luk 2010). Zonula Occludens not only provide the structural architecture necessary for the formation of tight junctions and cell polarity but participate in cellular signalling cascades responsible for regulating proliferation and differentiation (Matter & Balda

2003). A number of human cancers including HCC display dysregulated expression, and often decreased levels of Zonula Occludens (Martin & Jiang 2009). Low expression of ZO-1 has been linked to a poor prognosis in HCC cases and there is some suggestion of its use as a biomarker in the predicted progression of the disease (Nagai et al 2016). Little evidence exists regarding the role of ZO-2 and ZO-3 in the disease, but the trend in other cancers such as breast and lung suggest their levels correlate with the clinicopathological significance of ZO-1 (Lee & Luk 2010). Our data suggests that ZO-1, -2 and -3 are decreased significantly in both claudin-1 overexpressed and claudin-1 silenced cells. The dysregulation of claudin-1 in HCC likely causes the breakdown of tight junction complexes causing the dissociation of Zonula Occludens. Loss or dissociation of ZO-1 has been shown to increase proliferation and decrease cell polarity in a number of cancers (Yasen et al 2005). Therefore, the decreased expression of Zonula Occludens in these cells is likely to contribute to the reduction in cellular polarity and increased migratory phenotype observed in our experiments.

ZONAB is a Y-Box binding transcription factor strongly associated with tight junction complexes, especially ZO-1, via specific binding to the SH3 domain of Zonula Occludens (Balda & Garrett 2003). ZONAB typically shuttles between the tight junction and the nucleus, interacting with a number of proliferation related genes such as cyclin D1 and ERB receptors. Evidence suggests that ZO-1 regulates the expression and localisation of ZONAB in MDCK cells (Pozzi & Zent 2010). Decreased expression of ZO-1 causes an increase in expression of ZONAB and shifts its localisation from the tight junction to the nucleus. The result is an increase of direct transcription of proliferative genes such as cyclin D1 (Pozzi & Zent 2010). ZONAB overexpression potentially prevents polarization and differentiation while increasing proliferation in proximal tubule epithelial cells (Lima et al 2010). Increased ZONAB expression is associated with advanced stages of HCC, with an increased expression correlating with a poor prognosis (Yasen et al 2005). The overexpression of ZONAB combined with the

decreased expression of ZO-1, in both claudin-1 overexpressed and claudin-1 silenced cells, may in part account for the increases in proliferation observed. As there is little data regarding ZONAB in HCC, further investigation is needed. However, ZONAB provides a promising link between the dysregulation of claudin-1 and the increase in tumour progression outlined in this study and in the literature.

A comparison of tight junctional and associated genes between the claudin-1 overexpressing and silenced cells shows that while both groups may not present with identical patterns of expression there are many similarities. Increased expression of claudin-2 and decreased expression of claudins -4 and -5 along with occludin, and Zonula Occludens not only characterise the junctional profile of claudin-1 overexpressing and silenced cells but have been described as the pattern associated with a poor prognosis in the literature (Lee & Luk 2010). The correlation of the same pattern of dysregulated junctional constituents in both claudin-1 overexpressing and silenced cells and the literature gave the first indication that the aberrant expression of claudin-1 could be responsible for the poor prognosis associated with HCC cases with the same profile. While it is almost impossible to make conclusions about the underlying molecular mechanisms just off the junctional profile alone, it acts as an indicator of dysregulated cellular adherence and barrier function associated with EMT and tumour metastasis (Ikenouchi et al 2003)

4.1.2 The expression of epithelial to mesenchymal transition genes in claudin-1 overexpressing and silenced HepG2 cells.

Increasing evidence outlines epithelial-mesenchymal transition as the molecular switch in cancer progression, by which cancer cells gain the capacity to migrate away from the primary tumour and metastasise. The switch to a mesenchymal phenotype is characterised by a number of molecular mechanisms, most classically the downregulation of E-cadherin and the

upregulation of vimentin. The expression of vimentin was increased in both claudin-1 overexpressed and claudin-1 silenced HepG2 cells, although significantly more during claudin-1 overexpression. The epithelial marker E-cadherin was downregulated in both claudin-1 overexpressed and claudin-1 silenced HepG2 cells, again significantly more during claudin-1 overexpression. The low E-cadherin, high vimentin expression profile observed in both our claudin-1 overexpressing and silenced cells mimics that of invasive, poorly differentiated HCC (Van Zijl et al 2009). Studies correlate low E-cadherin (Cho et al 2008), and high vimentin (Hu et al 2004) expression in HCC with an increased metastatic potential, poor prognosis, and an increased rate of recurrence after surgical resection.

Cadherin switching, usually E- to N- cadherin is another hallmark of epithelial-mesenchymal transition (De Craene & Berx 2013). E-cadherin is typically only expressed in epithelial cells, whereas N-cadherin, R-cadherin, and cadherin-11 are expressed in mesenchymal cells. Therefore, the up-regulation of N-cadherin is classically seen as a hallmark of mesenchymal transition and is shown to promote invasion of surrounding tissues and metastasis in cancer (Wheelock et al 2008). The expression of N-cadherin was significantly decreased in claudin-1 overexpressing HepG2 cells, which is unexpected due to the assumption of EMT induction caused by the changes in E-cadherin and vimentin. However, N-cadherin is commonly downregulated in HCC, and interestingly this correlates with poor tumour differentiation, vascular invasion, and shorter postoperative disease-free survival (Zhan et al 2012). This suggests that N-cadherin expression and resultant prognosis in cancer is cell specific, and that in HCC, a reduced N-cadherin expression indicates an increase in tumorigenicity. The expression of N-cadherin was significantly increased in claudin-1 silenced HepG2 cells and therefore indicates classic cadherin switching seen in EMT initiation. However, due to fact N-cadherin is frequently decreased in HCC, the increase seen is unlikely to indicate a more tumour progressive phenotype. In fact, it may in part

explain why claudin-1 overexpression induces a more migratory phenotype in comparison to claudin-1 silencing in HepG2 cells.

In a similar pattern to N-cadherin, the expression of fibronectin was significantly decreased during claudin-1 overexpression and significantly increased during claudin-1 silencing. Fibronectin participates in the formation of a fibrotic extra cellular matrix which is modulated by inflammation, tissue fibrosis, and desmoplastic stroma in tumours. Conventionally fibronectin is seen as a bio-maker for EMT in the same way up-regulation of N-cadherin and vimentin are (Zeisberg & Neilson 2009). The increase of fibronectin in claudin-1 silenced HepG2 cells would further indicate EMT involvement due to its role in ECM remodelling and tumour progression. However, research suggests that fibronectin is abnormally localised and downregulated during HCC, which coincides with the decreased expression of fibronectin seen in claudin-1 overexpressing cells. Conventionally, both N-cadherin and fibronectin participate in the initiation of epithelial-mesenchymal transition, but in HCC their absence does not negatively regulate the process and may even be associated with a poorer prognosis in vivo.

The process of epithelial-mesenchymal transition is orchestrated by EMT related transcription factors in both normal development and in cancer. SNAIL, TWIST, and ZEB families represent the major groups of transcription factors regulating the process, although many other transcription factors are involved. The SNAIL family transcription factors showed dysregulated expression in both claudin-1 silenced and overexpressed HepG2 cells. SNAIL1 was significantly overexpressed during claudin-1 overexpression but only slightly overexpressed during claudin-1 silencing. SNAIL1 is classically known for decreasing E-cadherin expression and initiating the shift away from an epithelial phenotype. The increase in expression of SNAIL in both claudin-1 overexpressing and silenced cells inversely correlated, proportionally to the decrease in E-cadherin expression. SNAIL expression in

HCC is associated with decreased expression of E-cadherin and poor differentiation. The increased expression of SNAIL coupled with the decreased expression E-cadherin presents with a strong association with postoperative recurrence (Woo et al 2011). SNAIL2 (SLUG) was massively overexpressed during claudin-1 overexpression and almost silenced completely during claudin-1 silencing. SLUG is frequently overexpressed in HCC (Yang et al 2009). Experiments involving the overexpression of SLUG in HepG2 cells reported the induction of EMT with increased clonogenicity and presentation of stem cell markers (Sun et al 2014). The role of SNAIL3 in cancer is poorly understood, although it shares the same zinc-finger binding domains as SNAIL1 and 2 and is thought to bind to similar targets. No data is available about its expression in HCC, however its expression is increased in lung cancer and melanoma (Sánchez-Tilló et al 2012). There was no change in expression of SNAIL3 in claudin-1 overexpressing cells, but a significant decrease in claudin-1 silenced cells. Despite this, no data is available in the literature to draw conclusions from.

The large increases in expression of SNAIL 1 and 2 in claudin-1 overexpressing HepG2 cells indicate the activation of EMT. Evidence from the literature indicates HepG2 cells overexpressing these transcription factors present with increased proliferation and migration (Yang et al 2009). This suggests that SNAIL1 and 2 are likely involved in increasing the migratory capacity of claudin-1 overexpressing HepG2 and modulating gene expression of other EMT and tumour metastasis genes. The increase in SNAIL1 in claudin-1 silenced cells is relatively small. This may account for the slight decrease in E-cadherin observed, but in combination with the large decreases in SNAIL2 and 3, it is unlikely the SNAIL family transcription factors are responsible for the expression of EMT markers expressed in claudin-1 silenced cells.

TWIST1 is a transcriptional promotor of EMT, which was significantly increased in both claudin-1 silenced and claudin-1 overexpressed HepG2 cells. TWIST1 expression is

commonly increased in human cancers and correlates with poor prognosis in breast, prostate, lung, uterine, and several other tumour cell lines. TWIST1 is well defined as a E-cadherin repressor, and is involved in regulation of gene expression corresponding to the upregulation of mesenchymal markers, reduction of cell-cell adhesion, and increasing cell motility. Experiments involving the forced expression of TWIST1 in HepG2 cells, reported the induction of EMT, increased cell migration, and production of stem cell markers (Matsuo et al 2009). Given previous experimental evidence, the increase in TWIST1 expression in claudin-1 silenced and claudin-1 overexpressed HepG2 cells will certainly contribute to the increased migratory capacity observed. As the expression of TWIST1 is undetectable in wild type HepG2 cells, the induction of TWIST1 is modulated during claudin-1 silencing and claudin-1 overexpression.

ZEB1 and 2 were increased in both claudin-1 silenced and claudin-1 overexpressed HepG2 cells, however the increased expression of ZEB1 in claudin-1 silenced cells was not significant. Just like the SNAIL and TWIST family of transcription factors, ZEB1 and 2 downregulate the expression of E-cadherin via interactions with the E-box element of the E-cadherin promoter. ZEB1 and 2 are described as crucial promoters of metastasis in pancreatic and colon cancer by inducing EMT-activation, stem cell markers and associated characteristics (Hashiguchi et al 2013). ZEB1 is commonly upregulated in HCC, its increased expression is associated with a decrease in E-cadherin, an increase in metastasis, and a poor prognosis (Zhang et al 2013). The increased ZEB1 expression in claudin-1 overexpressing HepG2 cells further suggest the induction of EMT and explains the increased migratory capacity observed. The upregulation of ZEB1 and 2 in HCC is known to induce EMT and associated vasculogenic mimicry and metastasis (Liu et al 2016). Overexpression of ZEB2 in HepG2 cells increased cell migration, invasiveness, and vasculogenic mimicry, in vitro (Yang et al 2015). The increase of ZEB2 in claudin-1 overexpressing and silenced

HepG2 cells further strengthens the association with EMT induction and increased migratory capacity of the two groups.

The expression of EMT regulators TWIST1 and ZEB2, but not ZEB1, are upregulated in oral squamous cell Carcinoma. TWIST1 and ZEB2 in combination, cause an upregulation of EMT genes which correlate to a poor prognosis in oral squamous cell Carcinoma (Kong et al 2015). This upregulation of TWIST and ZEB2, but not ZEB1, mimics the profile observed in our claudin-1 silenced HepG2 cells, indicating that EMT can be induced without ZEB1, and the migratory phenotype observed may be modulated by a combination of TWIST and ZEB2.

Forkhead box C2 (FoxC2) is a member of the winged Helix/Forkhead family of transcription factors. The DNA binding domain of FoxC2 allows transcription of genes involved in various developmental and embryonic processes as well as cancer. High FoxC2 expression is linked with metastatic potential and a poor prognosis in serval human cancers such as breast, oesophageal, ovarian and colon (li et al 2015). FoxC2 is documented to be overexpressed in HCC and thought to activate MAPK and AKT/GSK-3β signalling pathways and induce EMT. FoxC2 was also reported to increase β1-integrin mediated cell migration in the HCC cell line, Huh-7 (Bai et al 2014). The expression of FoxC2 was increased in both claudin-1 silenced and overexpressed HepG2 cells. As FoxC2 induces EMT and increases cell migration in vivo and vitro, it is likely contributing to the increase in EMT markers and cell migration in both claudin-1 overexpressing and silenced HepG2 cells. The increase in FoxC2 expression was almost double in claudin-1 silenced cells compared to overexpressed. The upregulation of EMT markers seen in claudin-1 silenced cells may be regulated more by FoxC2 due to its significantly higher expression compared to core EMT transcription factors SNAIL, TWIST and ZEB1/2.

The homeobox goosecoid is a transcription factor involved in initiating EMT and cell migration in embryonic development. The expression has been correlated with

increased metastasis and a poor prognosis in breast (Hartwell et al 2006) and ovarian cancer (Kang et al 2014). Homeobox goosecoid is frequently upregulated in HCC and its expression is associated with a poor prognosis. The most invasive lung metastasis of HCC contains the highest expression of GSC, usually far higher than the primary tumour. The upregulation of GSC in metastatic tumours provides in vivo evidence of its participation in upregulating the invasive phenotype of HCC. Overexpression of homeobox goosecoid in the Hep3B HCC cell line induced EMT and significantly increased cell migration (Xue et al 2014). It is therefore possible for the increased expression of homeobox goosecoid, in both our claudin-1 overexpressing and silenced cells, to be responsible for the upregulation of EMT markers and increased migratory capacity observed.

Sox10 is part of the SRY-related HMG-box family of transcription factors most commonly known for its involvement in embryonic development. Its involvement in cancer is complex with tumour promoting and suppressive properties described in the literature (Zhou et al 2014). However, several studies reported upregulation of Sox10 and linked this phenotype with poor prognosis in breast cancer (Dravis et al 2015), HCC (Zhou et al 2014) and malignant Melanoma (Mohamed et al 2013). In vitro experiments overexpressing Sox10 in breast cancer cells, induced EMT and stem cell markers, increasing proliferation and invasive capacity (Dravis et al 2015). Forced expression of Sox10 in the HCC cell line Huh7 caused an increase in β-catenin expression and associated transcription factors TCF4 by facilitating the binding between them. Cell proliferation was subsequently increased by upregulated cyclin-D1 expression (Zhou et al 2014). Silenced Sox10 expression prevented binding of β-catenin and TCF4, reducing proliferation. The increased expression of Sox10 caused by claudin-1 overexpression could be responsible for the increased proliferation observed, by upregulating β-catenin and facilitating the binding of β-catenin to TCF, which are also upregulated. The decreased expression of Sox10 in claudin-1 silenced cells

correlates with the lower expression of β-catenin and associated target genes compared to claudin-1 overexpression.

Ca2+/calmodulin-dependent protein kinase II (CAMK2N1) is a serine/threonine kinase originally discovered for its role in neuron function, memory, and learning. CAMK2N1 has become a protein of interest in cancer due to its ability to activate signalling pathways and transcription factors. In HCC, CAMK2N1 induces TRAIL mediated apoptosis and inhibits MEK mediated cell proliferation (Wang et al 2015). CAMK2N1 is significantly downregulated during claudin-1 overexpression in HepG2 cell, reducing any inhibitory effects the kinase may have on tumour progression and apoptosis.

Desmoplakin is an essential part of the desmosomal plaque, forming adherence junctions between adjacent cells. Little is known about the role of desmoplakin in human cancers, although it is usually reported as downregulated. Increased desmoplakin is linked to β-catenin inhibition via upregulation of plakoglobin, although this is thought to be tissue specific. Downregulation was found to induce MAPK signalling, resulting in increased cell proliferation (Yang et al 2012). The role of desmoplakin in HCC is poorly documented, but the decreased expression observed during claudin-1 overexpression could indicate the involvement of MAPK signalling, a pathway commonly implicated in EMT induction.

Expression of EGFR is commonly upregulated in HCC, with its increased expression inducing proliferation and migration. EGFR is known to interact with C-X-C motif chemokine receptors and the MAPK pathway, promoting tumour progression (Huang et al 2014). The increase in expression of EGFR in claudin-1 silenced HepG2 cells could explain the increase in cell proliferation, and even possibly indicate the upregulation of EMT markers via the MAPK pathway (Wojciechowski et al 2017).

Nudix Hydrolase 13 (*NUDT13*) is a mitochondrial enzyme and microtubule-associated protein 1B (MAP1b) belonging to the microtubule-associated protein family. Both NUDT13

and MAP1b are aberrantly expressed in EMT, although their function in the process is unknown (Kanda et al 2016). An increase in MAP1b and a decrease in NUDT13 are associated with EMT induction and are described as novel EMT markers (Gröger et al 2012). The increased expression of both of these EMT markers in both claudin-1 overexpression and claudin-1 silenced HepG2 cells provides further evidence of the induction of EMT in these cells.

Moesin is a member of the EMR (Ezrin/Radixin/Moesin) family, which act as intermediate proteins between the plasma membrane and actin cytoskeleton. Moesin is localised and thus implicated in the filopodia in the leading edge of lamellipodia in migrating cells in normal pathology and cancer (Solinet et al 2013). In breast cancer, moesin expression correlates with invasive capacity and is directly targeted and repressed via miR-200b, an anti-EMT marker of epithelial cells (Li et al 2014). Moesin is documented to be highly expressed in HCC, with high levels of the protein correlating with poor relapse-free survival (Song et al 2016). The large increase in expression suggests a role of moesin in the increased migratory capacity seen during claudin-1 silencing in HepG2 cells.

Platelet-derived growth factor receptor B (PDGFRB) is a cell membrane embedded, tyrosine kinase receptor for platelet-derived growth factors. Binding to platelet-derived growth factors to their corresponding receptors induces cell proliferation. This mechanism is often exploited by cancer cells. PDGFRB is usually upregulated in mesenchymal stromal cells during wound healing and type 2 EMT but is also upregulated during type 3 EMT associated with cancer (Steller et al 2013). Platelet-derived growth factors as well as their receptors PDGF-R α and β are frequently upregulated in HCC as well as the autocrine secretion of PDGF. Autocrine and inflammation induced PDGF signalling upregulates non-canonical β-catenin signalling via the STAT3 pathway in HCC (Van Zijl et al 2009). The upregulation of platelet-derived growth factor receptor B in during claudin-1 overexpression in HepG2 cells

provides further evidence for EMT induction via non-canonical β-catenin signalling.

Versican is a large extracellular matrix proteoglycan that belongs to the lectican protein family. The increased expression of versican has been documented in a number of malignant human cancers such has breast, brain, prostate, ovary, and lung. In HCC, increased versican is regulated by EMT transcription factor FoxQ1 and the β-catenin/TCF4 complex (Xia et al 2014). Versican is involved in regulation of cell proliferation, metastasis, apoptosis, angiogenesis, and increasing the resistance to chemotherapy drugs. Versican contains a G3 domain that has two motifs similar to EGF and a G1 domain, both of which stimulate these cancer hallmarks via upregulation of the MAPK, and AKT signalling pathways (Du et al 2013). The upregulation of versican in claudin-1 overexpressing HepG2 cells correlates with the increase in cell migration and proliferation, implicating the proteoglycan in the process. The expression of versican also strengthens the argument that β-catenin regulates the process due to the association between Versican and the β-catenin/TCF4 complex.

4.1.3 The expression of caveolin-1 in claudin-1 overexpressing and silenced HepG2 cells.

Caveolin-1 (Cav-1) is the main structural component of caveolae and is known to be involved in vesicle transport, signal regulation and transduction. The expression of caveolin-1 is often dysregulated in a number of cancers with both increases, decreases, and mutations of the protein reported. However, the relationship between caveolin-1, tumour progression, and inhibition is multifaceted and appears to be cancer specific (Boscher & Nabi 2012).

Caveolin-1 is decreased in ovarian, lung, and mammary Carcinomas, whereas in bladder, oesophagus, thyroid, prostate, and pancreatic carcinomas it found to be is increased (Williams & Lisanti 2005). Caveolin-1 both positively and negatively regulates MAPK-ERK1/2, PTEN-AKT, and β-catenin-TCF/LEF signal transduction pathways, thereby initiating and

inhibiting EMT, and Rac1 mediated cell migration (Boscher, Nabi 2012).

The expression of caveolin-1 is commonly increased in HCC with its expression correlating with metastasis and a poor prognosis (Zhang et al 2009). Caveolin-1 expression was increased in both claudin-1 overexpressing and silenced HepG2 cells, especially during claudin-1 overexpression. The extent of the increase (40-fold) in claudin-1 overexpressing HepG2 cells indicates a significant involvement of the gene. A study by Yu et al (2014) demonstrated that overexpressing caveolin-1 in HepG2 cells increased β-catenin and ERK1/2 activation which presented with increased tumour size, migration, and proliferation via upregulation of EMT genes. It is therefore of interest that overexpression of claudin-1 caused a massive increase in caveolin-1 in our experiments, with an accompanying increase in associated EMT and tumour metastases genes.

A study comparing caveolin-1 expression in HCC cell lines has reported an increase in caveolin-1 expression inversely correlating with the differentiation and invasive nature of the cell line. HepG2 cells with a normally low caveolin-1 expression were described as well differentiated, whereas SNU-449 with a high caveolin-1 expression was very poorly differentiated (Cokakli et al 2009). What is also interesting is that SNU-449 cells have a significantly higher claudin-1 level than HepG2 cells, and express high levels of EMT markers such as vimentin, activated ERK1/2 and β-catenin (Suh et al 2013). Disruption of caveolin-1 containing caveolae using a cholesterol-depleting agent methyl-β-cyclodextrin (MBCD), significantly decreased mobility in SNU-449 cells by up to 10-fold (Cokakli et al 2009).

Claudin-1 demonstrates inclination to co-localise and co-precipitate, with caveolin-1 outlining the binding capacity of the two proteins (Itallie & Anderson 2012). Other studies have shown caveolin-1 to be involved in caveolae-mediated internalization of claudins and occludins in tight junction remodelling and during routine tight junction maintenance via continuous endocytic recycling of tight junction proteins (Stamatovic et al 2009) (Chalmers &

Whitley 2012). It is clear from our images that claudin-1 is internalised during overexpression, possibly by caveolin-1 containing caveolae. Internalisation of membrane bound proteins such as EGFR, by caveolin-1 containing caveolae, also results in the simultaneous co-internalisation of β-catenin/E-cadherin, this process activates the β-catenin-TCF/LEF signal transduction pathways resulting in EMT (Croager 2004). Caveolin-1 and a number of β-catenin-TCF/LEF and EMT associated genes were significantly up regulated during claudin-1 overexpression in HepG2 cells. Although further research is needed, it could be possible that internalisation and endocytic recycling of claudin-1 by caveolin-1 containing caveolae could participate in WNT/β-catenin and MAPK signalling, resulting in the EMT phenotype that was observed.

4.1.4 The expression of β-catenin and associated genes in claudin-1 overexpressing and silenced HepG2 cells.

The WNT/β-catenin pathway is involved in a number of normal and pathophysiological cellular processes. β-catenin maintains and stabilises junctional complexes and coordinates gene transcription when stabilised by canonical WNT signalling. β-catenin is implicated in the causation and progression of a number of human cancers such as breast, colon, ovarian, and melanoma (Rosenbluh et al 2014). Dysregulated canonical WNT/ β-catenin signalling is common in HCC, with reports of aberrant expression in up to 90% of cases. It is interesting that only approximately 40% of cases present with β-catenin or AXIN1/AXIN2 mutation, meaning in the remainder of the cases canonical WNT signalling is modulated by other pathways or external signals (Waisberg et al 2015). Stable β-catenin expression in HepG2 cells is present, but at relatively low levels. Both claudin-1 overexpression and silencing increases β-catenin mRNA and protein levels in HepG2 cells. Stable β-catenin is known to induce EMT and proliferation in HCC via the regulation of β-catenin associated transcription

factors. Once stabilised, cytosolic β-catenin is translocated to the nucleus, facilitated by Rac1, where it binds to TCF (T-cell factor)/LEF (lymphoid enhancer factor). The binding of β-catenin to TCF/LEF transcription factors displaces transcriptional repressors and recruits co activators to WNT gene target regions. The TCF/LEF family of transcription factors in humans consists of TCF1, LEF1 (TCF2), TCF3, and TCF4 (Kim et al 2013).

TCF1 was upregulated in both claudin-1 overexpressing and silenced HepG2 cells. Historically, TCF1, in association with β-catenin, has generally been linked with increased cell proliferation and differentiation via upregulation of WNT target genes (Giles et al 2003) However, TCF1 also has a tumour suppressing function in some cancers. Upregulation of TCF1 in leukaemia and colon cancer has correlated with an increased survival rate (Staal, Clevers 2012). With little data of regarding the role of TCF1 in HCC, it is difficult to speculate whether the increased expression of TCF1 is promoting tumour progression or inhibiting it.

LEF1 expression was upregulated during claudin-1 overexpression and slightly downregulated during claudin-1 silencing, although the change in expression in silenced cells was not significant. Like TCF1, LEF1 is another classic inducer of WNT target genes. It is commonly upregulated in HCC and shown to increase proliferation via upregulation of cyclinD1 (Liu et al 2016). Overexpression of LEF1 in MDCK cells induced epithelial to mesenchymal transition via SLUG, ZEB1, and ZEB2 (Kobayashi, Ozawa 2013) with the same process described in prostate cancer (Liang et al 2015). This evidence suggests that the increased expression of LEF1 during claudin-1 overexpression participates in the upregulation of EMT markers and associated transcription factors SLUG, ZEB1, and ZEB2. As no significant change in LEF1 was reported in claudin-1 was reported, it is unlikely LEF1 is responsible for the increase in EMT markers observed in these cells.

TCF3, otherwise known as TCF7L1, E47, or E2A, was previously reported to be dysregulated in a number of human cancers such as breast, colon, and HCC, correlating to

a poor prognosis (Berx et al 2007). TCF3 has the same basic helix-loop-helix structure as TWIST1 and demonstrates involvement in EMT activation and downregulation of E-cadherin through binding to E-boxes of the promoter E-pal and E3 (Voutsadakis 2016). Univariate Cox analysis of 128 HCC samples revealed that TCF3 was commonly upregulated in the disease and correlates with other EMT markers and a poor prognosis (Kim et al 2010). The increased expression of TCF3 in both claudin-1 overexpressing and silenced HepG2 cells indicates its likely participation in the upregulation of EMT target genes and the decreased expression of E-cadherin.

TCF4 otherwise known as TCF7L2 or E2-2, is commonly dysregulated in colon and breast cancers with its levels showing association with invasiveness in both diseases (Ravindranath et al 2011). Just like TCF3, TCF4 is a well-known inducer of EMT by directly binding to the ZEB1 promoter and activating its transcription (Sanchez-Tillo et al 2011). TCF4 also shows inclination for binding TWIST1, thereby upregulating EMT genes (Chang et al 2015). Upregulation of TCF4 in HCC results in increased expression of HIF-2α, EGFR, c-MYC and cyclinD1, thereby promoting cellular proliferation, angiogenesis, and increasing the resistance to anti-cancer drugs (Liu et al 2016). TCF4 was significantly upregulated in claudin-1 overexpressing HepG2 cells, increasing the likelihood of its participation in EMT induction. The increase in expression of TCF4 in claudin-1 silenced HepG2 cells was found not to be significant, thereby reducing the probability of its involvement in the upregulation of EMT makers observed.

Associated β-catenin target genes α-catenin, Frizzled-7 and RAC1 participate in the facilitation and modulation of the response to WNT/β-catenin signalling in HCC. Their expression appears to determine the outcome of β-catenin signalling in the disease. With its ability to bind to the E-cadherin/β-catenin complex at the membrane, α-catenin though F-actin binding, provides a scaffold between extracellular cadherins and intracellular

cytoskeleton (Drees et al 2005). Intracellular pools of α-catenin which are not associated with the E-cadherin/β-catenin complex at the membrane limit the actin polymerisation function of Arp2/3 and therefore decrease lamellipodial dynamics. α-catenin overexpression was found to inhibit the β-catenin/TCF response, indicating its role as a negative regulator in the WNT/β-catenin pathway (Daugherty et al 2014). In cancer, loss of α-catenin corresponds with increased cell proliferation and TCF-dependent transcription (Giannini et al 2000). Kaplan-Meier examination of patient survival suggested cases of HCC with decreased α-catenin and E-cadherin, and increased levels of β-catenin, had poor survival rates (Endo et al 2000). The decreased expression of α-catenin in claudin-1 overexpressing HepG2 cells correlates with the increased β-catenin/TCF associated gene expression and likely aids in the tumour progression of these cells. Low α-catenin levels would allow increased actin polymerisation associated with increased migration, and upregulation of TCF dependent transcription of EMT associated genes observed. The increased expression of α-catenin in claudin-1 silenced HepG2 cells correlates with the decreased β-catenin/TCF associated gene expression and may act as an inhibitor in this regard. It would also inhibit actin polymerisation, possibly explaining the difference in migratory capacity between claudin-1 overexpressed and claudin-1 silenced HepG2 cells.

Frizzled-7 is a transmembrane receptor involved in the canonical WNT signalling pathway. Binding of WNT signalling molecules to frizzled stabilises β-catenin by preventing its phosphorylation and targeted degradation. Frizzled-7 is commonly upregulated in colon, oesophageal, lung, and gastric cancer, as well as melanoma and lymphoblastic leukaemia (Ueno et al 2008). Frizzled-7 is also frequently upregulated in HCC, with functional studies providing evidence that increased Frizzled-7 mRNA increases cell migration via β-catenin mediated mechanism (Merle et al 2004). The increased expression of Frizzled-7 in claudin-1 overexpressing cells likely modulates and increases the stability of β-catenin promoting the

upregulation of TCF/LEF mediated transcription of EMT and cell proliferative genes. Claudin-1 silenced HepG2 cells also presented with increased Frizzled-7 providing a possible explanation for the increased β-catenin, although the complex interplay between α-Catenin, Rac1, and other β-catenin associated genes may mean that the stabilised β-catenin may not participate in tumour progression in these cells.

Rac1 is part of the RhoGTPase family that regulates the cellular machinery responsible for cytoskeleton formation and disassembly. Rac1 is involved in numerus processes regulating growth, cell migration, and apoptosis (Bid et al 2013). In cancer, evidence suggests Rac1 participates in the transformation necessary for invasion and metastasis. Reports suggest that levels of Rac1 are increased in high clinical stage HCC and have a strong association with vascular invasion (Yang et al 2010). Rac1 is a critical component of the WNT/β-catenin signalling pathway, especially as Rac1, in association with JNK kinase, phosphorylates β-catenin on critical residues. This promotes nuclear import and subsequent binding to TCF/LEF1 transcription factors (Wu et al 2008) and suggests that the upregulation of Rac1 seen in claudin-1 overexpressing HepG2 cells would promote mesenchymal-like migration though actin polymerisation, as well as supporting the nuclear transport of β-catenin. The decrease in Rac1 expression observed during claudin-1 silencing would suggest a decrease in nuclear transport of β-catenin, providing further evidence of the lack of β-catenin involvement in claudin-1 silenced cells.

In humans, there are 19 secreted WNT glycoproteins involved in canonical and non-canonical WNT signalling. They bind to several receptors, including frizzled family receptors, activating numerus downstream signal transduction pathways (Asem et al 2016). The role of non-canonical ligands, WNT5a and WNT5b, is complex in cancer and often circumstantial and tissue specific. Furthermore, the conditions for which WNT5a and 5b become oncogenic or tumour suppressive are poorly understood. Conflicting evidence exists about the specific

role of WNT5a and b in HCC. WNT5a acts in a tumour suppressive role in some thyroid and colorectal cancers, however, appears to promote cancer progression in pancreatic and gastric cancers, as well as melanoma (Asem et al 2016). In vitro experimental evidence suggests that overexpression of WNT5a in huh7 cells decreases cellular migration and proliferation by targeting non-canonical β-catenin signalling (Bi et al 2014). Further evidence of WNT5a as a tumour suppressor was documented by Geng et al (2012), suggesting that WNT5a was frequently decreased in HCC and led to an improved prognosis. In conflict to this, Yuzugullu et al (2009) reported that WNT5a and WNT5b were overexpressed in the majority of poorly differentiated HCC cell lines but were under expressed in well-differentiated cell lines. This gives more weight to other reports that WNT5a and b, along with their cognate receptor Fzd2, are frequently upregulated in late stage HCC as well as breast, lung, and colon cancers. The same report linked the expression of WNT5a and b with mesenchymal markers and inverse correlation of epithelia markers in breast, colon, liver, and lung cancer samples (Gujral et al 2014). It appears that WNT5a associates with EMT in poorly differentiated cancers promoting tumour progression but is inhibitory to well-differentiated cancers. The high expression of WNT5a and b in claudin-1 overexpressing cells, does not seem to inhibit its migratory capacity. Therefore, it likely that WNT5a and b further the initiation of the EMT phenotype observed in these cells, suggesting that claudin-1 overexpression mimics gene expression profile of poorly differentiated HCCs. The decreased expression of WNT5a in claudin-1 silenced cells suggests that the EMT markers produced as a result of claudin-1 silencing are likely not a result of canonical WNT signalling. It is interesting to note that the literature speculates that WNT5a and b decrease non-canonical β-catenin signalling in HCC, although the expression of β-catenin and associated transcription factors are increased in claudin-1 overexpressing HepG2 cells. It is possible that the induction of EMT may change the inhibitory/tumour suppressive response of WNT5a/b,

protecting non-canonical β-catenin signalling.

WNT11 is a secreted WNT glycoprotein involved in the canonical WNT signalling pathway. Just like WNT5a and b, its role in cancer progression is complex and cell specific. Reports indicate WNT11 is commonly upregulated in late stage colorectal cancer, its increased expression is associated with recurrence and a poor prognosis in the disease. In vitro experiments on colorectal cancer cell lines have shown the forced expression of WNT11 increases proliferation and migration via JNK signalling (Nishioka et al 2013). However, WNT11 mRNA and protein is significantly lower in HCC in comparison with normal liver tissue. An increase in WNT11 expression in HCC inhibits tumour progression via the induction of PKC signalling, that targets β-catenin for degradation, and reducing TCF/LEF1 mediated transcriptional activity. WNT11 was reported to upregulate ROCK activation in HCC, reducing migration and nuclear β-catenin translocation by suppressing Rac1 (Toyama et al 2010). The large decrease of WNT11 in claudin-1 overexpressing HepG2 cells concurs with these findings. β-catenin and associated TCF activity, along with Rac1 and associated cell migration, were all increased in these cells indicating no inhibition by WNT11. The decrease in WNT11 in claudin-1 silenced HepG2 cells was found not to be significant. Although, it is difficult to make firm conclusions without the protein expression, stable WNT11 levels may explain the lower levels of Rac1, β-catenin, and associated TCF activity in these cells.

4.1.5 The expression of tumour metastasis genes in claudin-1 overexpressing and silenced HepG2 cells.

Cancer progression and metastasis is reliant on tumour microenvironment modification orchestrated by matrix metalloproteinases (MMPs). In HCC, MMPs 2 and 9 in particular correlate with recurrence after resection and ultimately a poor prognosis. They are also

upregulated in breast, ovarian, and prostate cancers, as well as melanoma (Zhang et al 2006). MMPs -2 and -9 are both type IV collagenases with respective gelatinase A and B activity. MMPs -2 and -9 are vital for invasion and metastasis during tumour progression, as type IV collagen and gelatine are the two main components of the ECM and basement membrane (Roomi et al 2009). MMPs -2 and -9 in conjunction with CD44 have also shown the ability to activate latent TGF-β, inducting EMT and further upregulating MMPs -2 and -9 in a positive feedback mechanism, promoting tumour progression and angiogenesis (Yu, Stamenkovic 2000). Membrane bound insulin-like growth factor (IGF) can be released by MMP -2 and -9 from the binding proteins in which it is contained, thereby increasing the bioavailability of the growth factor, inducing downstream PI3K/*AKT* signalling and promoting proliferation and anti-apoptotic effects (Nakamura et al 2005).

In both claudin-1 overexpressing and silenced HepG2 cells, MMP-2 represented the largest increase of all the matrix metalloproteinases. The expression of MMP-9 was also overexpressed in these cells. The documented evidence in the literature clearly implements MMP-2 and -9 in cancer progression, thereby outlining more evidence that aberrant claudin-1 levels modulate tumour progression in HCC.

MMP-3 and -7, along with -10 and -11, are known as stromelysins and are capable of degrading a broad range of ECM substrates including a number of collagens, proteoglycans, laminin, fibronectin, and gelatines. However, they are unable to degrade triple-helical fibrillar collagens (Kousidou et al 2004). The upregulation of stromelysins, particularly MMP-3 and MMP-7, are associated with poor prognosis in a number of human cancers. They are reported to increase the bioavailability of insulin-like growth factor by degrading the associated binding proteins in a similar way to MMP-2 and -9 (Nakamura et al 2005). MMP-3 and MMP-7 also have the ability to increase the bioavailability of EGFR ligands by degrading the membrane bound heparin, thereby releasing bound EGF, TGF-α and amphiregulin (Gialeli et al 2011).

Binding of EGF ligands to EGFR can significantly increase cancer progression by inducing EMT and number of cancer hallmarks (Gialeli et al 2009). The transmembrane death receptor ligand FAS is also targeted by MMP-7 and -10. Proteolytic cleavage of FAS increases anti-apoptosis signals and chemoresistance in cancer cells, promoting cells survival and tumour progression (Mitsiades et al 2001). MMP-3 and MMP-7 can also target E-cadherin for proteolytic cleavage, producing a bioactive fragment capable of inducing and maintaining EMT, even if the MMPs are later downregulated (Radisky et al 2010). The shedding of E-cadherin by these MMPs has also shown to encourage β-catenin translocation to the nucleus, thereby inducing EMT and cell proliferation (Gialeli et al 2011). Taken together, the evidence surrounding MMP-3 and -7 suggests that they not only are produced in invasive cancers but are able to initiate an invasive phenotype and promote tumour progression.

The expression of MMP-3 and -7 were increased in claudin-1 silenced HepG2 cells, but decreased during claudin-1 overexpression. This implies that the expression of these MMPs in claudin-1 silenced cells might be modulated by a different mechanism. Classically, the upregulation of MMP-2, -9 and -13 are overexpressed in a conserved EMT related mechanism (Gialeli et al 2011). This provides further evidence that both cell types are expressing EMT-like phenotypes.

Tissue inhibitors of metalloproteinases (TIMPs) are a highly conserved family of protease inhibitors. The primary function of the four members TIMP-1, -2, -3 and 4 is to prevent degradation of the ECM via inhibition of matrix metalloproteinases. All MMPs can be inhibited by TIMPS, but the effectiveness of the inhibition depends on the TIMP family member. TIMP-1 predominantly inhibits MMP-1, -3, -7 and -9, whereas TIMP-2 is strongly associated with MMP-2. TIMP-3 shows preferential MMP-2 and -9 inhibition, while TIMP-4 inhibits MT1-MMP and MMP-2.

Tumour progression relies on an imbalance in the stoichiometry of the MMP/TIMP

equilibrium which enables initial invasion and subsequent metastasis. Emerging evidence suggests that TIMPS have a greater role in modulating the hallmarks of cancer that previously thought, which is much more complex than simply inhibiting MMPs (Bourboulia et al 2010). TIMP-1 demonstrates interaction with membrane bound CD63, which regulates cell survival and polarity via the CD63/B1 integrin signalling complex, thereby promoting cancer progression (Jung et al 2006). Reports have suggested that TIMP-1 may play an oncogenic role in HCC, with an increase in expression reported to correspond with apparent tumour stage, and ultimately patient prognosis (Song et al 2015). However, contrary reports state that an overexpression of TIMP-1 inhibits MMP-2 activation, with the result being a reduced metastatic potential in HepG2 cells (Wang et al 2012).

TIMP-2 interacts with the $\alpha_3\beta_1$ integrin complex, and in doing so inhibits the response of VEGF-A and FGF stimulated cell proliferation, thereby decreasing tumour progression. It can also induce G_1 cell cycle arrest via the upregulation of cyclin-dependent kinase inhibitor $p27^{KIP1}$ (Brew & Nagase 2010). In HCC, a decreased TIMP-2 expression is associated with increased tumour grade, metastatic potential and a poor survival rate (Giannelli et al 2002).

TIMP-3 induces apoptosis in a number of human cancers by stabilising the death receptors FAS, TNF-R1, and TRAIL. The pro-apoptotic effects of TIMP-3 reduce tumour progression in vitro and vivo (Ahonen et al 2003). Evidence also suggests TIMP-3 binds to VEGF and angiotensin II receptors, thereby blocking the angiogenic effects of their respective ligands on endothelial cells (Brew & Nagase 2010). The expression of TIMP-3 in HCC is frequently downregulated and associated with reduced tumour differentiation and increased metastatic potential. The transcriptional promotor of TIMP-3 was found to be hypermethylated in number of cases of HCC, which may account for its downregulation. In vitro overexpression of TIMP-3 in HCC cell lines induced apoptosis and suppressed proliferation, migration, and invasion (Zeng et al 2016).

TIMP-4 is the most recently discovered MMP inhibitor, with limited discussion of its role available in the literature. The expression of TIMP-4 in cancer is very much cell and circumstance specific, its expression appears to be increased in well differentiated and decreased in poorly differentiated Gliomas, breast, and prostate cancers. The decreased expression of TIMP-4 in these cancers has a relationship with their progression. TIMP-4 is known to inhibit MMP-2 and -9, and the decreased expression of TIMP-4 would consequently increase the proteolytic activity of these MMPs, and advance metastasis. The transcriptional promotor of TIMP-4 was found to be hypermethylated in a number of human cancers, reducing its expression in a similar way to TIMP-3 (Melendez-Zajgla et al 2008).

The expression of TIMP family members was significantly reduced in claudin-1 overexpressing and silenced HepG2 cells. The evidence reported in the literature indicates that the decreased expression of TIMPS is linked to cell survival, increased invasion, and angiogenesis in cancer. The general trend of decreased TIMP expression, coupled with the increase in MMP expression in both claudin-1 overexpressing and silenced HepG2 cells, provides evidence that aberrant levels of claudin-1 significantly enhances the metastatic potential of these cells.

Cathepsins are another proteolytic family, consisting of lysosomal proteinases and endopeptidases which are found to be commonly overexpressed in human cancers. In normal human physiology cathepsin K regulates bone remodelling in osteoporosis, but its role as a secreted cysteine protease has demonstrated its ability to degrade ECM components in several cancers, thereby promoting invasion and metastasis (Saftig et al 1998) (Gong-Jun et al 2013). Although the expression of cathepsin K is yet to be documented in HCC, the effect of overexpression on proteolytic ECM remodelling appears to be constant regardless of cancer type. The increased expression of cathepsin K in claudin-1 overexpression HepG2 cells infers an increased invasive capacity. *In vivo* cathepsin K could

promote tumour progression by degrading ECM components in a similar way documented in squamous cell carcinomas and many other cancers (Gong-Jun et al 2013).

Many cathepsins, including cathepsin L are activated by acidic conditions found in intracellular lysosomes. Increased anaerobic glycolysis in cancer cells lowers the pH, allowing inappropriate activation of cathepsins which promote extralysomal and extracellular activity. In this way, cathepsin L is able to degrade ECM components and specific nuclear transcription factors associated with cell cycle arrest (Morin et al 2008) (Gong-Jun et al 2013). Cathepsin L overexpression has been associated with increased tumour progression in a number of human cancers including HCC (Tumminello et al 1996) (Gong-Jun et al 2013). Knockdown of cathepsin L in experimental models appears to decrease cell proliferation and invasion of cancerous tumours (Gocheva et al 2006). Cathepsin L was found to be overexpressed in both HCC and liver cirrhosis, correlating with malignant lesions and associated poor prognosis. The increased expression of cathepsin L seen in claudin-1 overexpressing cells, in conjunction with existing evidence in the literature, suggests it could be responsible for promoting a more invasive phenotype.

CXCL12, otherwise known as stromal-derived factor 1, and its receptor CXCR4, are part of the C-X-C subfamily of chemokines. In normal physiology and embryonic development, they are involved in haematopoiesis, activation of leukocytes, and can cause strong chemotactic migration of embryonic and immune cells. In cancer, the CXCL12-CXCR4 axis is exploited in an auto/paracrine manner, driving angiogenesis, cellular migration/proliferation, and immune infiltration with associated upregulation of inflammatory cytokines (Ghanem et al 2014). In HCC, CXCL12 binding can induce EMT via upregulation of AKT, MAPK, and JNK/SAPK pathways, promoting cell proliferation and migration (Li et al 2014). CXCL12 is also found to induce angiogenesis under hypoxic conditions, both independently and in conjunction with VEGF in HCC. In vivo, the CXCL12-CXCR4 axis

recruits leukocytes and other immune cells, creating an inflammatory environment which contributes to tumour progression (Ghanem et al 2014). These findings correlate with the fact that patients with increased CXCL12-CXCR4 mRNA levels present with lower disease-free survival rates (Semaan et al 2016). Taken together, the increase in CXCL12-CXCR4 in claudin-1 overexpressing cells indicates a more invasive tumorigenic phenotype. It isn't clear if the increase in CXCL12-CXCR4 is in response to EMT, or aids in its initiation, either way it presents a clear indication of tumour progression in these cells. Interestingly, this axis is not overexpressed in claudin-1 silenced cells, suggesting differences in the underlying mechanism which promote the invasive phenotype observed.

Dysadherin (FXYD5) is a cell membrane associated glycoprotein and part of the FXYD family. Dysadherin is commonly overexpressed in several cancers such as breast, colon, HCC, pancreatic, stomach, and melanoma. The overexpression of dysadherin in these cancers all resulted in a poor prognosis and increased tumour progression (Mannan et al 2016). The mechanism in which dysadherin affects tumour progression is unknown, but its expression appears to correlate with EMT and cancer stem cell markers in some cancers (Raman et al 2015). In vivo experiments involving intrasplenic injection of dysadherin cDNA into HCC cells resulted in a decrease in E-cadherin, decreased cellular adhesion and formation of intrahepatic metastases (Ino et al 2002). Other experimental evidence has shown dysadherins have the ability to post-transnationally regulate E-cadherin, by preventing attachment of E-cadherin to the cytoskeleton via α-Catenin (Nam et al 2007). Dysadherin was overexpressed in both claudin-1 overexpressing and in claudin-1 silenced HepG2 cells. The overexpression of dysadherin in cancer and its links to EMT correlate with our findings during our experiments. It is therefore possible that dysadherin could aid in inducing the increased migratory capacity seen in both cell types.

KISS1 (Kisspeptin) and its G-coupled protein receptor KISS1R (GPR54) form a peptide hormone complex that acts as a metastasis suppressor in a number of cancers. KISS1/KISSR is found to be downregulated in bladder, colon, oesophageal, thyroid, and ovarian cancers, all of which present with a worse prognosis as a result (Makri et al 2008). Although the exact mechanism by which it suppresses metastatic activity is unknown. In HCC the downregulation of KISS1/KISS1R correlates with increased MMP-9, intrahepatic metastatic lesions, and a significantly poorer prognosis (Shengbing et al 2009). Yan et al (2001) proposed that high KISS1 levels reduce the binding of NF-kB p50/p65 to the MMP-9 promoter thereby reducing the expression of MMP-9, and subsequently reducing metastasis and invasion. The decreased expression of KISS1 and KISS1R correlates with both increased MMP-9 and migratory capacity in claudin-1 overexpressing and in claudin-1 silenced HepG2 cells. It is possible the decreased expression of KISS1/KISS1R aides in the tumour progressive capacity of these cells.

TRAIL, otherwise known as TNF-related apoptosis-inducing ligand is a protein-based ligand capable of binding to death receptors DR4 (TRAIL-RI) and DR5 (TRAIL-RII) and inducing caspase 8 dependent apoptosis. TRAIL demonstrates capacity to induce apoptosis in cancerous cells but not in normal tissue, providing a promising clinical avenue for treating the disease (Piras-Straub et al 2015). The expression of TRAIL in HCC was found to be significantly downregulated in comparison to surrounding non-cancerous liver tissue. The decreased expression of TRAIL in the disease is linked to increased tumour size and stage, with increased recurrence and ultimately a poor prognosis (Piras-Straub et al 2015). The decrease in expression of TRAIL in claudin-1 overexpressing cells correlates with the literature and suggests that these cells have an increased resistance to apoptosis. It also suggests that TRAIL based chemotherapy might provide a promising treatment option for this invasive subtype of HCC.

MTSS1 is known as Metastasis suppressor 1 (Missing in Metastasis), which is exactly what it is. Many cancers such as bladder, colon, and HCC contain low levels of the protein during metastasis. MTSS1 promotes disassembly of actin fibres at lamellipodia thereby preventing cell migration. The downregulation of MTSS1 is linked with the increase of miR-182 in HCC, resulting in shorter disease-free survival and a poor prognosis (Wang et al 2012). Claudin-1 silenced HepG2 cells presented with downregulated MTSS1 and upregulated miR-182 suggesting the underlying mechanism for this modulation of expression is altered in these cells thereby increasing the metastatic potential. It is also important to note that MTSS1 was reported to be downregulated in K19-possitve HCC, providing further evidence of invasive phenotype acquisition during claudin-1 silencing (Govaere et al 2014).

4.1.6 The expression of stem cell markers and markers associated with a hybrid EMT phenotype in claudin-1 overexpressing and silenced HepG2 cells.

Current clinical practice in oncology attempts to group cancers, not only by stage and grade but by the molecular markers expressed by the cells (Sharma 2009). In cases of HCC, the expression of NOTCH/JAGGED, CD44 and the cytokeratin profile have been strongly associated with a poor prognosis and shorter disease free survival in patients (Yu et al 2015). It is no coincidence that these markers are associated with cancer stem cells particularly hepatic progenitor cells (Fan et al 2012). It was originally thought that the subgroups of HCC cases expressing these markers originated directly from these lineages, however it has been proven experimentally that cells can be oncogenically reprogrammed to confer stem cell properties identical to cancer stem cells (Scaffidi & Misteli 2011). Interestingly, NOTCH/JAGGED, CD44 and the cytokeratins have also been implicated among the hallmarks of the hybrid EMT phenotype, with suggestions that this process may contribute to the induction of the cancer stem cell phenotype (Jolly et al 2015).

The NOTCH/JAGGED signalling pathway is highly conserved amongst mammals and is involved in proliferation, cellular differentiation and embryogenesis. The role of NOTCH/JAGGED signalling in cancer is complex and often controversial. The effect of its activation or inhibition depends on cellular and tissue context (Yuan et al 2015). HCC has been reported to have both upregulated and downregulated NOTCH signalling producing different results. In vitro NOTCH/JAGGED overexpression in HCC cell lines produced cell cycle arrest via downregulation of cyclin A, D1, and E (Qi et al 2003). This correlates with reports that suggest NOTCH/JAGGED expression is linked to reduced β-catenin expression in HCC. It is thought that NOTCH/JAGGED signalling can modulate β-catenin expression, thereby reducing proliferation by reduction of β-catenin target cyclins (Wang et al 2009). However, NOTCH signalling has also been shown to increase proliferation and induce epithelial-mesenchymal transition in rat hepatic stellate cells and HCC cell lines, irrespective of β-catenin related mechanisms (Zhang et al 2015). Increased NOTCH/JAGGED signalling has demonstrated links to the upregulation of stem cell markers and associated phenotype in a number of cell types (Lu et al 2016). Hepatic progenitor stem cells and associated cancer stem cells are thought to be modulated by NOTCH signalling, both showing increased expression of NOTCH1 and JAGGED1 (Morell et al 2014). Experiments using mice hepatocytes reported increased NOTCH/JAGGED signalling in conjunction with AKT overexpression induced an invasive subset of cells with a stem-cell-like K19 positive phenotype, usually only seen in hepatic progenitor cells (Fan et al 2012).

CD44 is a cell surface glycoprotein and a hepatic stem cell marker associated with increased tumour growth and metastasis in HCC. CD44 acts as a signalling hub, collaborating with other cell surface receptors and G-coupled protein receptors such as CXCR4, RTK, and Frizzled, thereby activating MAPK, AKT and β-catenin/WNT related pathways, promoting tumour progression. The expression of CD44 was found to have a role

in initiating EMT in HCC and remained upregulated during the EMT process (Orian-Rousseau 2015). CD44 positive HCC groups are associated with very poor prognosis (Luo, Tan 2016).

Cytokeratin -7, -14, and -19 are members of the intermediate filament family and major constituents of the cytoskeleton. Epithelial cells produce a cell specific profile of cytokeratins that can often change during carcinogenesis. Expression of cytokeratins associated with specialised cells of the mesenchymal organs such as -7, -8, -14, -18, -19, and -20 are associated with more invasive carcinomas (Pastuszak et al 2015). In HCC, the cytokeratins -7, -14 and -19 are markers of hepatic progenitor stem cells, and their expression correlates with a higher rate of recurrence after resection, and an overall worse prognosis (Durnez et al 2006). Cytokeratin 19 expression interestingly correlates with the most invasive subtypes of HCCs. K19-positive HCCs present with increased migration and invasion with resistance to chemotherapy drugs such as doxorubicin, 5-fluoruracil and sorafenib (Govaere et al 2014). They also show significantly higher levels of hepatic progenitor stem cell associated genes such as CD44, CD133, NOTCH1, and JAGGED1 (Govaere et al 2014). In vitro and in vivo evidence has also shown an increase in EMT markers in K19-positive HCCs (Kim et al 2011). Vimentin and MMP2 are shown to be significantly increased in K19-positive HCC samples and experiments, but E-cadherin is not frequently decreased (Takano et al 2016). This data has proven that K19-positive HCCs do not always derive from hepatic progenitor stem cells but can be induced by EMT and even act to directly induce EMT, although its role in carcinogenesis still remains unclear (Kim et al 2011).

The increased migratory capacity coupled with the upregulation of CK19, CD44, NOTCH1/JAGGED1 as well as vimentin and MMP2 in claudin-1 silenced cells, correlating with the findings of K19-positive HCCs as reported in the literature. However, the K19-possitve phenotype observed in claudin-1 silenced cells is as a result of molecular reprogramming and not arising from hepatic progenitor stem cells. This provides further

evidence that cells not directly derived from stem cell lineages can gain properties associated with these cells. A possible explanation for the acquisition of these traits comes from the concept of hybrid EMT. The co-expression of epithelial markers (E-cadherin/cytokeratin) and mesenchymal markers (vimentin) observed in cells with a hybrid EMT phenotype are known to possess stem cell-like properties and produce associated markers such as CK19, CD44, NOTCH1/JAGGED1 (Jolly et al 2015). Claudin-1 silenced cells have been shown to co-express epithelial and mesenchymal as well as stemness markers CK19, CD44, NOTCH1/JAGGED1 suggesting they possess this hybrid EMT phenotype. Claudin-1 overexpressing cells however show large decreases in almost all epithelial markers and large increases in mesenchymal markers which suggests the classical and complete shift to the mesenchymal phenotype. It could be a result of this complete transition that the same increases in stemness markers are not seen in these cells. The differing types of EMT observed in the claudin-1 overexpressing and silenced cells could potentially affect the ways these cells behave. Cells displaying complete EMT tend to favour single cell migration and invasion, while hybrid EMT cells use NOTCH/JAGGED signalling to migrate as a group (Jolly et al 2015). This may well explain the increased migratory rate in claudin-1 overexpressing cells compared to silenced in our experiments. While collective migration is often slower than single cell migration it has multiple advantages. Cells that migrate collectively show increased resistance to apoptosis, are much better at surviving mechanical stresses and display an increased plasticity when switching from mesenchymal to an epithelial phenotype during colonisation (Revenu & Gilmour 2009). These advantages have been observed in the literature showing that while only 3% of tumours circulate as clusters, these groups contribute to 50% of the total successful metastases (Aceto et al 2014).

4.1.7 The expression of miRNAs in claudin-1 overexpressing and silenced HepG2 cells.

The molecular reprogramming and phenotypic changes associated with epithelial to mesenchymal transition are significantly influenced by miRNA regulation and expression during normal development and cancer. Evidence suggests that a number of miRNAs directly regulate EMT transcriptional regulators, and other associated mechanisms, including NOTCH and WNT signalling pathways. The dysregulation of miRNAs can provide valuable hallmarks in malignant transformation and offer an insight and prediction into the progression of the disease.

The miR-200 family, consisting of miR-200a, miR-200b, miR-200c, miR-141, and miR-429 are known as metastasis suppressors in cancer via their role in targeting ZEB1/2, thereby inhibiting EMT. ZEB1/2 can also repress the miR-200 primary transcript in a double negative feedback loop (Peng & Croce 2016). In this way, the decreased expression of miR-200 family members is directly associated with mesenchymal phenotype in a number of cancers, including HCC. In HCC, the downregulation of miR-200 family members leads to increased invasion and a poor prognosis, with increased ZEB1/2, TWIST, and vimentin expression (Yeh et al 2014). The expression of miR-200 family members, 200a, 200b, and 200c were all downregulated in both claudin-1 overexpressing and claudin-1 silenced HepG2 cells. This correlates with the literature and also with the expression of EMT markers ZEB2, TWIST, and vimentin in these cells, providing further evidence of the mesenchymal transition. Interestingly, the expression of miR-429 is downregulated in claudin-1 overexpressing cells but increased in claudin-1 silenced cells. The downregulation of miR-429 is frequently associated with a poor prognosis though targeting ZEB1 (Ye et al 2015), however, the miRNA was found to be upregulated in an invasive K19 positive sub-group of HCCs. This is consistent with our findings, the increased expression of miR-429, cytokeratin-19 and the

lower expression of ZEB1 correlates with the molecular profile of these K19 positive sub-groups (Govaere et al 2014).

The role of miR-9 in HCC is complex, with reports suggesting both increased and decreased expression in the disease. Regardless of the expression, the dysregulation of miR-9 is strongly associated with higher tumour staging, an increased risk of venous infiltration, and an overall shorter survival (Cai et al 2014) (Zhang et al 2015). Overexpressed miR-9 directly targets E-cadherin and facilitates the activation of β-catenin, therefore increasing cell motility and invasiveness by inducing EMT (Cai et al 2014). Decreased expression induces EMT via the IGF2BP1/AKT and MAPK axis, promoting increased expression of c-Myc, Ki-67, or PTEN, and therefore cell proliferation (Zhang et al 2015). Interestingly, the expression of miR-9 was significantly increased in claudin-1 overexpressing cells but decreased in claudin-1 silenced cells. Although both of these circumstances are documented to correlate with a poor prognosis, the role of miR-9 in HCC is poorly understood and requires further investigation to provide more accurate links to its association with claudin-1.

The miR-26 family, 26a and 26b, were found to inhibit the initiation of EMT in HCC by targeting USP9X and zeste homolog 2 (EZH2) (Shen et al 2014). The expression of these miRNAs are commonly downregulated in the disease, with their expression inversely correlating with tumour grade (Ma et al 2016). miR-26a and b were found to be downregulated in both claudin-1 overexpressing and claudin-1 silenced HepG2 cells. The decreased levels of these miRNA coincide with the expression of EMT markers E-cadherin and vimentin, and migratory capacity of the cells.

MiR-30 is described as an EMT inhibitor by targeting EIF5A2 in a number of cancers (Tian et al 2015). The decreased expression of miR-30 seen in HCC is associated with increased EIF5A2, chemoresistance and initiation of EMT (Huang et al 2016). The decreased expression of miR-30 in claudin-1 overexpressing and claudin-1 silenced HepG2 cells

provides further evidence of EMT initiation and ultimately a poor prognosis in vivo. MiR-34 is a powerful tumour suppressor and negative regulator of EMT in numerous cancers *(*Zhu et al 2015). Its role includes significant downregulation of WNT/β-catenin, NOTCH1 and EMT transcriptional regulators SNAIL and ZEB1, as well as downstream targeting of genes c-Myc, cyclinD1, and Bcl-2. SNAIL appears to regulate miR-34 during EMT by binding to its promotor and preventing transcription, providing evidence of a double-negative feedback loop (Siemens et al 2011). In vitro and vivo evidence has linked decreased expression of miR-34 with increased cell migration and invasion in HCC (Misso et al 2014). The decreased expression of miR-34 commonly seen in HCC (Dang et al 2013) and in our claudin-1 overexpressing and silenced HepG2 cells, correlates with increased migration and invasion, and ultimately a poor prognosis in vivo.

miR-135a was upregulated in claudin-1 silenced HepG2 cells, but not during overexpression. In HCC the expression of miR-135 is also frequency increased both in tissue and HCC cell lines, correlating with a poor prognosis. miR-135 overexpression activates AKT signalling, upregulates SNAIL and MMP2 transcription, and inhibits FOXO1 and MTSS1 tumour suppressors (Zeng et al 2016). The initiation of EMT by miR-135 is well documented in HCC tissues and likely participates in claudin-1 silenced cells.

miR-138 is an inhibitor of epithelial to mesenchymal transition, which is downregulated in up to 77% of HCCs (Wang et al 2012). miR-138 is able to bind directly to the mRNA of vimentin, ZEB2, and EZH2 which prevents translation of these genes post-transcriptionally and subsequently inhibits EMT. miR-138 was also found to target RhoC and ROCK2, preventing cell migration and invasion (Liu et al 2011). The observed downregulation of miR-138 in claudin-1 overexpressing cells in conjunction with this evidence, suggests that miR-138 is in part responsible for the increased migratory capacity and EMT markers observed in these cells.

The overexpression of claudin-1 in HepG2 cells resulted in the increased expression of miR-10a, 10b, 95, 328, 221, 494, and 18b, which have all been previously linked to increased tumour progression in HCC. miR-10a and b were reported to induce migration and invasion by modulating RhoC and MMPs -2 and -9 (Liao et al 2014). Increased expression of miR-95-3p and miR-328 promotes cell proliferation and cell migration in HCC by targeting p21 and PTPRJ respectively (Ye et al 2016) (Luo et al 2015). Overexpression of miR-221 in vivo and in vitro experiments on HCC cell lines previously demonstrated an increase proliferation and inhibit apoptosis, although the mechanism by which it does this is unknown (Rong et al 2013). miR-494 targets PTEN, causing an increase in proliferation, migration and invasion, while the increased expression of miR-18b relates to the grade of malignancy and a poor prognosis (Liu et al 2015) (Murakami et al 2013).

In claudin-1 silenced HepG2 cells, miR-27, 331, 487, 362, 18, 501, 135, 222, and 331 were also overexpressed, all of which are implicated in increased tumour progression in HCC. Increased expression of these miRNAs is associated with increased proliferation and metastasis in HCC (Li et al 2015; Chang et al 2014; Chang et al 2016; Shen et al 2015; Ruan et al 2015; Zhang et al 2015; Yang et al 2014). miR-487 in particular is found to increase the expression of vimentin, suggesting a link between the miRNA and EMT (Ma et al 2016).

MicroRNAs 339, 140, 320, 30b, 365, 636, 185, 29, 202, and 150 are described as tumour suppressors in HCC, all of which are down regulated in claudin-1 overexpressing HepG2 cells. The decreased expression of miR-339 corresponds with increased invasion in HCC tissue (Wang et al 2016). MiR-140, 150, and 636 have been demonstrated to target MAPK signalling in HCC, reducing proliferation and migratory capacity (Yang et al 2013; Sun et al 2016; Jang et al 2013). miR-320 and miR-30b both suppress cell migration in HCC by post-transcriptionally regulating GNAI1 and CD90 respectively (Yao et al 2012). Mir-30 has also been shown to inhibit EMT via suppression of the transcriptional regulator SNAIL (Zhang

et al 2012). MiR-365 inhibits cell cycle progression and is linked to induction of apoptosis by targeting cyclinD1 and Bcl-2 (Nie et al 2012). MiR-185 inhibits proliferation in HCC by targeting the PTEN/AKT pathway (Qadir et al 2014), whereas miR-29a and 202 suppress cell proliferation by post-transcriptionally downregulating SPARC and LRP6 respectively (Zhu et al 2012; Zhang et al 2014).

In claudin-1 silenced cells, MicroRNAs 335, 145, 28, 100, 374, 128a, 132, 9, 342-3p, 138, 324-5p, 181a, 34a, 744, 455-3p, 339-5p, 130a, 376c, and 148a are all down regulated and are considered tumour suppressors in HCC. Both miR-335 and 145 appear to suppress cell proliferation and migration in HCC by targeting ROCK1 (Liu et al 2015; Ding et al 2016). MicroRNAs 28, 100, 374, 128a, 132, and 9 all suppress the PTEN/AKT pathway in HCC inhibiting cell proliferation, migration, and invasion (Shi et al 2015; Zhou et al 2014; Zhen et al 2016; Huang et al 2015; Liu et al 2015). MiR-100 also targets Rac1, further inhibiting cell migration (Zhou et al 2014). MiR-342-3p targets IKK-γ, TAB2, and TAB3 components of the NF-κB signalling pathway resulting in reduced proliferation in HCC (Zhao et al 2015). The expression of miR-138 is frequently downregulated in HCC as it suppresses cell proliferation and invasion by targeting SOX9 (Liu et al 2016). Mir-324-5p was found to target SP1, MMP-2, and -9 in HCC, preventing ECM degradation and associated invasion (Cao et al 2015). This also coincides with our findings in claudin-1 silenced cells, as the expression of mir-324-5p inversely correlates with the expression of SP1, MMP2, and -9. miR-181a and 34a both target the tumour promoting tyrosine-protein kinase c-MET in HCC, suppressing motility, invasion, and branching-morphogenesis as a result (Korhan et al 2014; Dang et al 2013). miR-744 and 455-3p suppress cell proliferation, migration, and invasion in HCC by targeting c-Myc and Runx2 respectively (Lin et al 2014; Qin et al 2016). The decreased expression of miR-339-5p, 130a, 376c and 148a are all associated with a poor prognosis and poor survival rate in HCC (Wang et al 2016; Li et al 2014; Formosa et al 2014; Ajdarkosh et al 2015).

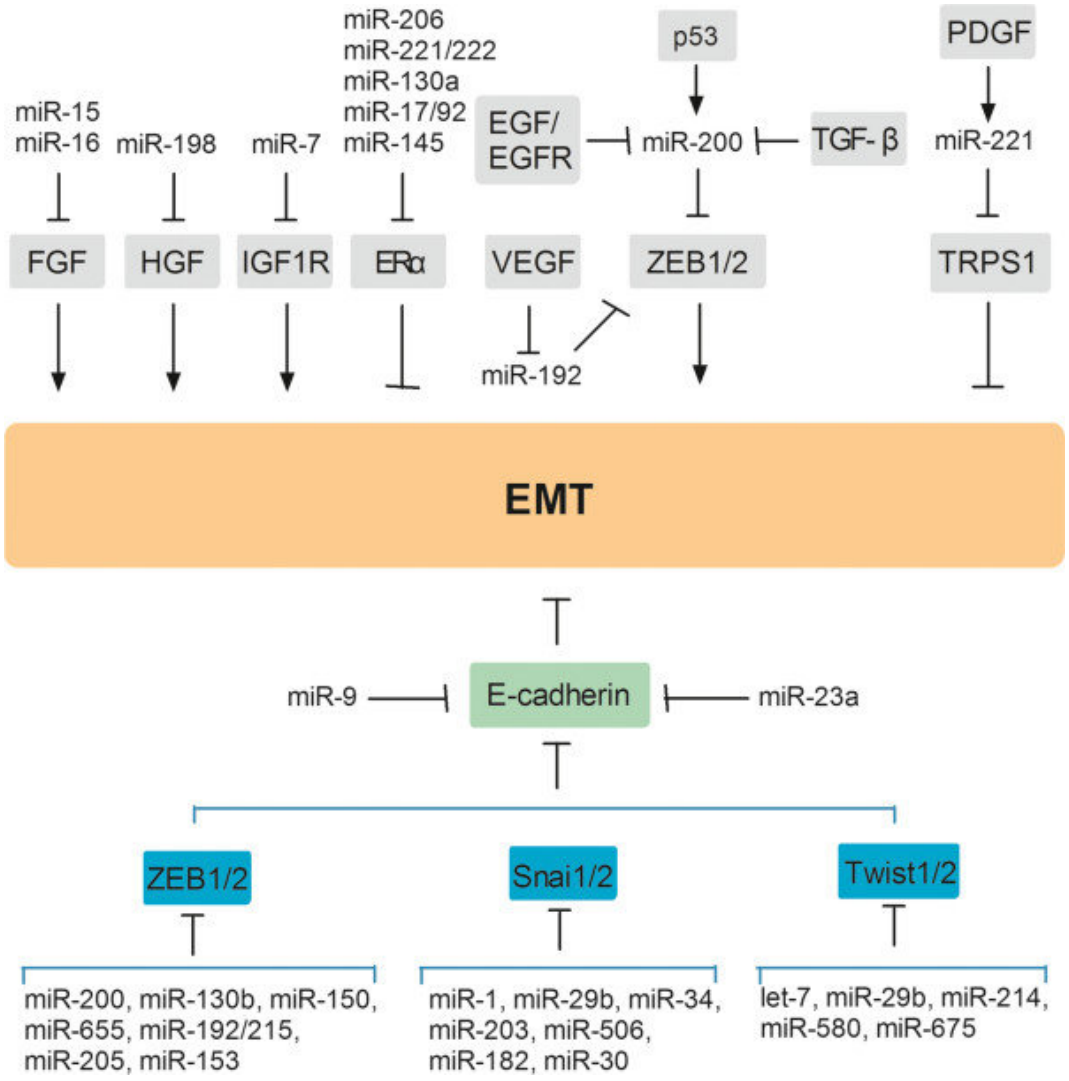

Figure 4.1: Regulation of EMT and associated signalling pathways by miRNAs. The figure outlines the influence of miRNAs on EMT via the targeting of ligands, receptors, signalling pathways and transcription factors. The expression of many of these miRNAs is altered during the overexpression and silencing of claudin-1 in HepG2 cells. Pointed lines represent activation and the blocked lines indicate inhibition.

4.2 Conclusions

Over the course of this project, our experiments have demonstrated that overexpressing claudin-1 produced cells that were significantly more migratory than both claudin-1 silenced, and wild type, HepG2 cells. Gene expression analysis revealed a substantial upregulation of mesenchymal and tumour metastasis genes such as vimentin, MMP -2, -9 and -13, as well

as EMT-TFs SNAIL, SLUG, TWIST, and ZEB1/2. A significant decrease of epithelial markers like E-cadherin, cytokeratin-7, -14, -19 and miR-200a, b, c, was also observed. Taken together the increase in mesenchymal markers with the decrease in epithelial makers provides strong evidence of the initiation of epithelial to mesenchymal transition in these cells.

Although our experiments were unable to identify the extract process by which claudin-1 drives this invasive phenotype, it is highly likely that it surrounds Wnt/β-catenin signalling. During claudin-1 overexpression, β-catenin and associated transcription factors LEF-1, TCF-3, and TCF-4 were significantly increased. It is well documented in the literature that β-catenin in conjunction with its associated transcription factors drive the EMT process by transcribing SNAIL, SLUG, TWIST, and ZEB1/2, as well as an array of tumour progressive genes.

The massive upregulation (~40 fold) of TCF-3 and -4 makes Wnt/β-catenin signalling the most likely contributor to the invasive phenotype observed during claudin-1 overexpression. However, it remains unclear how claudin-1 regulates Wnt/β-catenin signalling in these cells. Nevertheless, we theorise that caveolin-1 could provide the missing link between the claudin-1 and Wnt/β-catenin signalling. Overexpression of caveolin-1 in HepG2 cells is documented to cause increased β-catenin and ERK1/2 activation with associated increases in tumour size, migration, and proliferation via upregulation of EMT genes (Yu et al 2014). Based on this evidence, increased expression of caveolin-1 during claudin-1 overexpression may be driving the tumour progression of these cells by upregulating Wnt/β-catenin and associated EMT hallmarks.

The process by which claudin-1 silencing promotes tumour progression in HCC appears to be less straight forward. As with claudin-1 overexpression, claudin-1 silenced cells presented with a large increase in mesenchymal and tumour metastasis genes including vimentin, N-cadherin, Fibronectin, MMP -2, -9, and -13, as well as EMT-TFs, FOXC2, GSC, TWIST, and ZEB2. However, the expression of E-cadherin was not significantly decreased

and cytokeratin-7, -14, -19 were significantly increased. This co-expression of mesenchymal and epithelial markers can only be explained by the idea of hybrid EMT. This apparent contradictory notion is strengthened by the fact that these cells also present with an increase in hepatic stem cell markers CD44, CK19, NOTCH, and JAGGED, all hallmarks of this hybrid EMT phenotype.

Despite the slight observed increase in β-catenin, TCF-1 and -3, it is unlikely the invasive phenotype associated with claudin-1 knockdown is linked with Wnt/β-catenin signalling as a number of miRNAs expressed in these cells, along with NOTCH/JAGGED signalling, are known to inhibit this process. Although the underlying mechanisms involved during claudin-1 silencing requires more investigation, we propose that the AKT signalling pathway drives the progression of this phenotype.

Claudin-1 silenced cells show significantly reduced expression of miRNAs 28, 100, 374, 128a, 132, and 9 (Shi et al 2015; Zhou et al 2014; Zhen et al 2016; Huang et al 2015; Liu et al 2015). In HCC, these miRNAs suppress the PTEN/AKT pathway, therefore their downregulation in claudin-1 silenced cells would suggest an associated promotion of this pathway. Furthermore, the increased expression of JAM A in claudin-1 silenced cells has been linked with EMT induction via the PI3K/AKT pathway in other cancers (Tian et al 2015). The downregulation of afadin and nectin seen in claudin-1 silenced cells is also commonly regulated by AKT signalling in HCC and other cancers (Ma et al 2016). Most importantly, overexpression of AKT in mice hepatocytes resulted in an invasive subset of cells with a stem-cell-like K19 positive phenotype and increased NOTCH/JAGGED signalling, usually only seen in hepatic progenitor cells (Fan et al 2012). Although we have not definitively proven the involvement of AKT signalling in our claudin-1 silenced cells, our data in conjunction with the literature possibly implies that it is this signal transduction pathway that is driving the invasive phenotype observed.

We have successfully demonstrated that the aberrant expression of the tight junction constituent in claudin-1 overexpressing and silenced cells induces an invasive phenotype with increased migratory capacity that is consistent with the observational evidence published in the literature. Creating claudin-1 overexpressing and silenced HepG2 cells has allowed us to study the changes in gene expression and mechanisms in these cells that drive the observed increase in tumour progressive capacity. For the first time we have discovered that both an increased, and decreased, expression of claudin-1 in HCC induces hallmarks consistent with the initiation of epithelial to mesenchymal transition. We propose that it is this process that orchestrates the invasive capacity displayed in our experiments and in the literature. Interestingly, both claudin-1 overexpressing and silenced cells share a number of hallmarks that are associated with tumour progression, but the way in which they are initiated, and regulated, appears to be different. Our results indicate the claudin-1 overexpressing cells are regulated by Wnt/β-catenin signalling with involvement from caveolin-1. Whereas, our results indicate claudin-1 silence cells are regulated by AKT and NOTCH/JAGGED signalling.

4.3 Future investigation

The data generated from this thesis has revealed claudin-1 dysregulation as a potent inducer of invasive phenotype in HCC. However, future work must be focused around clarifying the mechanisms by which claudin-1 modulates these invasive malignancies, with the hope of exploring therapeutic avenues.

As previously mentioned, we propose that β-catenin and caveolin-1 co-operate to initiate EMT during claudin-1 overexpression in HepG2 cells. Functional siRNA mediated knockdown of β-catenin and/or caveolin-1 in these cells should determine their participation in initiating EMT. The tumour progressive nature of claudin-1 overexpressing HepG2 cells with silenced β-catenin and/or caveolin-1 would be investigated using migration assays and

RT-PCR to determine the migratory capacity and the expression profile of EMT genes. If silencing either of these genes indicates a tumour suppressive effect, immunocytochemistry might hopefully determine the extent of interactions between claudin-1, caveolin-1, and β-catenin. Once understood, these mechanisms could provide targets for therapeutic interventions, and possible avenues to suppressing the associated invasive phenotype. Data analysis of both claudin-1 overexpressing and silenced cells suggests the involvement and interaction of a number of signal transduction pathways. Claudin-1 overexpression seemed to be mediated by WNT/β-catenin and MAPK, whilst claudin-1 silenced cells appeared to have increased AKT signalling. However, as we did not investigate these signal transduction pathways directly, definitive conclusions cannot be drawn. Therefore, future investigation should focus around determining the level of expression and phosphorylation status/activation of these pathways, using western blotting techniques.

One of the limitations of siRNA gene silencing is that complete gene knockdown is not achievable. Which proposes the question, is the remaining level of claudin-1 involved in tumour progression, or is it inhibitory? Claudin-1 silencing induces a hybrid EMT profile, which can maintain clustered and group cell migration, and has been associated with a worse prognosis. It is possible that the low levels of claudin-1 could be supporting these weaker interactions, and mediating group cell migration, furthering disease progression. Further work exploring silencing of claudin-1 would be possible with the up and coming advent of technologies such as CRISPR/Cas9. The new techniques could allow us to study the effect of complete knockdown of claudin-1, and whether tumour progressive capacity would be increased or decreased if claudin-1 was completely absent in these cells. It would be interesting to see if the complete silencing of claudin-1 produces differing results from our current findings.

The data presented in this thesis has outlined just how important claudin-1 can be in

the initiation and progression of HCC. Further investigation will provide a greater understanding of its role in the disease, which will hopefully influence treatment options, and ultimately patient prognosis.

4.4 Summery

- Claudin-1 overexpression in HepG2 cells results in classical EMT initiation defined by a significant increase in expression of vimentin and EMT-TFs, with a significant decrease in expression of E-cadherin and cytokeratins.
- The EMT phenotype in claudin-1 overexpressing cells appears to be mediated by CAV1 and Wnt/β-catenin signalling
- Claudin-1 silenced HepG2 cells display a hybrid EMT phenotype with co-express of epithelial and mesenchymal markers.
- The hybrid EMT phenotype observed in claudin-1 silenced cells appears to be mediated by the AKT pathway with potential involvement from NOTCH/JAGGED signalling.
- Claudin-1 overexpressing and silenced HepG2 cells display invasive potential with increased migration, with increased expression of tumour metastasis genes and matrix metalloproteinases.
- Claudin-1 overexpressing and silenced HepG2 cells show distinct expression profiles of tight junctions and adhesion junctions which are thought to favour a migratory/invasive phenotype
- Claudin-1 overexpressing and silenced HepG2 cells shows a downregulation of tumour suppressive miRNAs and EMT suppressive miRNAs, with an increase in expression of miRNAs consistent with a poor prognosis in HCC.

Chapter 5: References

Abba, M. L., Patil, N., Leupold, J. H., and Allgayer, H (2016) 'MicroRNA Regulation of Epithelial to Mesenchymal Transition'*. Journal of Clinical Medicine* 5 (1), 8

Aceto, N., Bardia, A., Miyamoto, D. T., Donaldson, M. C., Wittner, B. S., Spencer, J. A., Yu, M., Pely, A., Engstrom, A., and Zhu, H (2014) 'Circulating Tumor Cell Clusters are Oligoclonal Precursors of Breast Cancer Metastasis'*. Cell* 158 (5), 1110-1122

Acharya, P., Beckel, J., Ruiz, W. G., Wang, E., Rojas, R., Birder, L., and Apodaca, G (2004) 'Distribution of the Tight Junction Proteins ZO-1, Occludin, and Claudin-4, -8, and -12 in Bladder Epithelium'*. American Journal of Physiology.Renal Physiology* 287 (2), F305-18

Ahonen, M., Poukkula, M., Baker, A. H., Kashiwagi, M., Nagase, H., Eriksson, J. E., and Kähäri, V. (2003) 'Tissue Inhibitor of Metalloproteinases-3 Induces Apoptosis in Melanoma Cells by Stabilization of Death Receptors'. *Oncogene,* 22 (14), 2121-2134

Aigner, K., Dampier, B., Descovich, L., Mikula, M., Sultan, A., Schreiber, M., Mikulits, W., Brabletz, T., Strand, D., Obrist, P., Sommergruber, W., Schweifer, N., Wernitznig, A., Beug, H., Foisner, R., and Eger, A. (2007) 'The Transcription Factor ZEB1 (deltaEF1) Promotes Tumour Cell Dedifferentiation by Repressing Master Regulators of Epithelial Polarity'*. Oncogene* 26 (49), 6979-6988

Ajdarkosh, H., Dadpay, M., Yahaghi, E., Pirzaman, E. R., Fayyaz, A. F., Darian, E. K., and Mokarizadeh, A. (2015) 'Decrease Expression and Clinicopathological Significance of miR-148a with Poor Survival in Hepatocellular Carcinoma Tissues'*. Diagnostic Pathology* 10 (1), 1

Anderson, J. M. and Van Itallie, C. M. (2009) 'Physiology and Function of the Tight Junction'. *Cold Spring Harbor Perspectives in Biology* 1 (2), 2584

Asem, M. S., Buechler, S., Wates, R. B., Miller, D. L., and Stack, M. S. (2016) 'WNT5a Signaling in Cancer'. *Cancers* 8 (9), 79

Bai, X., Wang, J., Guo, Y., Pan, J., Yang, Q., Zhang, M., Li, H., Zhang, L., Ma, J., and Shi, F. (2014) 'Prostaglandin E2 Stimulates β1-Integrin Expression in Hepatocellular Carcinoma through the EP1 receptor/PKC/NF-κB Pathway'. *Scientific Reports* 4, 6538

Balda, M. S., Garrett, M. D., and Matter, K. (2003) 'The ZO-1-Associated Y-Box Factor ZONAB Regulates Epithelial Cell Proliferation and Cell Density'. *The Journal of Cell Biology* 160 (3), 423-432

Balogh, J., David Victor III, Emad H Asham, Burroughs, S. G., Boktour, M., Saharia, A., Li, X., Ghobrial, R. M., and Monsour Jr, H. P. (2016) 'Hepatocellular Carcinoma: A Review'. *Journal of Hepatocellular Carcinoma* 3, 41

Banyard, J. and Bielenberg, D. R. (2015) 'The Role of EMT and MET in Cancer Dissemination'. *Connective Tissue Research* 56 (5), 403-413

Bauer, H., Zweimueller-Mayer, J., Steinbacher, P., Lametschwandtner, A., and Bauer, H. (2010) 'The Dual Role of Zonula Occludens (ZO) Proteins'. *BioMed Research International* 2010

Bazzoni, G. (2003) 'The JAM Family of Junctional Adhesion Molecules'. *Current Opinion in Cell Biology* 15 (5), 525-530

Bednarz-Knoll, N., Alix-Panabières, C., and Pantel, K. (2012) 'Plasticity of Disseminating Cancer Cells in Patients with Epithelial Malignancies'. *Cancer and Metastasis Reviews* 31 (3-4), 673-687

Beishline, K. and Azizkhan-Clifford, J. (2015) 'Sp1 and the ‘hallmarks of Cancer''. *FEBS Journal* 282 (2), 224-258

Bernstein, B. E., Mikkelsen, T. S., Xie, X., Kamal, M., Huebert, D. J., Cuff, J., Fry, B., Meissner, A., Wernig, M., and Plath, K. (2006) 'A Bivalent Chromatin Structure Marks Key Developmental Genes in Embryonic Stem Cells'. *Cell* 125 (2), 315-326

Berx, G., Raspé, E., Christofori, G., Thiery, J. P., and Sleeman, J. P. (2007) 'Pre-EMTing Metastasis? Recapitulation of Morphogenetic Processes in Cancer'. *Clinical & Experimental Metastasis* 24 (8), 587-597

Bhat, A. A., Ahmad, R., Uppada, S. B., Singh, A. B., and Dhawan, P. (2016) 'Claudin-1 Promotes TNF-α-Induced Epithelial-Mesenchymal Transition and Migration in Colorectal Adenocarcinoma Cells'. *Experimental Cell Research* 349 (1), 119-127

Bi, L., Liu, X., Wang, C., Cao, Y., Mao, R., Li, P., and Geng, M. (2014) 'WNT5a Involved in Regulation of the Biological Behaviour of Hepatocellular Carcinoma'. *Int J Clin Exp Pathol* 7 (3), 987-995

Bid, H. K., Roberts, R. D., Manchanda, P. K., and Houghton, P. J. (2013) 'RAC1: An Emerging Therapeutic Option for Targeting Cancer Angiogenesis and Metastasis'. *Molecular Cancer Therapeutics* 12 (10), 1925-1934

Bishayee, A. (2014) 'The Inflammation and Liver Cancer'. in *Inflammation and Cancer*. ed. *Springer*, 401-435

Boireau, S., Buchert, M., Samuel, M. S., Pannequin, J., Ryan, J. L., Choquet, A., Chapuis, H., Rebillard, X., Avances, C., Ernst, M., Joubert, D., Mottet, N., and Hollande, F. (2007) 'DNA-Methylation-Dependent Alterations of Claudin-4 Expression in Human Bladder Carcinoma'. *Carcinogenesis* 28 (2), 246-258

Bojarski, C., Weiske, J., Schoneberg, T., Schroder, W., Mankertz, J., Schulzke, J. D., Florian, P., Fromm, M., Tauber, R., and Huber, O. (2004) 'The Specific Fates of Tight Junction Proteins in Apoptotic Epithelial Cells'. *Journal of Cell Science* 117 (Pt 10), 2097-2107

Borka, K., Kaliszky, P., Szabó, E., Lotz, G., Kupcsulik, P., Schaff, Z., and Kiss, A. (2007) 'Claudin Expression in Pancreatic Endocrine Tumors as Compared with Ductal Adenocarcinomas'*. Virchows Archiv* 450 (5), 549

Boscher, C. and Nabi, I. R. (2012) 'Caveolin-1: Role in Cell Signaling'. in Caveolins and Caveolae. *Springer*, 29-50

Bouchagier, K. A., Assimakopoulos, S. F., Karavias, D. D., Maroulis, I., Tzelepi, V., Kalofonos, H., Karavias, D. D., Kardamakis, D., Scopa, C. D., and Tsamandas, A. C. (2014) 'Expression of Claudins-1, -4, -5, -7 and Occludin in Hepatocellular Carcinoma and their Relation with Classic Clinicopathological Features and Patients' Survival'. *In Vivo* (Athens, Greece) 28 (3), 315-326

Bourboulia, D. and Stetler-Stevenson, W. G. (eds.) (2010) Seminars in Cancer Biology. 'Matrix Metalloproteinases (MMPs) and Tissue Inhibitors of Metalloproteinases (TIMPs): Positive and Negative Regulators in Tumor Cell Adhesion': *Elsevier*. 89-95

Brandner, J. M., Kief, S., Grund, C., Rendl, M., Houdek, P., Kuhn, C., Tschachler, E., Franke, W. W., and Moll, I. (2002) 'Organization and Formation of the Tight Junction System in Human Epidermis and Cultured Keratinocytes'*. European Journal of Cell Biology* 81 (5), 253-263

Brew, K. and Nagase, H. (2010) 'The Tissue Inhibitors of Metalloproteinases (TIMPs): An Ancient Family with Structural and Functional Diversity'. *Biochimica Et Biophysica Acta (BBA)-Molecular Cell Research 1803* (1), 55-71

Brokalaki, E., Weber, F., Sotiropoulos, G., Daoudaki, M., Cicinnati, V., and Beckebaum, S. (eds.) (2012) Transplantation Proceedings. 'Claudin-7 Expression in Hepatocellular Carcinoma': *Elsevier*

Bustin, S. A., Benes, V., Garson, J. A., Hellemans, J., Huggett, J., Kubista, M., Mueller, R., Nolan, T., Pfaffl, M. W., Shipley, G. L., Vandesompele, J., and Wittwer, C. T. (2009) 'The MIQE Guidelines: Minimum Information for Publication of Quantitative Real-Time PCR Experiments'*. Clinical Chemistry* 55 (4), 611-622

Cai, L. and Cai, X. (2014) 'Up-Regulation of miR-9 Expression Predicate Advanced Clinicopathological Features and Poor Prognosis in Patients with Hepatocellular Carcinoma'. *Diagnostic Pathology* 9 (1), 1

Cao, L., Xie, B., Yang, X., Liang, H., Jiang, X., Zhang, D., Xue, P., Chen, D., and Shao, Z. (2015) 'MiR-324-5p Suppresses Hepatocellular Carcinoma Cell Invasion by Counteracting ECM Degradation through Post-Transcriptionally Downregulating ETS1 and SP1'*. PloS One* 10 (7), e0133074

Cavallaro, U. and Christofori, G. (2004) 'Cell Adhesion and Signalling by Cadherins and Ig-CAMs in Cancer'*. Nature Reviews Cancer* 4 (2), 118-132

Chaffer, C. L., San Juan, B. P., Lim, E., and Weinberg, R. A. (2016) 'EMT, Cell Plasticity and Metastasis'*. Cancer and Metastasis Reviews*, 1-10

Chalmers, A. D. and Whitley, P. (2012) 'Continuous Endocytic Recycling of Tight Junction Proteins: How and Why?'. *Essays in Biochemistry* 53, 41-54

Chang, R. M., Xiao, S., Lei, X., Yang, H., Fang, F., and Yang, L. Y. (2016) 'MiRNA-487a Promotes Proliferation and Metastasis in Hepatocellular Carcinoma'*. Clinical Cancer Research: An Official Journal of the American Association for Cancer Research*

Chang, R., Yang, H., Fang, F., Xu, J., and Yang, L. (2014) 'MicroRNA-331-3p Promotes Proliferation and Metastasis of Hepatocellular Carcinoma by Targeting PH Domain and leucine-rich Repeat Protein Phosphatase'*. Hepatology* 60 (4), 1251-1263

Chang, Y. W., Su, Y. J., Hsiao, M., Wei, K. C., Lin, W. H., Liang, C. L., Chen, S. C., and Lee, J. L. (2015) 'Diverse Targets of B-Catenin during the Epithelial-Mesenchymal Transition Define Cancer Stem Cells and Predict Disease Relapse'. *Cancer Research* 75 (16), 3398-3410

Chao, Y., Pan, S., Yang, S., Yu, S., Che, T., Lin, C., Tsai, M., Chang, G., Wu, C., and Wu, Y. (2009) 'Claudin-1 is a Metastasis Suppressor and Correlates with Clinical Outcome in Lung Adenocarcinoma'*. American Journal of Respiratory and Critical Care Medicine* 179 (2), 123-133

Chen, B., Sirota, M., Fan-Minogue, H., Hadley, D., and Butte, A. J. (2015) 'Relating Hepatocellular Carcinoma Tumor Samples and Cell Lines using Gene Expression Data in Translational Research'*. BMC Medical Genomics* 8 (2), 1

Cho, S. B., Lee, K. H., Lee, J. H., Park, S. Y., Lee, W. S., Park, C. H., Kim, H. S., Choi, S. K., and Rew, J. S. (2008) 'Expression of E-and N-Cadherin and Clinicopathology in Hepatocellular Carcinoma'. *Pathology International* 58 (10), 635-642

Chouaib, S., Janji, B., Tittarelli, A., Eggermont, A., and Thiery, J. P. (2014) 'Tumor Plasticity Interferes with Anti-Tumor Immunity'*. Critical Reviews™ in Immunology* 34 (2)

Clark, T., Maximin, S., Meier, J., Pokharel, S., and Bhargava, P. (2015) 'Hepatocellular Carcinoma: Review of Epidemiology, Screening, Imaging Diagnosis, Response Assessment, and Treatment'*. Current Problems in Diagnostic Radiology* 44 (6), 479-486

Cokakli, M., Erdal, E., Nart, D., Yilmaz, F., Sagol, O., Kilic, M., Karademir, S., and Atabey, N. (2009) 'Differential Expression of Caveolin-1 in Hepatocellular Carcinoma: Correlation with Differentiation State, Motility and Invasion'. *BMC Cancer* 9, 65-2407-9-65

Coyne, C. B., Gambling, T. M., Boucher, R. C., Carson, J. L., and Johnson, L. G. (2003) 'Role of Claudin Interactions in Airway Tight Junctional Permeability'*. American Journal of Physiology. Lung Cellular and Molecular Physiology* 285 (5), L1166-78

Croager, E. (2004) 'CAV1 Connection'. *Nature Reviews Cancer* 4 (2), 90-91

Cummins, P. M. (2012) 'Occludin: One Protein, Many Forms'*. Molecular and Cellular Biology* 32 (2), 242-250

Dang, Y., Luo, D., Rong, M., and Chen, G. (2013) 'Underexpression of miR-34a in Hepatocellular Carcinoma and its Contribution Towards Enhancement of Proliferating Inhibitory Effects of Agents Targeting c-MET'. *PloS One* 8 (4), e61054

Darby, I. A., Laverdet, B., Bonte, F., and Desmouliere, A. (2014) 'Fibroblasts and Myofibroblasts in Wound Healing'*. Clinical, Cosmetic and Investigational Dermatology* 7, 301-311

Daugherty, R. L., Serebryannyy, L., Yemelyanov, A., Flozak, A. S., Yu, H. J., Kosak, S. T., deLanerolle, P., and Gottardi, C. J. (2014) 'A-Catenin is an Inhibitor of Transcription'. *Proceedings of the National Academy of Sciences of the United States of America* 111 (14), 5260-5265

Davidson, L. A., Marsden, M., Keller, R., and DeSimone, D. W. (2006) 'Integrin α 5 β 1 and Fibronectin Regulate Polarized Cell Protrusions Required for Xenopus Convergence and Extension'*. Current Biology* 16 (9), 833-844

De Craene, B. and Berx, G. (2013) 'Regulatory Networks Defining EMT during Cancer Initiation and Progression'. *Nature Reviews Cancer* 13 (2), 97-110

de Oliveira, S. S., de Oliveira, I. M., De Souza, W., and Morgado-Díaz, J. A. (2005) 'Claudins Upregulation in Human Colorectal Cancer'*. FEBS Letters* 579 (27), 6179-6185

Dehn, P., White, C., Conners, D., Shipkey, G., and Cumbo, T. (2004) 'Characterization of the Human Hepatocellular Carcinoma (HepG2) Cell Line as an in Vitro Model for Cadmium Toxicity Studies'*. In Vitro Cellular & Developmental Biology-Animal* 40 (5), 172-182

Deryugina, E. I. and Quigley, J. P. (2006) 'Matrix Metalloproteinases and Tumor Metastasis'*. Cancer and Metastasis Reviews* 25 (1), 9-34

Dhawan, P., Ahmad, R., Chaturvedi, R., Smith, J. J., Midha, R., Mittal, M., Krishnan, M., Chen, X., Eschrich, S., and Yeatman, T. J. (2011) 'Claudin-2 Expression Increases Tumorigenicity of Colon Cancer Cells: Role of Epidermal Growth Factor Receptor Activation'. *Oncogene* 30 (29), 3234-3247

Ding, L., Lu, Z., Lu, Q., and Chen, Y. (2013) 'The Claudin Family of Proteins in Human Malignancy: A Clinical Perspective'. *Cancer Manag Res* 5 (8), 367-375

Ding, W., Tan, H., Zhao, C., Li, X., Li, Z., Jiang, C., Zhang, Y., and Wang, L. (2016) 'MiR-145 Suppresses Cell Proliferation and Motility by Inhibiting ROCK1 in Hepatocellular Carcinoma'*. Tumor Biology*, 1-6

Dravis, C., Spike, B. T., Harrell, J. C., Johns, C., Trejo, C. L., Southard-Smith, E. M., Perou, C. M., and Wahl, G. M. (2015) 'Sox10 Regulates stem/progenitor and Mesenchymal Cell States in Mammary Epithelial Cells'. *Cell Reports* 12 (12), 2035-2048

Drees, F., Pokutta, S., Yamada, S., Nelson, W. J., and Weis, W. I. (2005) 'A-Catenin is a Molecular Switch that Binds E-cadherin-β-catenin and Regulates Actin-Filament Assembly'. *Cell* 123 (5), 903-915

D'Souza, T., Sherman-Baust, C. A., Poosala, S., Mullin, J. M., and Morin, P. J. (2009) 'Age-Related Changes of Claudin Expression in Mouse Liver, Kidney, and Pancreas'*. The Journals of Gerontology. Series A, Biological Sciences and Medical Sciences* 64 (11), 1146-1153

Du, W. W., Yang, W., and Yee, A. J. (2013) 'Roles of Versican in Cancer Biology--Tumorigenesis, Progression and Metastasis'. *Histology and Histopathology* 28 (6), 701-713

Dube, E., Chan, P. T., Hermo, L., and Cyr, D. G. (2007) 'Gene Expression Profiling and its Relevance to the Blood-Epididymal Barrier in the Human Epididymis'*. Biology of Reproduction* 76 (6), 1034-1044

Durnez, A., Verslype, C., Nevens, F., Fevery, J., Aerts, R., Pirenne, J., Lesaffre, E., Libbrecht, L., Desmet, V., and Roskams, T. (2006) 'The Clinicopathological and Prognostic Relevance of Cytokeratin 7 and 19 Expression in Hepatocellular Carcinoma. A Possible Progenitor Cell Origin'. *Histopathology* 49 (2), 138-151

Duseja, A. (2014) 'Staging of Hepatocellular Carcinoma'*. Journal of Clinical and Experimental Hepatology* 4, S74-S79

Ebnet, K., Suzuki, A., Ohno, S., and Vestweber, D. (2004) 'Junctional Adhesion Molecules (JAMs): More Molecules with Dual Functions?'*. Journal of Cell Science* 117 (Pt 1), 19-29

Elloul, S., Kedrin, D., Knoblauch, N. W., Beck, A. H., and Toker, A. (2014) 'The Adherens Junction Protein Afadin is an AKT Substrate that Regulates Breast Cancer Cell Migration'. *Molecular Cancer Research*: MCR 12 (3), 464-476

El-Serag, H. B. (2012) 'Epidemiology of Viral Hepatitis and Hepatocellular Carcinoma'. *Gastroenterology* 142 (6), 1264-1273. e1

Endo, K., Ueda, T., Ueyama, J., Ohta, T., and Terada, T. (2000) 'Immunoreactive E-cadherin, A-Catenin, B-Catenin, and Gammα-Catenin Proteins in Hepatocellular Carcinoma: Relationships with Tumor Grade, Clinicopathological Parameters, and Patients' Survival'. *Human Pathology* 31 (5), 558-565

Ersoz, S., Mungan, S., Cobanoglu, U., Turgutalp, H., and Ozoran, Y. (2011) 'Prognostic Importance of Claudin-1 and Claudin-4 Expression in Colon Carcinomas'. *Pathology-Research and Practice* 207 (5), 285-289

Fan, B., Malato, Y., Calvisi, D. F., Naqvi, S., Razumilava, N., Ribback, S., Gores, G. J., Dombrowski, F., Evert, M., Chen, X., and Willenbring, H. (2012) 'CholangioCarcinomas can Originate from Hepatocytes in Mice'. *The Journal of Clinical Investigation* 122 (8), 2911-2915

Farahani, E., Patra, H. K., Jangamreddy, J. R., Rashedi, I., Kawalec, M., Rao Pariti, R. K., Batakis, P., and Wiechec, E. (2014) 'Cell Adhesion Molecules and their Relation to (Cancer) Cell Stemness'. *Carcinogenesis* 35 (4), 747-759

Farge, E. (2003) 'Mechanical Induction of Twist in the Drosophila foregut/stomodeal Primordium'. *Current Biology* 13 (16), 1365-1377

Findley, M. K. and Koval, M. (2009) 'Regulation and Roles for Claudin-family Tight Junction Proteins'. *IUBMB Life* 61 (4), 431-437

Fong, D., Spizzo, G., Mitterer, M., Seeber, A., Steurer, M., Gastl, G., Brosch, I., and Moser, P. (2012) 'Low Expression of Junctional Adhesion Molecule A is Associated with Metastasis and Poor Survival in Pancreatic Cancer'. *Annals of Surgical Oncology* 19 (13), 4330-4336

Formosa, A., Markert, E., Lena, A., Italiano, D., Finazzi-Agro, E., Levine, A., Bernardini, S., Garabadgiu, A., Melino, G., and Candi, E. (2014) 'MicroRNAs, miR-154, miR-299-5p, miR-376a, miR-376c, miR-377, miR-381, miR-487b, miR-485-3p, miR-495 and miR-654-3p, Mapped to the 14q32. 31 Locus, Regulate Proliferation, Apoptosis, Migration and Invasion in Metastatic Prostate Cancer Cells'. *Oncogene* 33 (44), 5173-5182

Foroni, C., Broggini, M., Generali, D., and Damia, G. (2012) 'Epithelial–mesenchymal Transition and Breast Cancer: Role, Molecular Mechanisms and Clinical Impact'. *Cancer Treatment Reviews* 38 (6), 689-697

Fujita, H., Chiba, H., Yokozaki, H., Sakai, N., Sugimoto, K., Wada, T., Kojima, T., Yamashita, T., and Sawada, N. (2006) 'Differential Expression and Subcellular Localization of Claudin-7, -8, -12, -13, and -15 Along the Mouse Intestine'. *The Journal of Histochemistry and Cytochemistry: Official Journal of the Histochemistry Society* 54 (8), 933-944

Furuse, M., Sasaki, H., and Tsukita, S. (1999) 'Manner of Interaction of Heterogeneous Claudin Species within and between Tight Junction Strands'. *The Journal of Cell Biology* 147 (4), 891-903

Furuse, M., Sasaki, H., Fujimoto, K., and Tsukita, S. (1998) 'A Single Gene Product, Claudin-1 Or -2, Reconstitutes Tight Junction Strands and Recruits Occludin in Fibroblasts'. *The Journal of Cell Biology* 143 (2), 391-401

Geng, M., Cao, Y., Chen, Y., Jiang, H., Bi, L., and Liu, X. (2012) 'Loss of WNT5a and Ror2 Protein in Hepatocellular Carcinoma Associated with Poor Prognosis'. *World J Gastroenterology* 18 (12), 1328-1338

Ghanem, I., Riveiro, M. E., Paradis, V., Faivre, S., de Parga, P., and Raymond, E. (2014) 'Insights on the CXCL12-CXCR4 Axis in Hepatocellular Carcinoma Carcinogenesis'. *Am J Transl Res* 6 (4), 340-352

Gialeli, C., Kletsas, D., Mavroudis, D., Kalofonos, H., Tzanakakis, G., and Karamanos, N. (2009) 'Targeting Epidermal Growth Factor Receptor in Solid Tumors: Critical Evaluation of the Biological Importance of Therapeutic Monoclonal Antibodies'. *Current Medicinal Chemistry* 16 (29), 3797-3804

Gialeli, C., Theocharis, A. D., and Karamanos, N. K. (2011) 'Roles of Matrix Metalloproteinases in Cancer Progression and their Pharmacological Targeting'. *FEBS Journal* 278 (1), 16-27

Giannelli, G., Bergamini, C., Marinosci, F., Fransvea, E., Quaranta, M., Lupo, L., Schiraldi, O., and Antonaci, S. (2002) 'Clinical Role of MMP-2/TIMP-2 Imbalance in Hepatocellular Carcinoma'. *International Journal of Cancer* 97 (4), 425-431

Giannini, A. L., Vivanco, M. d. M., and Kypta, R. M. (2000) 'A-Catenin Inhibits β-catenin Signaling by Preventing Formation of a β-catenin· T-Cell Factor· DNA Complex'. *Journal of Biological Chemistry* 275 (29), 21883-21888

Giepmans, B. N. and van IJzendoorn, S. C. (2009) 'Epithelial cell–cell Junctions and Plasma Membrane Domains'*. Biochimica Et Biophysica Acta (BBA)-Biomembranes* 1788 (4), 820-831

Giles, R. H., van Es, J. H., and Clevers, H. (2003) 'Caught Up in a Wnt Storm: Wnt Signaling in Cancer'*. Biochimica Et Biophysica Acta (BBA)-Reviews on Cancer* 1653 (1), 1-24

Gobardhan, P. D., Elias, S. G., Madsen, E. V., van Wely, B., van den Wildenberg, F., Theunissen, E. B., Ernst, M. F., Kokke, M. C., van der Pol, C., and Rinkes, I. H. B. (2011) 'Prognostic Value of Lymph Node Micrometastases in Breast Cancer: A Multicenter Cohort Study'*. Annals of Surgical Oncology* 18 (6), 1657-1664

Gocheva, V., Zeng, W., Ke, D., Klimstra, D., Reinheckel, T., Peters, C., Hanahan, D., and Joyce, J. A. (2006) 'Distinct Roles for Cysteine Cathepsin Genes in Multistage Tumorigenesis'. *Genes & Development* 20 (5), 543-556

Gomaa, A. I., Khan, S. A., Toledano, M. B., Waked, I., and Taylor-Robinson, S. D. (2008) 'Hepatocellular Carcinoma: Epidemiology, Risk Factors and Pathogenesis'*. World Journal of Gastroenterology* 14 (27), 4300-4308

Gong-Jun, Tan., Zheng-Ke, Peng., Jin-Ping, Lu., and Fa-Qing, Tang. (2013) 'Cathepsins mediate tumor metastasis'. *World J Biol Chem* 4 (4), 91-101

González-Mariscal, L., Tapia, R., and Chamorro, D. (2008) 'Crosstalk of Tight Junction Components with Signaling Pathways'*. Biochimica Et Biophysica Acta (BBA)-Biomembranes* 1778 (3), 729-756

Gopalakrishnan, S., Raman, N., Atkinson, S. J., and Marrs, J. A. (1998) 'Rho GTPase Signaling Regulates Tight Junction Assembly and Protects Tight Junctions during ATP Depletion'*. The American Journal of Physiology* 275 (3 Pt 1), C798-809

Govaere, O., Komuta, M., Berkers, J., Spee, B., Janssen, C., de Luca, F., Katoonizadeh, A., Wouters, J., van Kempen, L. C., Durnez, A., Verslype, C., De Kock, J., Rogiers, V., van

Gregory, P. A., Bert, A. G., Paterson, E. L., Barry, S. C., Tsykin, A., Farshid, G., Vadas, M. A., Khew-Goodall, Y., and Goodall, G. J. (2008) 'The miR-200 Family and miR-205 Regulate Epithelial to Mesenchymal Transition by Targeting ZEB1 and SIP1'*. Nature Cell Biology* 10 (5), 593

Grigore, A. D., Jolly, M. K., Jia, D., Farach-Carson, M. C., and Levine, H. (2016) 'Tumor Budding: The Name is EMT. Partial EMT.'*. Journal of Clinical Medicine* 5 (5), 51

Grise, F., Bidaud, A., and Moreau, V. (2009) 'Rho GTPases in Hepatocellular Carcinoma'. *Biochimica Et Biophysica Acta (BBA)-Reviews on Cancer* 1795 (2), 137-151

Gröger, C. J., Grubinger, M., Waldhör, T., Vierlinger, K., and Mikulits, W. (2012) 'Meta-Analysis of Gene Expression Signatures Defining the Epithelial to Mesenchymal Transition during Cancer Progression'. *PloS One* 7 (12), e51136

Grunsven, L. A., Topal, B., Pirenne, J., Vankelecom, H., Nevens, F., van den Oord, J., Pinzani, M., and Roskams, T. (2014) 'Keratin 19: A Key Role Player in the Invasion of Human Hepatocellular Carcinomas'. *Gut* 63 (4), 674-685

Guillemot, L., Paschoud, S., Pulimeno, P., Foglia, A., and Citi, S. (2008) 'The Cytoplasmic Plaque of Tight Junctions: A Scaffolding and Signalling Center'. *Biochimica Et Biophysica Acta (BBA)-Biomembranes* 1778 (3), 601-613

Gujral, T. S., Chan, M., Peshkin, L., Sorger, P. K., Kirschner, M. W., and MacBeath, G. (2014) 'A Non-canonical Frizzled2 Pathway Regulates Epithelial-Mesenchymal Transition and Metastasis'. *Cell* 159 (4), 844-856

Gunzel, D. and Yu, A. S. (2013) 'Claudins and the Modulation of Tight Junction Permeability'. *Physiological Reviews* 93 (2), 525-569

Guo, W. and Giancotti, F. G. (2004) 'Integrin Signalling during Tumour Progression'. *Nature Reviews Molecular Cell Biology* 5 (10), 816-826

Gupta, G. P. and Massagué, J. (2006) 'Cancer Metastasis: Building a Framework'. *Cell* 127 (4), 679-695

Hadj-Rabia, S., Baala, L., Vabres, P., Hamel-Teillac, D., Jacquemin, E., Fabre, M., Lyonnet, S., de Prost, Y., Munnich, A., and Hadchouel, M. (2004) 'Claudin-1 Gene Mutations in

Neonatal Sclerosing Cholangitis Associated with Ichthyosis: A Tight Junction Disease'. *Gastroenterology* 127 (5), 1386-1390

Hadler-Olsen, E., Winberg, J., and Uhlin-Hansen, L. (2013) 'Matrix Metalloproteinases in Cancer: Their Value as Diagnostic and Prognostic Markers and Therapeutic Targets'. *Tumor Biology* 34 (4), 2041-2051

Hanahan, D. and Weinberg, R. A. (2000) 'The Hallmarks of Cancer'. *Cell* 100 (1), 57-70

Hartwell, K. A., Muir, B., Reinhardt, F., Carpenter, A. E., Sgroi, D. C., and Weinberg, R. A. (2006) 'The Spemann Organizer Gene, Goosecoid, Promotes Tumor Metastasis'. *Proceedings of the National Academy of Sciences of the United States of America* 103 (50), 18969-18974

Hashiguchi, M., Ueno, S., Sakoda, M., Iino, S., Hiwatashi, K., Minami, K., Ando, K., Mataki, Y., Maemura, K., and Shinchi, H. (2013) 'Clinical Implication of ZEB-1 and E-cadherin Expression in Hepatocellular Carcinoma (HCC)'. *BMC Cancer* 13 (1), 1

Hayes, J., Peruzzi, P. P., and Lawler, S. (2014) 'MicroRNAs in Cancer: Biomarkers, Functions and Therapy'. *Trends in Molecular Medicine* 20 (8), 460-469

He, S., Xiang, C., Zhang, Y., Lu, X., Chen, H., and Xiong, L. (2017) 'Recent Progress on the Effects of microRNAs and Natural Products on Tumor epithelial–mesenchymal Transition'. *OncoTargets and Therapy* 10, 3435

Herbst, D. A. and Reddy, K. R. (2012) 'Risk Factors for Hepatocellular Carcinoma'. *Clinical Liver Disease* 1 (6), 180-182

Herranz, N., Pasini, D., Diaz, V. M., Franci, C., Gutierrez, A., Dave, N., Escriva, M., Hernandez-Munoz, I., Di Croce, L., Helin, K., Garcia de Herreros, A., and Peiro, S. (2008)

'Polycomb Complex 2 is Required for E-cadherin Repression by the Snail1 Transcription Factor'. *Molecular and Cellular Biology* 28 (15), 4772-4781

Hewitt, K. J., Agarwal, R., and Morin, P. J. (2006) 'The Claudin Gene Family: Expression in Normal and Neoplastic Tissues'. *BMC Cancer* 6, 186

Higashi, Y., Suzuki, S., Sakaguchi, T., Nakamura, T., Baba, S., Reinecker, H., Nakamura, S., and Konno, H. (2007) 'Loss of Claudin-1 Expression Correlates with Malignancy of Hepatocellular Carcinoma'. *Journal of Surgical Research* 139 (1), 68-76

Hoevel, T., Macek, R., Mundigl, O., Swisshelm, K., and Kubbies, M. (2002) 'Expression and Targeting of the Tight Junction Protein CLDN1 in CLDN1-negative Human Breast Tumor Cells'. *Journal of Cellular Physiology* 191 (1), 60-68

Holczbauer, A., Gyongyosi, B., Lotz, G., Szijarto, A., Kupcsulik, P., Schaff, Z., and Kiss, A. (2013) 'Distinct Claudin Expression Profiles of Hepatocellular Carcinoma and Metastatic Colorectal and Pancreatic Carcinomas'. *The Journal of Histochemistry and Cytochemistry: Official Journal of the Histochemistry Society* 61 (4), 294-305.

Holczbauer, Á., Gyöngyösi, B., Lotz, G., Törzsök, P., Kaposi-Novák, P., Szijártó, A., Tátrai, P., Kupcsulik, P., Schaff, Z., and Kiss, A. (2014) 'Increased Expression of Claudin-1 and Claudin-7 in Liver Cirrhosis and Hepatocellular Carcinoma'. *Pathology & Oncology Research* 20 (3), 493-502

Holmes, J. L., Van Itallie, C. M., Rasmussen, J. E., and Anderson, J. M. (2006) 'Claudin Profiling in the Mouse during Postnatal Intestinal Development and Along the Gastrointestinal Tract Reveals Complex Expression Patterns'. *Gene Expression Patterns* 6 (6), 581-588

Hong, J., Zhou, J., Fu, J., He, T., Qin, J., Wang, L., Liao, L., and Xu, J. (2011) 'Phosphorylation of Serine 68 of Twist1 by MAPKs Stabilizes Twist1 Protein and Promotes Breast Cancer Cell Invasiveness'. *Cancer Research* 71 (11), 3980-3990

Hoover, K. B., Liao, S., and Bryant, P. J. (1998) 'Loss of the Tight Junction MAGUK ZO-1 in Breast Cancer: Relationship to Glandular Differentiation and Loss of Heterozygosity'. *The American Journal of Pathology* 153 (6), 1767-1773

Hu, L., Lau, S. H., Tzang, C., Wen, J., Wang, W., Xie, D., Huang, M., Wang, Y., Wu, M., and Huang, J. (2004) 'Association of Vimentin Overexpression and Hepatocellular Carcinoma Metastasis'. *Oncogene* 23 (1), 298-302

Huang, C., Huang, X., Zhu, J., Chen, Z., Li, X., Zhang, X., Huang, S., He, J., Lian, F., and Zhao, Y. (2015) 'MiR-128-3p Suppresses Hepatocellular Carcinoma Proliferation by Regulating PIK3R1 and is Correlated with the Prognosis of HCC Patients'. *Oncology Reports* 33 (6), 2889-2898

Huang, J., Li, J., Qu, Y., Zhang, J., Zhang, L., Chen, X., Liu, B., and Zhu, Z. (2014) 'The Expression of Claudin 1 Correlates with β-catenin and is a Prognostic Factor of Poor Outcome in Gastric Cancer'. *International Journal of Oncology* 44 (4), 1293-1301

Huang, P., Xu, X., Wang, L., Zhu, B., Wang, X., and Xia, J. (2014) 'The Role of EGF-EGFR Signalling Pathway in Hepatocellular Carcinoma Inflammatory Microenvironment'. *Journal of Cellular and Molecular Medicine* 18 (2), 218-230

Huang, R. Y., Guilford, P., and Thiery, J. P. (2012) 'Early Events in Cell Adhesion and Polarity during Epithelial-Mesenchymal Transition'. *Journal of Cell Science* 125 (Pt 19), 4417-4422

Huang, W., Chen, Z., He, R., Wu, Y., Yin, S., Liang, X., Chen, G., Yang, H., Peng, Z., and Yang, L. (2016) 'Clinicopathological Role of Mir-30a-5p in Hepatocellular Carcinoma Tissues and Prediction of its Function with Bioinformatics Analysis'. *OncoTargets and Therapy* 9, 5061

HUANG, Y., WANG, Z., ZHAO, J., and ZHANG, J. (2008) 'Bone Morphogenic Protein-7 Induces Mesenchymal to Epithelial Transition in Adult Renal Fibroblasts'*. Acta Academiae Medicinae Militaris Tertiae* 13, 009

Huang, Z., Huang, L., Shen, S., Li, J., Lu, H., Mo, W., Dang, Y., Luo, D., Chen, G., and Feng, Z. (2015) 'Sp1 Cooperates with Sp3 to Upregulate MALAT1 Expression in Human Hepatocellular Carcinoma'. *Oncology Reports* 34 (5), 2403-2412

Huber, M. A., Kraut, N., and Beug, H. (2005) 'Molecular Requirements for epithelial–mesenchymal Transition during Tumor Progression'*. Current Opinion in Cell Biology* 17 (5), 548-558

Hutchinson, L. (2015) 'Understanding Metastasis'*. Nature Reviews Clinical Oncology* 12 (5), 247-247

Ikenouchi, J., Furuse, M., Furuse, K., Sasaki, H., Tsukita, S., and Tsukita, S. (2005) 'Tricellulin Constitutes a Novel Barrier at Tricellular Contacts of Epithelial Cells'*. The Journal of Cell Biology* 171 (6), 939-945

Ikenouchi, J., Matsuda, M., Furuse, M., and Tsukita, S. (2003) 'Regulation of Tight Junctions during the Epithelium-Mesenchyme Transition: Direct Repression of the Gene Expression of claudins/occludin by Snail'*. Journal of Cell Science* 116 (Pt 10), 1959-1967

Ikenouchi, J., Sasaki, H., Tsukita, S., Furuse, M., and Tsukita, S. (2008) 'Loss of Occludin Affects Tricellular Localization of Tricellulin'. *Molecular Biology of the Cell* 19 (11), 4687-4693

Ino, Y., Gotoh, M., Sakamoto, M., Tsukagoshi, K., and Hirohashi, S. (2002) 'Dysadherin, a Cancer-Associated Cell Membrane Glycoprotein, Down-Regulates E-cadherin and Promotes Metastasis'. *Proceedings of the National Academy of Sciences of the United States of America* 99 (1), 365-370

Ioachim, E., Charchanti, A., Briasoulis, E., Karavasilis, V., Tsanou, H., Arvanitis, D., Agnantis, N., and Pavlidis, N. (2002) 'Immunohistochemical Expression of Extracellular Matrix Components Tenascin, Fibronectin, Collagen Type IV and Laminin in Breast Cancer: Their Prognostic Value and Role in Tumour Invasion and Progression'. *European Journal of Cancer* 38 (18), 2362-2370

Iorio, M. V. and Croce, C. M. (2017) 'MicroRNA Dysregulation in Cancer: Diagnostics, Monitoring and Therapeutics. A Comprehensive Review'. *EMBO Molecular Medicine* 9 (6), 852

Ip, Y. C., Cheung, S. T., Lee, Y. T., Ho, J. C., and Fan, S. T. (2007) 'Inhibition of Hepatocellular Carcinoma Invasion by Suppression of Claudin-10 in HLE Cells'. *Molecular Cancer Therapeutics* 6 (11), 2858-2867

Itallie, C. M. V. and Anderson, J. M. (2012) 'Caveolin Binds Independently to Claudin-2 and Occludin'. *Annals of the New York Academy of Sciences* 1257 (1), 103-107

Itoh, M. and Bissell, M. J. (2003) 'The Organization of Tight Junctions in Epithelia: Implications for Mammary Gland Biology and Breast Tumorigenesis'. *Journal of Mammary Gland Biology and Neoplasia* 8 (4), 449-462

Jakab, C., Halász, J., Szász, A., Kiss, A., Schaff, Z., Rusvai, M., Gálfi, P., and Kulka, J. (2008) 'Expression of Claudin-1, -2, -3, -4, -5 and-7 Proteins in Benign and Malignant Canine Mammary Gland Epithelial Tumours'*. Journal of Comparative Pathology* 139 (4), 238-245

Jakab, C., Kiss, A., Schaff, Z., Szabo, Z., Rusvai, M., Galfi, P., Szabara, A., Sterczer, A., and Kulka, J. (2010) 'Claudin-7 Protein Differentiates Canine CholangioCarcinoma from Hepatocellular Carcinoma'*. Histology and Histopathology* 25 (7), 857-864

Jang, J., Lee, Y., Jeon, Y., Lee, K., Jang, J., and Kim, C. (2013) 'ANT2 Suppression by shRNA Restores miR-636 Expression, Thereby Downregulating Ras and Inhibiting Tumorigenesis of Hepatocellular Carcinoma'*. Experimental & Molecular Medicine* 45 (1), e3

Jiang, L., Yang, Y., Fu, L., Xu, W., Liu, D., Liang, Q., Zhang, X., Xu, L., Guan, X., and Wu, B. (2014) 'CLDN3 Inhibits Cancer Aggressiveness Via WNT-EMT Signaling and is a Potential Prognostic Biomarker for Hepatocellular Carcinoma'. *Oncotarget*

Johansson, N., Ahonen, M., and Kähäri, V. (2000) 'Matrix Metalloproteinases in Tumor Invasion'*. Cellular and Molecular Life Sciences* 57 (1), 5-15

Jolly, M. K., Boareto, M., Huang, B., Jia, D., Lu, M., Ben-Jacob, E., Onuchic, J. N., and Levine, H. (2015) 'Implications of the Hybrid epithelial/mesenchymal Phenotype in Metastasis'*. Frontiers in Oncology* 5

Jones, S. (2004) 'An Overview of the Basic Helix-Loop-Helix Proteins'*. Genome Biology* 5 (6), 1

Jung, K. K., Liu, X. W., Chirco, R., Fridman, R., and Kim, H. R. (2006) 'Identification of CD63 as a Tissue Inhibitor of Metalloproteinase-1 Interacting Cell Surface Protein'. *The EMBO Journal* 25 (17), 3934-3942

Kahle, K. T., Gimenez, I., Hassan, H., Wilson, F. H., Wong, R. D., Forbush, B., Aronson, P. S., and Lifton, R. P. (2004) 'WNK4 Regulates Apical and Basolateral Cl- Flux in Extrarenal Epithelia'. *Proceedings of the National Academy of Sciences of the United States of America* 101 (7), 2064-2069

Kalluri, R. and Neilson, E. G. (2003) 'Epithelial-Mesenchymal Transition and its Implications for Fibrosis'*. The Journal of Clinical Investigation* 112 (12), 1776-1784

Kalluri, R. and Weinberg, R. A. (2009) 'The Basics of Epithelial-Mesenchymal Transition'*. The Journal of Clinical Investigation* 119 (6), 1420-1428

Kanda, M., Shimizu, D., Tanaka, H., Shibata, M., Iwata, N., Hayashi, M., Kobayashi, D., Tanaka, C., Yamada, S., Fujii, T., Nakayama, G., Sugimoto, H., Koike, M., Fujiwara, M., and Kodera, Y. (2016) 'Metastatic Pathway-Specific Transcriptome Analysis Identifies MFSD4 as a Putative Tumor Suppressor and Biomarker for Hepatic Metastasis in Patients with Gastric Cancer'. *Oncotarget* 7 (12), 13667-13679

Kang, K., Lee, M., Song, J., Jeong, J., Kim, Y., Lee, C., Kim, T., Kwak, K., Kim, O., and Ann, H. J. (2014) 'Overexpression of Goosecoid Homeobox is Associated with Chemoresistance and Poor Prognosis in Ovarian Carcinoma'. *Oncology Reports* 32 (1), 189-198

Kanwal, F., Hoang, T., Kramer, J. R., Asch, S. M., Goetz, M. B., Zeringue, A., Richardson, P., and El–Serag, H. B. (2011) 'Increasing Prevalence of HCC and Cirrhosis in Patients with Chronic Hepatitis C Virus Infection'*. Gastroenterology* 140 (4), 1182-1188. e1

Karlsson, M. C., Gonzalez, S. F., Welin, J., and Fuxe, J. (2017) 'Epithelial-Mesenchymal Transition in Cancer Metastasis through the Lymphatic System'*. Molecular Oncology*

Katoh, M. and Katoh, M. (2003) 'CLDN23 Gene, Frequently Down-Regulated in Intestinal-Type Gastric Cancer, is a Novel Member of CLAUDIN Gene Family'. *International Journal of Molecular Medicine* 11 (6), 683-689

Katyal, S., Oliver III, J. H., Peterson, M. S., Ferris, J. V., Carr, B. S., and Baron, R. L. (2000) 'Extrahepatic Metastases of Hepatocellular Carcinoma 1'. *Radiology* 216 (3), 698-703

Kida, Y., Asahina, K., Teraoka, H., Gitelman, I., and Sato, T. (2007) 'Twist Relates to Tubular Epithelial-Mesenchymal Transition and Interstitial Fibrogenesis in the Obstructed Kidney'. *The Journal of Histochemistry and Cytochemistry: Official Journal of the Histochemistry Society* 55 (7), 661-673

Kim, H., Choi, G. H., Na, D. C., Ahn, E. Y., Kim, G. I., Lee, J. E., Cho, J. Y., Yoo, J. E., Choi, J. S., and Park, Y. N. (2011) 'Human Hepatocellular Carcinomas with “Stemness”-related Marker Expression: Keratin 19 Expression and a Poor Prognosis'. *Hepatology* 54 (5), 1707-1717

Kim, J., Hong, S. J., Park, J. Y., Park, J. H., Yu, Y., Park, S. Y., Lim, E. K., Choi, K. Y., Lee, E. K., and Paik, S. S. (2010) 'Epithelial–mesenchymal Transition Gene Signature to Predict Clinical Outcome of Hepatocellular Carcinoma'. *Cancer Science* 101 (6), 1521-1528

Kim, W., Kim, M., and Jho, E. H. (2013) 'WNT/β-catenin Signalling: From Plasma Membrane to Nucleus'. *The Biochemical Journal* 450 (1), 9-21

Kinsey, D. L. (1960) 'An Experimental Study of Preferential Metastasis'. *Cancer* 13 (4), 674-676

Kitajiri, S., Furuse, M., Morita, K., Saishin-Kiuchi, Y., Kido, H., Ito, J., and Tsukita, S. (2004) 'Expression Patterns of Claudins, Tight Junction Adhesion Molecules, in the Inner Ear'. *Hearing Research* 187 (1), 25-34

Kleeff, J., Shi, X., Bode, H. P., Hoover, K., Shrikhande, S., Bryant, P. J., Korc, M., Büchler, M. W., and Friess, H. (2001) 'Altered Expression and Localization of the Tight Junction Protein ZO-1 in Primary and Metastatic Pancreatic Cancer'. *Pancreas* 23 (3), 259-265

Kobayashi, W. and Ozawa, M. (2013) 'The Transcription Factor LEF-1 Induces an epithelial–mesenchymal Transition in MDCK Cells Independent of β-catenin'. *Biochemical and Biophysical Research Communications* 442 (1), 133-138

Koch, U., Lehal, R., and Radtke, F. (2013) 'Stem Cells Living with a Notch'. *Development (Cambridge, England)* 140 (4), 689-704

Kong, Y. H., Zanaruddin, S. N. S., Lau, S. H., Ramanathan, A., Kallarakkal, T. G., Vincent-Chong, V. K., Mustafa, W. M. W., Abraham, M. T., Rahman, Z. A. A., and Zain, R. B. (2015) 'Co-Expression of TWIST1 and ZEB2 in Oral Squamous Cell Carcinoma is Associated with Poor Survival'. *PloS One* 10 (7), e0134045

Konopka, G., Tekiela, J., Iverson, M., Wells, C., and Duncan, S. A. (2007) 'Junctional Adhesion Molecule-A is Critical for the Formation of Pseudocanaliculi and Modulates E-cadherin Expression in Hepatic Cells'. *The Journal of Biological Chemistry* 282 (38), 28137-28148

Korhan, P., Erdal, E., and Atabey, N. (2014) 'MiR-181a-5p is Downregulated in Hepatocellular Carcinoma and Suppresses Motility, Invasion and Branching-Morphogenesis by Directly Targeting c-Met'. *Biochemical and Biophysical Research Communications* 450 (4), 1304-1312

Kousidou, O. C., Roussidis, A. E., Theocharis, A. D., and Karamanos, N. K. (2004) 'Expression of MMPs and TIMPs Genes in Human Breast Cancer Epithelial Cells Depends on Cell Culture Conditions and is Associated with their Invasive Potential'. *Anticancer Research* 24 (6), 4025-4030

Koval, M. (2013) 'Differential Pathways of Claudin Oligomerization and Integration into Tight Junctions'. *Tissue Barriers* 1 (3), e24518

Krämer, F., White, K., Kubbies, M., Swisshelm, K., and Weber, B. H. (2000) 'Genomic Organization of Claudin-1 and its Assessment in Hereditary and Sporadic Breast Cancer'. *Human Genetics* 107 (3), 249-256

Krause, G., Winkler, L., Mueller, S. L., Haseloff, R. F., Piontek, J., and Blasig, I. E. (2008) 'Structure and Function of Claudins'. *Biochimica Et Biophysica Acta (BBA)-Biomembranes* 1778 (3), 631-645

Kwon, M. J. (2013) 'Emerging Roles of Claudins in Human Cancer'. *International Journal of Molecular Sciences* 14 (9), 18148-18180

Lal-Nag, M. and Morin, P. J. (2009) 'The Claudins'. *Genome Biol* 10 (8), 235

Lamouille, S., Xu, J., and Derynck, R. (2014) 'Molecular Mechanisms of Epithelial-Mesenchymal Transition'. *Nature Reviews. Molecular Cell Biology* 15 (3), 178-196

Landy, J., Ronde, E., English, N., Clark, S. K., Hart, A. L., Knight, S. C., Ciclitira, P. J., and Al-Hassi, H. O. (2016) 'Tight Junctions in Inflammatory Bowel Diseases and Inflammatory Bowel Disease Associated Colorectal Cancer'. *World Journal of Gastroenterology* 22 (11), 3117-3126

Langley, R. R. and Fidler, I. J. (2011) 'The Seed and Soil Hypothesis revisited—The Role of tumor-stroma Interactions in Metastasis to Different Organs'. *International Journal of Cancer* 128 (11), 2527-2535

Latorre, I. J., , K. K., and Javier, R. T. (2006) 'Tight Junction Proteins and Cancer'. in *Tight Junctions*. ed. by Anon: Springer, 116-134

Laurila, J. J., Karttunen, T., Koivukangas, V., Laurila, P. A., Syrjala, H., Saarnio, J., Soini, Y., and Ala-Kokko, T. I. (2007) 'Tight Junction Proteins in Gallbladder Epithelium: Different Expression in Acute Acalculous and Calculous Cholecystitis'*. The Journal of Histochemistry and Cytochemistry: Official Journal of the Histochemistry Society* 55 (6), 567-573

Lee, S. H. (2015) 'Intestinal Permeability Regulation by Tight Junction: Implication on Inflammatory Bowel Diseases'*. Intestinal Research* 13 (1), 11-18

Levrero, M. and Zucman-Rossi, J. (2016) 'Mechanisms of HBV-Induced Hepatocellular Carcinoma'*. Journal of Hepatology* 64 (1), S84-S101

Li, B., Huang, P., Qiu, J., Liao, Y., Hong, J., and Yuan, Y. (2014) 'MicroRNA-130a is Down-Regulated in Hepatocellular Carcinoma and Associates with Poor Prognosis'*. Medical Oncology* 31 (10), 1-6

Li, J., Xin, J., Zhang, L., Wu, J., Jiang, L., Zhou, Q., Li, J., Guo, J., Cao, H., and Li, L. (2013) 'Human Hepatic Progenitor Cells Express Hematopoietic Cell Markers CD45 and CD109'*. International Journal of Medical Sciences* 11 (1), 65-79

Li, Q., Wu, J., Wei, P., Xu, Y., Zhuo, C., Wang, Y., Li, D., and Cai, S. (2015) 'Overexpression of Forkhead Box C2 Promotes Tumor Metastasis and Indicates Poor Prognosis in Colon Cancer Via Regulating Epithelial-Mesenchymal Transition'. *American Journal of Cancer Research* 5 (6), 2022

Li, S., Li, J., Fei, B. Y., Shao, D., Pan, Y., Mo, Z. H., Sun, B. Z., Zhang, D., Zheng, X., Zhang, M., Zhang, X. W., and Chen, L. (2015) 'MiR-27a Promotes Hepatocellular Carcinoma Cell Proliferation through Suppression of its Target Gene Peroxisome Proliferator-Activated Receptor Gamma'*. Chinese Medical Journal* 128 (7), 941-947

Li, X., Li, P., Chang, Y., Xu, Q., Wu, Z., Ma, Q., and Wang, Z. (2014) 'The SDF-1/CXCR4 Axis Induces epithelial–mesenchymal Transition in Hepatocellular Carcinoma'. *Molecular and Cellular Biochemistry* 392 (1-2), 77-84

Li, X., Roslan, S., Johnstone, C., Wright, J., Bracken, C., Anderson, M., Bert, A., Selth, L., Anderson, R., and Goodall, G. (2014) 'MiR-200 can Repress Breast Cancer Metastasis through ZEB1-Independent but Moesin-Dependent Pathways'. *Oncogene* 33 (31), 4077-4088

Li, Y., Yang, J., Dai, C., Wu, C., and Liu, Y. (2003) 'Role for Integrin-Linked Kinase in Mediating Tubular Epithelial to Mesenchymal Transition and Renal Interstitial Fibrogenesis'. *The Journal of Clinical Investigation* 112 (4), 503-516

Liang, J., Li, Y., Daniels, G., Sfanos, K., De Marzo, A., Wei, J., Li, X., Chen, W., Wang, J., Zhong, X., Melamed, J., Zhao, J., and Lee, P. (2015) 'LEF1 Targeting EMT in Prostate Cancer Invasion is Regulated by miR-34a'. *Molecular Cancer Research: MCR* 13 (4), 681-688

Liao, C., Kong, L., Zhou, P., Yang, X., Huang, J., Zhang, H., and Lu, N. (2014) 'MiR-10b is Overexpressed in Hepatocellular Carcinoma and Promotes Cell Proliferation, Migration and Invasion through RhoC, uPAR and MMPs'. *Journal of Translational Medicine* 12 (1), 1

Lima, W. R., Parreira, K. S., Devuyst, O., Caplanusi, A., N'kuli, F., Marien, B., Van Der Smissen, P., Alves, P. M., Verroust, P., Christensen, E. I., Terzi, F., Matter, K., Balda, M. S., Pierreux, C. E., and Courtoy, P. J. (2010) 'ZONAB Promotes Proliferation and Represses Differentiation of Proximal Tubule Epithelial Cells'. *Journal of the American Society of Nephrology: JASN* 21 (3), 478-488

Lin, F., Ding, R., Zheng, S., Xing, D., Hong, W., Zhou, Z., and Shen, J. (2014) 'Decrease Expression of microRNA-744 Promotes Cell Proliferation by Targeting c-Myc in Human Hepatocellular Carcinoma'. *Cancer Cell International* 14 (1), 1

Lin, Y., Dong, C., and P Zhou, B. (2014) 'Epigenetic Regulation of EMT: The Snail Story'. *Current Pharmaceutical Design* 20 (11), 1698-1705

Lippoldt, A., Liebner, S., Andbjer, B., Kalbacher, H., Wolburg, H., Haller, H., and Fuxe, K. (2000) 'Organization of Choroid Plexus Epithelial and Endothelial Cell Tight Junctions and Regulation of claudin-1, -2 and-5 Expression by Protein Kinase C'. *Neuroreport* 11 (7), 1427-1431

Liu, C. Y., Lin, H. H., Tang, M. J., and Wang, Y. K. (2015) 'Vimentin Contributes to Epithelial-Mesenchymal Transition Cancer Cell Mechanics by Mediating Cytoskeletal Organization and Focal Adhesion Maturation'. *Oncotarget* 6 (18), 15966-15983

Liu, H., Li, W., Chen, C., Pei, Y., and Long, X. (2015) 'MiR-335 Acts as a Potential Tumor Suppressor miRNA Via Downregulating ROCK1 Expression in Hepatocellular Carcinoma'. *Tumor Biology* 36 (8), 6313-6319

Liu, K., Li, X., Cao, Y., Ge, Y., Wang, J., and Shi, B. (2015) 'MiR-132 Inhibits Cell Proliferation, Invasion and Migration of Hepatocellular Carcinoma by Targeting PIK3R3'. *International Journal of Oncology* 47 (4), 1585-1593

Liu, K., Liu, S., Zhang, W., Jia, B., Tan, L., Jin, Z., and Liu, Y. (2015) 'MiR-494 Promotes Cell Proliferation, Migration and Invasion, and Increased Sorafenib Resistance in Hepatocellular Carcinoma by Targeting PTEN'. *Oncology Reports* 34 (2), 1003-1010

Liu, L. J., Xie, S. X., Chen, Y. T., Xue, J. L., Zhang, C. J., and Zhu, F. (2016) 'Aberrant Regulation of WNT Signaling in Hepatocellular Carcinoma'. *World Journal of Gastroenterology* 22 (33), 7486-7499

Liu, Q., Qiao, L., Liang, N., Xie, J., Zhang, J., Deng, G., Luo, H., and Zhang, J. (2016) 'The Relationship between Vasculogenic Mimicry and epithelial-mesenchymal Transitions'*. Journal of Cellular and Molecular Medicine* 20 (9), 1761-1769

Liu, X., Wang, C., Chen, Z., Jin, Y., Wang, Y., Kolokythas, A., Dai, Y., and Zhou, X. (2011) 'MicroRNA-138 Suppresses Epithelial-Mesenchymal Transition in Squamous Cell Carcinoma Cell Lines'*. The Biochemical Journal* 440 (1), 23-31

Liu, Y., El-Naggar, S., Darling, D. S., Higashi, Y., and Dean, D. C. (2008) 'Zeb1 Links Epithelial-Mesenchymal Transition and Cellular Senescence'*. Development (Cambridge, England)* 135 (3), 579-588

Liu, Y., Zhang, W., Liu, K., Liu, S., Ji, B., and Wang, Y. (2016) 'MiR-138 Suppresses Cell Proliferation and Invasion by Inhibiting SOX9 in Hepatocellular Carcinoma'*. Am J Transl Res* 8 (5), 2159-2168

Lódi, C., Szabó, E., Holczbauer, A., Batmunkh, E., Szíjártó, A., Kupcsulik, P., Kovalszky, I., Paku, S., Illyés, G., and Kiss, A. (2006) 'Claudin-4 Differentiates Biliary Tract Cancers from Hepatocellular Carcinomas'*. Modern Pathology* 19 (3), 460-469

Lu, J., Xia, Y., Chen, K., Zheng, Y., Wang, J., Lu, W., Yin, Q., Wang, F., Zhou, Y., and Guo, C. (2016) 'Oncogenic Role of the Notch Pathway in Primary Liver Cancer (Review)'. *Oncology Letters* 12 (1), 3-10

Luo, X., Yang, S., Zhou, C., Pan, F., Li, Q., and Ma, S. (2015) 'MicroRNA-328 Enhances Cellular Motility through Posttranscriptional Regulation of PTPRJ in Human Hepatocellular Carcinoma'. *OncoTargets and Therapy* 8, 3159

Luo, Y. and Tan, Y. (2016) 'Prognostic Value of CD44 Expression in Patients with Hepatocellular Carcinoma: Meta-Analysis'. *Cancer Cell International* 16 (1), 47

Ma, D., Chai, Z., Zhu, X., Zhang, N., Zhan, D., Ye, B., Wang, C., Qin, C., Zhao, Y., and Zhu, W. (2016) 'MicroRNA-26a Suppresses Epithelial-Mesenchymal Transition in Human Hepatocellular Carcinoma by Repressing Enhancer of Zeste Homolog 2'. *Journal of Hematology & Oncology* 9 (1), 1

Ma, J., Sheng, Z., Lv, Y., Liu, W., Yao, Q., Pan, T., Xu, Z., Zhang, C., and Xu, G. (2016) 'Expression and Clinical Significance of Nectin-4 in Hepatocellular Carcinoma'. *OncoTargets and Therapy* 9, 183

Ma, L. and Weinberg, R. A. (2008) 'Micromanagers of Malignancy: Role of microRNAs in Regulating Metastasis'. *Trends in Genetics* 24 (9), 448-456

Ma, M., He, M., Jiang, Q., Yan, Y., Guan, S., Zhang, J., Yu, Z., Chen, Q., Sun, M., and Yao, W. (2016) 'MiR-487a Promotes TGF-β1-Induced EMT, the Migration and Invasion of Breast Cancer Cells by Directly Targeting MAGI2'. *International Journal of Biological Sciences* 12 (4), 397

MacDonald, B. T., Tamai, K., and He, X. (2009) 'Wnt/β-catenin Signaling: Components, Mechanisms, and Diseases'. *Developmental Cell* 17 (1), 9-26

Makri, A., Pissimissis, N., Lembessis, P., Polychronakos, C., and Koutsilieris, M. (2008) 'The Kisspeptin (KiSS-1)/GPR54 System in Cancer Biology'. *Cancer Treatment Reviews* 34 (8), 682-692

Malek, N. P., Schmidt, S., Huber, P., Manns, M. P., and Greten, T. F. (2014) 'The Diagnosis and Treatment of Hepatocellular Carcinoma'*. Deutsches Arzteblatt International* 111 (7), 101-106

Mannan, A. and Hahn-Stromberg, V. (2016) 'Dysadherin Expression is Associated with Advanced Tumor stage while Complexity Index is Related to Poorly Differentiated Tumors in Colon Carcinoma'. *Diagn Pathol Open* 1 (111), 2

Margetts, P. J. (2012) 'Twist: A New Player in the Epithelial-Mesenchymal Transition of the Peritoneal Mesothelial Cells'*. Nephrology, Dialysis, Transplantation: Official Publication of the European Dialysis and Transplant Association - European Renal Association* 27 (11), 3978-3981

Maria, O. M., Kim, J. W., Gerstenhaber, J. A., Baum, B. J., and Tran, S. D. (2008) 'Distribution of Tight Junction Proteins in Adult Human Salivary Glands'*. The Journal of Histochemistry and Cytochemistry: Official Journal of the Histochemistry Society* 56 (12), 1093-1098

Mariano, C., Sasaki, H., Brites, D., and Brito, M. A. (2011) 'A Look at Tricellulin and its Role in Tight Junction Formation and Maintenance'*. European Journal of Cell Biology* 90 (10), 787-796

Markov, A. G., Kruglova, N. M., Fomina, Y. A., Fromm, M., and Amasheh, S. (2012) 'Altered Expression of Tight Junction Proteins in Mammary Epithelium After Discontinued Suckling in Mice'*. Pflügers Archiv-European Journal of Physiology* 463 (2), 391-398

Martin, T. A. and Jiang, W. G. (2009) 'Loss of Tight Junction Barrier Function and its Role in Cancer Metastasis'. *Biochimica Et Biophysica Acta (BBA)-Biomembranes* 1788 (4), 872-891

Martin, T. A., Mason, M. D., and Jiang, W. G. (2011) 'Tight Junctions in Cancer Metastasis'. *Frontiers in Bioscience (Landmark Edition)* 16, 898-936

Matsuo, N., Shiraha, H., Fujikawa, T., Takaoka, N., Ueda, N., Tanaka, S., Nishina, S., Nakanishi, Y., Uemura, M., and Takaki, A. (2009) 'Twist Expression Promotes Migration and Invasion in Hepatocellular Carcinoma'. *BMC Cancer* 9 (1), 240

Matter, K. and Balda, M. S. (2003) 'Signalling to and from Tight Junctions'. *Nature Reviews Molecular Cell Biology* 4 (3), 225-237

McGlynn, K. A., Petrick, J. L., and London, W. T. (2015) 'Global Epidemiology of Hepatocellular Carcinoma: An Emphasis on Demographic and Regional Variability'. *Clinics in Liver Disease* 19 (2), 223-238

Medici, D., Hay, E. D., and Olsen, B. R. (2008) 'Snail and Slug Promote Epithelial-Mesenchymal Transition through Beta-Catenin-T-Cell Factor-4-Dependent Expression of Transforming Growth Factor-beta3'. *Molecular Biology of the Cell* 19 (11), 4875-4887

Mee, C. J., Harris, H. J., Farquhar, M. J., Wilson, G., Reynolds, G., Davis, C., van IJzendoorn, S. C., Balfe, P., and McKeating, J. A. (2009) 'Polarization Restricts Hepatitis C Virus Entry into HepG2 Hepatoma Cells'. *Journal of Virology* 83 (12), 6211-6221

Melendez-Zajgla, J., Del Pozo, L., Ceballos, G., and Maldonado, V. (2008) 'Tissue Inhibitor of Metalloproteinases-4. the Road Less Travelled'. *Molecular Cancer* 7 (1), 1

Mendez, M. G., Kojima, S., and Goldman, R. D. (2010) 'Vimentin Induces Changes in Cell Shape, Motility, and Adhesion during the Epithelial to Mesenchymal Transition'. *FASEB Journal: Official Publication of the Federation of American Societies for Experimental Biology* 24 (6), 1838-1851

Merle, P., de la Monte, S., Kim, M., Herrmann, M., Tanaka, S., Von Dem Bussche, A., Kew, M. C., Trepo, C., and Wands, J. R. (2004) 'Functional Consequences of Frizzled-7 Receptor Overexpression in Human Hepatocellular Carcinoma'. Gastroenterology 127 (4), 1110-1122

Michlig, S., Damak, S., and Le Coutre, J. (2007) 'Claudin-based Permeability Barriers in Taste Buds'*. Journal of Comparative Neurology* 502 (6), 1003-1011

Misso, G., Di Martino, M. T., De Rosa, G., Farooqi, A. A., Lombardi, A., Campani, V., Zarone, M. R., Gulla, A., Tagliaferri, P., and Tassone, P. (2014) 'Mir-34: A New Weapon Against Cancer?'. *Molecular Therapy—Nucleic Acids* 3 (9), e194

Mitsiades, N., Yu, W. H., Poulaki, V., Tsokos, M., and Stamenkovic, I. (2001) 'Matrix Metalloproteinase-7-Mediated Cleavage of Fas Ligand Protects Tumor Cells from Chemotherapeutic Drug Cytotoxicity'. *Cancer Research* 61 (2), 577-581

Mittal, S. and El-Serag, H. B. (2013) 'Epidemiology of Hepatocellular Carcinoma: Consider the Population'*. Journal of Clinical Gastroenterology* 47 Supplement, S2-6

Mohamed, A., Gonzalez, R. S., Lawson, D., Wang, J., and Cohen, C. (2013) 'SOX10 Expression in Malignant Melanoma, Carcinoma, and Normal Tissues'. *Applied Immunohistochemistry & Molecular Morphology: AIMM* 21 (6), 506-510

Moldvay, J., Jäckel, M., Páska, C., Soltész, I., Schaff, Z., and Kiss, A. (2007) 'Distinct Claudin Expression Profile in Histologic Subtypes of Lung Cancer'*. Lung Cancer* 57 (2), 159-167

Moniz, S. and Jordan, P. (2010) 'Emerging Roles for WNK Kinases in Cancer'. *Cellular and Molecular Life Sciences* 67 (8), 1265-1276

Morell, C. M. and Strazzabosco, M. (2014) 'Notch Signaling and New Therapeutic Options in Liver Disease'. *Journal of Hepatology* 60 (4), 885-890

Moreno-Bueno, G., Portillo, F., and Cano, A. (2008) 'Transcriptional Regulation of Cell Polarity in EMT and Cancer'*. Oncogene* 27 (55), 6958

Morin, P. J., Kinzler, K. W., and Sparks, A. B. (2016) 'Beta-Catenin Mutations: Insights into the APC Pathway and the Power of Genetics'*. Cancer Research* 76 (19), 5587-5589

Morin, V., Sanchez, A., Quinones, K., Huidobro, J. G., Iribarren, C., Bustos, P., Puchi, M., Geneviève, A. M., and Imschenetzky, M. (2008) 'Cathepsin L Inhibitor I Blocks Mitotic Chromosomes Decondensation during Cleavage Cell Cycles of Sea Urchin Embryos'. *Journal of Cellular Physiology* 216 (3), 790-795

Morita, K., Sasaki, H., Fujimoto, K., Furuse, M., and Tsukita, S. (1999) 'Claudin-11/OSP-Based Tight Junctions of Myelin Sheaths in Brain and Sertoli Cells in Testis'*. The Journal of Cell Biology* 145 (3), 579-588

Morohashi, S., Kusumi, T., Sato, F., Odagiri, H., Chiba, H., Yoshihara, S., Hakamada, K., Sasaki, M., and Kijima, H. (2007) 'Decreased Expression of Claudin-1 Correlates with Recurrence Status in Breast Cancer'*. International Journal of Molecular Medicine* 20 (2), 139-144

Morrow, C. M., Mruk, D., Cheng, C. Y., and Hess, R. A. (2010) 'Claudin and Occludin Expression and Function in the Seminiferous Epithelium'*. Philosophical Transactions of the Royal Society of London. Series B, Biological Sciences* 365 (1546), 1679-1696

Murakami, Y., Tamori, A., Itami, S., Tanahashi, T., Toyoda, H., Tanaka, M., Wu, W., Brojigin, N., Kaneoka, Y., and Maeda, A. (2013) 'The Expression Level of miR-18b in

Hepatocellular Carcinoma is Associated with the Grade of Malignancy and Prognosis'. *BMC Cancer* 13 (1), 1

Muresan, Z., Paul, D. L., and Goodenough, D. A. (2000) 'Occludin 1B, a Variant of the Tight Junction Protein Occludin'. *Molecular Biology of the Cell* 11 (2), 627-634

Myal, Y., Leygue, E., and Blanchard, A. A. (2010) 'Claudin 1 in Breast Tumorigenesis: Revelation of a Possible Novel "Claudin High" Subset of Breast Cancers'. *Journal of Biomedicine & Biotechnology* 2010, 956897

Nagai, T., Arao, T., Nishio, K., Matsumoto, K., Hagiwara, S., Sakurai, T., Minami, Y., Ida, H., Ueshima, K., Nishida, N., Sakai, K., Saijo, N., Kudo, K., Kaneda, H., Tamura, D., Aomatsu, K., Kimura, H., Fujita, Y., Haji, S., and Kudo, M. (2016) 'Impact of Tight Junction Protein ZO-1 and TWIST Expression on Postoperative Survival of Patients with Hepatocellular Carcinoma'. *Digestive Diseases (Basel, Switzerland)* 34 (6), 702-707

Nakamura, M., Miyamoto, S., Maeda, H., Ishii, G., Hasebe, T., Chiba, T., Asaka, M., and Ochiai, A. (2005) 'Matrix Metalloproteinase-7 Degrades all Insulin-Like Growth Factor Binding Proteins and Facilitates Insulin-Like Growth Factor Bioavailability'. *Biochemical and Biophysical Research Communications* 333 (3), 1011-1016

Nakanishi, Y., Uemura, M., and Takaki, A. (2009) 'TWIST Expression Promotes Migration and Invasion in Hepatocellular Carcinoma'. *BMC Cancer* 9 (1), 1

Nam, E. H., Lee, Y., Moon, B., Lee, J. W., and Kim, S. (2015) 'Twist1 and AP-1 Cooperatively Upregulate Integrin alpha5 Expression to Induce Invasion and the Epithelial-Mesenchymal Transition'. *Carcinogenesis* 36 (3), 327-337

Nam, J., Hirohashi, S., and Wakefield, L. M. (2007) 'Dysadherin: A New Player in Cancer Progression'. *Cancer Letters* 255 (2), 161-169

Natsuizaka, M., Omura, T., Akaike, T., Kuwata, Y., Yamazaki, K., Sato, T., Karino, Y., Toyota, J., Suga, T., and Asaka, M. (2005) 'Clinical Features of Hepatocellular Carcinoma with Extrahepatic Metastases'. *Journal of Gastroenterology and Hepatology* 20 (11), 1781-1787

Nawshad, A., Lagamba, D., Polad, A., and Hay, E. D. (2005) 'Transforming Growth Factor-Beta Signaling during Epithelial-Mesenchymal Transformation: Implications for Embryogenesis and Tumor Metastasis'. *Cells, Tissues, Organs* 179 (1-2), 11-23

Nejjari, M., Hafdi, Z., Gouysse, G., Fiorentino, M., Béatrix, O., Dumortier, J., Pourreyron, C., Barozzi, C., D'Errico, A., and Grigioni, W. F. (2002) 'Expression, Regulation, and Function of αV Integrins in Hepatocellular Carcinoma: An in Vivo and in Vitro Study'. *Hepatology* 36 (2), 418-426

Nie, J., Liu, L., Zheng, W., Chen, L., Wu, X., Xu, Y., Du, X., and Han, W. (2012) 'MicroRNA-365, Down-Regulated in Colon Cancer, Inhibits Cell Cycle Progression and Promotes Apoptosis of Colon Cancer Cells by Probably Targeting Cyclin D1 and Bcl-2'. *Carcinogenesis* 33 (1), 220-225

Niessen, C. M. (2007) 'Tight junctions/Adherens Junctions: Basic Structure and Function'. *Journal of Investigative Dermatology* 127 (11), 2525-2532

Nieto, M. A. (2009) 'Epithelial-Mesenchymal Transitions in Development and Disease: Old Views and New Perspectives'. *The International Journal of Developmental Biology* 53 (8-10), 1541-1547

Nishioka, M., Ueno, K., Hazama, S., Okada, T., Sakai, K., Suehiro, Y., Okayama, N., Hirata, H., Oka, M., and Imai, K. (2013) 'Possible Involvement of WNT11 in Colorectal Cancer Progression'. *Molecular Carcinogenesis* 52 (3), 207-217

Nordenstedt, H., White, D. L., and El-Serag, H. B. (2010) 'The Changing Pattern of Epidemiology in Hepatocellular Carcinoma'. *Digestive and Liver Disease* 42, S206-S214

Ogden, A., Rida, P. C., and Aneja, R. (2013) 'Heading Off with the Herd: How Cancer Cells might Maneuver Supernumerary Centrosomes for Directional Migration'. *Cancer and Metastasis Reviews* 32 (1-2), 269-287

Okuda, H. (2007) 'Hepatocellular Carcinoma Development in Cirrhosis'. *Best Practice & Research Clinical Gastroenterology* 21 (1), 161-173

Ombrato, L. and Malanchi, I. (2014) 'The EMT Universe: Space between Cancer Cell Dissemination and Metastasis Initiation'. *Critical Reviews™ in Oncogenesis* 19 (5)

Orbán, E., Szabó, E., Lotz, G., Kupcsulik, P., Páska, C., Schaff, Z., and Kiss, A. (2008) 'Different Expression of Occludin and ZO-1 in Primary and Metastatic Liver Tumors'. *Pathology & Oncology Research* 14 (3), 299-306

Orian-Rousseau, V. (2015) 'CD44 Acts as a Signaling Platform Controlling Tumor Progression and Metastasis'. *Frontiers in Immunology* 6, 154

Osanai, M., Murata, M., Nishikiori, N., Chiba, H., Kojima, T., and Sawada, N. (2006) 'Epigenetic Silencing of Occludin Promotes Tumorigenic and Metastatic Properties of Cancer Cells Via Modulations of Unique Sets of Apoptosis-Associated Genes'. *Cancer Research* 66 (18), 9125-9133

Osanai, M., Murata, M., Nishikiori, N., Chiba, H., Kojima, T., and Sawada, N. (2007) 'Occludin-mediated Premature Senescence is a fail-safe Mechanism Against Tumorigenesis in Breast Carcinoma Cells'. *Cancer Science* 98 (7), 1027-1034

Osanai, M., Nishikiori, N., Murata, M., Chiba, H., Kojima, T., and Sawada, N. (2006) 'Occludin Expression Inhibits Tumorigenicity and Metastasis'. *The FASEB Journal* 20, A223

Paget, S. (1889) 'The Distribution of Secondary Growths in Cancer of the Breast. 1889'. *Cancer Metastasis Reviews* 8 (2), 98-101

Paoli, P., Giannoni, E., and Chiarugi, P. (2013) 'Anoikis Molecular Pathways and its Role in Cancer Progression'. *Biochimica Et Biophysica Acta (BBA)-Molecular Cell Research* 1833 (12), 3481-3498

Park, J. and Schwarzbauer, J. E. (2014) 'Mammary Epithelial Cell Interactions with Fibronectin Stimulate Epithelial-Mesenchymal Transition'. *Oncogene* 33 (13), 1649-1657

Parri, M. and Chiarugi, P. (2010) 'Rac and Rho GTPases in Cancer Cell Motility Control'. *Cell Communication and Signaling* 8 (1), 1

Paschoud, S., Bongiovanni, M., Pache, J., and Citi, S. (2007) 'Claudin-1 and Claudin-5 Expression Patterns Differentiate Lung Squamous Cell Carcinomas from Adenocarcinomas'. *Modern Pathology* 20 (9), 947-954

Pastuszak, M., Groszewski, K., Pastuszak, M., Dyrla, P., Wojtuń, S., and Gil, J. (2015) 'Cytokeratins in Gastroenterology. Systematic Review'. *Przeglad Gastroenterologiczny* 10 (2), 61

Peinado, H., Olmeda, D., and Cano, A. (2007) 'Snail, Zeb and bHLH Factors in Tumour Progression: An Alliance Against the Epithelial Phenotype?'. *Nature Reviews Cancer* 7 (6), 415-428

Peiro, S., Escriva, M., Puig, I., Barbera, M.J., Dave, N., Herranz, N., Larriba, M.J., Takkunen, M., Francí, C., Munoz, A. and Virtanen, I., (2006) 'Snail1 transcriptional repressor binds to its own promoter and controls its expression'. *Nucleic acids research*, *34*(7), pp.2077-2084.

Peng, Y. and Croce, C. M. (2016) 'The Role of MicroRNAs in Human Cancer'. *Signal Transduction and Targeted Therapy* 1, 15004

Piras-Straub, K., Khairzada, K., Trippler, M., Baba, H. A., Kaiser, G. M., Paul, A., Canbay, A., Weber, F., Gerken, G., and Herzer, K. (2015) 'TRAIL Expression Levels in Human Hepatocellular Carcinoma have Implications for Tumor Growth, Recurrence and Survival'*. International Journal of Cancer* 136 (4), E154-E160

Polacheck, W. J., Zervantonakis, I. K., and Kamm, R. D. (2013) 'Tumor Cell Migration in Complex Microenvironments'*. Cellular and Molecular Life Sciences* 70 (8), 1335-1356

Postigo, A. A. (2003) 'Opposing Functions of ZEB Proteins in the Regulation of the TGFbeta/BMP Signaling Pathway'*. The EMBO Journal* 22 (10), 2443-2452

Pozzi, A. and Zent, R. (2010) 'ZO-1 and ZONAB Interact to Regulate Proximal Tubular Cell Differentiation'. *Journal of the American Society of Nephrology: JASN* 21 (3), 388-390

Puisieux, A., Brabletz, T., and Caramel, J. (2014) 'Oncogenic Roles of EMT-Inducing Transcription Factors'*. Nature Cell Biology* 16 (6), 488-494

Qadir, X. V., Han, C., Lu, D., Zhang, J., and Wu, T. (2014) 'MiR-185 Inhibits Hepatocellular Carcinoma Growth by Targeting the DNMT1/PTEN/Akt Pathway'*. The American Journal of Pathology* 184 (8), 2355-2364

Qi, R., An, H., Yu, Y., Zhang, M., Liu, S., Xu, H., Guo, Z., Cheng, T., and Cao, X. (2003) 'Notch1 Signaling Inhibits Growth of Human Hepatocellular Carcinoma through Induction of Cell Cycle Arrest and Apoptosis'. *Cancer Research* 63 (23), 8323-8329

Qin, L., Zhang, Y., Lin, J., Shentu, Y., and Xie, X. (2016) 'MicroRNA-455 Regulates Migration and Invasion of Human Hepatocellular Carcinoma by Targeting Runx2'*. Oncology Reports* 36 (6), 3325-3332

Radisky, E. S. and Radisky, D. C. (2010) 'Matrix Metalloproteinase-Induced Epithelial-Mesenchymal Transition in Breast Cancer'. *Journal of Mammary Gland Biology and Neoplasia* 15 (2), 201-212

Rahner, C., Mitic, L. L., and Anderson, J. M. (2001) 'Heterogeneity in Expression and Subcellular Localization of Claudins 2, 3, 4, and 5 in the Rat Liver, Pancreas, and Gut'*. Gastroenterology* 120 (2), 411-422

Raman, P., Purwin, T., Pestell, R., and Tozeren, A. (2015) 'FXYD5 is a Marker for Poor Prognosis and a Potential Driver for Metastasis in Ovarian Carcinomas'. *Cancer Informatics* 14, 113

Ravindranath, A., Yuen, H., Chan, K., Grills, C., Fennell, D., Lappin, T., and El-Tanani, M. (2011) 'WNT–β-catenin–Tcf-4 Signalling-Modulated Invasiveness is Dependent on Osteopontin Expression in Breast Cancer'. *British Journal of Cancer* 105 (4), 542-551

Raza, S. A., Clifford, G. M., and Franceschi, S. (2007) 'Worldwide Variation in the Relative Importance of Hepatitis B and Hepatitis C Viruses in Hepatocellular Carcinoma: A Systematic Review'*. British Journal of Cancer* 96 (7), 1127-1134

Resnick, M. B., Konkin, T., Routhier, J., Sabo, E., and Pricolo, V. E. (2005) 'Claudin-1 is a Strong Prognostic Indicator in Stage II Colonic Cancer: A Tissue Microarray Study'*. Modern Pathology* 18 (4), 511-518

Revenu, C. and Gilmour, D. (2009) 'EMT 2.0: Shaping Epithelia through Collective Migration'*. Current Opinion in Genetics & Development* 19 (4), 338-342

Riazuddin, S., Ahmed, Z. M., Fanning, A. S., Lagziel, A., Kitajiri, S., Ramzan, K., Khan, S. N., Chattaraj, P., Friedman, P. L., and Anderson, J. M. (2006) 'Tricellulin is a Tight-Junction

Protein Necessary for Hearing'. *The American Journal of Human Genetics* 79 (6), 1040-1051

Ridley, A. J. (2015) 'Rho GTPase Signalling in Cell Migration'. *Current Opinion in Cell Biology* 36, 103-112

Rimassa, L. and Santoro, A. (2009) 'Sorafenib Therapy in Advanced Hepatocellular Carcinoma: The SHARP Trial'. *Expert Review of Anticancer Therapy* 9 (6), 739-745

Rong, M., Chen, G., and Dang, Y. (2013) 'Increased miR-221 Expression in Hepatocellular Carcinoma Tissues and its Role in Enhancing Cell Growth and Inhibiting Apoptosis in Vitro'. *BMC Cancer* 13 (1), 1

Roomi, M., Monterrey, J., Kalinovsky, T., Rath, M., and Niedzwiecki, A. (2009) 'Patterns of MMP-2 and MMP-9 Expression in Human Cancer Cell Lines.'. Oncology Reports 21 (5), 1323

Rosenbluh, J., Wang, X., and Hahn, W. C. (2014) 'Genomic Insights into WNT/β-catenin Signaling'. *Trends in Pharmacological Sciences* 35 (2), 103-109

Ruan, D., Li, Y., and Jiang, N. (eds.) (2015) 'Effect of MiR-501-5p on CYLD Expression and Cell Proliferation in Human Hepatocellular Carcinoma.' *ASCO Annual Meeting Proceedings*. 88-95

Runkle, E. A. and Mu, D. (2013) 'Tight Junction Proteins: From Barrier to Tumorigenesis'. *Cancer Letters* 337 (1), 41-48

Ruscetti, M., Quach, B., Dadashian, E. L., Mulholland, D. J., and Wu, H. (2015) 'Tracking and Functional Characterization of Epithelial-Mesenchymal Transition and Mesenchymal Tumor Cells during Prostate Cancer Metastasis'. *Cancer Research* 75 (13), 2749-2759

Saftig, P., Hunziker, E., Wehmeyer, O., Jones, S., Boyde, A., Rommerskirch, W., Moritz, J. D., Schu, P., and Von Figura, K. (1998) 'Impaired Osteoclastic Bone Resorption Leads to Osteopetrosis in Cathepsin-K-Deficient Mice'*. Proceedings of the National Academy of Sciences* 95 (23), 13453-13458

Sahlgren, C., Gustafsson, M. V., Jin, S., Poellinger, L., and Lendahl, U. (2008) 'Notch Signaling Mediates Hypoxia-Induced Tumor Cell Migration and Invasion'*. Proceedings of the National Academy of Sciences of the United States of America* 105 (17), 6392-6397

Saitou, M., Furuse, M., Sasaki, H., Schulzke, J. D., Fromm, M., Takano, H., Noda, T., and Tsukita, S. (2000) 'Complex Phenotype of Mice Lacking Occludin, a Component of Tight Junction Strands'*. Molecular Biology of the Cell* 11 (12), 4131-4142

Sakai, N., Chiba, H., Fujita, H., Akashi, Y., Osanai, M., Kojima, T., and Sawada, N. (2007) 'Expression Patterns of Claudin Family of Tight-Junction Proteins in the Mouse Prostate'*. Histochemistry and Cell Biology* 127 (4), 457-46

Sanchez-Tillo, E., de Barrios, O., Siles, L., Cuatrecasas, M., Castells, A., and Postigo, A. (2011) 'B-Catenin /TCF4 Complex Induces the Epithelial-to-Mesenchymal Transition (EMT)-Activator ZEB1 to Regulate Tumor Invasiveness'. *Proceedings of the National Academy of Sciences of the United States of America* 108 (48), 19204-19209

Sanchez-Tillo, E., Lazaro, A., Torrent, R., Cuatrecasas, M., Vaquero, E., Castells, A., Engel, P., and Postigo, A. (2010) 'ZEB1 Represses E-cadherin and Induces an EMT by Recruiting the SWI/SNF Chromatin-Remodeling Protein BRG1'*. Oncogene* 29 (24), 3490

Sánchez-Tilló, E., Liu, Y., de Barrios, O., Siles, L., Fanlo, L., Cuatrecasas, M., Darling, D. S., Dean, D. C., Castells, A., and Postigo, A. (2012) 'EMT-Activating Transcription Factors in Cancer: Beyond EMT and Tumor Invasiveness'. *Cellular and Molecular Life Sciences* 69 (20), 3429-3456

Sassen, S., Miska, E. A., and Caldas, C. (2008) 'MicroRNA—implications for Cancer'. *Virchows Archiv* 452 (1), 1-10

Scaffidi, P. and Misteli, T. (2011) 'In Vitro Generation of Human Cells with Cancer Stem Cell Properties'. *Nature Cell Biology* 13 (9), 1051-1061

Semaan, A., Dietrich, D., Bergheim, D., Dietrich, J., Kalff, J. C., Branchi, V., Matthaei, H., Kristiansen, G., Fischer, H., and Goltz, D. (2016) 'CXCL12 Expression and PD-L1 Expression Serve as Prognostic Biomarkers in HCC and are Induced by Hypoxia'. *Virchows Archiv*, 1-12

Sharma, S. (2009) 'Tumor Markers in Clinical Practice: General Principles and Guidelines'. *Indian Journal of Medical and Paediatric Oncology : Official Journal of Indian Society of Medical & Paediatric Oncology* 30 (1), 1-8

Shen, G., Lin, Y., Yang, X., Zhang, J., Xu, Z., and Jia, H. (2014) 'MicroRNA-26b Inhibits Epithelial-Mesenchymal Transition in Hepatocellular Carcinoma by Targeting USP9X'. *BMC Cancer* 14 (1), 1

Shen, H., Li, W., Tian, Y., Xu, P., Wang, H., Zhang, J., and Li, Y. (2015) 'Upregulation of miR-362-3p Modulates Proliferation and Anchorage-Independent Growth by Directly Targeting Tob2 in Hepatocellular Carcinoma'. *Journal of Cellular Biochemistry* 116 (8), 1563-1573

Shengbing, Z., Jing Feng, L., Bin, W., Lingyun, G., and Aimin, H. (2009) 'Expression of KiSS-1 Gene and its Role in Invasion and Metastasis of Human Hepatocellular Carcinoma'. *The Anatomical Record* 292 (8), 1128-1134

Shi, X. and Teng, F. (2015) 'Down-Regulated miR-28-5p in Human Hepatocellular Carcinoma Correlated with Tumor Proliferation and Migration by Targeting Insulin-Like Growth Factor-1 (IGF-1)'. *Molecular and Cellular Biochemistry* 408 (1-2), 283-293

Shi, Y. and Massagué, J. (2003) 'Mechanisms of TGF-β Signaling from Cell Membrane to the Nucleus'. *Cell* 113 (6), 685-700

Shi, Y., Sawada, J., Sui, G., Affar, E. B., Whetstine, J. R., Lan, F., Ogawa, H., Luke, M. P., Nakatani, Y., and Shi, Y. (2003) 'Coordinated Histone Modifications Mediated by a CtBP Co-Repressor Complex'. *Nature* 422 (6933), 735-738

Shimizu, M., Goto, T., Sato, A., and Shibuya, H. (2013) 'WNK4 is an Essential Effector of Anterior Formation in FGF Signaling'. *Genes to Cells* 18 (6), 442-449

Shin, K., Fogg, V. C., and Margolis, B. (2006) 'Tight Junctions and Cell Polarity'. *Annu.Rev.Cell Dev.Biol.* 22, 207-235

Siemens, H., Jackstadt, R., Hünten, S., Kaller, M., Menssen, A., Götz, U., and Hermeking, H. (2011) 'MiR-34 and SNAIL Form a Double-Negative Feedback Loop to Regulate Epithelial-Mesenchymal Transitions'. *Cell Cycle* 10 (24), 4256-4271

Simske, J. S. (2013) 'Claudins Reign: The claudin/EMP/PMP22/γ Channel Protein Family in C. Elegans'. *Tissue Barriers* 1 (3), e25502

Singh, A. B., Sharma, A., and Dhawan, P. (2010) 'Claudin Family of Proteins and Cancer: An Overview'. *Journal of Oncology* 2010, 541957

Solinet, S., Mahmud, K., Stewman, S. F., Ben El Kadhi, K., Decelle, B., Talje, L., Ma, A., Kwok, B. H., and Carreno, S. (2013) 'The Actin-Binding ERM Protein Moesin Binds to and Stabilizes Microtubules at the Cell Cortex'. *The Journal of Cell Biology* 202 (2), 251-260

Song, L., Liu, Q., Meng, X., Li, S. L., Wang, L., Fan, Q., and Xuan, X. (2016) 'DLC-1 is an Independent Prognostic Marker and Potential Therapeutic Target in Hepatocellular Cancer'. *Diagnostic Pathology* 11 (1), 1

Song, T., Dou, C., Jia, Y., Tu, K., and Zheng, X. (2015) 'TIMP-1 Activated Carcinoma-Associated Fibroblasts Inhibit Tumor Apoptosis by Activating SDF1/CXCR4 Signaling in Hepatocellular Carcinoma'. *Oncotarget* 6 (14), 12061-12079

Staal, F. J. and Clevers, H. (2012) 'Tales of the Unexpected: Tcf1 Functions as a Tumor Suppressor for Leukemias'. *Immunity* 37 (5), 761-763

Stamatovic, S. M., Keep, R. F., Wang, M. M., Jankovic, I., and Andjelkovic, A. V. (2009) 'Caveolae-Mediated Internalization of Occludin and Claudin-5 during CCL2-Induced Tight Junction Remodelling in Brain Endothelial Cells'. *The Journal of Biological Chemistry* 284 (28), 19053-19066

Steller, E. J., Raats, D. A., Koster, J., Rutten, B., Govaert, K. M., Emmink, B. L., Snoeren, N., van Hooff, S. R., Holstege, F. C., and Maas, C. (2013) 'PDGFRB Promotes Liver Metastasis Formation of Mesenchymal-Like Colorectal Tumor Cells'. *Neoplasia* 15 (2), 204-IN30

Stemmer, V., De Craene, B., Berx, G., and Behrens, J. (2008) 'Snail Promotes Wnt Target Gene Expression and Interacts with β-catenin'*. Oncogene* 27 (37), 5075-5080

Sugarbaker, E. D. (1952) 'The Organ Selectivity of Experimentally Induced Metastases in Rats'*. Cancer* 5 (3), 606-612

Suh, Y., Yoon, C., Kim, R., Lim, E., Oh, Y., Hwang, S., An, S., Yoon, G., Gye, M., and Yi, J. (2013) 'Claudin-1 Induces epithelial–mesenchymal Transition through Activation of the c-Abl-ERK Signaling Pathway in Human Liver Cells'. *Oncogene* 32 (41), 4873-4882

Sun, W., Zhang, Z., Wang, J., Shang, R., Zhou, L., Wang, X., Duan, J., Ruan, B., Gao, Y., Dai, B., Qu, S., Liu, W., Ding, R., Wang, L., Wang, D., and Dou, K. (2016) 'MicroRNA-150 Suppresses Cell Proliferation and Metastasis in Hepatocellular Carcinoma by Inhibiting the GAB1-ERK Axis'*. Oncotarget* 7 (10), 11595-11608

Sun, Y., Song, G., Sun, N., Chen, J., and Yang, S. (2014) 'SLUG Overexpression Induces Stemness and Promotes Hepatocellular Carcinoma Cell Invasion and Metastasis'. *Oncology Letters* 7 (6), 1936-1940

Takano, M., Shimada, K., Fujii, T., Morita, K., Takeda, M., Nakajima, Y., Nonomura, A., Konishi, N., and Obayashi, C. (2016) 'Keratin 19 as a Key Molecule in Progression of Human Hepatocellular Carcinomas through Invasion and Angiogenesis'. *BMC Cancer* 16 (1), 903

Tam, W. L. and Weinberg, R. A. (2013) 'The Epigenetics of Epithelial-Mesenchymal Plasticity in Cancer'*. Nature Medicine* 19 (11), 1438-1449

Thiery, J. P. (2002) 'Epithelial–mesenchymal Transitions in Tumour Progression'*. Nature Reviews Cancer* 2 (6), 442-454

Tian, S., Yu, J., Liu, Y., Kang, W., Ma, Z., Ye, X., and Yan, C. (2015) 'MiR-30b Suppresses Tumor Migration and Invasion by Targeting EIF5A2 in Gastric Cancer'. *World Journal of Gastroenterology: WJG* 21 (31), 9337

Tian, Y., Tian, Y., Zhang, W., Wei, F., Yang, J., Luo, X., Zhou, T., Hou, B., Qian, S., Deng, X., Qiu, Y., and Yao, K. (2015) 'Junctional Adhesion Molecule-A, an Epithelial-Mesenchymal Transition Inducer, Correlates with Metastasis and Poor Prognosis in Human Nasopharyngeal Cancer'. *Carcinogenesis* 36 (1), 41-48

Tobioka, H., Tokunaga, Y., Isomura, H., Kokai, Y., Yamaguchi, J., and Sawada, N. (2004) 'Expression of Occludin, a Tight-Junction-Associated Protein, in Human Lung Carcinomas'. *Virchows Archiv* 445 (5), 472-476

Toivola, D. M., Tao, G., Habtezion, A., Liao, J., and Omary, M. B. (2005) 'Cellular Integrity Plus: Organelle-Related and Protein-Targeting Functions of Intermediate Filaments'. *Trends in Cell Biology* 15 (11), 608-617

Tőkés, A., Kulka, J., Paku, S., Szik, Á., Páska, C., Novák, P. K., Szilák, L., Kiss, A., Bögi, K., and Schaff, Z. (2005) 'Claudin-1, -3 and-4 Proteins and mRNA Expression in Benign and Malignant Breast Lesions: A Research Study'. *Breast Cancer Research* 7 (2), R296

Toyama, T., Lee, H. C., Koga, H., Wands, J. R., and Kim, M. (2010) 'Non-canonical WNT11 Inhibits Hepatocellular Carcinoma Cell Proliferation and Migration'. *Molecular Cancer Research: MCR* 8 (2), 254-265

Trimble, W. S. and Grinstein, S. (2015) 'Barriers to the Free Diffusion of Proteins and Lipids in the Plasma Membrane'. *The Journal of Cell Biology* 208 (3), 259-271

Tumminello, F., Leto, G., Pizzolanti, G., Candiloro, V., Crescimanno, M., Crosta, L., Flandina, C., Montalto, G., Soresi, M., and Carroccio, A. (1996) 'Cathepsin D, B and L Circulating Levels as Prognostic Markers of Malignant Progression'. *Anticancer Research* 16 (4), 2315-2320

Ueno, K., Hiura, M., Suehiro, Y., Hazama, S., Hirata, H., Oka, M., Imai, K., Dahiya, R., and Hinoda, Y. (2008) 'Frizzled-7 as a Potential Therapeutic Target in Colorectal Cancer'. *Neoplasia* 10 (7), 697-705

van IJzendoorn, S. C., Zegers, M. M., Kok, J. W., and Hoekstra, D. (1997) 'Segregation of Glucosylceramide and Sphingomyelin Occurs in the Apical to Basolateral Transcytotic Route in HepG2 Cells'. *The Journal of Cell Biology* 137 (2), 347-357

Van Zijl, F., Zulehner, G., Petz, M., Schneller, D., Kornauth, C., Hau, M., Machat, G., Grubinger, M., Huber, H., and Mikulits, W. (2009) 'Epithelial-Mesenchymal Transition in Hepatocellular Carcinoma'. *Future Oncology* 5 (8), 1169-1179

Venook, A. P., Papandreou, C., Furuse, J., and de Guevara, L. L. (2010) 'The Incidence and Epidemiology of Hepatocellular Carcinoma: A Global and Regional Perspective'. *The Oncologist* 15 Suppl 4, 5-13

Voutsadakis, I. A. (2016) 'Epithelial-Mesenchymal Transition (EMT) and Regulation of EMT Factors by Steroid Nuclear Receptors in Breast Cancer: A Review and in Silico Investigation'. *Journal of Clinical Medicine* 5 (1), 11

Waisberg, J. and Saba, G. T. (2015) 'WNT-/-β-catenin Pathway Signaling in Human Hepatocellular Carcinoma'. *World Journal of Hepatology* 7 (26), 2631

Wang, F., Daugherty, B., Keise, L. L., Wei, Z., Foley, J. P., Savani, R. C., and Koval, M. (2003) 'Heterogeneity of Claudin Expression by Alveolar Epithelial Cells'. *American Journal of Respiratory Cell and Molecular Biology* 29 (1), 62-70

Wang, J., Li, J., Shen, J., Wang, C., Yang, L., and Zhang, X. (2012) 'MicroRNA-182 Downregulates Metastasis Suppressor 1 and Contributes to Metastasis of Hepatocellular Carcinoma'. *BMC Cancer* 12 (1), 1

Wang, J., Scully, K., Zhu, X., Cai, L., Zhang, J., Prefontaine, G. G., Krones, A., Ohgi, K. A., Zhu, P., and Garcia-Bassets, I. (2007) 'Opposing LSD1 Complexes Function in Developmental Gene Activation and Repression Programmes'. *Nature* 446 (7138), 882-887

Wang, M., Xue, L., Cao, Q., Lin, Y., Ding, Y., Yang, P., and Che, L. (2009) 'Expression of Notch1, Jagged1 and B-Catenin and their Clinicopathological Significance in Hepatocellular Carcinoma'. *Neoplasma* 56 (6), 533-541

Wang, N., Zhu, M., Tsao, S., Man, K., Zhang, Z., and Feng, Y. (2012) 'Up-Regulation of TIMP-1 by Genipin Inhibits MMP-2 Activities and Suppresses the Metastatic Potential of Human Hepatocellular Carcinoma'. *PLoS One* 7 (9), e46318

Wang, W., Zhao, L. J., Tan, Y. X., Ren, H., and Qi, Z. T. (2012) 'MiR-138 Induces Cell Cycle Arrest by Targeting Cyclin D3 in Hepatocellular Carcinoma'*. Carcinogenesis* 33 (5), 1113-1120

Wang, Y. Y., Zhao, R., and Zhe, H. (2015) 'The Emerging Role of CaMKII in Cancer'. *Oncotarget* 6 (14), 11725-11734

Wang, Y., Chen, C., Wang, X., and Wang, L. (2016) 'Effects of miR-339-5p on Invasion and Prognosis of Hepatocellular Carcinoma'*. Clinics and Research in Hepatology and Gastroenterology* 40 (1), 51-56

Wheelock, M. J., Shintani, Y., Maeda, M., Fukumoto, Y., and Johnson, K. R. (2008) 'Cadherin Switching'. *Journal of Cell Science* 121 (Pt 6), 727-735

White, L. R., Blanchette, J. B., Ren, L., Awn, A., Trpkov, K., and Muruve, D. A. (2007) 'The Characterization of alpha5-Integrin Expression on Tubular Epithelium during Renal Injury'*. American Journal of Physiology.Renal Physiology* 292 (2), F567-76

Williams, K., Motiani, K., Giridhar, P. V., and Kasper, S. (2013) 'CD44 Integrates Signaling in Normal Stem Cell, Cancer Stem Cell and (Pre) Metastatic Niches'*. Experimental Biology and Medicine* 238 (3), 324-338

Williams, T. M. and Lisanti, M. P. (2005) 'Caveolin-1 in Oncogenic Transformation, Cancer, and Metastasis'. American Journal of Physiology. *Cell Physiology* 288 (3), C494-506

Wojciechowski, M. C., Mahmutovic, L., Shu, D. Y., and Lovicu, F. J. (2017) 'ERK1/2 Signaling is Required for the Initiation but Not Progression of TGFβ-Induced Lens Epithelial to Mesenchymal Transition (EMT)'*. Experimental Eye Research* 159, 98-113

Wong, R. and Frenette, C. (2011) 'Updates in the Management of Hepatocellular Carcinoma'*. Gastroenterol Hepatol (NY)* 7 (1), 16-24

Wong, V. (1997) 'Phosphorylation of Occludin Correlates with Occludin Localization and Function at the Tight Junction'*. The American Journal of Physiology* 273 (6 Pt 1), C1859-67

Woo, H. Y., Min, A. L., Choi, J. Y., Bae, S. H., Yoon, S. K., and Jung, C. K. (2011) 'Clinicopathological Significance of the Expression of SNAIL in Hepatocellular Carcinoma'. *The Korean Journal of Hepatology* 17 (1), 12-18

Wu, X., Tu, X., Joeng, K. S., Hilton, M. J., Williams, D. A., and Long, F. (2008) 'Rac1 Activation Controls Nuclear Localization of β-catenin during Canonical WNT Signaling'. *Cell* 133 (2), 340-353

Wu, Y., Deng, J., Rychahou, P. G., Qiu, S., Evers, B. M., and Zhou, B. P. (2009) 'Stabilization of Snail by NF-κB is Required for Inflammation-Induced Cell Migration and Invasion'*. Cancer Cell* 15 (5), 416-428

Xia, L., Huang, W., Tian, D., Zhang, L., Qi, X., Chen, Z., Shang, X., Nie, Y., and Wu, K. (2014) 'Forkhead Box Q1 Promotes Hepatocellular Carcinoma Metastasis by Transactivating ZEB2 and VersicanV1 Expression'. *Hepatology* 59 (3), 958-973

Xu, H., Dawson, R., Crane, I. J., and Liversidge, J. (2005) 'Leukocyte Diapedesis in Vivo Induces Transient Loss of Tight Junction Protein at the Blood-Retina Barrier'. *Investigative Ophthalmology & Visual Science* 46 (7), 2487-2494

Xue, T., Ge, N., Zhang, L., Cui, J., Chen, R., You, Y., Ye, S., and Ren, Z. (2014) 'Goosecoid Promotes the Metastasis of Hepatocellular Carcinoma by Modulating the Epithelial-Mesenchymal Transition'. *PloS One* 9 (10), e109695

Yamaguchi, H., Hsu, J., and Hung, M. (2012) 'Regulation of Ubiquitination-Mediated Protein Degradation by Survival Kinases in Cancer'. *Frontiers in Oncology* 2, 15

Yan, C., Wang, H., and Boyd, D. D. (2001) 'KiSS-1 Represses 92-kDa Type IV Collagenase Expression by Down-Regulating NF-Kappa B Binding to the Promoter as a Consequence of Ikappa Balpha -Induced Block of p65/p50 Nuclear Translocation'. *The Journal of Biological Chemistry* 276 (2), 1164-1172

Yan, J., Gumireddy, K., Li, A., and Huang, Q. (2013) 'Regulation of Mesenchymal Phenotype by MicroRNAs in Cancer'. *Current Cancer Drug Targets* 13 (9), 930-934

Yang, F., Sun, L., Li, Q., Han, X., Lei, L., Zhang, H., and Shang, Y. (2012) 'SET8 Promotes Epithelial-Mesenchymal Transition and Confers TWIST Dual Transcriptional Activities'. *The EMBO Journal* 31 (1), 110-123

Yang, H., Fang, F., Chang, R., and Yang, L. (2013) 'MicroRNA-140-5p Suppresses Tumor Growth and Metastasis by Targeting Transforming Growth Factor β Receptor 1 and Fibroblast Growth Factor 9 in Hepatocellular Carcinoma'. *Hepatology* 58 (1), 205-217

Yang, J., Liu, X., Yuan, X., and Wang, Z. (2015) 'MiR-99b Promotes Metastasis of Hepatocellular Carcinoma through Inhibition of Claudin 11 Expression and may Serve as a Prognostic Marker'. *Oncology Reports* 34 (3), 1415-1423

Yang, J., Mani, S. A., Donaher, J. L., Ramaswamy, S., Itzykson, R. A., Come, C., Savagner, P., Gitelman, I., Richardson, A., and Weinberg, R. A. (2004) 'Twist, a Master Regulator of Morphogenesis, Plays an Essential Role in Tumor Metastasis'. *Cell* 117 (7), 927-939

Yang, L., Chen, Y., Cui, T., Knosel, T., Zhang, Q., Albring, K. F., Huber, O., and Petersen, I. (2012) 'Desmoplakin Acts as a Tumor Suppressor by Inhibition of the WNT/β-catenin Signaling Pathway in Human Lung Cancer'. *Carcinogenesis* 33 (10), 1863-1870

Yang, M., Chen, C., Chau, G., Chiou, S., Su, C., Chou, T., Peng, W., and Wu, J. (2009) 'Comprehensive Analysis of the Independent Effect of TWIST and SNAIL in Promoting Metastasis of Hepatocellular Carcinoma'. *Hepatology* 50 (5), 1464-1474

Yang, M., Wu, M., Chiou, S., Chen, P., Chang, S., Liu, C., Teng, S., and Wu, K. (2008) 'Direct Regulation of TWIST by HIF-1α Promotes Metastasis'. *Nature Cell Biology* 10 (3), 295-305

Yang, W., Lv, S., Liu, X., Liu, H., Yang, W., and Hu, F. (2010) 'Up-Regulation of Tiam1 and Rac1 Correlates with Poor Prognosis in Hepatocellular Carcinoma'. *Japanese Journal of Clinical Oncology* 40 (11), 1053-1059

Yang, Y., Wang, F., Xiao, J., Song, Y., Zhao, Y., Cao, Y., Bei, Y., and Yang, C. (2014) 'MiR-222 Overexpression Promotes Proliferation of Human Hepatocellular Carcinoma HepG2 Cells by Downregulating p27'. *Int J Clin Exp Med* 7 (4), 893-902

Yang, Z., Sun, B., Li, Y., Zhao, X., Zhao, X., Gu, Q., An, J., Dong, X., Liu, F., and Wang, Y. (2015) 'ZEB2 Promotes Vasculogenic Mimicry by TGF-β1 Induced Epithelial-to-Mesenchymal Transition in Hepatocellular Carcinoma'. *Experimental and Molecular Pathology* 98 (3), 352-359

Yao, J., Liang, L., Zhang, Y., Ding, J., Tian, Q., Li, J., and He, X. (2012) 'GNAI1 Suppresses Tumor Cell Migration and Invasion and is Post-Transcriptionally Regulated by Mir-320a/c/d in Hepatocellular Carcinoma'. *Cancer Biology & Medicine* 9 (4), 234-241

Yasen, M., Kajino, K., Kano, S., Tobita, H., Yamamoto, J., Uchiumi, T., Kon, S., Maeda, M., Obulhasim, G., Arii, S., and Hino, O. (2005) 'The Up-Regulation of Y-Box Binding Proteins (DNA Binding Protein A and Y-Box Binding Protein-1) as Prognostic Markers of Hepatocellular Carcinoma'. Clinical Cancer Research: *An Official Journal of the American Association for Cancer Research* 11 (20), 7354-7361

Ye, J., Yao, Y., Song, Q., Li, S., Hu, Z., Yu, Y., Hu, C., Da, X., Li, H., and Chen, Q. (2016) 'Up-Regulation of miR-95-3p in Hepatocellular Carcinoma Promotes Tumorigenesis by Targeting p21 Expression'. *Scientific Reports* 6

Ye, Z., Ma, G., Zhao, Y., Xiao, Y., Zhan, Y., Jing, C., Gao, K., Liu, Z., and Yu, S. (2015) 'MiR-429 Inhibits Migration and Invasion of Breast Cancer Cells in Vitro'. *International Journal of Oncology* 46 (2), 531-538

Yeh, T. S., Wang, F., Chen, T. C., Yeh, C. N., Yu, M. C., Jan, Y. Y., and Chen, M. F. (2014) 'Expression Profile of microRNA-200 Family in Hepatocellular Carcinoma with Bile Duct Tumor Thrombus'. *Annals of Surgery* 259 (2), 346-354

Yook, J. I., Li, X., Ota, I., Hu, C., Kim, H. S., Kim, N. H., Cha, S. Y., Ryu, J. K., Choi, Y. J., and Kim, J. (2006) 'A Wnt–Axin2–GSK3β Cascade Regulates Snail1 Activity in Breast Cancer Cells'. *Nature Cell Biology* 8 (12), 1398-1406

Yoon, C. H., Kim, M. J., Park, M. J., Park, I. C., Hwang, S. G., An, S., Choi, Y. H., Yoon, G., and Lee, S. J. (2010) 'Claudin-1 Acts through c-Abl-Protein Kinase Cdelta (PKC delta) Signaling and has a Causal Role in the Acquisition of Invasive Capacity in Human Liver Cells'. *The Journal of Biological Chemistry* 285 (1), 226-233

Yoshida, Y., Ban, Y., and Kinoshita, S. (2009) 'Tight Junction Transmembrane Protein Claudin Subtype Expression and Distribution in Human Corneal and Conjunctival Epithelium'. *Investigative Ophthalmology & Visual Science* 50 (5), 2103-2108

Yu, D. D., Jing, Y. Y., Guo, S. W., Ye, F., Lu, W., Li, Q., Dong, Y. L., Gao, L., Yang, Y. T., Yang, Y., Wu, M. C., and Wei, L. X. (2015) 'Overexpression of Hepatocyte Nuclear Factor-1beta Predicting Poor Prognosis is Associated with Biliary Phenotype in Patients with Hepatocellular Carcinoma'. *Scientific Reports* 5, 13319

Yu, H., Shen, H., Zhang, Y., Zhong, F., Liu, Y., Qin, L., and Yang, P. (2014) 'CAV1 Promotes HCC Cell Progression and Metastasis through WNT/β-catenin Pathway'. *PloS One* 9 (9), e106451

Yu, Q. and Stamenkovic, I. (2000) 'Cell Surface-Localized Matrix Metalloproteinase-9 Proteolytically Activates TGF-Beta and Promotes Tumor Invasion and Angiogenesis'. *Genes & Development* 14 (2), 163-176

Yu, W., Kamara, H., and Svoboda, K. K. (2008) 'The Role of Twist during Palate Development'. *Developmental Dynamics* 237 (10), 2716-2725

Yuan, X., Wu, H., Xu, H., Xiong, H., Chu, Q., Yu, S., Wu, G. S., and Wu, K. (2015) 'Notch Signaling: An Emerging Therapeutic Target for Cancer Treatment'. *Cancer Letters* 369 (1), 20-27

Yuzugullu, H., Benhaj, K., Ozturk, N., Senturk, S., Celik, E., Toylu, A., Tasdemir, N., Yilmaz, M., Erdal, E., and Akcali, K. C. (2009) 'Canonical WNT Signaling is Antagonized by Non-canonical WNT5a in Hepatocellular Carcinoma Cells'. *Molecular Cancer* 8 (1), 1

Zeisberg, M. and Neilson, E. G. (2009) 'Biomarkers for Epithelial-Mesenchymal Transitions'. *The Journal of Clinical Investigation* 119 (6), 1429-1437

Zeng, W., LI, Y., Aoxian, Y., and Yuqiang, N. (2016) 'Expression and Inhibitory Role of TIMP-3 in Hepatocellular Carcinoma' *Oncology Reports* 36 (1), 494-502

Zeng, Y., Liang, X., Zhang, G., Jiang, N., Zhan, D., Wei, S., Liu, C., Liang, B., Ji, G., Chen, X., Xiong, M., and Huang, Z. (2012) 'Reduced N-Cadherin Expression is Associated with Metastatic Potential and Poor Surgical Outcomes of Hepatocellular Carcinoma'. *Journal of Gastroenterology and Hepatology* 27 (1), 173-180

Zeng, Y., Liang, X., Zhang, G., Jiang, N., Zhang, T., Huang, J., Zhang, L., and Zeng, X. (2016) 'MiRNA-135a Promotes Hepatocellular Carcinoma Cell Migration and Invasion by Targeting Forkhead Box O1'*. Cancer Cell International* 16 (1), 63

Zhang, G., Zhou, T., Tian, H., Liu, Z., and Xia, S. (2013) 'High Expression of ZEB1 Correlates with Liver Metastasis and Poor Prognosis in Colorectal Cancer'. *Oncology Letters* 5 (2), 564-568

Zhang, J., Cheng, J., Zeng, Z., Wang, Y., Li, X., Xie, Q., Jia, J., Yan, Y., Guo, Z., Gao, J., Yao, M., Chen, X., and Lu, F. (2015) 'Comprehensive Profiling of Novel microRNA-9 Targets and a Tumor Suppressor Role of microRNA-9 Via Targeting IGF2BP1 in Hepatocellular Carcinoma'. *Oncotarget* 6 (39), 42040-42052

Zhang, J., Zhang, H., Liu, J., Tu, X., Zang, Y., Zhu, J., Chen, J., Dong, L., and Zhang, J. (2012) 'MiR-30 Inhibits TGF-β1-Induced Epithelial-to-Mesenchymal Transition in Hepatocyte by Targeting SNAIL1'*. Biochemical and Biophysical Research Communications* 417 (3), 1100-1105

Zhang, P., Sun, Y., and Ma, L. (2015) 'ZEB1: At the Crossroads of Epithelial-Mesenchymal Transition, Metastasis and Therapy Resistance'*. Cell Cycle* 14 (4), 481-487

Zhang, Q., Chen, X., Zhou, J., Zhang, L., Zhao, Q., Chen, G., Xu, J., Feng, Q., and Chen, Z. (2006) 'CD147, MMP-2, MMP-9 and MVD-CD34 are Significant Predictors of Recurrence After Liver Transplantation in Hepatocellular Carcinoma Patients'. *Cancer Biology & Therapy* 5 (7), 808-814

Zhang, Q., Xu, M., Cai, X., Qu, Y., Li, Z., and Lu, L. (2015) 'Myofibroblastic Transformation of Rat Hepatic Stellate Cells: The Role of Notch Signaling and Epithelial-Mesenchymal Transition Regulation'. *Eur Rev Med Pharmacol Sci* 19 (21), 4130-4138

Zhang, Y., Wang, Y., Guo, Y., Liao, Z., Xu, R., and Ruan, Z. (2015) 'MiR-135b Promotes the Invasion and Metastasis of Hepatocellular Carcinoma Cells'*. Xi Bao Yu Fen Zi Mian Yi Xue Za Zhi = Chinese Journal of Cellular and Molecular Immunology* 31 (10), 1316-1321

Zhang, Y., Zheng, D., Xiong, Y., Xue, C., Chen, G., Yan, B., and Ye, Q. (2014) 'MiR-202 Suppresses Cell Proliferation in Human Hepatocellular Carcinoma by Downregulating LRP6 post-transcriptionally'*. FEBS Letters* 588 (10), 1913-1920

Zhang, Z., Cai, L., Zheng, S., Xiong, Y., and Dong, J. (2009) 'Overexpression of Caveolin-1 in Hepatocellular Carcinoma with Metastasis and Worse Prognosis: Correlation with Vascular Endothelial Growth Factor, Microvessel Density and Unpaired Artery'. *Pathology & Oncology Research* 15 (3), 495-502

Zhao, L. and Zhang, Y. (2015) 'MiR-342-3p Affects Hepatocellular Carcinoma Cell Proliferation Via Regulating NF-κB Pathway'*. Biochemical and Biophysical Research Communications* 457 (3), 370-377

Zhen, Y., Fang, W., Zhao, M., Luo, R., Liu, Y., Fu, Q., Chen, Y., Cheng, C., Zhang, Y., and Liu, Z. (2016) 'MiR-374a-CCND1-pPI3K/AKT-c-JUN Feedback Loop Modulated by PDCD4 Suppresses Cell Growth, Metastasis, and Sensitizes Nasopharyngeal Carcinoma to Cisplatin'*. Oncogene*

Zheng, A., Yuan, F., Li, Y., Zhu, F., Hou, P., Li, J., Song, X., Ding, M., and Deng, H. (2007) 'Claudin-6 and Claudin-9 Function as Additional Co-receptors for Hepatitis C Virus'. *Journal of Virology* 81 (22), 12465-12471

Zhou, B.P., Deng, J., Xia, W., Xu, J., Li, Y.M., Gunduz, M. and Hung, M.C., (2004) 'Dual regulation of Snail by GSK-3β-mediated phosphorylation in control of epithelial–mesenchymal transition'. *Nature cell biology*, *6*(10), pp.931-940.

Zhou, D., Bai, F., Zhang, X., Hu, M., Zhao, G., Zhao, Z., and Liu, R. (2014) 'SOX10 is a Novel Oncogene in Hepatocellular Carcinoma through WNT/β-catenin/TCF4 Cascade'. *Tumor Biology* 35 (10), 9935-9940

Zhou, H. C., Fang, J. H., Luo, X., Zhang, L., Yang, J., Zhang, C., and Zhuang, S. M. (2014) 'Downregulation of microRNA-100 Enhances the ICMT-Rac1 Signaling and Promotes Metastasis of Hepatocellular Carcinoma Cells'. *Oncotarget* 5 (23), 12177-12188

Zhu, L., Gao, J., Huang, K., Luo, Y., Zhang, B., and Xu, W. (2015) 'MiR-34a Screened by miRNA Profiling Negatively Regulates WNT/β-catenin Signaling Pathway in Aflatoxin B1 Induced Hepatotoxicity'. *Scientific Reports* 5, 16732

Zhu, X., Dong, Q., Zhang, X., Deng, B., Jia, H., Ye, Q., Qin, L., and Wu, X. (2012) 'MicroRNA-29a Suppresses Cell Proliferation by Targeting SPARC in Hepatocellular Carcinoma'. *International Journal of Molecular Medicine* 30 (6), 1321-1326

Zhu, Y., Brännström, M., Janson, P., and Sundfeldt, K. (2006) 'Differences in Expression Patterns of the Tight Junction Proteins, Claudin 1, 3, 4 and 5, in Human Ovarian Surface Epithelium as Compared to Epithelia in Inclusion Cysts and Epithelial Ovarian Tumours'. *International Journal of Cancer* 118 (8), 1884-1891

Newell, P., Toffanin, S., Villanueva, A., Chiang, D. Y., Minguez, B., Cabellos, L., Savic, R., Hoshida, Y., Lim, K. H., and Melgar-Lesmes, P. (2009) 'Ras Pathway Activation in Hepatocellular Carcinoma and Anti-Tumoral Effect of Combined Sorafenib and Rapamycin in Vivo'*. Journal of Hepatology* 51 (4), 725-733

He, A. R. and Goldenberg, A. S. (2013) 'Treating Hepatocellular Carcinoma Progression Following First-Line Sorafenib: Therapeutic Options and Clinical Observations'*. Therapeutic Advances in Gastroenterology* 6 (6), 447-458

Piris, M. A. (2011) 'The use of Molecular Profiling for Diagnosis and Research in Non-Hodgkin's Lymphoma'*. Hematology Reports* 3 (3s), e2

Wu, Y. and Zhou, B. P. (2010) 'Snail: More than EMT'*. Cell Adhesion & Migration* 4 (2), 199-203

Nissinen, L. and Kähäri, V. (2014) 'Matrix Metalloproteinases in Inflammation'*. Biochimica Et Biophysica Acta (BBA)-General Subjects* 1840 (8), 2571-2580

Etienne-Manneville, S. and Hall, A. (2002) 'Rho GTPases in Cell Biology'*. Nature* 420 (6916), 629

Thomas, S., Liao, Z., Clark, D., Chen, Y., Samadani, R., Mao, L., Ann, D., Baulch, J., Shapiro, P., and Yang, A. (2013) 'Exosomal Proteome Profiling: A Potential Multi-Marker Cellular Phenotyping Tool to Characterize Hypoxia-Induced Radiation Resistance in Breast Cancer'*. Proteomes* 1 (2), 87-108

'EMT, CSCs, and Drug Resistance: The Mechanistic Link and Clinical Implications'*. Nature Reviews Clinical Oncology* 14 (10), 611

Biswas, S. and Rao, C. M. (2017) 'Epigenetics in Cancer: Fundamentals and Beyond'. *Pharmacology & Therapeutics* 173, 118-134

Kim, J., Kong, J., Chang, H., Kim, H., and Kim, A. (2016) 'EGF Induces Epithelial-Mesenchymal Transition through Phospho-Smad2/3-Snail Signaling Pathway in Breast Cancer Cells'. *Oncotarget* 7 (51), 85021-85032

Hecht, J. R., Douillard, J., Schwartzberg, L., Grothey, A., Kopetz, S., Rong, A., Oliner, K. S., and Sidhu, R. (2015) 'Extended RAS Analysis for Anti-Epidermal Growth Factor Therapy in Patients with Metastatic Colorectal Cancer'. *Cancer Treatment Reviews* 41 (8), 653-659

Ocana, O. H. and Nieto, M. A. (2008) 'A New Regulatory Loop in Cancer-Cell Invasion'. *EMBO Reports* 9 (6), 521-522

Lin, S. and Gregory, R. I. (2015) 'MicroRNA Biogenesis Pathways in Cancer'. *Nature Reviews Cancer* 15 (6), 321

Chi, Y. and Zhou, D. (2016) 'MicroRNAs in Colorectal Carcinoma-from Pathogenesis to Therapy'*. Journal of Experimental & Clinical Cancer Research* 35 (1), 43

Ombrato, L. and Malanchi, I. (2014) 'The EMT Universe: Space between Cancer Cell Dissemination and Metastasis Initiation'*. Critical Reviews™ in Oncogenesis* 19 (5)

Oliveira, S. and Morgado-Diaz, J. (2007) 'Claudins: Multifunctional Players in Epithelial Tight Junctions and their Role in Cancer'. *Cellular and Molecular Life Sciences* 64 (1), 17-28

Capaldo, C. T. and Nusrat, A. (2015) Seminars in Cell & Developmental Biology. 'Claudin Switching: Physiological Plasticity of the Tight Junction': *Elsevier* 85-95